Institut für Anorganische Chemie

Synthesis, Characterization, and Reactivity Studies of Low-valent 3d Metal Complexes with N-Heterocyclic Carbene and α-Diimine Ligands

Dissertation

Zur Erlangung des Doktorgrades der Naturwissenschaften

Dr. rer. nat.

an der Fakultät Chemie und Pharmazie der Universität Regensburg

vorgelegt von:

Stefan Pelties

aus Nordhorn

Regensburg 2016

Der experimentelle Teil der vorliegenden Arbeit wurde in der Zeit zwischen November 2012 und Februar 2016 unter Anleitung von Prof. Dr. Robert Wolf am Institut für Anorganische Chemie der Universität Regensburg und unter Anleitung von Prof. Dr. Michael K. Whittlesey am Department of Chemistry, University of Bath, UK (Juni 2015 und Juli 2016) angefertigt.

Die Arbeit wurde angeleitet von:		Prof. Dr. Robert Wolf
Promotionsgesuch eingereicht am:		17.03.2016
Tag der mündlichen Prüfung:		02.05.2016
Promotionsausschuss:	Vorsitz	Prof. Dr. Olga Garcia Mancheño
	Erstgutachter	Prof. Dr. Robert Wolf
	Zweitgutachter	Prof. Dr. Manfred Scheer
	Dritter Prüfer	Prof. Dr. Axel Jacobi von Wangelin

Prologue

This thesis reports on the synthesis and characterization of reactive 3d metal complexes with N-heterocyclic carbene (NHC) and α-diimine ligands. Chapter 1 reviews the chemistry of mononuclear phosphane and NHC nickel(I) complexes. Besides the synthesis and structural motifs of the nickel(I) radicals, this chapter also deals with the reactivity of these species. In chapter 2-5 the synthesis, characterization, and reactivity studies of monomeric NHC nickel(I) complexes is discussed. Chapter 6 covers the synthesis and structural characterization of iron(II), cobalt(II), and nickel(II) complexes with a cyclic (alkyl)(amino)carbene ligand. Investigations concerning the synthesis and characterization of NHC manganese(II) complexes is reported in chapter 7. In chapter 8 the synthesis, characterization, and first reactivity studies of a highly reduced cobalt complex with an α-diimine ligand is discussed. The final chapter 9 summarizes the results of this thesis and gives a brief outlook.

Table of Contents

1 The Chemistry of Mononuclear Phosphane and N-Heterocyclic Carbene Nickel(I) Complexes: Synthesis, Structural Motifs, and Reactivity

1.1 Introduction

Although the importance of nickel(I) species in catalytic cycles has been recognized early,[1] much of the literature pays particular attention to the chemistry of nickel(0) compounds.[2] By contrast, nickel(I) chemistry has remained less developed. Monovalent nickel species play a key role in many enzymatic processes.[3] For example, methyl-coenzyme M reductase (MCR) contains the coenzyme F430 with a nickel(I) center as part of its active site, which catalyzes the conversion of methyl-coenzyme M and coenzyme B into methane and the heterodisulfide of coenzyme M (HS-CoM) and coenzyme B (HS-CoB) (Chart 1, left).[4] Isotopic exchange experiments and ESR studies indicate the formation of a σ-alkane-nickel complex as intermediate in this process.[5] Moreover, the active site of CO dehydrogenase/acetyl-coenzyme A synthase, the so-called A-cluster, possesses a three-coordinate nickel(I) ion, which reversible coordinates carbon monoxide before its methylation to yield the acetyl group (Chart 1, right).[6]

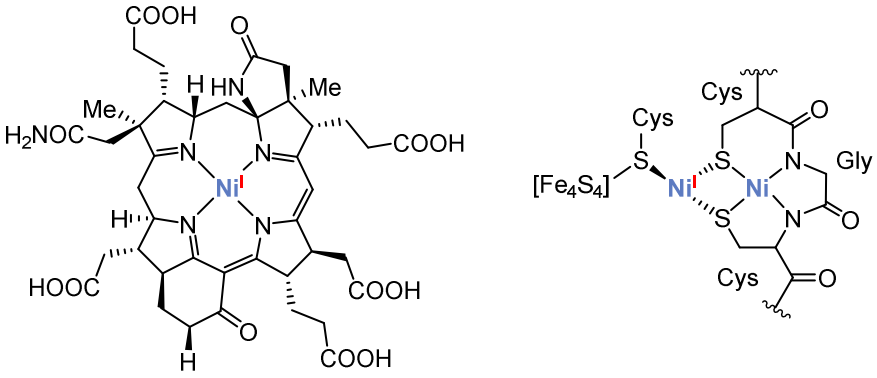

Chart 1. Cofactor F430 (left) and A-cluster of acetyl-coenzyme A synthase (right).

In recent years, the chemistry of nickel(I) has undergone a significant upsurge, taking it from a proposed oxidation state of importance[1,7] to one that has been thoroughly investigated in relation to both stoichiometric and catalytic transformations.[8] Moreover, nickel(I) compounds such as the first structurally characterized nickel(I) monomer **I** supported by a macrocyclic nitrogen donor ligand (Scheme 1, left) are of much current interest as enzyme model complexes (*vide supra*).[9,10] Another important class of compounds are nickel(I) β-diketiminato (or "nacnac") complexes,[11] which can exhibit high reactivity toward element−element (element = O, S, Se, Te, P) bonds, such as the dimeric β-diketiminato nickel(I) complex **II** (Scheme 1, right). Remarkably, the reaction of **II** with white phosphorus (P_4) yields the dinuclear complex **III**, in which the P_4 ligand shows a rare η^3-coordination to each nickel center and the metal ions remain monovalent.[12]

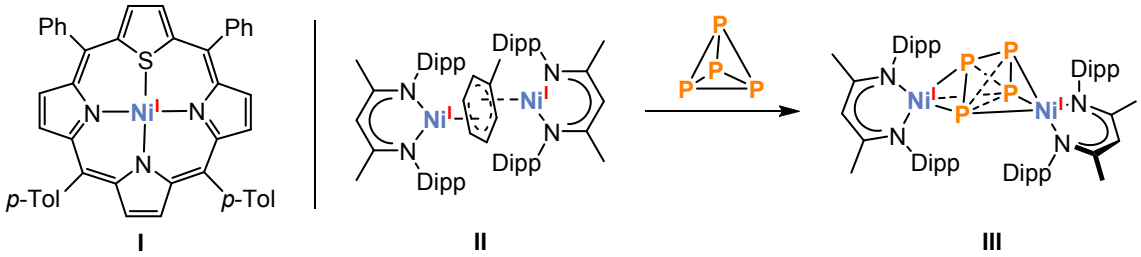

Scheme 1. Example for a mononuclear nickel(I) macrocycle (**I**, left) and reactivity of the dimeric β-diketiminato complex **II** toward white phosphorus (right); *o*-Tol = *ortho*-tolyl, Dipp = 2,6-diisopropylphenyl.[9,12]

A vast number of oligonuclear complexes with Ni(I)−Ni(I) bonds or interactions have been stabilized by various ligands, e.g. guanidinato, α-diimines, pincer ligands, and thioethers. Such oligonuclear, nickel-nickel-bonded complexes are beyond the scope of this review, however.[13]

In the past, the chemistry of 4d and 5d metal NHC and phosphane complexes has been extensively investigated.[14,15] Because of their intrinsically poor availability, the concomitant economic costs, and the high toxicity of the heavy metals, it is of high importance to develop new procedures using 3d metal complexes. As one of the earth-abundant metals, nickel is a promising candidate in this regard.

Due to our primary interest in NHC nickel(I) monomers, it is the aim of the introductory chapter of this thesis to give an overview of the dynamically emerging field of mononuclear NHC nickel(I) complexes. The chemistry of these compounds has evolved from that of the related nickel(I) phosphane compounds, and therefore, is closely intertwined. This review will try to highlight the analogies and differences between and within these two classes. In this paper, we will categorize the known monomeric phosphane and NHC nickel(I) complexes. After a brief introduction about synthetic access strategies, this work will discuss phosphane nickel(I) halides and related cationic nickel(I) complexes with weakly coordinating counteranions, followed by phosphane complexes with ancillary N-donors, pincer complexes, phosphane complexes with additional S-donors, and a brief section on piano-stool hydrocarbyl complexes. Finally the chemistry of NHC nickel(I) complexes will be described.

1.2 General Synthetic Access

Various methods have been described for the preparation of nickel(I) compounds, which generally can be subdivided in four different synthetic access routes (Scheme 2). The first mononuclear nickel(I) complexes were described in 1964 by Heimbach.[16] Remarkably, he reported three different preparation methods for the compounds of type $[NiX(PPh_3)_3]$ (**1a**, X = Cl, Br, I, Chart 2) in his publication, each of which still is applied these days. For example, the oxidation (**A**) of the nickel(0) complex $[Ni(PPh_3)_4]$ with elemental halides (Cl_2, Br_2, I_2) afforded compounds of type **1**. Nickel(I) complexes **1** are also formed in the comproportionation (**B**) of the nickel(II) salts $[NiX_2(PPh_3)_2]$ (X = Cl, Br, I) with $[Ni(PPh_3)_4]$. This represents one of the most used methods nowadays due to the good access to suitable nickel(II) and nickel(0) precursors,

many of which are commercially available. The third route reported by Heimbach (**C**) is the reduction of the nickel(II) compound $[(\eta^3\text{-allyl})NiBr]_2$ by PPh_3, affording $[NiBr(PPh_3)_3]$, although the mechanism is rather unclear. More commonly applied reducing agents for the synthesis of nickel(I) compounds from nickel(II) halides are hydrides, e.g. $NaBH_4$, and electropositive metals such as sodium or potassium.

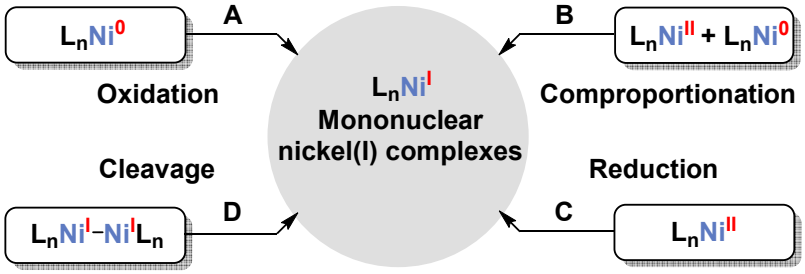

Scheme 2. Common synthetic routes toward mononuclear phosphane and NHC nickel(I) compounds.

Another method (**D**) was discovered by the group of Hoberg and coworkers in 1985. Cleavage of the dimer $[Ni(1,5\text{-cod})I]_2$ (1,5-cod = 1,5-cyclooctadiene) is observed when sterically demanding phosphanes are introduced, forming complexes $[NiI(PCy_3)_2]$ (**2c**) and $[Ni(1,5\text{-cod})I(PPh_3)]$ (**3**, Chart 2).[17] Sterically demanding ligands prevent metal-metal bond formation. Although its molecular structure was not determined at the time, complex **3** was characterized by elemental analysis, infrared spectroscopy, and its magnetic moment, which gives credence to the presence of a mononuclear structure.

1.3 Nickel(I) Phosphane Complexes

1.3.1 Mononuclear Phosphane Nickel(I) Halides and Related Cationic Nickel(I) Complexes with Weakly Coordinating Counteranions

The early coordination chemistry of nickel(I) was dominated by phosphane-stabilized halide compounds such as the type **1** complexes first synthesized by Heimbach (Chart 1). Related compounds have been prepared by many other groups after Heimbach's discovery.[18,19] The general structure motif of complexes **1** was first revealed in 1974 by the single crystal X-ray structure of [NiI(triphos)] (**1c**), Chart 2, triphos = 1,1,1-tris(diphenylphosphinomethyl)ethane) reported by Sacconi and coworkers.[20]

Furthermore, cryoscopic weight determinations by Heimbach indicated the dissociation of one phosphane ligand in complexes **1a**, yielding structures of type $[NiX(PPh_3)_2]$ (**2a**) in solution.[16] He also obtained complexes of type **2a** by comproportionation of $[NiX_2(PPh_3)_2]$ and $[(\eta^2\text{-}C_2H_4)Ni(PPh_3)_2]$. Besides **2a**−**2c**[21] bearing monodentate phosphanes, related complexes are also known with bidentate ligands (**2d**−**2h**, Chart 2).[22]

Very recently, Fink, Eichhöfer *et al.* investigated complexes **1a** (X = Cl), **2a**, and **21** (Chart 4) by experimental (X-ray diffraction and magnetic measurements) and theoretical methods (DFT).[23] Their structural analysis revealed Y-distorted structures for the trigonal planar complexes **2a** and

21, which is not only caused by Jahn-Teller-distortion but also by π-π interactions of the phenyl groups bound to the phosphane ligand. In addition, their DFT calculations and magnetic measurements showed a small magnetic anisotropy for compounds **2a** and **21**. Moreover, slow magnetic relaxation at low temperatures indicated single-molecule magnet behavior.

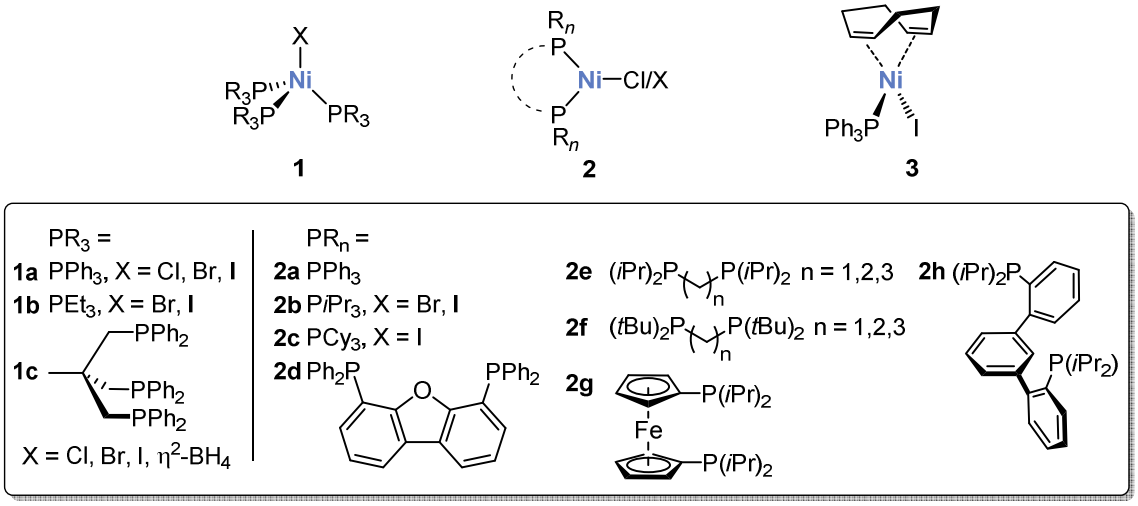

Chart 2. Monomeric phosphane nickel(I) complexes.[18–27]

One of the first reactivity studies was done by the group of Royo, who reacted complexes **1a** (X = Cl, Br, I) with carbon monoxide and obtained compounds with the composition $[NiX(CO)_2(PPh_3)_2]$ (**4**). These complexes were characterized by elemental analysis, infrared spectroscopy, and the determination of their magnetic moments in solution (2.0 − 2.3 μ_B).[24]

In the 1980s, the attention focused increasingly on mechanistic aspects in the context of nickel catalyzed coupling reactions, in particular the oxidative addition of alkyl and aryl halides to the metal center. These investigations showed that a radical mechanism involving nickel(I) intermediates might play a key role in nickel(0) and nickel(II)-based conversions.[1,25]

Complexes **1a** and **2a** were found to act as precatalyst in *cis*-isomerization reactions, such as the conversion of 1-butene to *cis*-2-butene. The active catalyst was presumed to be a nickel(II) hydride species as a result of a hydrogen abstraction from the olefin by the nickel(I) complex.[21a,26]

More recent work by Lu and coworkers showed that the three-coordinate complex **2d** readily reacts with vinyl halides, forming a nickel(II) dihalide and the corresponding vinyl nickel(II) complex in a 1:1 ratio through the homolytic cleavage of the carbon halide bond.[22c] Complex **2d** proved to be catalytically active in Kumada cross coupling reactions of vinyl chloride and phenyl Grignard reagents. Very recently, Hazari *et al.* showed that the related complex **2g** is an active catalyst in Suzuki-Miyaura couplings.[27]

Although the molecular structure of complex **2f** (n = 2) has been unambiguously determined to be dimeric in the solid-state, mass spectrometric data showed molecular ion peaks of monomeric complexes for the related compounds **2e** (n = 2, 3) (Chart 2), which indicates the presence of easily cleaved dimers.[21b,28] In any case, complex **2f** (n = 2) has proven to act as an extraordinarily

versatile starting material for the preparation of all different types of monomeric nickel(I) compounds (Scheme 3). Complex **2f** is readily accessible by reducing the respective nickel(II) dichloride with potassium graphite.

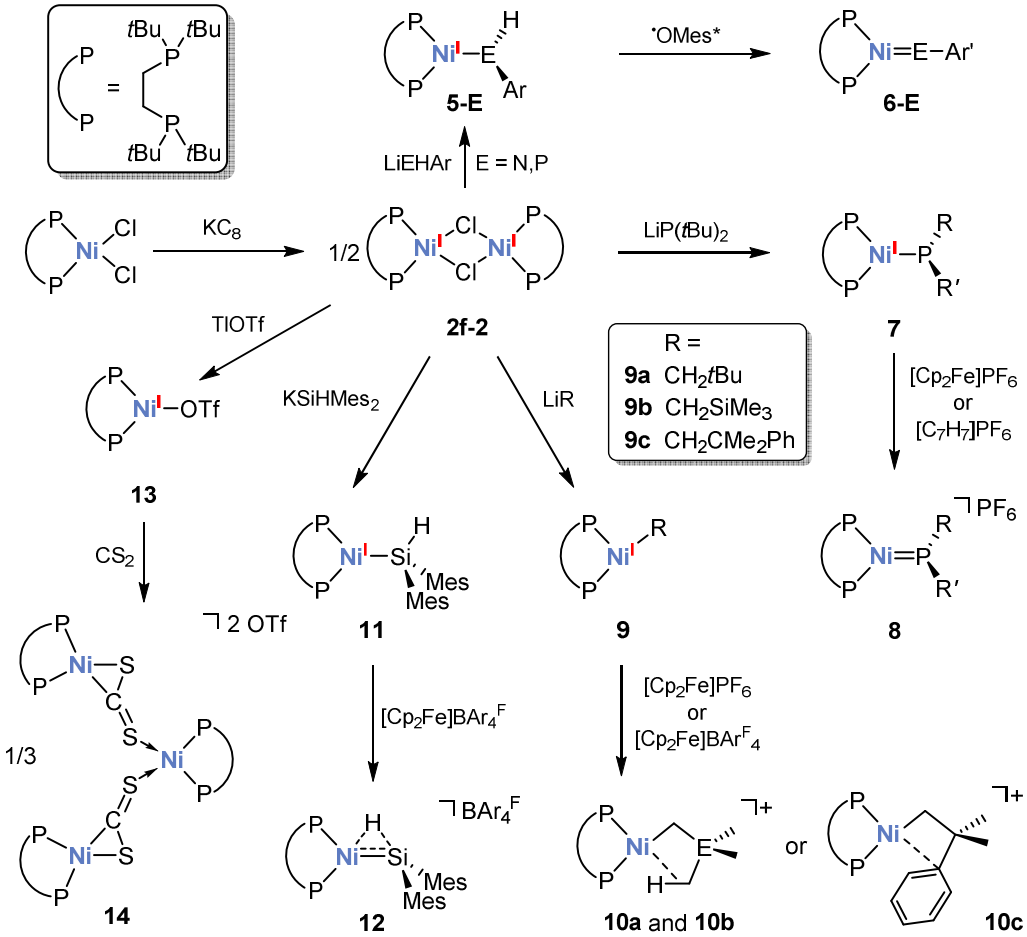

Scheme 3. Synthesis of nickel(I) monomers through salt metathesis reactions with the nickel(I) dimer **2f** (Ar = Dipp, dmp 2,6-bis(2,4,6-trimethylphenyl)phenyl); Mes = 2,4,6-trimethylphenyl; R = R' = *tert*-butyl; R = H, R' = dmp; Mes* = 2,4,6-tris(*tert*-butyl)phenyloxyl.[28–33]

Starting in 2001, Hillhouse *et al.* demonstrated that route **D** (Scheme 2) offers a versatile and powerful method for the synthesis of nickel(I) monomers by introducing sterically demanding ligands by salt metathesis of the dimeric nickel(I) halide **2f** with s-block metal amides, phosphides, and alkyls, potassium dimesitylsilanide, and thallium triflate (Scheme 3). Amide and related phosphide complexes **5-E** are formed in the reaction of the appropriate lithium amide/phosphide and **2f**. Interestingly, H-atom abstraction from **5-E** resulted in the formation of rare imide and phosphinidene complexes (**6-E**).[29] A similar reactivity was also observed with Li*P*t*Bu*$_2$, which gave access to complex **7** (Scheme 3). Subsequent oxidation with either ferrocenium or tropylium hexafluorophosphate formed the nickel(II) phosphinidene **8**. Another example is the synthesis of the T-shaped complexes **9** by reacting **2f** with lithium alkyls (Scheme 3).[30] The one-electron oxidation of complexes **9** gave the cations **10a**−**c** featuring intramolecular Ni-C−H bond interactions. While the cationic amido and phosphido complexes **5-E** undergo α-

deprotonation to afford imido and phosphinidene derivatives, the addition of a Brønsted base to **10a**−**c** resulted in γ-deprotonation of a methyl group, affording nickelacyclobutanes.

Hillhouse *et al.* isolated the Y-shaped nickel(I) monomer **11** by reaction of **2f** with $KSiHMes_2$ (Scheme 3). One-electron oxidation of **11** gave complex **12** with an unusual 3-center-2-electron bond between Ni, Si, and the bridging H bonding as an outcome of the partial 1,2-H migration from silicon to nickel.[31]

According to Scheme 3, nickel(I) triflate **13** can be accessed by reacting **2f** with TlOTf.[32] Complex **13** readily reacts with carbon disulfide yielding the unprecedented trinuclear complex **14**, where two nickel(II) centers and one nickel(0) center are present.[33]

Another access to nickel(I) alkyl complexes was found very recently by the Hillhouse group in the conversion of the nickel(0) carbene complex **15** with $[Cp_2Fe]BAr^F_4$, leading to the cation **16** as a result of an unusual intramolecular rearrangement (Scheme 4).[34] Initiated by the oxidation, the carbene atom is probably attacked by one of the phosphorus atoms of the bidentate ligand, forming **16**. The metal center in **16** displays an additional η^2-interaction with the mesityl substituent.

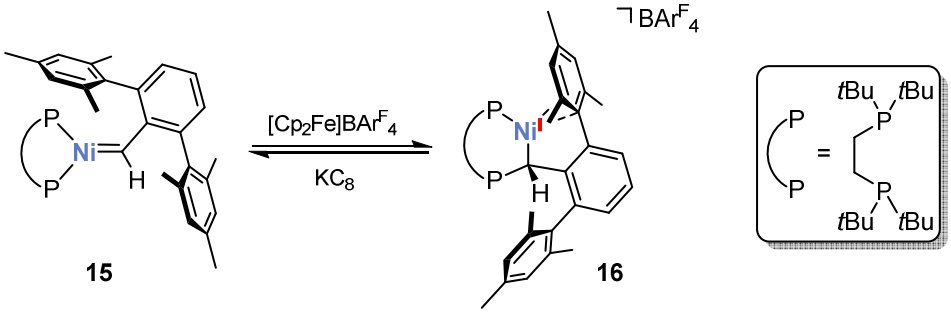

Scheme 4. Synthesis of the nickel(I) cation **15**.[34]

The first cationic nickel(I) monomer **17a** was synthesized by Klein, Dartiguenave, and coworkers (Chart 3).[35] Initially, Klein *et al.* attempted to synthesize complexes of type $[NiX(CH_3)(PMe_3)_4]$ starting from the nickel(II) (pseudo)halides $[NiX(CH_3)(PMe_3)_2]$ (X = Cl, Br, I, NCS) and two equivalents of PMe_3, followed by salt elimination with $NaBPh_4$. Interestingly, cation **17a** was obtained as a result of methyl radical elimination. Analogous complexes with bidentate ligands have also been prepared by the reducing nickel(II) precursors of type $[Ni(L)_2]^{2+}$,[36] or the comproportionation of nickel(II) compounds of type $[Ni(L)_2]^{2+}$ and nickel(0) compounds $(Ni(L)_2)$.[37]

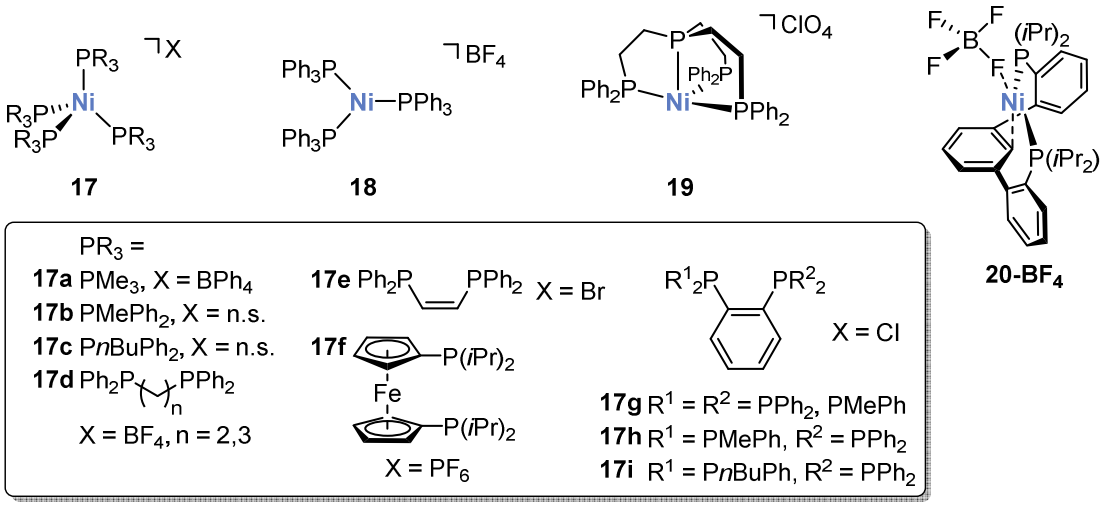

Chart 3. Cationic nickel(I) monomers with weakly coordinating anions.[35–41]

The unique tris(phosphane) complex **18** was isolated by reacting $[Ni(PPh_3)_4]$ with $BF_3{\cdot}OEt_2$ and extensively investigated by EPR spectroscopy.[38] Complex **18** was found to be the active species in the styrene oligomerization catalyst system $[Ni(PPh_3)_4]/BF_3{\cdot}OEt_2$.[39] The related trigonal pyramidal complex **19** was obtained by oxidation of $[Ni(\eta^2\text{-}C_2H_4)(PPh_3)_2]$ with $[C_3Ph_3]ClO_4$ in the presence of the tetradentate ligand $P(CH_2CH_2PPh_2)_3$.[40]

Recently, the group of Agapie prepared cation **20-BF$_4$** by reacting **2h** with $NaBF_4$. Interestingly, the BF_4^- ion in complex **20-BF$_4$** strongly interacts with the nickel(I) ion.[41]

1.3.2 Mononuclear Nickel(I) Phosphane Complexes with Ancillary N-Donors

Nickel(I) phosphane complexes with additional N-donor ligands are the structurally most versatile subclass of nickel(I) monomers. A variety of complexes are known (Chart 4) which comprise oligodentate P,N ligands or a phosphane and a separate N-donor ligand, e.g. an amide ligand. The nickel atoms assumes coordination numbers ranging from two to five in these complexes.

The first example of this subclass, three-coordinate complex **21**, was synthesized by Bradley, Hursthouse and co-workers upon converting $[NiCl_2(PPh_3)_3]$ with two equivalents $LiN(SiMe_3)_2$ in 1972.[42] Although the authors did not comment on the reaction mechanism, they demonstrated the generality by using a range of different phosphanes. A few years later, Sacconi and coworkers synthesized complexes of type **22** by reacting divalent nickel(II) halides and $NaBH_4$ with the tetradentate ligand $N(CH_2CH_2PPh_2)_3$.[43] **22-CN** was prepared by adding sodium cyanide to **22-I**.

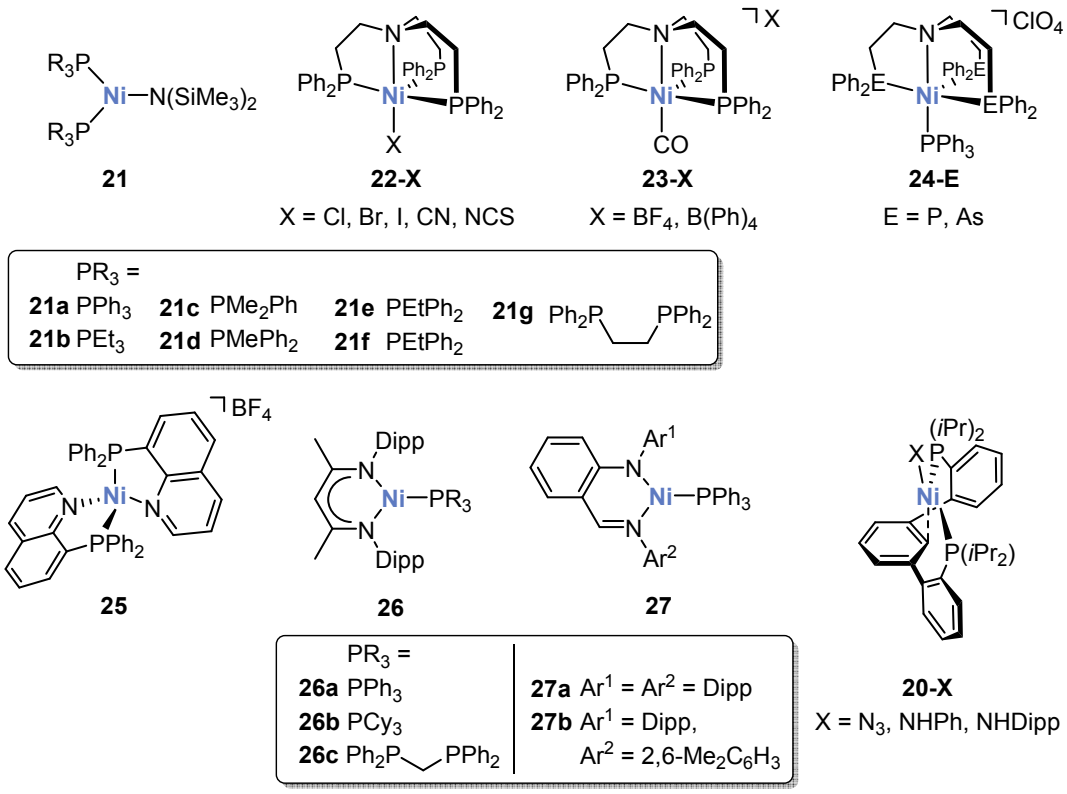

Chart 4. Nickel(I) monomers with ancillary N-donors.[42–46]

Related complexes **23** are accessible in a similar manner using CO instead of $NaBH_4$. Complexes **24-E**, bearing an additional PPh_3 ligand, were synthesized in an analogous procedure as for **19** (Chart 3) by reacting $[Ni(\eta^2\text{-}C_2H_4)(PPh_3)_2]$ with $[C_3Ph_3]ClO_4$ in the presence of $N(CH_2CH_2EPh_2)_3$ (E = P, As).[40] The metal atom in cation **25** adopts a distorted tetrahedral environment with a quinoline derivative as donor-ligand. Complex **25** was recently synthesized by the group of Takagi upon reduction of the corresponding, dicationic nickel(II) complex with zinc powder.[44]

In the context of the extensive investigations of low-valent β-diketiminato nickel(I) complexes,[11] phosphane-supported nickel(I) monomers were isolated. For example, complexes **26a** and **27**, possessing a T-shaped structure, are formed from $[NiCl(Ph)(PPh_3)_2]$ and the lithium β-diketiminate salt.[45] Stephan *et al.* synthesized the related complexes **26b** and **26c** by adding phosphanes to the dimeric precursor $[HC\{C(Me)NDipp\}_2Ni]_2$(toluene).[46] Compounds **26a** and **27** catalyze norbornene polymerization to afford addition-type polynorbornene after being activated with methylaluminoxane.[45]

Salt metathesis of **20-Cl**, bearing the *meta*-terphenyl diphosphine *m*-P_2, with NaN_3, LiNHPh and LiNHDipp afforded **20-X** (Chart 4).[41] Attempts to abstract a hydrogen atom from the amido complexes **20-NHPh** and **20-NHDipp** (in a similar fashion as in the work of Hillhouse with compounds **5-E**, Scheme 3) resulted in the formation of mixtures of the mono- and bis-Staudinger oxidation products of the free ligand *m*-P_2 (phosphoranimine) and the nickel(0) complex [(*m*-

P_2)Ni]. The formation of the latter complex indicates the presence of the desired imido nickel(II) complex as intermediate species.

The electronically unsaturated nickel(I) monomer **29** was synthesized by Hor *et al.* upon reacting the nickel(II) precursor **28** with MeLi (Scheme 5).[47] Complex **29** features a hemilabile imino moiety, which slips to an η^2-coordination by treatment with $AlMe_3$ or MAO (methylaluminoxane). Moreover, compounds **29** and **30** catalyze ethylene oligomerization using MAO (Al/Ni ratio of 1000) as cocatalyst with turnover numbers of 21000 (**29**) and 14666 (**30**).

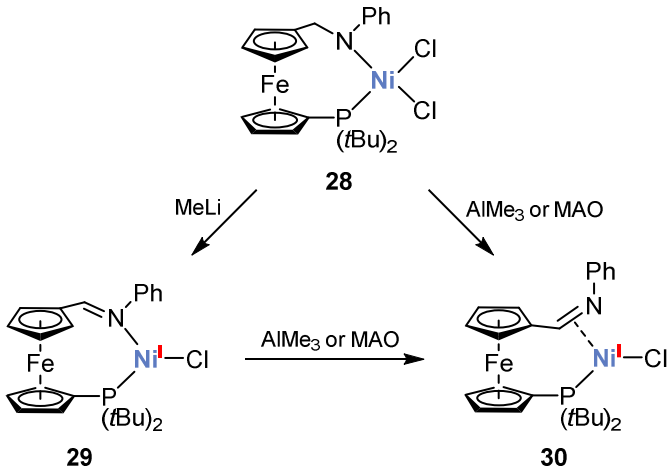

Scheme 5. Synthesis of the imino complex **29** and **30**; MAO = methylaluminoxane.[47]

The first structurally characterized σ-alkyl nickel(I) complex **31** was isolated by Eaborn, Smith *et al.* in 2000 by reacting [$NiCl_2(PPh_3)_2$] with Li{$C(SiMe_3)_2(SiMe_2C_5H_4N)$} (Chart 5).[48] Compound **31** displays a T-shaped structure, where nickel is also coordinated by a pyridine moiety and triphenylphosphane. The mechanism of the formation of **31** could not be fully elucidated, but it is likely that the reaction involves an intermediate alkyl nickel(II) chloride, which is reduced by another molecule of the lithium salt, yielding **31**.

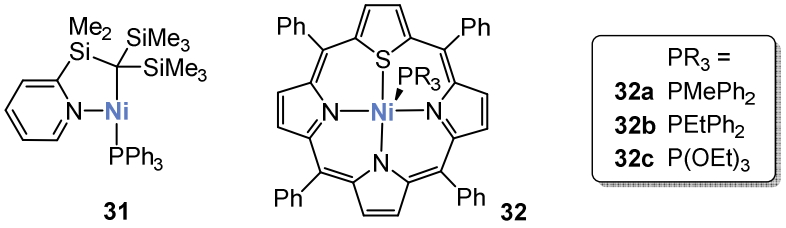

Chart 5. Nickel(I) monomers with ancillary N-donors.[48,49]

Five-coordinate complexes **32** were obtained from the reaction of [Ni(STPP)] (STPP = tetraphenyl-21-thiaporphyrin) with $PMePh_2$, $PEtPh_2$, and $P(OEt)_3$.[49] The molecular structure of **32** was not determined, but EPR measurements indicated a five-coordinate nickel(I) macrocycle

with relatively large ^{31}P superhyperfine coupling constants of A^P = 0.0124 to 0.0133 cm^{-1}. According to the EPR data, spin density is present on the metal and the ligand.

The group of Kraikivskii reported a coordination induced homolytic Ni−C bond cleavage of the imine-amide complex **34** (Scheme 6). Reaction of the nickel(II) allyl compound **33** with PMe_3 affords the five-coordinate nickel(II) species **34**, which spontaneously gives nickel(I) complex **35** and cyclohexene as the cyclodimerization product of two allyl radicals.[50] Unfortunately, the isolated nickel complexes are X-ray amorphous, but they were studied by EPR and 2D NMR techniques.

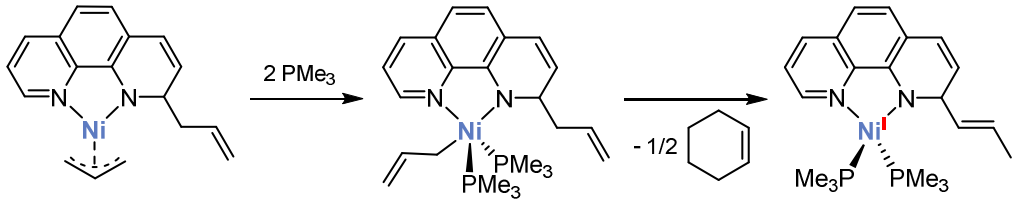

Scheme 6. Nickel(I) monomer formation through coordination induced Ni−C bond cleavage.[50]

Very recently, the group of Tilley presented the synthesis of unique two-coordinate phosphane nickel(I) complexes [(L)Ni(N(Dipp)($SiMe_3$))] (**86**, tBu_3P, iPr_3P, $Ph_2P(CH_2)_2PPh_2$) and compared their reactivity toward the phenol derivative 2,6-tBu_2-4-Me-C_6H_2OH with their NHC analogue (Scheme 20, chapter 1.3).[51]

1.3.3 Pincer Complexes

Pincer complexes with P- and N-donor functions are an important subclass of nickel(I) compounds, which were only recently discovered. In 2008, the groups of Mindiola prepared the dinuclear nickel(I) complex **37** by reduction of **36-Cl** with potassium graphite (Scheme 7).[52] Single-crystal X-ray diffraction revealed that the Ni-atoms are bridged by the N-atom of the pincer ligands. In addition, solid-state magnetization and solid-state EPR spectroscopic data are consistent with an equilibrium between a monomer and a dimer in solution. An S = 0 ground state with a low-lying S = 1 excited state was determined for the dimer. The radical nature of complex **37** was further proven by reactions with H−X (X = H, OH, OMe, PHPh, and B(catechol)) and X−X bonds (X = B(catechol), SPh, and SePh), which yielded homolytic bond cleavage products (**36-X**/**36-H**). The three-coordinate complex **38** was obtained through insertion of the terminal nitrogen of diphenyl diazomethane into a P−Ni bond of **37**. It was presumed that the insertion more likely occurs from the monomeric species.

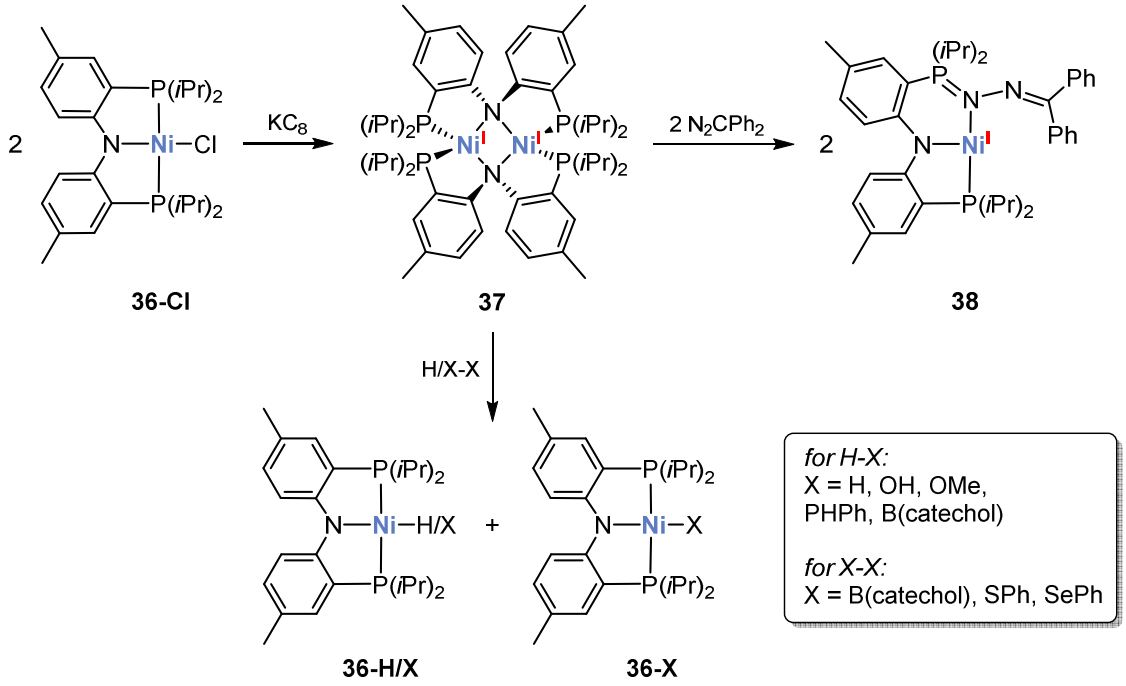

Scheme 7. Synthesis of the nickel(I) pincer complexes **37** and **38**.[52]

In the same year, Caulton *et al.* reported the synthesis of compound **40** by converting the nickel(II) halide **39** with an excess of elemental magnesium (Scheme 8).[53] Complex **40** reacts rapidly with CO_2 at low temperatures and in a very selective fashion to yield complex **41**, in which the oxygen of CO_2 is transposed with the amide N.

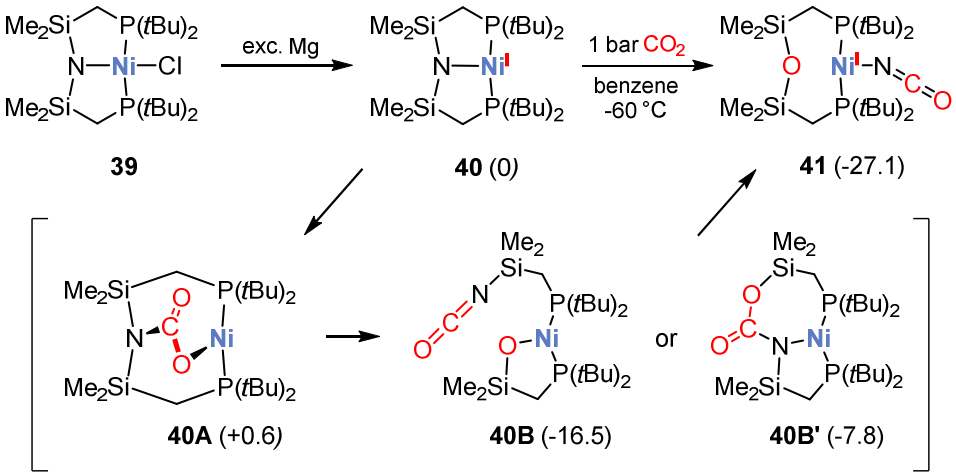

Scheme 8. Synthesis and reactivity of **40** toward CO_2 and postulated intermediates with their relative, DFT-calculated electronic energies (kcal/mol) compared to free **40** and CO_2 in parenthesis.[53]

Reaction of **40** with CO_2 affords the cyanate complex **41**. Interestingly, the oxidation state of the nickel(I) center did not change. Similar to **40**, **41** has a T-shaped structure. An electron transfer from nickel to the substrate occurs at some point in the reaction, which leads to an increased nucleophilic character of oxygen in CO_2. DFT calculations indicate that the reaction is

presumably initiated by the insertion of one C=O double bond of CO_2 into the Ni−N bond to produce **40A** (Scheme 8). Subsequently, the intermediate **40B** with a cyanate group bound at Si is formed under C−O and N−Si bond cleavage as well as Si−O bond formation. The cyanate moiety is subsequently transferred to the nickel center, yielding **41**. Another possible pathway, though energetically less favored according to the DFT calculations, involves the intermediate **40B'**, formed through insertion of the C=O double bond of **40A** into one Si−N bond, which subsequently gives **41**.

Pincer complexes are of significant interest as model complexes for the three-coordinate nickel(I) ion in the A-cluster of CO dehydrogenase/acetyl-coenzyme A synthase (*vide supra*). For example, the group of Lee explored the reactivity of pincer complex **42-CO** toward alkyl iodides and observed the first methylation of a nickel(I) compound giving a nickel acetyl complex (Scheme 9).[54] In the 1:1 reaction of **42-CO** with methyl iodine the formation of 50% of complex **42-I** (relative to **42-CO**) and a mixture of compounds **43** and **44** (R = Me, 37%:13%) was observed. Complexes of type **43** (R = *i*Pr, *t*Bu) are predominantly formed with sterically more demanding alkyls such as *iso*-propyl or *tert*-butyl groups, while **44** was not detected with these residues. DFT calculations indicate that the mechanism involves an initial alkyl radical abstraction with concomitant iodine radical generation. In addition, these calculations suggests that the direct C−C coupling is mainly responsible for the formation of main product **43**; its formation through migratory insertion of a CO ligand from the five-coordinate intermediate **42-COR** appears energetically less favored. Coupling of the alkyl radical with the nickel(I) center (Ni−C coupling) to form **42-COR** with subsequent loss of CO seems to be the main access route for compound **44**.

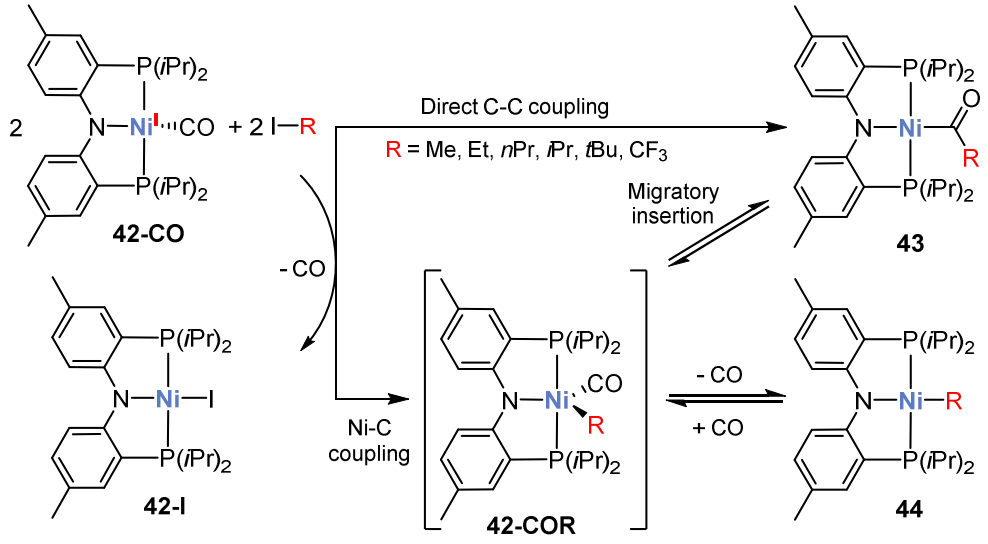

Scheme 9. Reactivity of **42-CO** toward alkyl radicals.[54]

1.3.4 Mononuclear Nickel(I) Complexes with Additional S-Donor Ligands

Alkyl radical formation is also important in the context of the enzyme methyl-coenzyme M reductase (*vide supra*), in which a nickel-promoted C−S bond cleavage of the substrate takes place.[4,55] Interestingly, the S-ligated nickel complex **45** produces methyl radicals upon irradiation

with visible light for 30 minutes, which recombine to ethane. The intermediate nickel(I) species **46** was detected by EPR spectroscopy (Scheme 10).[56] When solutions of **45** were irradiated for prolonged times, the formation of nickel(II) compound **47** was observed. Complex **46** decomposes at room temperature, and therefore, could not be fully characterized.

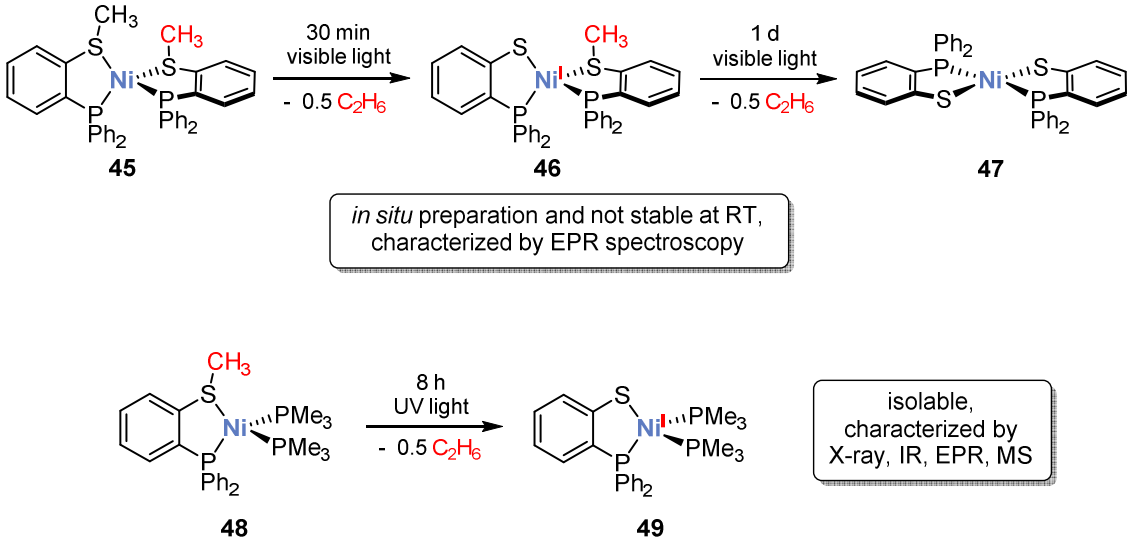

Scheme 10. Methyl radical formation of the nickel(0) complexes **45** and **48**.[56,57]

A similar reactivity was observed when the nickel(0) complex **48** was irradiated with UV light for eight hours to form **49**.[57] In contrast to the formation of **46**, complex **49** can be isolated and was described as thermally stable up to 42 °C. The formation of **49** from **48** formally proceeds via elimination of methyl radicals. Although ethane was not detected in this case, it is likely one of the products of this elimination reaction.

The group of Riordan obtained the nickel(I) complex **51** in the reaction of **50** with MeLi by trapping an *in situ* formed nickel species with PMe_3 (Scheme 11). Methyl radical formation was not proven in this case.[58]

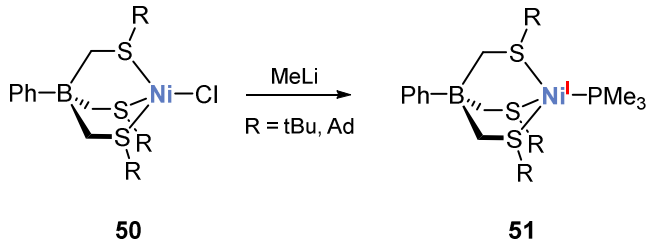

Scheme 11. Synthesis of complex **51**.[58]

The five-coordinate monovalent nickel species **53** synthesized by Holm *et al.* has been applied in the evolution of dihydrogen from protons (Scheme 12).[59] Complex **53** features a distorted trigonal bipyramidal structure and can be prepared by electrochemical or chemical reduction of the respective dication **52**. Interestingly, **53** was found to produce dihydrogen in almost quantitative amounts upon treatment with one equivalent of a Brønsted acid such as HCl in diethyl ether/DMF.

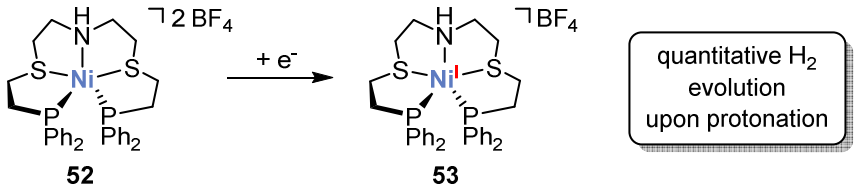

Scheme 12. Five-coordinate nickel(I) complex **53**.[59]

Phosphane-stabilized nickel(I) monomers with monodentate thiolate ligands are rather scarce. Tatsumi and coworkers showed that even very small changes at the ligand can have a huge influence on the reactivity.[60] Conversion of the monovalent nickel amide **21** with an *m*-terphenylthiol afforded the dinuclear complex **54** under elimination of the free amine (Scheme 13). By use of a slightly sterically more encumbering thiol carrying mesityl instead of xylyl groups, they isolated the nickel(I) monomer **55**. Its radical nature was shown by trapping **55** with the presistent radical TEMPO, yielding the square planar nickel(II) complex **56**.

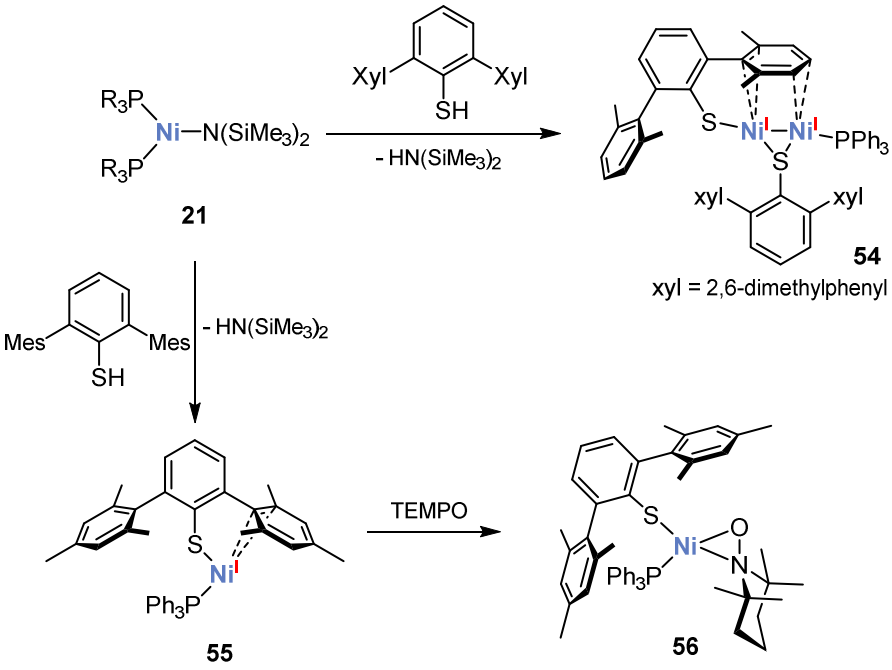

Scheme 13. Preparation of the dinuclear complex **54** and the monomer **55**, and its reactivity toward TEMPO.[60]

1.3.5 Piano Stool Complexes with Cyclobutadiene and Cyclopentadienyl Ligands

The chemistry of half-sandwich nickel(I) monomers is less-well developed in comparison with the substance classes mentioned before, probably due to the extraordinarily labile nature of half-sandwich nickel(I) compounds and their tendency to aggregate via Ni-Ni bond formation.[61] The first half-sandwich nickel(I) complex **57c** was isolated as early as 1974 by Uhlig and Walther from the reaction of nickelocene (Cp_2Ni) and PPh*n*Bu_2 (Chart 6).[62] Complex **57c** was also synthesized by converting Cp_2Ni with [Ni(PPh*n*Bu_2)$_4$] via comproportionation.

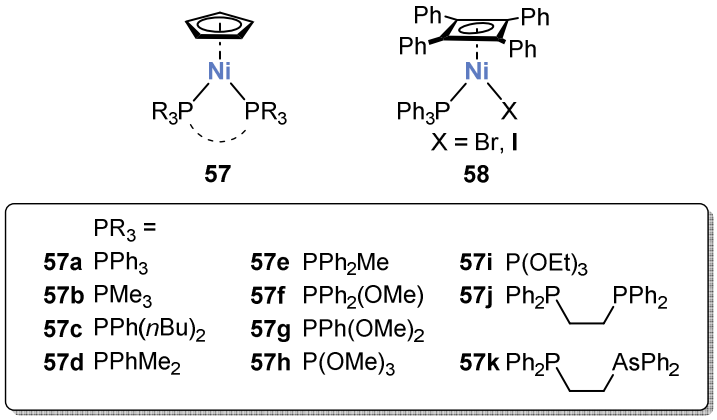

Chart 6. Half-sandwich nickel(I) complexes.[62–67]

Various other preparation methods for complexes of type **57** have been reported subsequently. These include the reaction of NaCp with **1a**, $[(\eta^5\text{-Cp})Ni(PR_3)_2]PF_6$, and $NiX_2(PR_3)_2$ (X = Cl, Br; probably under elimination of a Cp radical), ligand substitution of NO and CO, respectively, by an excess of phosphanes in the complexes $[(\eta^5\text{-Cp})Ni(NO)]$ and $[(\eta^5\text{-Cp})Ni(CO)]_2$,[63] and the (electro-)chemical reduction of cationic complexes of type $[(\eta^5\text{-Cp})Ni(PR_3)_2]^+$.[64] Compounds of type **57** are highly sensitive toward oxygen, thermally unstable, and they easily decompose to Cp_2Ni and $[Ni(PR_3)_4]$. A possible reason for this facile decomposition is the fact that complexes **57** easily lose one phosphane ligand in solution, forming unstable $17e^-$ radicals of type $[CpNi(PR_3)]$.[64b] Although the structures **57a-k** were not confirmed by single-crystal X-ray diffraction, their molecular structures probably exhibit a two-legged piano stool geometry with an η^5-coordinated Cp-ring similar to the related complex CpNi(bpy) (bpy = 2,2-bypiridine).[63] In this context, EPR investigations indicate the presence of nonequivalent ^{31}P nuclei of the phosphane ligands in **57i** due a slight deviation from the expected C_{2V} symmetry (Jahn-Teller distortion).[65] The sole reactivity study on a complex of type **57** was carried out by the group of Saraev.[66] They observed the substitution of the phosphane ligands in the reaction of **57a** with (di)phenylacetylene, yielding complexes $[CpNi(\eta^2\text{-}C_2PhR)_2]$ (R = H, Ph). Saraev and coworkers also showed that oligomerization of the substrate occurs when an excess of the acetylene was used. The outcome was found to be highly dependent on the applied temperature: 1,2,4-triphenylbenzene was the main product at 20 °C, the main products are linear oligomers with an average molecular weight of 1050 $g \cdot mol^{-1}$ at 40 °C.

Related tetraphenylcyclobutadiene (Cb*) complexes of type **58** (Chart 5) were prepared by reacting $[Cb^*NiBr_2]$ with sodium in the presence of PPh_3 (**58-Br**) or [Cb*Ni(1,5-cod)] with 0.5 equivalents of iodine in presence of PPh_3 (**58-I**).[67] In marked contrast to the cyclopentadienyl complexes of type **57**, the cyclobutadiene complexes **58** are thermally stable up to 192 °C (**58-Br**) and 212 °C (**58-I**), respectively. Similar to **57**, compounds **58** are extremely air-sensitive.

1.4 Mononuclear N-Heterocyclic Carbene Nickel(I) Complexes

The chemistry of monomeric NHC nickel(I) complexes started to develop in 2008.[68] Only a few publications exist to date. An important starting material for the synthesis of mononuclear nickel(I) complexes is Sigman's dimer **59**, which is accessible according to Scheme 14 by the comproportionation of Ni(1,5-cod)$_2$ and NiCl$_2$(dme) in presence of free carbene (IDipp = 1,3-bis(2,6-diisopropylphenyl)imidazolin-2-ylidene, SIDipp = 1,3-bis(2,6-diisopropylphenyl)imidazolidine-2-ylidene).[69] Hillhouse and coworkers demonstrated that the reaction of **59** with sterically encumbered s-block amides and organyls results in the formation of unprecedented two-coordinate nickel(I) compounds **60**−**63** (Scheme 14). The salt metathesis procedure is similar to that described for compound **2f** (n = 2) (Scheme 3, *vide supra*).[68,70,71]

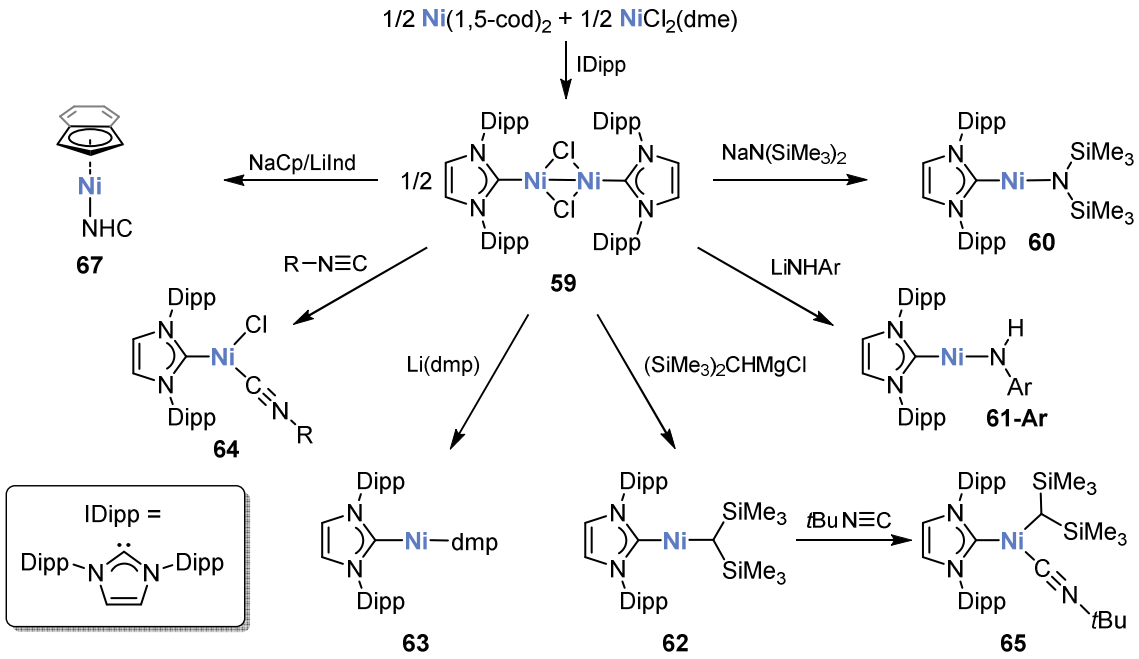

Scheme 14. Synthesis of NHC nickel(I) complexes using Sigman's dimer (**59**) (1,5-cod = 1,5-cyclooctadiene, dme = 1,2-dimethoxyethane, Ar = Dipp, dmp (2,6-bis(2,4,6-trimethylphenyl)phenyl)), dppp (2,6-bis(2,6-diisopropylphenyl)phenyl)); R = CH_2Ph, *t*Bu; Ind = Indenyl; NHC = IDipp, SIDipp.[68–71]

Furthermore, the three-coordinate complexes **64**[72] and **65**[71] were prepared by addition of isonitriles to **59** and **62**, respectively. In the reaction of **62** with primary and secondary alkyl halides, Hillhouse *et al.* found evidence for a radical mechanism for the oxidative addition of the substrate.

Reactivity studies with complexes **60** and **61-Ar** further revealed the propensity for single-electron transfer (SET), which gave unique nickel(II) complexes. For example, the oxidation of **60** with one equivalent of $[Cp_2Fe]BAr^F{}_4$ in diethyl ether resulted in the formation of iminosilane **68** with a 14e$^-$ nicke(II) center as an outcome of a β-methyl elimination from the cationic intermediate $[(IDipp)Ni(N(SiMe_3)_2)]^+$ (Scheme 15).[68]

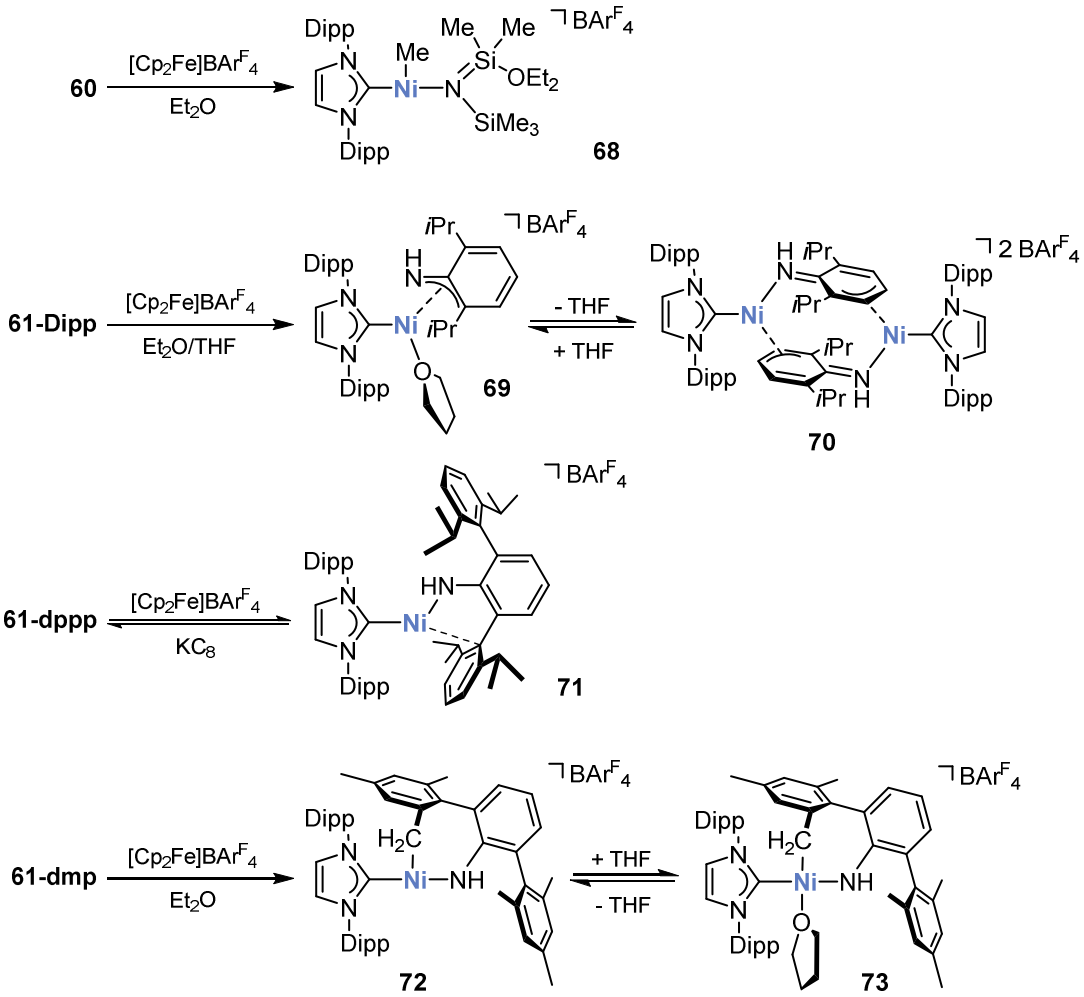

Scheme 15. Reactivity of the nickel(I) amides **60** and **61-Ar**.[68,70]

By contrast, a different reactivity was observed upon oxidation of arylamide nickel(I) complexes **61-Dipp**, **61-dppp**, and **61-dmp** (Scheme 15). One-electron oxidation of **61-Dipp** yields cation **69**, in which the nickel(II) ion is coordinated by the amide ligand in an allyl-like fashion and a THF molecule. Compound **69** reversibly rearranges to dimeric **70** when dissolved in dichloromethane. By use of a sterically encumbering *m*-terphenyl substituent, cation **71** was isolated by oxidation with $[Cp_2Fe]BAr^F_4$. The structure of **71** features an intramolecular Ni-*ipso*-carbon-interaction between nickel and one of the flanking aryl moieties. Complex **71** can be reduced with KC_8 to form **61-dppp** back.[70] Interestingly, the similarly sterically demanding complex **61-dmp** gave the low-coordinate cation **72** upon one-electron oxidation. A C−H bond activation on one *ortho*-methyl group occurred in this case to form a seven-membered nickelacycle. Complex **72** reversibly coordinates a THF molecule in a similar manner as **70**, forming square-planar **73** when dissolved in THF. These examples impressively demonstrate the ability of NHC ligands to stabilize unusual coordination modes in a very flexible way.

The group of Hazari applied Sigman's dimer **59** for the synthesis of nickel(I) monomers. Complexes of type **67** were formed by reacting **59** with one equivalent of NaCp or LiInd,

respectively (Scheme 16).[73] Interestingly, nickel(I) dimers **66** were isolated from the 1:1 reaction of **59** with NaCp and LiInd. Conversion with a second equivalent of NaCp or LiInd gave the monomeric compounds of type **67**, which represent the first examples of 17e⁻ nickel(I) species bearing cyclopentadienyl or indenyl ligands. In marked contrast to phosphane complexes **57** (Chart 5), which undergo facile dissociation of one phosphane ligand and concomitant disproportionation, complexes **67** are indefinitely stable under an inert gas atmosphere.

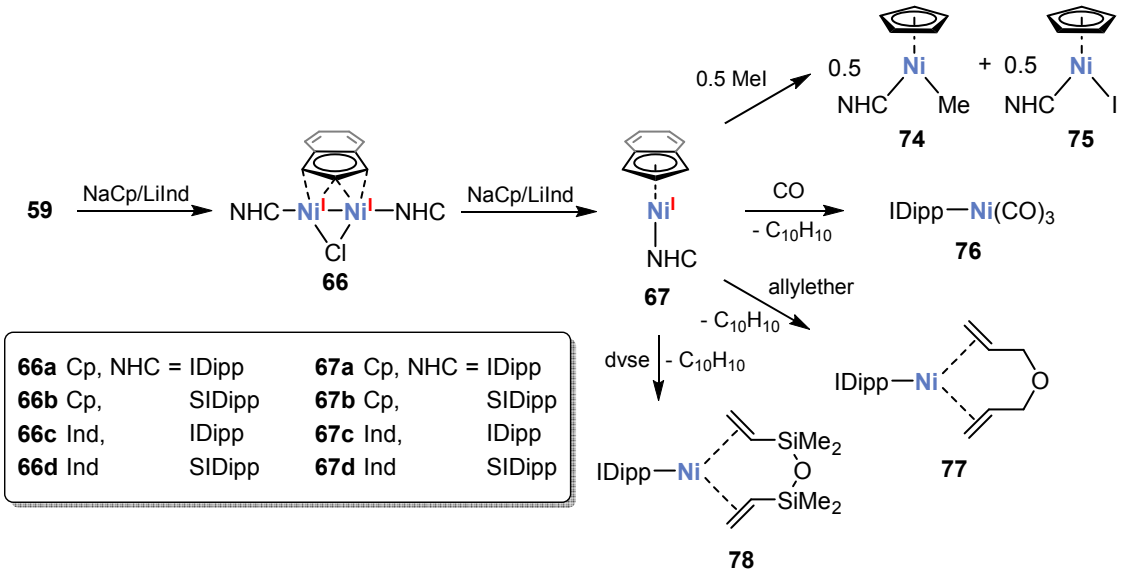

Scheme 16. Synthesis of dimers **66** and monomers **67**; NHC = IDipp, SIDipp; dvse = dimethyl silyl ether.[73]

Representatively, the stoichiometric reactivity of **67a** toward mild oxidizing and reducing agents was tested. Complex **67a** homolytically cleaves the C−I bond of MeI to afford the nickel(II) complexes **74** and **75**, while the reaction with CO affords the nickel(0) complex **66** together with dicyclopentadienyl ($C_{10}H_{10}$). Upon conversion with dvse (dimethyl silyl ether) and allylether, nickel(0) bisalkene complexes **77** and **78** were fomed. Furthermore, complexes **63** are precatalysts for the Suzuki-Miyaura coupling of phenylboronic acid and *p*-chlorotoluene.

Homolytic cleavage of carbon halide bonds by low-valent nickel compounds was used to synthesize T-Shaped nickel(I) complexes. As shown in Scheme 17, monomer **80** was prepared by reacting the two-coordinate zerovalent nickel complexes of type **79**,[74] bearing sterically demanding NHC ligands, with aryl halides.[75] Three-coordinate complexes **80** are active catalysts for Kumada and Suzuki cross-couplings as well as Buchwald-Hartwig aminations.

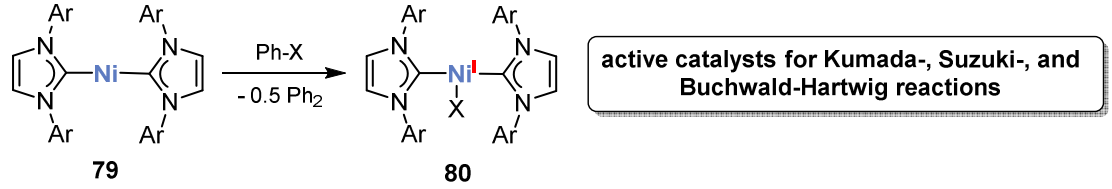

Scheme 17. Synthesis of catalytically active NHC nickel(I) compounds **80**; Ar = Dipp, Mes, X = Cl, Br, I.[74,75]

Another example for a coordinatively unsaturated nickel(I) NHC species was reported by the group of Tatsumi and coworkers.[60] Reaction of the phosphane precursor **55** with the free carbene IMes (1,3-bis(2,4,6-trimethylphenyl)imidazolin-2-ylidene) gave the thiolate **81**. The triphenylphosphane ligand in **55** was thus replaced by IMes, demonstrating a stronger metal-ligand bond for the NHC than for the phosphane (Scheme 18).

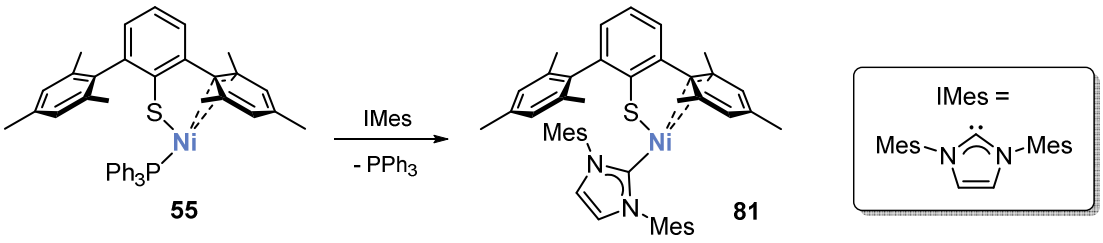

Scheme 18. Synthesis of NHC complex **81** by phosphane exchange.[60]

A very convenient preparation method for a series of three-coordinate nickel(I) compounds was developed by the group of Whittlesey. Comproportionation of $[Ni(1,5\text{-cod})_2]$ and $[NiX_2(PPh_3)_2]$ (X = Cl, Br), followed by the addition of an *in situ* generated ring-expanded carbene, yielded complexes of type **73** (Scheme 19).[76]

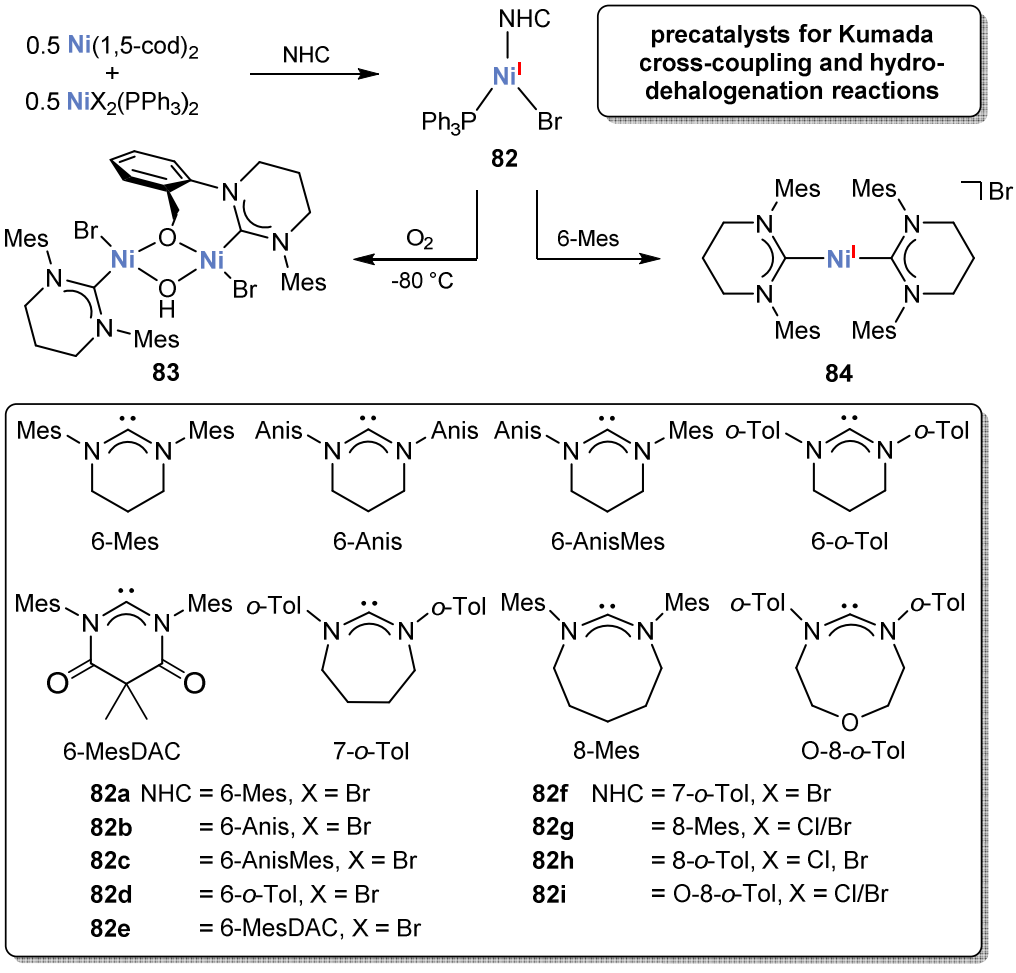

Scheme 19. Synthesis of the three- and two-coordinate nickel(I) complexes **82** and **84**, as well as the reactivity of **82** toward O_2. Anis = *para*-methoxyphenyl; *o*-Tol = *ortho*-tolyl.[76–78]

DFT and EPR studies on these compounds revealed a mixed composition of the SOMO with main contributions from the $3d_{z^2}$ and $3d_{x^2-y^2}$.[77] Complexes **82** proved active for the Kumada cross-coupling of aryl chlorides and fluorides as well as for hydrodefluorination reactions. In addition, Whittlesey *et al.* investigated the reactivity of complexes **82** toward O_2 and observed a stereoelectronic dependency by use of different carbenes.[78] Dinuclear **83** was formed in the reaction of **82a** with O_2 at −80 °C through C−H bond activation of one *ortho*-methyl group of the carbene's Mes substituent. Using **82d** and **82f**, containing less bulky ligands, resulted in simple nickel(II) bromides [(NHC)$NiBr_2(PPh_3)$] and other not identifiable products.

The two-coordinate cation **84** was isolated by ligand substitution of PPh_3 with 6-Mes (Scheme 19).[79] Remarkably, complex **84** represents the first mononuclear nickel complex exhibiting magnetic anisotropy due to an unquenched orbital angular momentum. This behavior is indicative for a single-molecule magnet and a result of the partially-filled and near-degenerate d_{xz} and d_{yz} orbitals in the linear complex.

Very recently, the Tilley and co-workers presented a new versatile approach for the synthesis of nickel(I) carbene and phosphane species.[51] Complexes of type **86** were formed by protonation of the anionic complex **85** with a mild Brønsted base in the presence of an NHC or phosphane (Scheme 20). The reaction with sterically encumbering 2,6-bis(*tert*-butyl)-4-methylphenol gave aryl oxides **87** and **88**. While the aryloxide ligand coordinates via oxygen in the IDipp complex **87**, the molecular structure of the tri-*tert*-butylphosphane complex **88** features a dearomatized, η^5-coordinated aryloxide ligand.

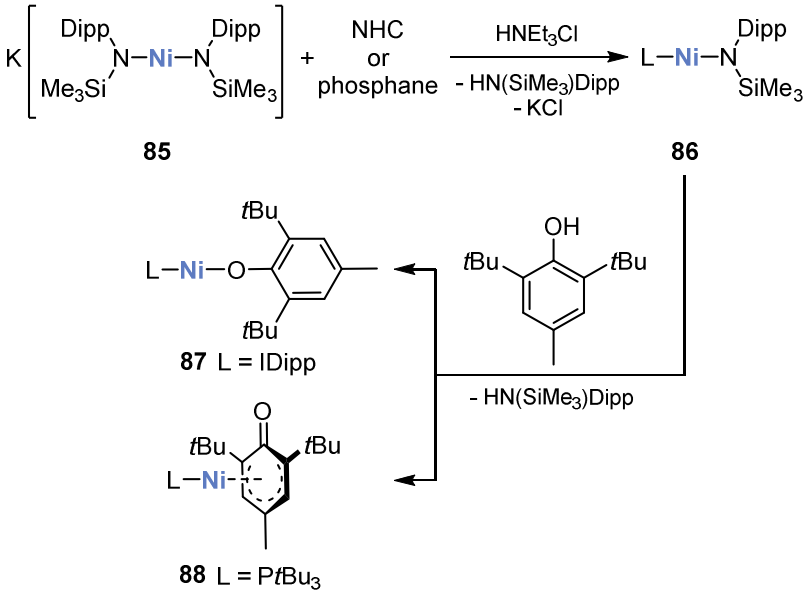

Scheme 20. Synthesis of low-coordinate nickel(I) complexes (L = IDipp, tBu_3P, iPr_3P, $Ph_2P(CH_2)_2PPh_2$).[51]

1.5 Conclusion

Following Heimbach's pioneering work, the chemistry of phosphane- and NHC-stabilized nickel(I) monomers has developed into a thriving research over the last decades. Progress in this field was inhibited for a long time, because these nickel(I) radicals are often difficult to isolate as a result of their high air-sensivity and the tendency to disproportionate and aggregate. Furthermore, the characterization can be complicated due to the paramagnetic nature of nickel(I) monomers. With their d^9 configuration and one unpaired electron in their valence shell, monovalent nickel(I) species have a propensity to react with organic and inorganic substrates via single electron transfer (SET). They often give meaningful EPR spectra due to their substantial metalloradical nature,[80] Due to these characteristic features, mononuclear nickel(I) compounds attract interest far beyond organometallic chemistry.

Monomeric nickel(I) compounds display a substantial range of different coordination modes. Four-coordinate complexes are most common with tetrahedral compounds being more frequently observed than trigonal pyramidal ones. In addition, three-coordinate complexes with distorted Y-shaped motifs have been observed more frequently compared to T-shaped environments, which came up more recently. Five-coordinate trigonal bipyramidal structures and linear two-coordinate complexes are less common. The former coordination mode was exclusively observed with phosphane ligands and latter predominantly for complexes with bulky NHCs. Furthermore, there are only three different types of complexes known featuring cyclopentadienyl and cyclobutadiene ligands ("Two-legged piano-stool" motif).

It is noteworthy that low-coordinate motifs occur more frequently with carbene ligands, due to the ability of bulky NHCs to kinetically stabilize low-coordinate metal centers more efficiently than the usually sterically less protective phosphane ligands. In accord with Pauling's electroneutrality principle[81] another reason is the ability of NHCs to form stronger σ-bonds with transition metals due to the more directional nature of the sp^2-type lone pair of the carbene in contrast to the non-directional s-type lone pair in phosphanes, which results in a higher electron density localized on the metal center.[82]

Chelating phosphanes are commonly applied in nickel(I) chemistry, while analogous NHC complexes are unprecedented. A more frequent use of less conventional carbenes (e.g. ring-expanded carbenes or diamidocarbenes) would be desirable in order to assess the electronic and steric influence of the NHC ligand on the reactivity and structural properties of monovalent nickel complexes. The phosphane ligand exchange in monovalent nickel species offers a route to the corresponding NHC complexes, representing a link between both compound classes.

In summary, NHC nickel(I) compounds are far less explored as compared to phosphane nickel(I) complexes. Although different preparative methods for nickel(I) NHC compounds have been developed in the recent years, only a few publications deal with their reactivity. Nonetheless, the

introduction of NHC ligands in nickel(I) chemistry certainly gave new impetus to the field, enabling unique coordination modes and unprecedented reactions.

References

1 a) T. T. Tsou, J. K. Kochi, *J. Am. Chem. Soc.* **1979**, *101*, 6319–6332; b) T. T. Tsou, J. K. Kochi, *J. Am. Chem. Soc.* **1979**, *101*, 7547–7560.

2 a) J. Montgomery, *Angew. Chem. Int. Ed.* **2004**, *43*, 3890–3908; J. Montgomery, *Angew. Chem.* **2004**, *116*, 3980–3998; b) S. Z. Tasker, E. A. Standley, T. F. Jamison, *Nature* **2014**, *509*, 299–309; c) E. A. Standley, S. Z. Tasker, K. L. Jensen, T. F. Jamison, *Acc. Chem. Res.* **2015**, *48*, 1503–1514.

3 S. W. Ragsdale, *Chem. Rev.* **2006**, *106*, 3317–3337.

4 a) U. Ermler, *Dalton Trans.* **2005**, 3451–3458; b) S. Scheller, M. Goenrich, R. Boecher, R. K. Thauer, B. Jaun, *Nature* **2010**, *465*, 606–608.

5 S. Scheller, M. Goenrich, S. Mayr, R. K. Thauer, B. Jaun, *Angew. Chem. Int. Ed.* **2010**, *49*, 8112–8115; *Angew. Chem.* **2010**, *122*, 8289–8292.

6 a) V. J. DeRose, J. Telser, M. E. Anderson, P. A. Lindahl, B. M. Hoffman, *J. Am. Chem. Soc.* **1998**, *120*, 8767–8776; b) S. W. Ragsdale, *Crit. Rev. Biochem. Mol.* **2004**, *39*, 165–195; c) D. J. Evans, *Coord. Chem. Rev.* **2005**, *249*, 1582–1595; d) J.-H. Jeoung, H. Dobbek, *Science* **2007**, *318*, 1461–1464; e) M. Can, F. A. Armstrong, S. W. Ragsdale, *Chem. Rev.* **2014**, *114*, 4149–4174.

7 K. Nag, A. Chakravorty, *Coord. Chem. Rev.* **1980**, *33*, 87–147.

8 a) T. J. Anderson, G. D. Jones, D. A. Vicic, *J. Am. Chem. Soc.* **2004**, *126*, 8100–8101; b) G. D. Jones, C. McFarland, T. J. Anderson, D. A. Vicic, *Chem. Commun.* **2005**, 4211–4213; c) G. D. Jones, J. L. Martin, C. McFarland, O. R. Allen, R. E. Hall, A. D. Haley, R. J. Brandon, T. Konovalova, P. J. Desrochers, P. Pulay, D. A. Vicic, *J. Am. Chem. Soc.* **2006**, *128*, 13175–13183; d) V. B. Phapale, E. Buñuel, M. García-Iglesias, D. J. Cárdenas, *Angew. Chem. Int. Ed.* **2007**, *46*, 8790–8795; *Angew. Chem.* **2007**, *119*, 8946–8951; e) X. Hu, *Chem. Sci.* **2011**, *2*, 1867–1886; f) M. Vogt, B. de Bruin, H. Berke, M. Trincado, H. Grützmacher, *Chem. Sci.* **2011**, *2*, 723–727; g) B. Horn, C. Limberg, C. Herwig, B. Braun, *Chem. Commun.* **2013**, *49*, 10923–10925; h) J. Breitenfeld, J. Ruiz, M. D. Wodrich, X. Hu, *J. Am. Chem. Soc.* **2013**, *135*, 12004–12012; i) J. Breitenfeld, M. D. Wodrich, X. Hu, *Organometallics* **2014**, *33*, 5708–5715; j) J.-J. Meng, M. Gao, M. Dong, Y.-P. Wei, W.-Q. Zhang, *Tetrahedron Lett.* **2014**, *55*, 2107–2109; k) M. I. Lipschutz, T. D. Tilley, *Angew. Chem. Int. Ed.* **2014**, *53*, 7290–7294; *Angew. Chem.* **2014**, *126*, 7418–7422.

9 L. Latos-Grazynski, M. M. Olmstead, A. L. Balch, *Inorg. Chem.* **1989**, *28*, 4065–4066.

10 Selected publications on nickel(I) complexes with macrocyclic ligands: a) C. Gosden, K. P. Healy, D. Pletcher, *J. Chem. Soc., Dalton Trans.* **1978**, 972–976; b) B. Jaun, A. Pfaltz, *J. Chem. Soc., Chem. Commun.* **1986**, 1327–1329, c) M. W. Renner, L. R. Furenlid, K. M. Barkigia, A. Forman, H. K. Shim, D. J. Simpson, K. M. Smith, J. Fajer, *J. Am. Chem. Soc.* **1991**, *113*, 6891–6898; d) L. R. Furenlid, M. W. Renner, E. Fujita, *Physica B* **1995**, *208–*

209, 739–742; e) G. N. Sinyakov, A. M. Shulga, *J. Struct. Chem.* **1996**, *37*, 442–446; f) M. T. Kieber-Emmons, C. G. Riordan, *Acc. Chem. Res.* **2007**, *40*, 618–625; g) M. T. Kieber-Emmons, K. M. Van Heuvelen, T. C. Brunold, C. G. Riordan, *J. Am. Chem. Soc.* **2009**, *131*, 440–441; h) C. Uyeda, J. C. Peters, *Chem. Sci.* **2012**, *4*, 157–163.

11 a) S. Yao, M. Driess, *Acc. Chem. Res.* **2012**, *45*, 276–287; b) Y.-C. Tsai, *Coord. Chem. Rev.* **2012**, *256*, 722–758.

12 S. Yao, Y. Xiong, C. Milsmann, E. Bill, S. Pfirrmann, C. Limberg, M. Driess, *Chem. Eur. J.* **2010**, *16*, 436–439.

13 Selected publications on oligonuclear nickel(I) complexes: a) O. Jarchow, H. Schulz, R. Nast, *Angew. Chem. Int. Ed. Engl.* **1970**, *9*, 71–71; *Angew. Chem.* **1970**, *82*, 43–44; b) D. L. DeLaet, R. Del Rosario, P. E. Fanwick, C. P. Kubiak, *J. Am. Chem. Soc.* **1987**, *109*, 754–758; c) K. S. Ratliff, R. E. Lentz, C. P. Kubiak, *Organometallics* **1992**, *11*, 1986–1988; d) D. A. Morgenstern, R. E. Wittrig, P. E. Fanwick, C. P. Kubiak, *J. Am. Chem. Soc.* **1993**, *115*, 6470–6471; e) D. A. Vicic, T. J. Anderson, J. A. Cowan, A. J. Schultz, *J. Am. Chem. Soc.* **2004**, *126*, 8132–8133; f) A. L. Keen, S. A. Johnson, *J. Am. Chem. Soc.* **2006**, *128*, 1806–1807; g) A. L. Keen, M. Doster, S. A. Johnson, *J. Am. Chem. Soc.* **2007**, *129*, 810–819; h) A. Velian, S. Lin, A. J. M. Miller, M. W. Day, T. Agapie, *J. Am. Chem. Soc.* **2010**, *132*, 6296–6297; i) C. Jones, C. Schulten, L. Fohlmeister, A. Stasch, K. S. Murray, B. Moubaraki, S. Kohl, M. Z. Ertem, L. Gagliardi, C. J. Cramer, *Chem. Eur. J.* **2011**, *17*, 1294–1303; j) M. Tanabe, R. Yumoto, K. Osakada, *Chem. Commun.* **2012**, *48*, 2125–2127; k) S. Suseno, K. T. Horak, M. W. Day, T. Agapie, *Organometallics* **2013**, *32*, 6883–6886; l) R. Beck, S. A. Johnson, *Organometallics* **2013**, *32*, 2944–2951; m) C. Rettenmeier, H. Wadepohl, L. H. Gade, *Chem. Eur. J.* **2014**, *20*, 9657–9665; n) B. R. Reed, S. A. Stoian, R. L. Lord, S. Groysman, *Chem. Commun.* **2015**, *51*, 6496–6499; o) F. Koch, H. Schubert, P. Sirsch, A. Berkefeld, *Dalton Trans.* **2015**, *44*, 13315–13324.

14 Reviews on reactions involving active transition metal catalysts with phosphane ligands: a) C. A. Tolman, *Chem. Rev.* **1977**, *77*, 313–348; b) T. Hayashi, M. Kumada, *Acc. Chem. Res.* **1982**, *15*, 395–401; c) T. Hayashi, *Acc. Chem. Res.* **2000**, *33*, 354–362; d) P. C. J. Kamer, P. W. N. M. van Leeuwen, J. N. H. Reek, *Acc. Chem. Res.* **2001**, *34*, 895–904; e) U. Christmann, R. Vilar, *Angew. Chem. Int. Ed.* **2005**, *44*, 366–374; *Angew. Chem.* **2005**, *117*, 370–378; f) Y.-M. Li, F.-Y. Kwong, W.-Y. Yu, A. S. C. Chan, *Coord. Chem. Rev.* **2007**, *251*, 2119–2144; g) M. L. Clarke, J. J. R. Frew, *Organometzallic Chemistry: Volume 35*, Royal Society of Chemistry, Cambridge, **2009**; h) C. D. Swor, D. R. Tyler, *Coord. Chem. Rev.* **2011**, *255*, 2860–2881; i) T. M. Shaikh, C.-M. Weng, F.-E. Hong, *Coord. Chem. Rev.* **2012**, *256*, 771–803. M; j) P. Carroll, P. J. Guiry, *Chem. Soc. Rev.* **2014**, *43*, 819–833; k) Y.-M. Wang, A. D. Lackner, F. D. Toste, *Acc. Chem. Res.* **2014**, *47*, 889–901.

15 Reviews on reactions involving active transition metal catalysts with NHC ligands: a) W. A. Herrmann, *Angew. Chem. Int. Ed.* **2002**, *41*, 1290–1309; *Angew. Chem.* **2002**, *114*, 1342–1363; b) E. A. B. Kantchev, C. J. O'Brien, M. G. Organ, *Angew. Chem. Int. Ed.* **2007**, *46*, 2768–2813; *Angew. Chem.* **2007**, *119*, 2824–2870; c) S. Würtz, F. Glorius, *Acc. Chem. Res.* **2008**, *41*, 1523–1533; d) G. C. Vougioukalakis, R. H. Grubbs, *Chem. Rev.* **2010**, *110*, 1746–1787; e) S. Díez-González, N. Marion, S. P. Nolan, *Chem. Rev.* **2009**, *109*, 3612–3676; f) T. Hatakeyama, S. Hashimoto, K. Ishizuka, M. Nakamura, *J. Am. Chem. Soc.* **2009**, *131*, 11949–11963. g) K. Riener, S. Haslinger, A. Raba, M. P. Högerl, M. Cokoja, W. A. Herrmann, F. E. Kühn, *Chem. Rev.* **2014**, *114*, 5215–5272.

16 P. Heimbach, *Angew. Chem.* **1964**, *76*, 586–586.

17 H. Hoberg, K. Radine, C. Krüger, M. J. Romãn, *Z. Naturforsch.* **1985**, *40*, 607–614.

18 Publications on the synthesis of complexes of type **1**: a) L. Porri, M. C. Gallazzi, G. Vitulli, *Chem. Commun.* **1967**, 228–228; b) C. S. Cundy, H. Nöth, *J. Organomet. Chem.* **1971**, *30*, 135–143; c) L. Sacconi, S. Midollini, *J. Chem. Soc., Dalton Trans.* **1972**, 1213–1216; d) D. G. Holah, A. N. Hughes, B. C. Hui, K. Wright, *Can. J. Chem.* **1974**, *52*, 2990–2999; e) D. G. Holah, A. N. Hughes, B. C. Hui, *Inorg. Nucl. Chem. Lett.* **1974**, *10*, 427–429; f) A. Bencini, C. Benelli, D. Gatteschi, L. Sacconi, *Inorg. Chim. Acta* **1979**, *37*, 195–199; g) E. Uhlig, B. Nestler, *Z. Anorg. Allg. Chem.* **1980**, *460*, 56–64; h) M. Gómez, P. Royo, I. Sáez, A. Arcas, *Transition Met. Chem.* **1982**, *7*, 294–297; i) P. B. Kraikivskii, V. V. Saraev, D. A. Matveev, S. N. Zelinskii, V. S. Tkach, *Russ. J. Coord. Chem.* **2003**, *29*, 431–434; j) M. Kandiah, G. S. McGrady, A. Decken, P. Sirsch, *Inorg. Chem.* **2005**, *44*, 8650–8652.

19 Structural characterization of complexes of type **1** and **2**: X-ray of $[NiBr(PPh_3)_3]$: a) C. Mealli, P. Dapporto, V. Sriyunyongwat, T. A. Albright, *Acta Cryst. C* **1983**, *39*, 995–996; b) $[NiCl(PPh_3)_3]$: J. M. Cassidy, K. H. Whitmire, *Acta Cryst. C* **1991**, *47*, 2094–2098; c) $[NiCl(PPh_3)_2]$: D. D. Ellis, A. L. Spek, *Acta Cryst. C* **2000**, *56*, 1067–1070.

20 a) Preliminary description of the structure: P. Dapporto, G. Fallani, S. Midollini, L. Sacconi, *J. Chem. Soc., Chem. Commun.* **1972**, 1161–1161; b) P. Dapporto, G. Fallani, L. Sacconi, *Inorg. Chem.* **1974**, *13*, 2847–2850.

21 a) H. Kanai, *J. Chem. Soc., Chem. Commun.* **1972**, 203–204; b) F. Scott, C. Krüger, P. Betz, *J. Organomet. Chem.* **1990**, *387*, 113–121.

22 a) F. Scott, C. Krüger, P. Betz, *J. Organomet. Chem.* **1990**, *387*, 113–121; b) J. Langer, R. Fischer, H. Görls, N. Theyssen, D. Walther, *Z. Anorg. Allg. Chem.* **2007**, *633*, 557–562; c) E. E. Marlier, S. J. Tereniak, K. Ding, J. E. Mulliken, C. C. Lu, *Inorg. Chem.* **2011**, *50*, 9290–9299; d) S. T. Chao, N. C. Lara, S. Lin, M. W. Day, T. Agapie, *Angew. Chem. Int. Ed.* **2011**, *50*, 7529–7532; *Angew. Chem.* **2011**, *123*, 7671–7674; e) R. Beck, M. Shoshani, J. Krasinkiewicz, J. A. Hatnean, S. A. Johnson, *Dalton Trans.* **2013**, *42*, 1461–1475.

23 W. Lin, T. Bodenstein, V. Mereacre, K. Fink, A. Eichhöfer, *Inorg. Chem.* **2016**, DOI 10.1021/acs.inorgchem.5b02497.

24 F. Caballero, M. Gómez, P. Royo, *Transition Met. Chem.* **1977**, *2*, 130–132.

25 a) A. Morvillo, A. Turco, *J. Organomet. Chem.* **1982**, *224*, 387–397; b) M. Anton, N. Clos, G. Müller, *J. Organomet. Chem.* **1984**, *267*, 213–219.

26 a) M. J. D'Aniello, E. K. Barefield, *J. Am. Chem. Soc.* **1978**, *100*, 1474–1481; b) H. Kanai, K. Kushi, K. Sakanoue, N. Kishimoto, *Bull. Chem. Soc. Jpn.* **1980**, *53*, 2711–2715.

27 L. M. Guard, M. Mohadjer Beromi, G. W. Brudvig, N. Hazari, D. J. Vinyard, *Angew. Chem. Int. Ed.* **2015**, *54*, 13352–13356; *Angew. Chem.* **2015**, *127*, 13550–13554.

28 D. J. Mindiola, R. Waterman, D. M. Jenkins, G. L. Hillhouse, *Inorg. Chim. Acta* **2003**, *345*, 299–308.

29 a) D. J. Mindiola, G. L. Hillhouse, *J. Am. Chem. Soc.* **2001**, *123*, 4623–4624; b) R. Melenkivitz, D. J. Mindiola, G. L. Hillhouse, *J. Am. Chem. Soc.* **2002**, *124*, 3846–3847; c) V. M. Iluc, G. L. Hillhouse, *J. Am. Chem. Soc.* **2010**, *132*, 15148–15150.

30 K. D. Kitiachvili, D. J. Mindiola, G. L. Hillhouse, *J. Am. Chem. Soc.* **2004**, *126*, 10554–10555.

31 V. M. Iluc, G. L. Hillhouse, *J. Am. Chem. Soc.* **2010**, *132*, 11890–11892.

32 V. M. Iluc, A. J. M. Miller, G. L. Hillhouse, *Chem. Commun.* **2005**, 5091–5093.

33 J. S. Anderson, V. M. Iluc, G. L. Hillhouse, *Inorg. Chem.* **2010**, *49*, 10203–10207.

34 V. M. Iluc, G. L. Hillhouse, *J. Am. Chem. Soc.* **2014**, *136*, 6479–6488.

35 a) H.-F. Klein, H. H. Karsch, W. Buchner, *Chem. Ber.* **1974**, *107*, 537–546; b) A. Gleizes, M. Dartiguenave, Y. Dartiguenave, J. Galy, H. F. Klein, *J. Am. Chem. Soc.* **1977**, *99*, 5187–5189.

36 a) M. Martelli, G. Pilloni, G. Zotti, S. Daolio, *Inorg. Chim. Acta* **1974**, *11*, 155–158; b) G. A. Bowmaker, P. D. W. Boyd, G. K. Campbell, J. M. Hope, R. L. Martin, *Inorg. Chem.* **1982**, *21*, 1152–1159; c) G. A. Bowmaker, J. P. Williams, *J. Chem. Soc., Dalton Trans.* **1994**, 1231–1236; d) G. Pilloni, A. Toffoletti, G. Bandoli, B. Longato, *Inorg. Chem.* **2006**, *45*, 10321–10328.

37 a) A. Miedaner, R. C. Haltiwanger, D. L. DuBois, *Inorg. Chem.* **1991**, *30*, 417–427; b) V. V. Saraev, P. B. Kraikivskii, D. A. Matveev, A. S. Kuzakov, A. I. Vil'ms, A. A. Fedonina, *Russ. J. Coord. Chem.* **2008**, *34*, 438–442.

38 V. V. Saraev, P. B. Kraikivskii, I. Svoboda, A. S. Kuzakov, R. F. Jordan, *J. Phys. Chem. A* **2008**, *112*, 12449–12455.

39 V. V. Saraev, P. B. Kraikivskii, V. V. Annenkov, A. I. Vil'ms, D. A. Matveev, E. N. Danilovtseva, T. G. Ermakova, N. P. Kuznetsova, K. Lammertsma, *Kinet. Catal.* **2005**, *46*, 712–718.

40 F. Cecconi, S. Midollini, A. Orlandini, *J. Chem. Soc., Dalton Trans.* **1983**, 2263–2268.

41 D. E. Herbert, N. C. Lara, T. Agapie, *Chem. Eur. J.* **2013**, *19*, 16453–16460.

42 D. C. Bradley, M. B. Hursthouse, R. J. Smallwood, A. J. Welch, *J. Chem. Soc., Chem. Commun.* **1972**, 872–873.

43 L. Sacconi, C. A. Ghilardi, C. Mealli, F. Zanobini, *Inorg. Chem.* **1975**, *14*, 1380–1386.

44 A. Hashimoto, H. Yamaguchi, T. Suzuki, K. Kashiwabara, M. Kojima, H. D. Takagi, *Eur. J. Inorg. Chem.* **2010**, *2010*, 39–47.

45 D. Zhang, G.-X. Jin, L.-H. Weng, F. Wang, *Organometallics* **2004**, *23*, 3270–3275. H.-Y. Wang, X. Meng, G.-X. Jin, *Dalton Trans.* **2006**, 2579–2585.

46 G. Bai, P. Wei, D. W. Stephan, *Organometallics* **2005**, *24*, 5901–5908.

47 Z. Weng, S. Teo, L. L. Koh, T. S. A. Hor, *Angew. Chem. Int. Ed.* **2005**, *44*, 7560–7564; *Angew. Chem.* **2005**, *117*, 7732–7736.

48 C. Eaborn, M. S. Hill, P. B. Hitchcock, J. D. Smith, *Chem. Commun.* **2000**, 691–692.

49 P. J. Chmielewski, L. Latos-Grażyński, E. Pacholska, *Inorg. Chem.* **1994**, *33*, 1992–1999.

50 P. B. Kraikivskii, V. V. Saraev, R. Meusinger, V. V. Bocharova, I. A. Ushakov, S. K. Petrovskii, *J. Organomet. Chem.* **2012**, *715*, 43–47.

51 M. I. Lipschutz, T. D. Tilley, *Organometallics* **2014**, *33*, 5566–5570.

52 D. Adhikari, S. Mossin, F. Basuli, B. R. Dible, M. Chipara, H. Fan, J. C. Huffman, K. Meyer, D. J. Mindiola, *Inorg. Chem.* **2008**, *47*, 10479–10490.

53 B. C. Fullmer, H. Fan, M. Pink, K. G. Caulton, *Inorg. Chem.* **2008**, *47*, 1865–1867.

54 a) C. Yoo, S. Oh, J. Kim, Y. Lee, *Chem. Sci.* **2014**, *5*, 3853–3858; b) C. Yoo, M. J. Ajitha, Y. Jung, Y. Lee, *Organometallics* **2015**, *34*, 4305–4311.

55 M. Cha, S. C. Shoner, J. A. Kovacs, *Inorg. Chem.* **1993**, *32*, 1860–1863.

56 J. S. Kim, J. H. Reibenspies, M. Y. Darensbourg, *J. Am. Chem. Soc.* **1996**, *118*, 4115–4123.

57 P. B. Kraikivskii, M. Frey, H. A. Bennour, A. Gembus, R. Hauptmann, I. Svoboda, H. Fuess, V. V. Saraev, H.-F. Klein, *J. Organomet. Chem.* **2009**, *694*, 1869–1876.

58 a) P. J. Schebler, B. S. Mandimutsira, C. G. Riordan, L. M. Liable-Sands, C. D. Incarvito, A. L. Rheingold, *J. Am. Chem. Soc.* **2001**, *123*, 331–332; b) K. Fujita, A. L. Rheingold, C. G. Riordan, *Dalton Trans.* **2003**, 2004–2008.

59 T. L. James, L. Cai, M. C. Muetterties, R. H. Holm, *Inorg. Chem.* **1996**, *35*, 4148–4161.

60 M. Ito, T. Matsumoto, K. Tatsumi, *Inorg. Chem.* **2009**, *48*, 2215–2223.

61 a) E. O. Fischer, C. Palm, *Chem. Ber.* **1958**, *91*, 1725–1731; b) O. S. Mills, B. W. Shaw, *Acta Cryst.* **1965**, *18*, 562; c) O. S. Mills, B. W. Shaw, *J. Organomet. Chem.* **1968**, *11*, 595–600; d) M. S. Paquette, L. F. Dahl, *J. Am. Chem. Soc.* **1980**, *102*, 6621–6623; e) L. R. Byers, L. F. Dahl, *Inorg. Chem.* **1980**, *19*, 680–692; f) L. R. Byers, V. A. Uchtman, L. F. Dahl, *J. Am. Chem. Soc.* **1981**, *103*, 1942–1951; g) J. J. Maj, A. D. Rae, L. F. Dahl, *J. Am. Chem. Soc.* **1982**, *104*, 3054–3063; h) J. J. Schneider, R. Goddard, C. Krüger, S. Werner, B. Metz, *Chem. Ber.* **1991**, *124*, 301–308; i) U. Denninger, J. J. Schneider, G. Wilke, R.

Goddard, C. Krüger, *Inorg. Chim. Acta* **1993**, *213*, 129–140; j) J. J. Schneider, U. Denninger, R. Goddard, C. Krüger, C. W. Lehmann, *J. Organomet. Chem.* **1999**, *582*, 188–194. W; k) Buchowicz, B. Herbaczyńska, L. B. Jerzykiewicz, T. Lis, S. Pasynkiewicz, A. Pietrzykowski, *Inorg. Chem.* **2012**, *51*, 8292–8297.

62 E. Uhlig, H. Walther, *Z. Anorg. Allg. Chem.* **1974**, *409*, 89–96.

63 E. K. Barefield, D. A. Krost, D. S. Edwards, D. G. Van Derveer, R. L. Trytko, S. P. O'Rear, A. N. Williamson, *J. Am. Chem. Soc.* **1981**, *103*, 6219–6222.

64 a) E. Hernandez, P. Royo, *J. Organomet. Chem.* **1985**, *291*, 387–392; b) C. Amatore, O. Buriez, H.-N. Verpeaux, *Acta Chem. Scand.* **1999**, *53*, 920–927.

65 V. V. Saraev, P. B. Kraikivskii, S. N. Zelinskii, A. I. Vil'ms, D. A. Matveev, A. Y. Yunda, A. A. Fedonina, K. Lammertsma, *Russ. J. Coord. Chem.* **2006**, *32*, 397–401.

66 V. V. Saraev, P. B. Kraikivskii, A. I. Vilms, S. N. Zelinskii, A. Y. Yunda, E. N. Danilovtseva, A. S. Kuzakov, *Kinet. Catal.* **2007**, *48*, 778–784.

67 H. Hoberg, W. Richter, C. Fröhlich, *J. Organomet. Chem.* **1981**, *213*, C49–C52.

68 C. A. Laskowski, G. L. Hillhouse, *J. Am. Chem. Soc.* **2008**, *130*, 13846–13847.

69 B. R. Dible, M. S. Sigman, A. M. Arif, *Inorg. Chem.* **2005**, *44*, 3774–3776.

70 C. A. Laskowski, G. R. Morello, C. T. Saouma, T. R. Cundari, G. L. Hillhouse, *Chem. Sci.* **2012**, *4*, 170–174.

71 C. A. Laskowski, D. J. Bungum, S. M. Baldwin, S. A. Del Ciello, V. M. Iluc, G. L. Hillhouse, *J. Am. Chem. Soc.* **2013**, *135*, 18272–18275.

72 C. A. Laskowski, G. L. Hillhouse, *Organometallics* **2009**, *28*, 6114–6120.

73 J. Wu, A. Nova, D. Balcells, G. W. Brudvig, W. Dai, L. M. Guard, N. Hazari, P.-H. Lin, R. Pokhrel, M. K. Takase, *Chem. Eur. J.* **2014**, *20*, 5327–5337.

74 A. J. Arduengo, S. F. Gamper, J. C. Calabrese, F. Davidson, *J. Am. Chem. Soc.* **1994**, *116*, 4391–4394.

75 a) S. Miyazaki, Y. Koga, T. Matsumoto, K. Matsubara, *Chem. Commun.* **2010**, *46*, 1932–1934; b) S. Nagao, T. Matsumoto, Y. Koga, K. Matsubara, *Chem. Lett.* **2011**, *40*, 1036–1038; c) K. Zhang, M. Conda-Sheridan, S. R. Cooke, J. Louie, *Organometallics* **2011**, *30*, 2546–2552.

76 C. J. E. Davies, M. J. Page, C. E. Ellul, M. F. Mahon, M. K. Whittlesey, *Chem. Commun.* **2010**, *46*, 5151–5153.

77 M. J. Page, W. Y. Lu, R. C. Poulten, E. Carter, A. G. Algarra, B. M. Kariuki, S. A. Macgregor, M. F. Mahon, K. J. Cavell, D. M. Murphy, M. K. Whittlesey, *Chem. Eur. J.* **2013**, *19*, 2158–2167.

78 R. C. Poulten, I. López, A. Llobet, M. F. Mahon, M. K. Whittlesey, *Inorg. Chem.* **2014**, *53*, 7160–7169.

79 R. C. Poulten, M. J. Page, A. G. Algarra, J. J. Le Roy, I. López, E. Carter, A. Llobet, S. A. Macgregor, M. F. Mahon, D. M. Murphy, M. K. Whittlesey, *J. Am. Chem. Soc.* **2013**, *135*, 13640–13643.

80 B. De Bruin, D. G. H. Hetterscheid, A. J. J. Koekkoek and H. Grutzmacher, *Progr. Inorg. Chem.* **2007**, 247.

81 L. Pauling, *J. Chem. Soc.* **1948**, 1461–1467.

82 a) W. A. Herrmann, M. Elison, J. Fischer, C. Köcher, G. R. J. Artus, *Angew. Chem. Int. Ed. Engl.* **1995**, *34*, 2371–2374; *Angew. Chem.* **1995**, *107*, 2602–2605; b) R. H. Crabtree, *J. Organomet. Chem.* **2005**, *690*, 5451–5457; c) H. Jacobsen, A. Correa, A. Poater, C. Costabile, L. Cavallo, *Coord. Chem. Rev.* **2009**, *253*, 687–703; d) G. C. Fortman, S. P. Nolan, *Chem. Soc. Rev.* **2011**, *40*, 5151–5169; e) D. J. D. Wilson, S. A. Couchman, J. L. Dutton, *Inorg. Chem.* **2012**, *51*, 7657–7668.

2 Selective P_4 Activation by an Organometallic Nickel(I) Radical: Formation of a Dinuclear Nickel(II) Tetraphosphide and Related Di- and Trichalcogenides[a,b,c]

Stefan Pelties, Dirk Herrmann, Bas de Bruin, František Hartl, and Robert Wolf

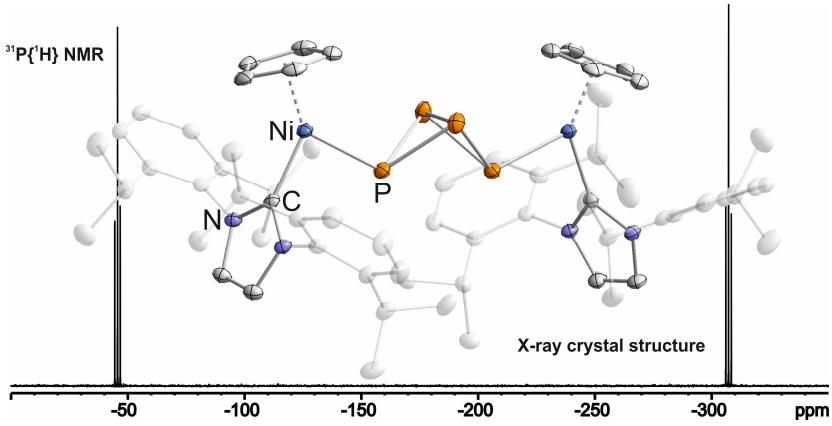

[a] Reproduced from S. Pelties, D. Herrmann, B. de Bruin, F. Hartl, R. Wolf, *Chem. Commun.* **2014**, 50, 7014–7016 with permission from *The Royal Society of Chemistry*.
[b] Bas de Bruin performed and analyzed the EPR measurements (Figures 1, S14, and Table 2) and carried out the DFT calculations. Dirk Herrmann and František Hartl performed the spectroelectrochemistry and analyzed the results (Figures 1, S12, and S13).
[c] During the preparation of this manuscript, Hazari *et al.* reported the synthesis and characterization of **1**, **1-THF** and closely related mono- and dinuclear species by a different synthetic route (J. Wu, A. Nova, D. Balcells, G. W. Brudvig, W. Dai, M. L. M. Guard, N. Hazari, P.-H. Lin, R. Pokhrel and M. K. Takase, *Chem. Eur. J.* **2014**, *18*, 5327).

2.1 Introduction

The P_4 molecule is the most reactive allotrope of phosphorus; its activation and transformation by transition metal compounds has attracted substantial interest over the years.[1] While many low-valent metal complexes, e.g. transition metal carbonyls or anionic metalates**,** react with P_4, it is still challenging to design highly selective transformations.[2,3] White phosphorus is able to efficiently trap organic and main group element radicals.[4] Therefore, one potential solution to the selectivity issue is to use a radical pathway in transition metal-mediated P_4 transformations. While 2nd and 3rd row metalloradicals are well-established,[5] nickel(I) radicals have attracted significant attention recently.[6,7] Importantly, Drieß *et al*. have shown that reactions of β-diketiminato nickel(I) complexes with P_4 yield dinuclear complexes $[(L^RNi)_2(\mu\text{-}\eta^3\text{:}\eta^3\text{-}P_4)]$ (L^R = HC[CMeN(2,6-$R_2C_6H_3$)]$_2$ with R = Et, *i*Pr).[8] The P–P bond activation in the doubly η^3-coordinated ligand is reversible and occurs without the reduction of P_4 to formally P_4^{2-}.

We have been interested in designing new reactive nickel(I) radicals (see chapter 1 for an overview over mononuclear nickel(I) phosphane and N-heterocyclic carbene complexes), which may be utilized for element-element bond activations. We now report the synthesis of complexes **1**–**3**, featuring an NHC and a cyclopentadienyl ligand, and an initial reactivity study of complex **1** with P_4 and related small molecules**.**

2.2. Results and Discussion

Complexes **1**–**3** are accessible according to Scheme 1 by the reduction of the appropriate nickel(II) halides with KC_8 in THF.¶ ^{1}H NMR monitoring shows that **1**–**3** are formed very selectively; they can be isolated as yellow crystalline solids in modest to high yields.

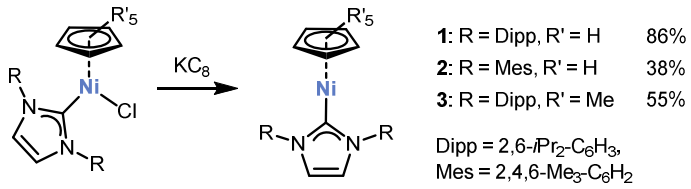

Scheme 1. Synthesis of nickel(I) complexes **1**–**3**.

Single X-ray structure analyses revealed that the nickel centre is surrounded by the carbene carbon and one η^5-coordinated Cp or Cp* moiety (Figure 1). No further significant interactions between nickel and the diisopropylphenyl groups are apparent. Nonetheless, the cyclopentadienyl ligand is tilted with respect to the nickel carbene bond with an angle $C_{carbene}$–Ni–$(C_5R_5)_{centroid}$ of 154.3(1)° for **1**, 151.9(1)° for **2** and 164.6(1)° for **3**.§

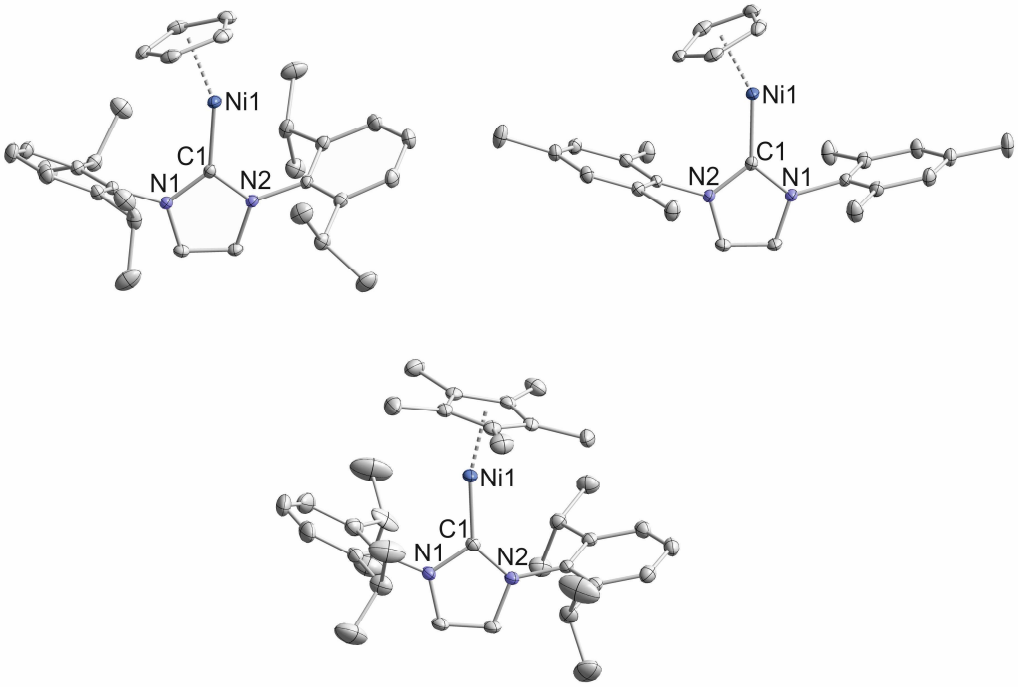

Figure 1. Solid-state molecular structure of **1** (left top), **2** (right top) and **3** (bottom). The hydrogen atoms are omitted for clarity. Thermal ellipsoids are drawn at 40% level. Selected bond lengths [Å] and angles [°]: Ni1-C1 1.877(1), $(C_5H_5)_{centroid}$-Ni1 1.79(1), C1-Ni1-$(C_5H_5)_{centroid}$ 154.3(1); **2**: Ni1-C1 1.876(2), $(C_5H_5)_{centroid}$-Ni1 1.80(1), C1-Ni1-$(C_5H_5)_{centroid}$ 152.0(1); **3**: Ni1-C1 1.880(1), $(C_5Me_5)_{centroid}$-Ni1 1.79(1), C1-Ni1-$(C_5H_5)_{centroid}$ 164.8(1).

Cyclic voltammograms show one electrochemically quasi-reversible wave at $E_{1/2}$ = –1.02 and –1.06 V vs. Fc/Fc^+ for Cp-substituted **1** and **2**, respectively, and a reversible wave at

–1.18 V vs. Fc/Fc^+ for the Cp* complex **3** (Supporting Information, SI). UV/vis-spectroelectrochemistry (see Figure 2 for **1**) confirms that these processes correspond to chemically reversible oxidations of neutral **1**–**3** to stable cationic nickel(II) complexes, which probably bind THF in the case of **1** and **2**. Indeed, the preparative oxidation of **1** with $[Cp_2Fe]PF_6$ affords the THF adduct $[(C_5H_5)Ni(IDipp)(THF)]PF_6$ (**1-THF**) (Figure 3, left).

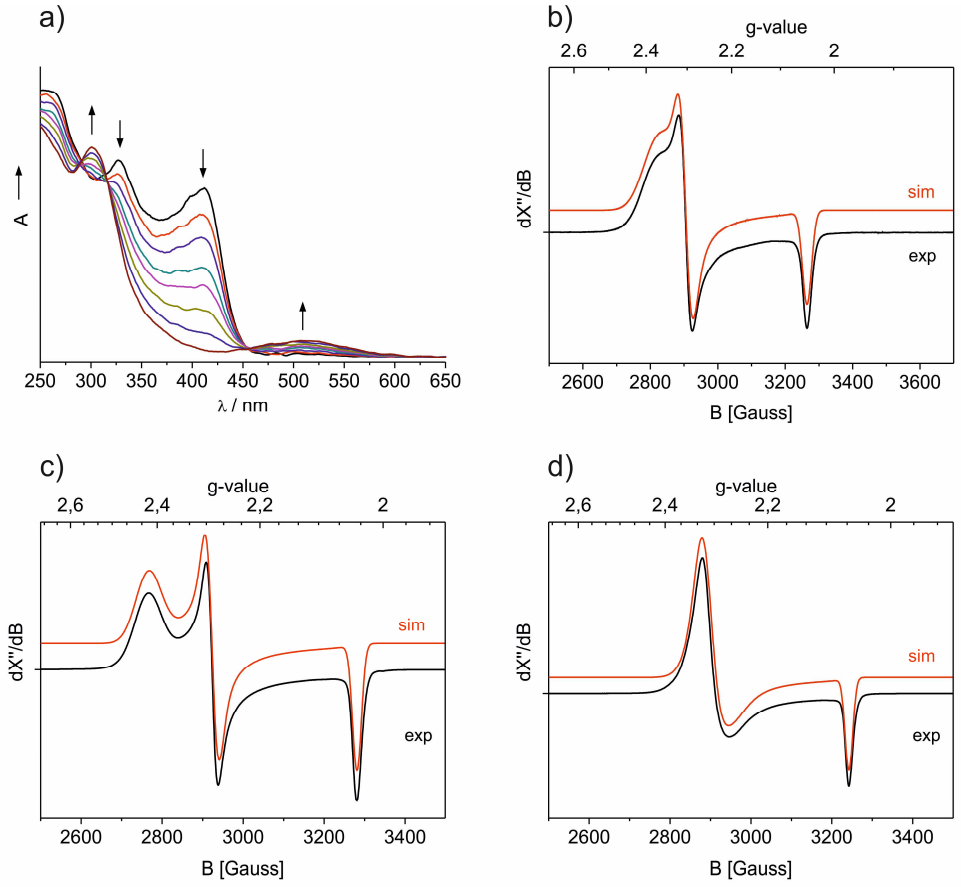

Figure 2. a) UV/Vis monitoring of the oxidation of **1** performed at –0.83 V vs. Fc/Fc^+ within an OTTLE cell equipped with a Pt minigrid working electrode, THF/TBAH under Ar, 293 K; Experimental and simulated X-band EPR spectrum of **1** (b), **2** (c) and **3** (d) in frozen THF. Freq. 9.3646 GHz, 0.063 mW, 20 K, mod. 4 Gauss; g-tensor parameters obtained from simulations and DFT calculations (b3-lyp, def2-TZVP) for **1**: g_{11} = 2.377 (2.220), g_{22} = 2.306 (2.187), g_{33} = 2.050 (2.078); **2**: g_{11} = 2.420 (2.225), g_{22} = 2.289 (2.210), g_{33} = 2.039 (2.076); **3**: g_{11} = 2.315 (2.228), g_{22} = 2.305 (2.179), g_{33} = 2.064 (2.087) (DFT-calculated values in parentheses).

Complexes **1**–**3** feature identical magnetic moments of 2.3(1), 2.3(1) and 2.2(1) μ_B in $[D_8]$THF (Evans method), which indicate the presence of one unpaired electron per molecule. The EPR spectrum of **1**, **2** and **3** are characteristic for an S = ½ system and reveal a rhombic g-tensor with significant deviations from g_e in case of **1** and **2** pointing to metalloradical character. In contrast, complex **2** shows an axial g-tensor, again with a substantial deviations from g_e. The DFT calculated g_{11} and g_{22} values are somewhat smaller than the experimental ones, but are generally in good agreement with the ones obtained from the simulations (Figure 2). Furthermore, the g_{11}-g_{22}-separation seem to correlate with

the degree of distortion in the structure, in particular with the $C_{carbene}$–Ni–$(C_5R_5)_{centroid}$ angle, while the difference between g_{22} and g_{33} remains nearly the same for all compounds. The highest g_{11}-g_{22}-separation ($\Delta g_{11/22}$ = 131) shows complex **2** having the smallest $C_{carbene}$–Ni–$(C_5R_5)_{centroid}$ angle. While complex **1** still features a difference of $\Delta g_{11/22}$ = 71, complex **3** possesses an axial spectrum ($\Delta g_{11/22}$ = 10) with an only slightly tilted structure.

Initial reactivity studies of **1** established its behavior as a typical metal-centered radical. The reactions of phenyl disulfide and TEMPO with **1** in THF afforded the known thiolate [(C_5H_5)Ni(SPh)(IDipp)] (**4**)[9] and the new TEMPO adduct **5** in quantitative yield (Figure 3). The molecular structure of **5** shows a side-on η^2-coordinated TEMPO ligand and an η^1-coordinated Cp ligand at the distorted square planar nickel(II) atom. The structural parameters agree with presence of a formally anionic $TEMPO^-$ ligand.[10] A sharp ^{1}H NMR singlet at 5.93 ppm is observed for the Cp moiety even at –90 °C presumably due to rapid haptotropic migration (Figure S4, SI).

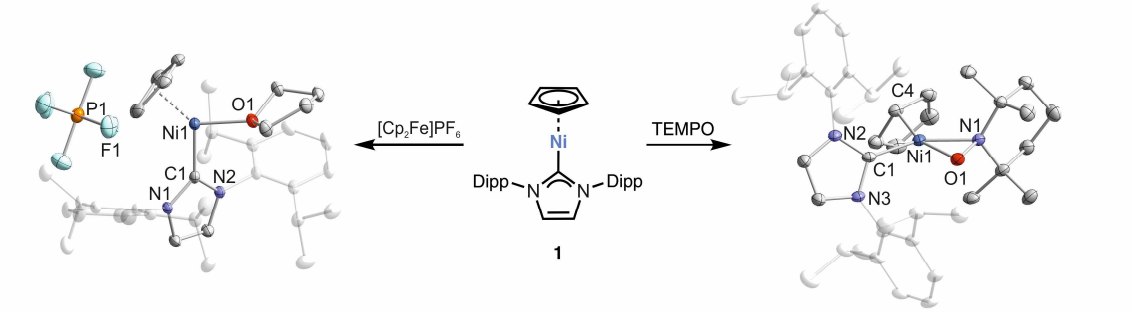

Figure 3. Reaction of **1** with TEMPO and $[Cp_2Fe]PF_6$, and solid-state molecular structures of [(C_5H_5)Ni(IDipp)(THF)] (**1-THF**, left) and [(C_5H_5)Ni(TEMPO)(IDipp)] (**5**, right). The hydrogen atoms are omitted for clarity. Thermal ellipsoids are drawn at 40% level. Selected bond lengths [Å] and angles [°] **1-THF**: Ni1-C1 1.903(2), $(C_5H_5)_{centroid}$-Ni1 1.77(1), C1-Ni1-$(C_5H_5)_{centroid}$ 131.3(1); **5**: Ni1-O1 1.8408(14), Ni1-N1 1.9581(16), N1-O1 1.3989(20), Ni1-C1 1.8824(19), Ni1-C4 2.034(2), C1-Ni1-O1 104.50(7), O1-Ni1-N1 43.07(6), C1-Ni1-C4 97.104(4), N1-Ni1-C4 115.325(2).

We next investigated the reactivity of **1** with the heavier chalcogens. The reaction with 1/8 S_8 gave the blue disulfide **6-S** and the purple trisulfide **7-S** (Figure 4 and 5) in a 7:3 ratio according to ^{1}H NMR analysis. **6-S** is soluble in *n*-hexane and diethyl ether and can thus be separated from **7-S** by extraction and subsequent crystallisation (SI). Disulfide-bridged dinuclear complexes with an M-S-S-M motif are well-known,[11] while complexes with an unsupported μ-S_3^{2-} bridge are still rather scarce.[11a,b,12]

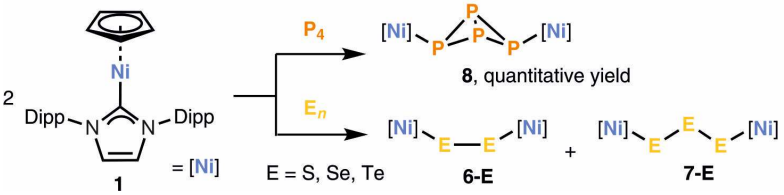

^{1}H NMR yield (isolated yield)		
E_n	6-E	7-E
S_8	70% (45%)	30% (15%)
Se_∞	82% (31%)	5% (/)
Te_∞	quant.(31%)	/

Figure 4. Reactions of **1** with P_4, S_8, Se_∞ and Te_∞.

The structure of **7-S** shows a similar S1-S2-S3 angle and S-S bond lengths as the structure of [{(C_5H_5)Fe(CO)$_2$}$_2$(μ-S_3)].[11a] Diselenide **6-Se** (31% isolated) is the major reaction product of **1** with one equivalent of elemental selenium. A ^{1}H NMR spectrum of the reaction mixture (THF, room temperature) shows that **6-Se** is formed in more than 80% yield whereas the triselenide **7-Se** is a minor by-product. Ditelluride **6-Te** was the only product to be detected after stirring **1** with one equivalent of grey tellurium for seven days. It was isolated as a dark brown crystalline solid in 31% yield. The molecular structures of **6-Se**, **6-Te** and **7-Se** are analogous to the corresponding sulfides **6-S** and **7-S** (Figure 5).

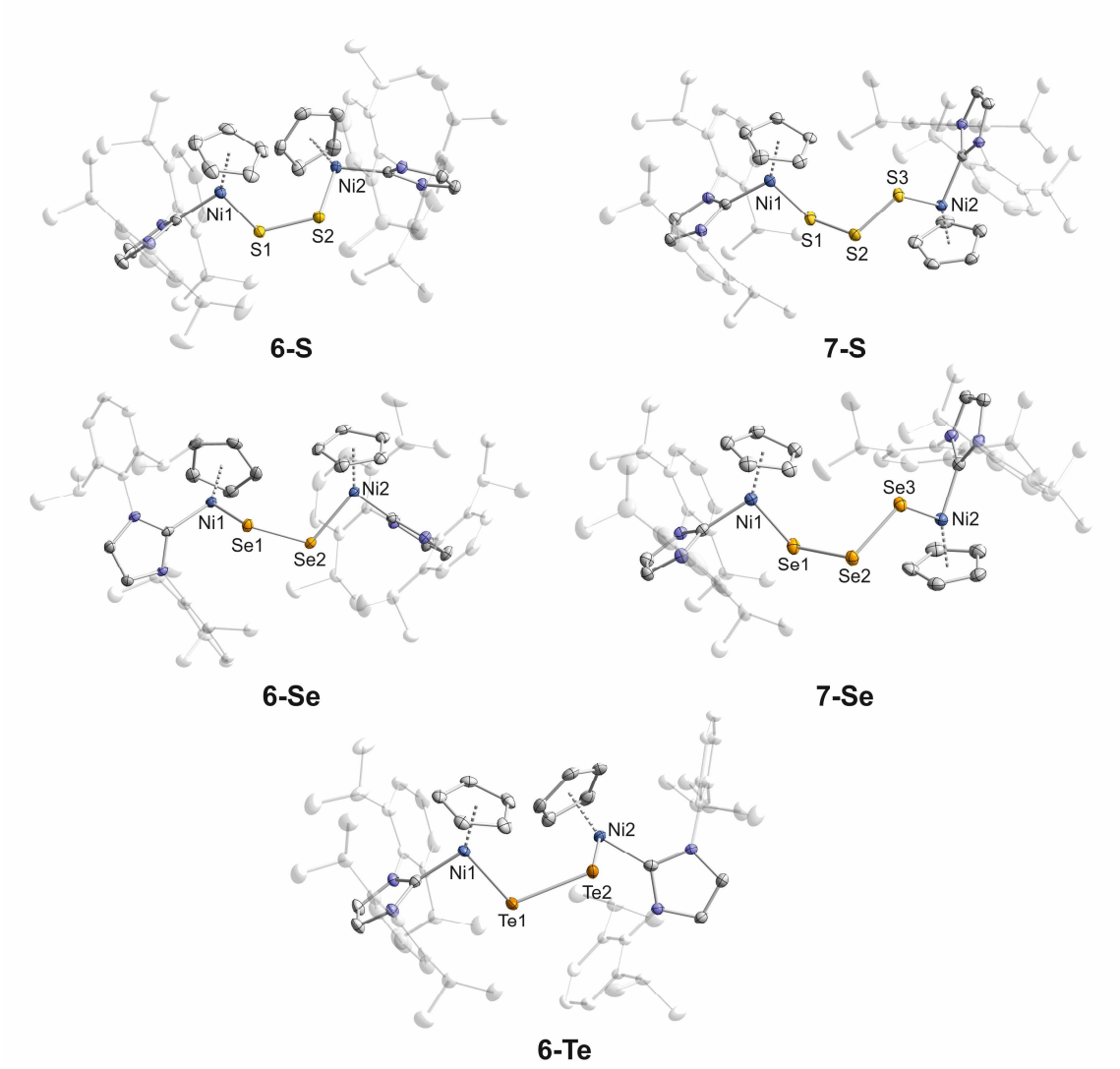

Figure 5. Solid-state molecular structures of the products **6-S** (left top), **7-S** (right top), **6-Se** (left centre), **7-Se** (right centre) and **6-Te** (bottom). The hydrogen atoms are omitted for clarity. Thermal ellipsoids are drawn at 40% level. Selected bond lengths [Å] and angles [°]: **6-S**: Ni1-S1/Ni2-S2 2.1800(1)/2.1797(1), S1-S2 2.0476(1), Ni1-S1-S2-Ni2 78.601(5); **7-S**: Ni1-S1/Ni2-S3 2.1936(6)/2.1748(5), S1-S2/S2-S3 2.0561(7)/2.0522(7), S1-S2-S3 111.58(3); **6-Se**: Ni1-Se1/Ni2-Se2 2.3013(4)/2.2998(4), Se1-Se2 2.3361(3), Ni1-Se1-Se2 109.039(1), Ni1-Se1-Se2-Ni2 91.174(1); **7-Se**: (the analogous bond distances and angles of a second crystallographically independent molecule in the asymmetric unit are given in parentheses) Ni1-Se1/Ni2-Se3 2.3068(6)/2.2838(6) (2.2847(6)/2.3341(5)), Se1-Se2/Se2-Se3 2.3335(4)/2.3318(5) (2.3282(5)/2.3341(5)), Ni1-Se1-Se2 108.480(2) (110.150(2)), Se1-Se2-Se3 109.117(2) (108.352(2)); **6-Te**: Ni1-Te1/Ni2-Te2 2.4769(4)/2.4741(4), Te1-Te2 2.7063(2), Ni1-Te1-Te2 108.928(1), Ni1-Se1-Se2-Ni2 93.951(1).

Considering that a mixture of at least two products is formed with sulfur and selenium, it was gratifying to discover that complex **1** reacts with P_4 in a highly selective fashion in THF at room temperature, giving tetraphosphide **8** as the sole product (Figure 4). The reaction is instantaneous, and compound **8** can be isolated as an analytically pure, dark purple powder in quantitative yield simply by removing the solvent.

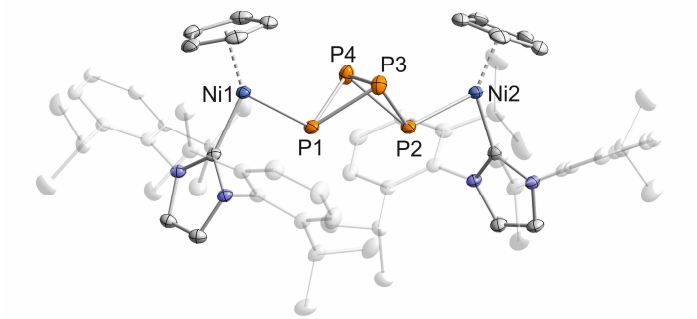

Figure 6. Solid-state molecular structures of **8**. The hydrogen atoms are omitted for clarity. Thermal ellipsoids are drawn at 40% level. Selected bond lengths [Å] and angles [°]: Ni1-P1/Ni2-P2 2.2107(6)/2.2103(6), P1-P3/P4 2.2334(7)/2.2111(7), P3-P4 2.1649(7), P1-P2 2.8897(8).

Its molecular structure (Figure 6) shows an exo/exo configuration for the two [(C_5H_5)Ni(IDipp)] units. The P−P bond lengths (2.2111(7) − 2.2334(7) Å) are very similar to those in P_4 (P−P 2.21 Å). The $^{31}P\{^1H\}$ NMR spectrum shows two triplets at δ = −307.4 and −45.8 ppm with $^1J_{P\text{-}P}$ = −190.5 Hz. These values are similar to those of [{$Cp^RFe(CO)_2$}$_2$(μ-η^1:η^1-P_4)] (Cp^R = C_5H_3-1,3-*t*Bu_2, C_5H_2-1,2,4-*t*Bu_3, C_5H-*i*Pr_4, C_5Me_5) and [{Cp*$Cr(CO)_3$}$_2$(μ-η^1:η^1-P_4)], which also display a tetraphospha[1.1.0]bicyclobutane framework.[13]

2.3 Conclusion

In conclusion, we have pepared rare mononuclear cyclopentadienyl nickel(I) complexes **1**–**3** with significant metalloradical character.[6,7] This feature was successfully utilized for the high-yield synthesis of the novel tetraphosphido complex [{(C_5H_5)Ni(IDipp)}$_2$(μ-η^1:η^1P_4)] (**8**), which features an uncommon μ-η^1:η^1-bridging P_4^{2-} ligand.[14] Further reactivity studies of **1**–**3** and **8** are in progress; the results will be reported in due course.

Notes and References

¶The hydride complex [(C_5H_5)NiH(IDipp)] (**1-H**) was identified as a minor by-product (5%) of the synthesis of **1**. Compound **1-H** was prepared independently and features a distinct molecular structure from **1**; see the supporting information (SI) for details.

§Based on DFT calculations, Hazari *et al.* attributed the bending of the $C_{carbene}$–Ni–$(C_5H_5)_{centroid}$ angle in the structure of **1** to the asymmetric spin density distribution.[7]

1 a) B. M. Cossairt, N. A. Piro, C. C. Cummins, *Chem. Rev.* **2010**, *110*, 4164; b) M. Caporali, L. Gonsalvi, A. Rossin, M. Peruzzini, *Chem. Rev.* **2010**, *110*, 4178; c) M. Scheer, G. Balázs, A. Seitz, *Chem. Rev.* **2010**, *110*, 4236.

2 a) G. L. Simon, L. F. Dahl, *J. Am. Chem. Soc.* **1973**, *95*, 2175; b) O. J. Scherer, H. Sitzmann, G. Wolmershäuser, *Angew. Chem. Int. Ed. Engl.* **1985**, *24*, 351; c) O. J. Scherer, T. Brück, *Angew. Chem. Int. Ed. Engl.* **1987**, *26*, 59; d) O. J. Scherer, M. Swarowsky, H. Swarowsky, G. Wolmershäuser, *Angew. Chem. Int. Ed. Engl.* **1988**, *27*, 694; e) M. Scheer, U. Becker, *Chem. Ber.* **1996**, *129*, 1307.

3 a) E. Urnežius, W. W. Brennessel, C. J. Cramer, J. E. Ellis, P. von R. Schleyer, *Science* **2002**, *295*, 832; b) E.-M. Schnöckelborg, J. J. Weigand, R. Wolf, *Angew. Chem. Int. Ed.* **2011**, *50*, 6657.

4 a) D. H. R. Barton, J. Zhu, *J. Am. Chem. Soc.* **1993**, *115*, 2071; b) D. H. Barton, R. A. Vonder Embse, *Tetrahedron* **1998**, *54*, 12475; c) S. L. Hinchley, C. A. Morrison, D. W. H. Rankin, C. L. B. Macdonald, R. J. Wiacek, A. Voigt, A. H. Cowley, M. F. Lappert, G. Gundersen, J. A. C. Clyburne, P. P. Power, *J. Am. Chem. Soc.* **2001**, *123*, 9045; d) N. A. Giffin, A. D. Hendsbee, T. L. Roemmele, M. D. Lumsden, C. C. Pye, J. D. Masuda, *Inorg. Chem.* **2012**, *51*, 11837.

5 B. de Bruin, D. G. H. Hetterscheid, A. J. J. Koekkoek, H. Grützmacher, *Progr. Inorg. Chem.* **2007**, 247.

6 a) P. L. Holland, T. R. Cundari, L. L. Perez, N. A. Eckert, R. J. Lachicotte, *J. Am. Chem. Soc.* **2002**, *124*, 14416; b) N. A. Eckert, A. Dinescu, T. R. Cundari, P. L. Holland, *Inorg. Chem.* **2005**, *44*, 7702; c) B. R. Dible, M. S. Sigman, A. M. Arif, *Inorg. Chem.* **2005**, *44*, 3774; d) C. A. Laskowski, G. L. Hillhouse, *J. Am. Chem. Soc.* **2008**, *130*, 13846; e) S. Yao, Y. Xiong, C. Milsmann, E. Bill, S. Pfirrmann, C. Limberg, M. Driess, *Chem. Eur. J.* **2010**, *16*, 436; f) C. J. E. Davies, M. J. Page, C. E. Ellul, M. F. Mahon, M. K. Whittlesey, *Chem. Commun.* **2010**, *46*, 5151; g) M. Vogt, B. de Bruin, H. Berke, M. Trincado, H. Grützmacher, *Chem. Sci.* **2011**, *2*, 723. h) K. Zhang, M. Conda-Sheridan, S. R. Cooke, J. Louie, *Organometallics* **2011**, *30*, 2546; i) S. Nagao, T. Matsumoto, Y. Koga, K. Matsubara, *Chem. Lett.* **2011**, *40*, 1036; j) C. A. Laskowski, D. J. Bungum, S. M. Baldwin, S. A. Del Ciello, V. M. Iluc, G. L. Hillhouse, *J. Am. Chem. Soc.* **2013**, *135*, 18272; k) M.

J. Page, W. Y. Lu, R. C. Poulten, E. Carter, A. G. Algarra, B. M. Kariuki, S. A. Macgregor, M. F. Mahon, K. J. Cavell, D. M. Murphy, M. K. Whittlesey, *Chem. Eur. J.* **2013**, *19*, 2158; l) R. C. Poulten, M. J. Page, A. G. Algarra, J. J. Le Roy, I. López, E. Carter, A. Llobet, S. A. Macgregor, M. F. Mahon, D. M. Murphy, M. Murugesu, M. K. Whittlesey, *J. Am. Chem. Soc.* **2013**, *135*, 13640.

7 J. Wu, A. Nova, D. Balcells, G. W. Brudvig, W. Dai, M. L. M. Guard, N. Hazari, P.-H. Lin, R. Pokhrel, M. K. Takase, *Chem. Eur. J.* **2014**, *18*, 5327.

8 S. Yao, Y. Xiong, C. Milsmann, E. Bill, S. Pfirrmann, C. Limberg, M. Driess, *Chem. Eur. J.* **2010**, *16*, 436.

9 D. A. Malyshev, N. M. Scott, N. Marion, E. D. Stevens, V. P. Ananikov, I. P. Beletskaya, S. P. Nolan, *Organometallics* **2006**, *25*, 446.

10 a) M. H. Dickman, R. J. Doedens, *Inorg. Chem.* **1982**, *21*, 682; b) M. K. Mahanthappa, K.-W. Huang, A. P. Cole, R. M. Waymouth, *Chem. Commun.* **2002**, 502; c) D. Isrow, B. Captain, *Inorg. Chem.* **2011**, *50*, 5864. d) D. G. H. Hetterscheid, J. Kaiser, E. Reijerse, T. P. J. Peters, S. Thewissen, A. N. J. Blok, J. M. M. Smits, R. de Gelder, B. de Bruin, *J. Am. Chem. Soc.* **2005**, *127*, 1895.

11 Selected examples: a) M. A. El-Hinnawi, A. A. Aruffo, B. D. Santarsiero, D. R. McAlister, V. Schomaker, *Inorg. Chem.* **1983**, *22*, 1585; b) N. Zhu, S. Du, X. Wu, J. Lu, *Angew. Chem. Int. Ed. Engl.* **1992**, *31*, 87; d) M. Emirdag-Eanes, J. A. Ibers, *Inorg. Chem.* **2001**, *40*, 6910; e) J. T. York, E. C. Brown, W. B. Tolman, *Angew. Chem. Int. Ed.* **2005**, *44*, 7745; f) J. Hu, G. Liu, Q. Jiang, R. Zhang, W. Huang, H. Yan, *Inorg. Chem.* **2010**, *49*, 11199; g) L.-P. Wei, Z.-G. Ren, L.-W. Zhu, W.-Y. Yan, S. Sun, H.-F. Wang, J.-P. Lang, Z.-R. Sun, *Inorg. Chem.* **2011**, *50*, 4493; h) E. M. Matson, M. D. Goshert, J. J. Kiernicki, B. S. Newell, P. E. Fanwick, M. P. Shores, J. R. Walensky, S. C. Bart, *Chem. Eur. J.* **2013**, *19*, 16167; i) J. Wallick, C. G. Riordan, G. P. A. Yap, *J. Am. Chem. Soc.* **2013**, *135*, 14972.

12 a) R. Steudel, M. Kustos, A. Prenzel, *Z. Naturforschung B; Chem. Sci.* **1997**, 79; b) E. Galardon, H. Daguet, P. Deschamps, P. Roussel, A. Tomas, I. Artaud, *Dalton Trans.* **2013**, *42*, 2817.

13 a) L. Weber, U. Sonnenberg, *Chem. Ber.* **1991**, 124, 725; b) P. Jutzi and S. Opiela, *J. Organomet. Chem.* **1992**, *431*, C29; c) O. J. Scherer, G. Schwarz, G. Wolmershäuser, *Z. Anorg. Allg. Chem.* **1996**, *622*, 95; d) O. J. Scherer, T. Hilt, G. Wolmershäuser, *Organometallics* **1998**, *17*, 4110; e) C. Schwarzmaier, PhD thesis, University of Regensburg **2012**.

14 For related work on P_4 activation by Ni^0 complexes, see: B. Zarzycki, T. Zell, D. Schmidt, U. Radius, *Eur. J. Inorg. Chem.* **2013**, 2051, and literature cited therein.

2.4 Supporting Information (SI)

2.4.1 General Procedures

All experiments were performed under an atmosphere of dry argon using standard Schlenk techniques or an MBraun UniLab glovebox. Solvents were purified, dried, and degassed with an MBraun SPS800 solvent purification system. NMR spectra were recorded on Bruker Avance 300 and Avance 400 spectrometers at 300 K and internally referenced to residual solvent resonances.[1,2] Melting points were measured on samples in sealed capillaries on a Stuart SMP10 melting point apparatus. UV/Vis spectra were recorded on a Varian Cary 50 spectrophotometer. Elemental analyses were determined by the analytical department of Regensburg University. The starting materials [IMesH]Cl, [(C_5H_5)NiCl(IDipp)], [(C_5Me_5)NiCl(IDipp)] were prepared according to literature procedures.[3–5] Yellow sulfur, grey selenium, grey tellurium, TEMPO, and $LiBEt_3H$ (1M solution in THF) were purchased from Aldrich and used as received.

2.4.2 Synthesis of [(C_5H_5)NiCl(IMes)]

The preparation of [CpNiCl(IMes)] is based on a published synthesis of [CpNiCl(IDipp)].[4] Cp_2Ni (2.00 g, 10.6 mmol, 1.0 eq.) and [IMesH]Cl (3.79 g, 11.1 mmol) were dissolved in THF (100 mL). The suspension was refluxed for 16 h. A colour change to dark purple was observed in the first 30 min. The solvent was subsequently removed and the residue was extracted with toluene (ca. 100 mL). The resulting solution was concentrated to ca. 20 mL. Purple crystals of [CpNiCl(IMes)] formed upon standing at room temperature. These were isolated, washed with *n*-pentane (10 mL), and dried *in vacuo*. Yield: 2.99 g (61%); m.p. >140 °C (slow decomp. to a black solid); UV/Vis (THF, λ_{max} /nm (ε_{max} /L·mol^{-1}·cm^{-1})): 321 (7300), 511 (400); elemental analysis calcd. for $C_{26}H_{29}ClN_2Ni$ (M = 465.7): C 67.06, H 6.71, N 6.02, found: C 67.36, H 6.22, N 5.91; ^{1}H NMR (d_8-THF, 300 K, 400.13 MHz) δ/ppm = 2.13 (s, 18H, CH_3), 4.71 (s, 5H, Cp), 6.19 (s, 2H, NC-H), 6.87 (s, 4H, *meta*-H_{Ar}); $^{13}C\{^1H\}$ NMR (d_8-THF, 300 K, 100.61 MHz) δ /ppm = 18.6 (CH_3), 21.1 (CH_3), 92.3 (Cp), 124.0 (N*C*-H), 129.4 (C_{Ar}), 137.3 (C_{Ar}), 139.0 (C_{Ar}), 168.8 (N*C*N).

2.4.3 Synthesis of [(C_5H_5)Ni(IDipp)] (1)

KC_8 (467 mg, 3.46 mmol, 1.1 eq) was added in small portions to a cooled (−80 °C) solution of [CpNiCl(IDipp)] (1.722 g, 3.143 mmol, 1.0 eq) in THF (100 mL). After stirring the reaction mixture for three days at room temperature, the solvent was removed, and the dark residue was extracted with toluene (6×120 mL). The solvent was removed, and the yellow solid was dried *in vacuo*. Compound **1** was isolated as yellow powder in 86% yield. In some instances, the ^{1}H NMR spectrum showed small signals of unknown impurities, which were removed by recrystallization from toluene giving yellow crystals of **1** in 51% yield; m.p. >95 °C (slow decomp. to a dark brown solid); UV/Vis (*n*-hexane, λ_{max} /nm (ε_{max} /L·mol^{-1}·cm^{-1})): 324 (8300), 402 (8100); effective magnetic moment (C_6D_6): μ_{eff} = 2.3(1) μ_B; elemental analysis calcd. for $C_{26}H_{29}N_2Ni$ (M = 428.2):

C 75.01, H 8.07, N 5.47, found: C 75.02, H 7.94, N 5.43; ^{1}H NMR (C_6D_6, 300 K, 300.13 MHz) δ/ppm = −40.7 (br s, 5H, Cp), 1.3 (br s, 12H, CH(CH_3)$_2$), 2.0 (br s, 12H, CH(CH_3)$_2$), 3.5 (br s, 2H, *para*-H_{Ar}), 5.1 (br s, 4H, *meta*-H_{Ar}), 6.8 (br s, 4H, CH(CH$_3$)$_2$), 26.5 (br s, 2H, NC-H).

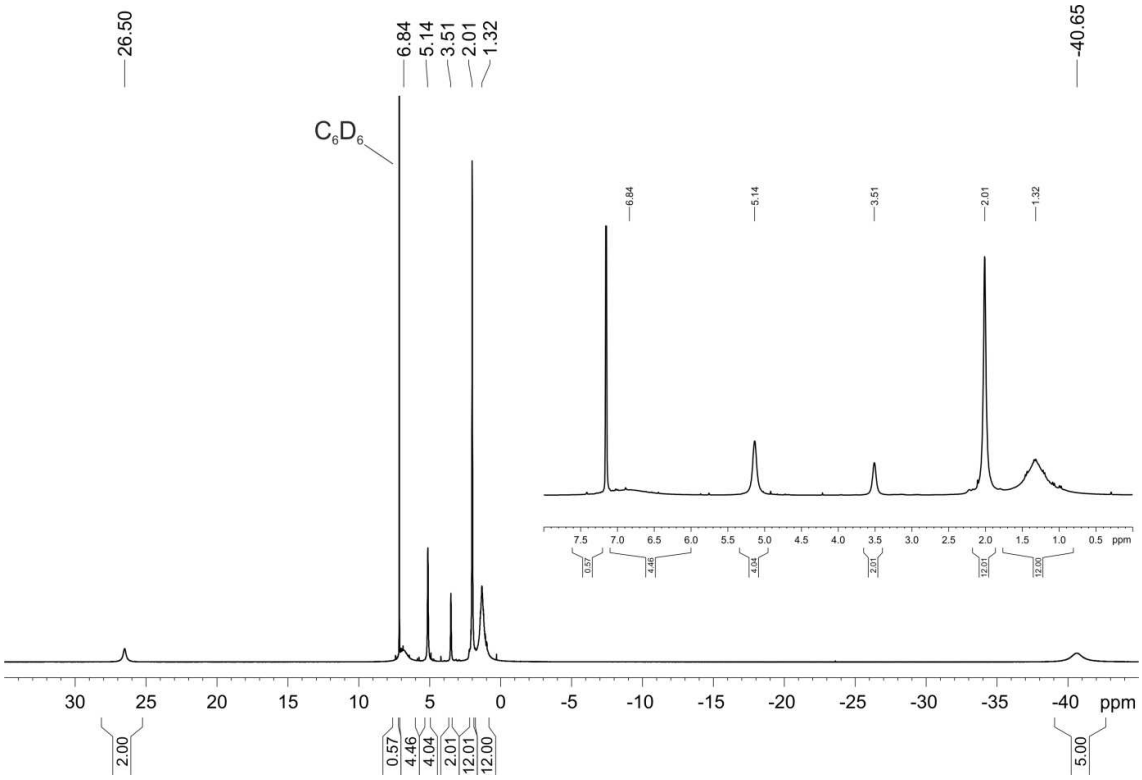

Figure S1. ^{1}H NMR spectrum of [(C_5H_5)Ni(IDipp)] (**1**, C_6D_6, 300 K, 400.13 MHz).

2.4.4 Synthesis of [(C_5H_5)Ni(IMes)] (2)

KC_8 (154.2 mg, 1.141 mmol, 1.05 eq) was added in small portions to a cooled (−80 °C) solution of [CpNiCl(IMes)] (503.7 g, 1.086 mmol, 1.0 eq) in THF (20 mL). The reaction mixture was stirred for 14 h at room temperature. The solvent was subsequently removed, and the dark residue was extracted with toluene (20 mL). The solution was concentrated to ca. 7 mL. Yellow crystals of **2** formed upon cooling this solution to −15 °C. Yield: 178 mg (38%); m.p. >87 °C (slow decomp. to a brown solid); UV/Vis (THF, λ_{max} /nm (ε_{max} /L·mol^{-1}·cm^{-1})): 337 (5400), 400 (4900), 425 (5700); effective magnetic moment (C_6D_6): μ_{eff} = 2.3(1) μ_B; elemental analysis calcd. for $C_{26}H_{29}N_2Ni$ (M = 428.2): C 72.93, H 6.83, N 6.54, found: C 73.39, H , N 6.78, N 6.44; ^{1}H NMR (C_6D_6, 300 K, 400.13 MHz) δ /ppm = −38.2 (br s, 5H, Cp), 1.6 (br s, 6H, *para*-CH_3), 3.5 (br s, 12H, *ortho*-CH_3), 4.6 (br s, 4H, *meta*-H_{Ar}), 25.4 (br s, 2H, NC-H). Compound **2** contains a small amount (<5% according to the ^{1}H NMR analysis) of putative [CpNiH(IMes)], which could not be removed by recrystallisation (see Figure S2).

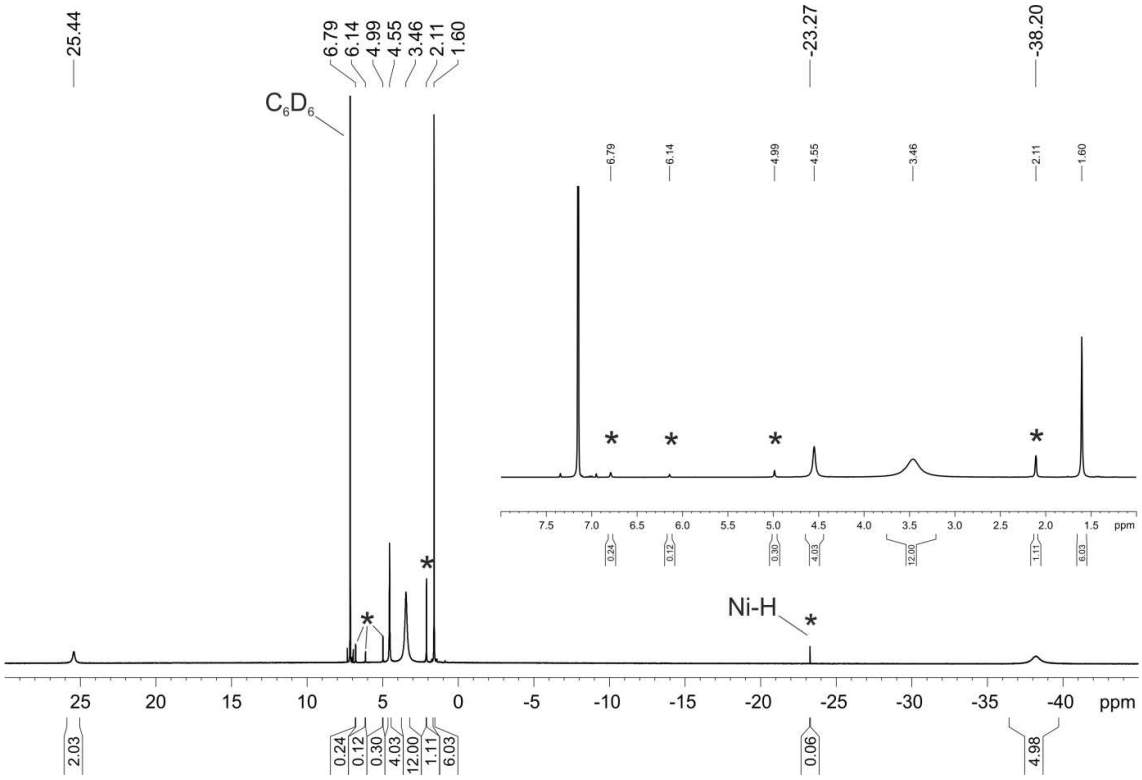

Figure S2. ^{1}H NMR spectrum of [(C_5H_5)Ni(IMes)] (**2**, C_6D_6, 300 K, 400.13 MHz). The signals assigned to the by-product [(C_5H_5)NiH(IMes)] are labeled with an asterisk.

2.4.5 Synthesis of [(C_5Me_5)Ni(IDipp)] (3)

KC_8 (115 mg, 0.853 mmol, 1.1 eq) was added in small portions to a cooled (−80 °C) solution of [(C_5Me_5)NiCl(IDipp)] (479 g, 0.775 mmol, 1.0 eq) in THF (20 mL). The solvent was removed after stirring the reaction mixture for four days at room temperature, and the dark residue was extracted with toluene (10 mL and 5 mL). The solution was concentrated to ca. 3 mL. Yellow crystals of **3** formed upon cooling this solution to −35 °C Yield: 246 mg (55%); m.p. >98 °C (slow decomp. to a black solid); UV/Vis (*n*-hexane, λ_{max} /nm (ε_{max} /L·mol^{-1}·cm^{-1})): sh351 (6600), 371 (7100), 476 (9400); effective magnetic moment (C_6D_6): μ_{eff} = 2.2(1) μ_B; elemental analysis calcd. for $C_{37}H_{51}N_2Ni$ (M = 582.5): C 76.29, H 8.83, N 4.81, found: C 76.56, H , N 8.67, N 4.69; ^{1}H NMR (C_6D_6, 300 K, 400.13 MHz) δ/ppm = 1.8 (br s, 12H, CH(CH_3)$_2$), 2.7−2.9 (br m, 16H, CH(CH_3)$_2$/*para*-H), 5.6 (br s, 4H, *meta*-H_{Ar}), 6.30 (br s, 4H, CH(CH_3)$_2$), 30.8 (br s, 2H, NC-H), 103.6 (br s, 15H, C_5Me_5).

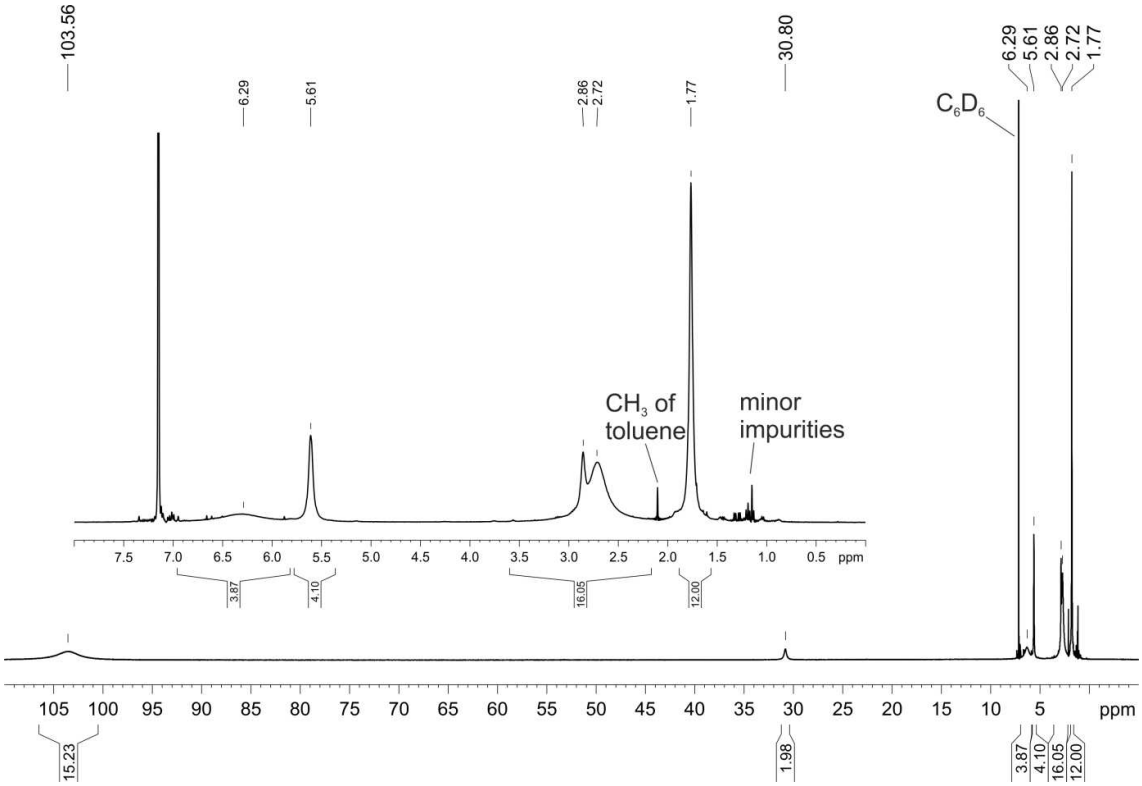

Figure S3. ^{1}H NMR spectrum of [(C_5Me_5)Ni(IDipp)] (**3**, C_6D_6, 300 K, 400.13 MHz).

2.4.6 Synthesis of [(C_5H_5)Ni(SPh)(IDipp)] (4)

A solution of **1** (28.2 mg, 0.0550 mmol, 2.0 eq.) in THF (3 mL) was added to a solution of phenyl disulfide (6.0 mg, 0.027 mmol, 1.0 eq.) in THF (3 mL) at room temperature. The solvent was removed after stirring the reaction solution for 20 min, and the crude product was extracted with *n*-hexane. Dark brown crystals formed upon cooling the solution to −35 °C. Yield: 21 mg (62%); elemental analysis calcd. for $C_{38}H_{46}N_2NiS$ (*M* = 621.6): C 73.43, H 7.46, N 4.51, found: C 73.20, H 7.49, N 4.23; ^{1}H NMR ($CDCl_3$, 300 K, 400.13 MHz) δ/ppm = 1.08 (d, $^{3}J_{HH}$ = 6.9 Hz, 12H, CH(C*H*$_3$)$_2$), 1.39 (d, $^{3}J_{HH}$ = 6.9 Hz, 12H, CH(C*H*$_3$)$_2$), 2.90 (bs, 4H, C*H*(CH$_3$)$_2$), 4.56 (s, 5H, Cp), 6.64 (m, 3H, *meta*-/*para*-H$_{Ph}$), 6.86 (m, 2H, *ortho*-H$_{Ph}$), 7.09 (s, 2H, NC-H), 7.30 (d, $^{3}J_{HH}$ = 7.8 Hz, 4H, *meta*- H$_{Dipp}$), 7.46 (t, $^{3}J_{HH}$ = 7.8 Hz, 2H, *para*- H$_{Dipp}$); ^{13}C{^{1}H} NMR (ppm): 22.5, 26.2, 28.8, 92.1, 120.0, 123.9, 125.2, 126.2, 129.9, 137.1, 146.2, 148.2 174.4.

2.4.7 Synthesis of [(C_5H_5)Ni(TEMPO)(IDipp)] (5)

A solution of TEMPO (19.4 mg, 0.124 mmol, 1.0 eq.) in toluene (2 mL) was added to a solution of **1** (63.6 mg, 0.124 mmol, 1.0 eq.) in toluene (2 mL) at room temperature. The reaction solution was slightly reduced in volume after stirring for 1 h. Dark pink X-ray quality crystals of **5** formed after cooling the solution to −35 °C. Yield: 68 mg (65%); m.p. >70 °C (slow decomp. to a dark brown oil); UV/Vis (*n*-hexane, λ_{max} /nm (ε_{max} /L·mol^{-1}·cm^{-1})): 510 (593); elemental analysis calcd. for $C_{41}H_{59}N_3NiO$ (*M* = 668.6): C 73.65, H 8.89, N 6.28, found: C 73.69, H 8.77, N 6.34; ^{1}H NMR (C_6D_6, 300 K, 400.13 MHz) δ/ppm = 0.89 (s, 6H, CH$_3$-TEMPO), 0.96−1.28 (m, 4H,

CH_2), 1.00 (d, $^3J_{HH}$ = 6.8 Hz, 12H, CH(C*H*$_3$)$_2$), 1.46-1.56 (m, 2H, CH_2), 1.46 (d, $^3J_{HH}$ = 6.8 Hz, 12H, CH(C*H*$_3$)$_2$), 1.67 (s, 6H, CH_3-TEMPO), 3.12 (sept, $^3J_{HH}$ = 6.8 Hz, 4H, C*H*(CH$_3$)$_2$), 5.93 (s, 5H, Cp), 6.61 (s, 2H, NC-H), 7.24 (d, $^3J_{HH}$ = 7.5 Hz, 4H, *meta*-H$_{Ar}$), 7.32 (t, $^3J_{HH}$ = 7.7 Hz, 2H, *para*-H$_{Ar}$); $^{13}C\{^1H\}$ NMR (C_6D_6, 300 K, 100.61 MHz) δ/ppm = 16.9 (N-CH$_2$-*C*H$_2$), 22.6 (CH(*C*H$_3$)$_2$), 23.3 (CH_3-TEMPO), 26.5 (CH(*C*H$_3$)$_2$), 29.1 (*C*H(CH$_3$)$_2$), 31.9 (CH_3-TEMPO), 37.1 (N-*C*H$_2$-CH$_2$), 63.1 (ON*C*), 109.6 (Cp), 124.0 (*meta*-C), 125.5 (N*C*-H), 130.1 (p*ara*-C), 137.3 (*ipso*-C), 147.0 (*ortho*-C), 183.6 (N*C*N).

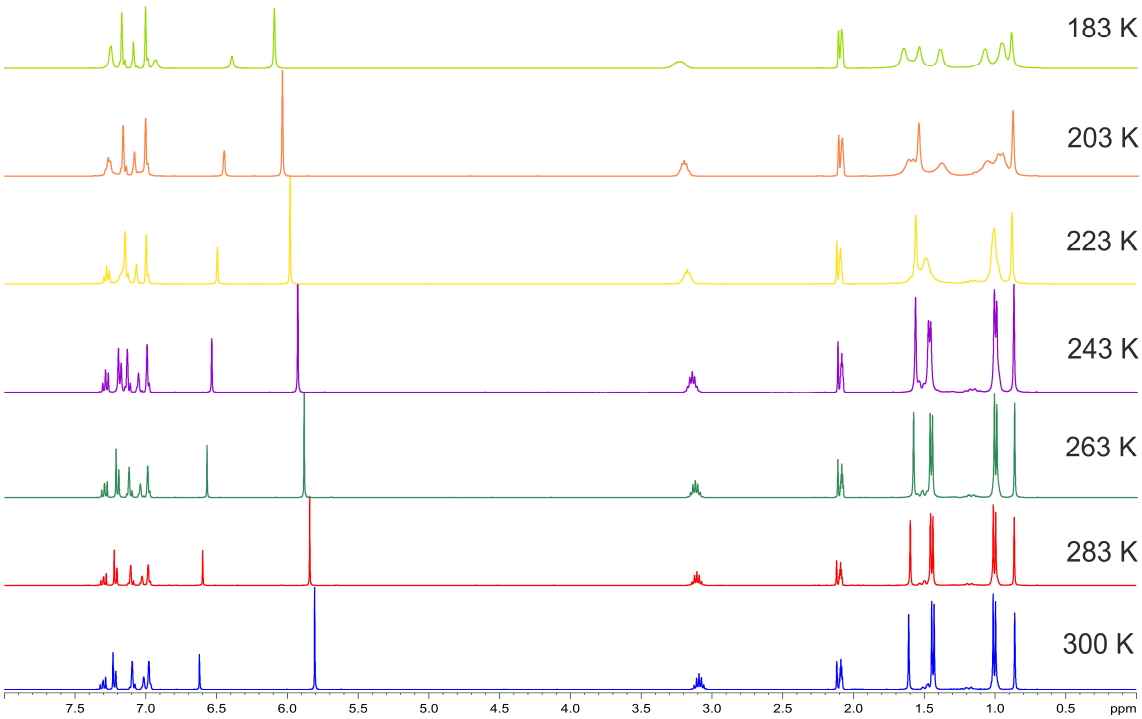

Figure S4. ^{1}H NMR spectrum of **[**(C_5H_5)Ni(TEMPO)(IDipp)] (**5**, C_7D_8, 400.13 MHz) at different temperatures.

2.4.8 Synthesis of [(C_5H_5)Ni(IDipp)$_2$(μ-η^1:η^1-S_2)] (6-S) and [(C_5H_5)Ni(IDipp)$_2$(μ-η^1:η^1-S_3)] (7-S)

S_8 (6.7 mg, 0.026 mmol, 1.0 eq.) was added to a solution of **1** (107.1 mg, 0.209 mmol, 8.0 eq.) in THF (5 mL) at room temperature. The resulting dark green solution was stirred for 14 h, and the solvent was removed afterwards. Blue X-ray quality crystals of **6-S** were obtained by extracting the raw product with *n*-hexane and cooling the solution to −35 °C. Yield (**6-S**): 47 mg (42%). The solid residue of the *n*-hexane extract was washed with diethyl ether. **7-S** was obtained as a purple powder by extracting the residue with THF and removing of the solvent of this filtrate. Yield (**7-S**): 18 mg (15%). X-ray quality crystals were obtained by cooling a concentrated solution of **7-S** in toluene to −35 °C. Analytical data for **6-S**: m.p. >195 °C (slow decomp. to a dark grey solid); UV/Vis (*n*-hexane, λ_{max} /nm (ε_{max} /L·mol^{-1}·cm^{-1})): 415 (5900), sh540 (4238), 635 (10046); elemental analysis calcd. for $C_{64}H_{82}N_4Ni_2S_2$ (*M* = 1088.9): C 70.59, H 7.59, N 5.15, found: C 70.57, H 7.44, N 4.95; ^{1}H NMR (C_6D_6, 300 K, 400.13 MHz) δ/ppm = 0.96 (d, $^3J_{HH}$ = 6.7 Hz, 24H,

CH(C*H*$_3$)$_2$), 1.52 (d, $^3J_{HH}$ = 6.7 Hz, 24H, CH(C*H*$_3$)$_2$), 3.14 (bs, 8H, C*H*(CH$_3$)$_2$), 4.65 (s, 10H, Cp), 6.45 (s, 4H, NC-H), 7.17−7.26 (m, 12H, H$_{Ar}$); ^{13}C{^{1}H} NMR (C$_6$D$_6$, 300 K, 100.61 MHz) δ/ppm = 23.2 (CH(*C*H$_3$)$_2$), 26.0 (CH(*C*H$_3$)$_2$), 28.9 (*C*H(CH$_3$)$_2$), 94.1 (Cp), 124.1 (N*C*-H), 124.7 (*meta*-C), 130.0 (p*ara*-C), 137.8 (*ipso*-C), 146.2 (*ortho*-C), 181.3 (N*C*N). Analytical data for **7-S**: m.p. >173 °C (slow decomp. to a dark solid); UV/Vis (THF, λ_{max} /nm (ε_{max} /L·mol^{-1}·cm^{-1})): 370 (6000), 531 (8455); elemental analysis calcd. for C$_{64}$H$_{82}$N$_4$Ni$_2$S$_3$·C$_4$H$_8$O (*M* = 1121.0): C 68.46, H 7.60, N 4.70, found: C 68.04, H 7.14, N 4.67; ^{1}H NMR (*d*$_8$-THF, 300 K, 400.13 MHz) δ/ppm = 0.94 (d, $^3J_{HH}$ = 6.7 Hz, 24H, CH(C*H*$_3$)$_2$), 1.47 (d, $^3J_{HH}$ = 6.7 Hz, 24H, CH(C*H*$_3$)$_2$), 3.06 (bs, 8H, C*H*(CH$_3$)$_2$), 5.21 (s, 10H, Cp), 6.50 (s, 4H, NC-H), 7.19-7.33 (m, 12H, H$_{Ar}$); ^{13}C{^{1}H} NMR (*d*$_8$-THF, 300 K, 100.61 MHz) δ/ppm = 23.0 (CH(*C*H$_3$)$_2$), 26.1 (CH(*C*H$_3$)$_2$), 29.3 (*C*H(CH$_3$)$_2$), 92.2 (Cp), 124.3 (N*C*-H), 126.2 (*meta*-C), 130.1 (p*ara*-C), 138.3 (*ipso*-C), 147.1 (*ortho*-C), 178.6 (N*C*N).

2.4.9 Synthesis of [(C$_5$H$_5$)Ni(IDipp)$_2$(*μ*-η^1:η^1-Se$_2$)] (6-Se)

Grey selenium (28.1 mg, 0.357 mmol, 1.0 eq.) was added to a solution of **1** (183.0 mg, 0.357 mmol, 1.0 eq.) in THF (5 mL) at room temperature. The resulting dark green solution was stirred for 16 h, and the solvent was removed afterwards. The residue was extracted with toluene, and the solution was layered with *n*-hexane to afford X-ray quality crystals of **6-Se** at room temperature overnight. The ^{1}H NMR spectrum of these crystals shows the presence of compound **7-Se** (ca. 10%) which was characterised by X-ray crystallography. Yield: 30 mg (31%); m.p. >173 °C (decomp. to a black oil); UV/Vis (THF, λ_{max} /nm (ε_{max} /L·mol^{-1}·cm^{-1})): 435 (6000), 650 (5500); elemental analysis calcd. for C$_{64}$H$_{82}$N$_4$Ni$_2$Se$_2$·0.5(C$_6$H$_{14}$) (*M* = 1225.8): C 65.65, H 7.32, N 4.57, found: C 66.05, H 7.33, N 4.49; ^{1}H NMR (C$_6$D$_6$, 300 K, 400.13 MHz) δ/ppm = 0.95 (d, $^3J_{HH}$ = 6.7 Hz, 24H, CH(C*H*$_3$)$_2$, **6-Se**), 1.14 (d, $^3J_{HH}$ = 6.9 Hz, 2.4H, CH(C*H*$_3$)$_2$, **7-Se**), 1.48 (d, $^3J_{HH}$ = 6.9 Hz, 2.4H, CH(C*H*$_3$)$_2$, **7-Se**), 1.52 (d, $^3J_{HH}$ = 6.7 Hz, 24H, CH(C*H*$_3$)$_2$, **6-Se**), 2.87 (sept., 0.8H, $^3J_{HH}$ = 6.9 Hz, C*H*(CH$_3$)$_2$, **7-Se**), 3.11 (br s, 8H, C*H*(CH$_3$)$_2$, **6-Se**), 4.65 (s, 10H, Cp, **6-Se**), 5.18 (s, 1H, Cp, **7-Se**), 6.30 (s, 0.4H, NC-H, **7-Se**), 6.51 (s, 4H, NC-H, **6-Se**), 7.12−7.27 (m, 13H, H$_{Ar}$, 6-**Se**/**7-Se**); ^{13}C{^{1}H} NMR (C$_6$D$_6$, 300 K, 100.61 MHz) δ/ppm = 23.1 (CH(*C*H$_3$)$_2$), 26.2 (CH(*C*H$_3$)$_2$), 29.0 (*C*H(CH$_3$)$_2$), 94.4 (Cp), 124.0 (N*C*-H), 124.9 (*meta*-C), 130.0 (p*ara*-C), 137.8 (*ipso*-C), 146.4 (*ortho*-C), 182.4 (N*C*N).

2.4.10 Synthesis of [(C$_5$H$_5$)Ni(IDipp)$_2$(*μ*-η^1:η^1-Te$_2$)] (6-Te)

Grey tellurium (18.1 mg, 0.142 mmol, 1.0 eq.) was added to a solution of **1** (72.7 mg, 0.142 mmol, 1.0 eq.) in THF (5 mL) at room temperature. The suspension was stirred for 7 days. A slow colour change from dark yellow to dark brown was observed. The solvent was removed, and the dark residue was extracted with diethyl ether. Cooling to −35 °C gave dark brown crystals of **6-Te**. Yield: 30 mg (31%) X-ray quality crystals were grown from a concentrated solution of

6-Te in *n*-hexane at room temperature; m.p. >165 °C (slow decomp. to a grey solid); UV/Vis (THF, λ_{max} /nm (ε_{max} /L·mol^{-1}·cm^{-1})): 308 (27800), 460 (6670), 521 (5670), 669 (5170); elemental analysis calcd. for $C_{64}H_{82}N_2Ni_2S_2 \cdot 0.5(C_4H_{10}O)$ (*M* = 1317.0): C 60.19, H 6.66, N 4.25, found: C 60.31, H 6.54, N 4.27; ^{1}H NMR (C_6D_6, 300 K, 400.13 MHz) δ/ppm = 0.93 (d, $^3J_{HH}$ = 6.7 Hz, 24H, CH(C*H*$_3$)$_2$), 1.51 (d, $^3J_{HH}$ = 6.7 Hz, 24H, CH(C*H*$_3$)$_2$), 3.15 (bs, 8H, C*H*(CH$_3$)$_2$), 4.70 (s, 10H, Cp), 6.45 (s, 4H, NC-H), 7.16 (m, 4H, *ortho*-H$_{Ar}$), 7.22 (m, 8H, *meta*- H$_{Ar}$); ^{13}C{^{1}H} NMR (C_6D_6, 300 K, 100.61 MHz) δ/ppm = 23.5 (CH(*C*H$_3$)$_2$), 26.2 (CH(*C*H$_3$)$_2$), 29.2 (*C*H(CH$_3$)$_2$), 94.9 (Cp), 124.1 (N*C*-H), 125.2 (*meta*-C), 130.0 (p*ara*-C), 138.0 (*ipso*-C), 146.4 (*ortho*-C), 186.3 (N*C*N).

2.4.11 Synthesis of [(C$_5$H$_5$)Ni(IDipp)$_2$(*μ*-η^1:η^1-P$_4$)] (8)

P_4 (79.4 mg, 0.641 mmol, 1.0 eq.) was added to a solution of **1** (656.7 mg, 1.28 mmol, 2.0 eq.) in THF (20 mL) at room temperature. The resulting dark red solution was stirred for 2 h. Afterward, the solvent was removed completely. Compound **8** remained as an analytically pure, red powder. Yield: 727 mg (99%). Dark purple X-ray quality crystals formed by diffusing *n*-hexane into a concentrated THF solution of **8**; m.p. >160 °C (slow decomp. to a black and colourless solid); UV/Vis (THF, λ_{max} /nm (ε_{max} /L·mol^{-1}·cm^{-1})): 395 (23700), 420 (10700), 508 (10700); elemental analysis calcd. for $C_{64}H_{82}N_4Ni_2P_4$ (*M* = 1148.7): C 66.92, H 7.20, N 4.88, found: C 66.85, H 7.23, N 4.61; ^{1}H NMR (d$_8$-THF, 300 K, 400.13 MHz) δ/ppm = 1.06 (d, $^3J_{HH}$ = 6.8 Hz, 24H, CH(C*H*$_3$)$_2$), 1.43 (d, $^3J_{HH}$ = 6.8 Hz, 24H, CH(C*H*$_3$)$_2$), 3.03 (bs, 8H, C*H*(CH$_3$)$_2$), 4.29 (s, 10H, Cp), 7.29 (s, 4H, NC-H), 7.36 (d, $^3J_{HH}$ = 7.8 Hz, 8H, *meta*-H$_{Ar}$), 7.49 (t, $^3J_{HH}$ = 7.8 Hz, 4H, *para*-H$_{Ar}$); ^{13}C{^{1}H} NMR (d$_8$-THF, 300 K, 100.61 MHz) δ/ppm = 23.6 (CH(*C*H$_3$)$_2$), 26.2 (CH(*C*H$_3$)$_2$), 29.4 (*C*H(CH$_3$)$_2$), 91.0 (Cp), 124.4 (*meta*-C), 125.7 (N*C*-H), 130.2 (p*ara*-C), 138.4 (*ipso*-C), 147.0 (*ortho*-C), 185.6 (N*C*N); ^{31}P{^{1}H} NMR: (d$_8$-THF, 300 K, 121.49 MHz) δ/ppm = −307.4 (t, $^1J_{PP}$ = −190.5 Hz, 2P), −45.8 (t, $^1J_{PP}$ = −190.5 Hz, 2P).

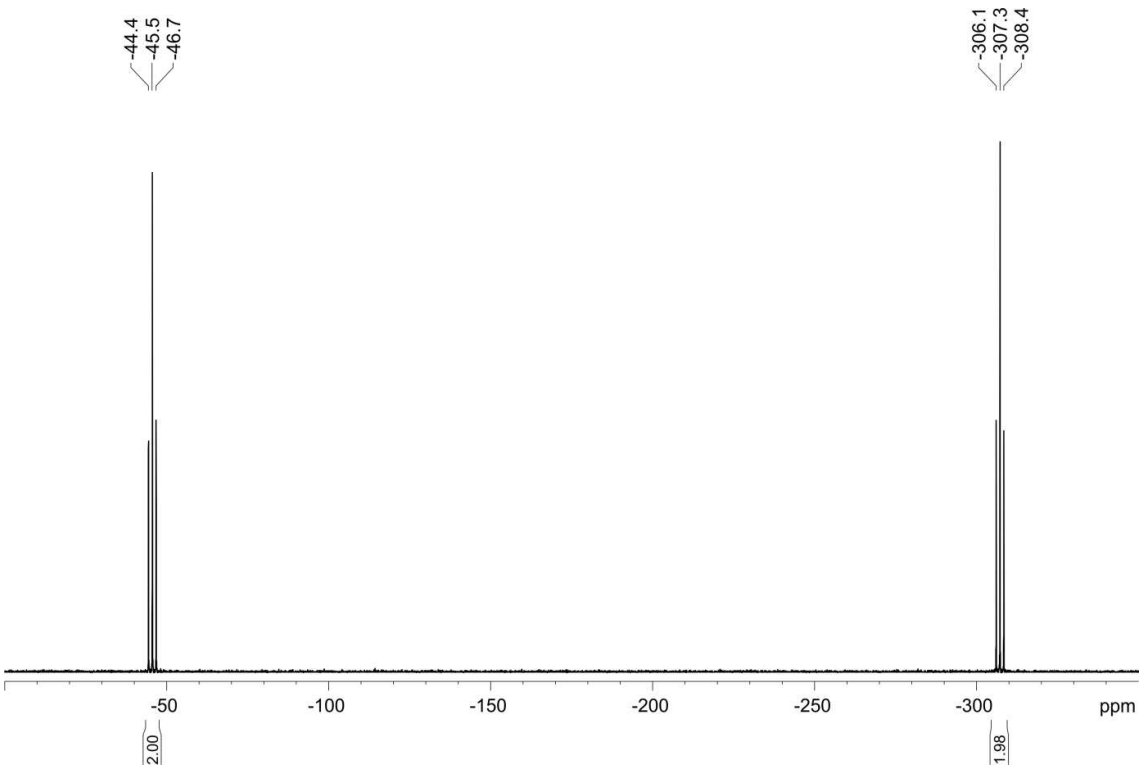

Figure S5. $^{31}P\{^{1}H\}$ NMR spectrum of the reaction solution of [(C_5H_5)Ni(IDipp)(μ-η^1:η^1-P_4)] (**8**, C_6D_6, 300 K, 121.49 MHz,).

2.4.12 Synthesis of 1-H

An 1M solution of $LiBEt_3H$ (0.50 mL, 0.50 mmol, 1.0 eq.) was added to a solution of [(C_5H_5)NiCl(IDipp)] (274 mg, 0.500 mmol, 1.0 eq.) in THF (10 mL) dropwise at 0 °C. The solution was allowed to warm up to room temperature, and was stirred for 14 h. The solvent of the resulting red solution was removed and extracted with 20 mL *n*-hexane. X-ray quality, red crystals of **1-H** formed upon cooling the solution to −15 °C. Yield: 98 mg (38%); m.p. >185 °C (slow decomp. to a dark green solid); UV/Vis (*n*-hexane, λ_{max} /nm (ε_{max} /L·mol^{-1}·cm^{-1})): 365 (4500), 429 (710), 510 (150); elemental analysis calcd. for $C_{32}H_{42}N_2Ni$ (*M* = 513.4): C 74.86, H 8.25, N 5.46, found: C 74.65, H 8.20, N 5.35; ^{1}H NMR (C_6D_6, 300 K, 400.13 MHz) δ/ppm = −23.64 (s,1H, Ni-H),1.07 (d, $^{3}J_{HH}$ = 6.8 Hz, 12H, CH(CH_3)$_2$), 1.45 (d, $^{3}J_{HH}$ = 6.8 Hz, 12H, CH(CH_3)$_2$), 2.92 (sept, $^{3}J_{HH}$ = 6.8 Hz, 4H, CH(CH$_3$)$_2$), 4.91 (s, 5H, Cp), 6.45 (s, 2H, NC-H), 7.14 (d, $^{3}J_{HH}$ = 7.7 Hz, 4H, *meta*- H_{Ar}), 7.24 (t, $^{3}J_{HH}$ = 7.7 Hz, 2H, *para*- H_{Ar}); $^{13}C\{^{1}H\}$ NMR (C_6D_6, 300 K, 100.61 MHz) δ/ppm = 23.1 (CH(*C*H$_3$)$_2$), 24.9 (CH(*C*H$_3$)$_2$), 28.9 (*C*H(CH$_3$)$_2$), 86.9 (Cp), 122.5 (N*C*-H), 124.0 (*meta*-C), 129.7 (p*ara*-C), 138.7 (*ipso*-C), 146.2 (*ortho*-C), 188.6 (N*C*N).

2.4.13 Synthesis of 1-THF

[Cp_2Fe]PF_6 (10.8 mg, 0.0326 mmol, 1.0 eq.) was added to a solution of **1** (16.7 mg, 0.0326 mmol, 1.0 eq.) in THF (3 mL) at room temperature. The suspension was stirred for 14 h, and the solvent was removed afterwards. The residue was washed with *n*-hexane (ca. 3 mL) and extracted with THF (1.5 mL). Dark pink X-ray quality crystals of **1-THF** formed upon diffusing *n*-hexane into

the THF solution. The ^{1}H NMR spectrum of these crystals shows the presence of an unidentified by-product (ca. 10%). Yield: 10 mg (42%); m.p. >120 °C (decomp. to a brown solid); UV/Vis (THF, λ_{max} /nm (ε_{max} /L·mol^{-1}·cm^{-1})): 516 (467); elemental analysis calcd. for $C_{36}H_{49}N_2F_6NiOP$ (M = 729.46): C 59.28, H 6.77, N 3.84, found: C 58.84, H 6.52, N 3.79; ^{1}H NMR (d_8-THF, 300 K, 400.13 MHz) δ/ppm = 1.20 (d, $^3J_{HH}$ = 6.6 Hz, 12H, CH(CH_3)$_2$, **1-THF**), 1.24 (d, $^3J_{HH}$ = 6.7 Hz, 1.2H, CH(CH_3)$_2$, by-product), 1.32 (d, $^3J_{HH}$ = 6.7 Hz, 1.2H, CH(CH_3)$_2$, by-product), 1.50 (d, $^3J_{HH}$ = 6.6 Hz, 12H, CH(CH_3)$_2$, **1-THF**), 1.80 (m, 4H, THF), 2.54 (m, 0.4H, CH(CH$_3$)$_2$, by-product), 3.13 (m, 4H, CH(CH$_3$)$_2$, **1-THF**), 4.60 (s, 5H, Cp, **1-THF**), 7.46 – 7.64 (m, 0.3H, H$_{Ar}$, by-product), 7.48−7.67 (m, 6H, H$_{Ar}$, **1-THF**), 7.73 (s, 2H, NC-H, **1-THF**) 8.17 (s, 0.2H, NC-H, by-product) 9.44 (s, 0.1H, NCHN, by-product); ^{13}C{^{1}H} NMR (C_6D_6, 300 K, 100.61 MHz) δ/ppm = 22.5 (CH(*C*H$_3$)$_2$), 29.8 (*C*H(CH$_3$)$_2$), 94.9 (Cp), 125.4 (N*C*-H), 129.1 (*meta*-C), 131.5 (p*ara*-C), 132.8 (*ipso*-C), 146.2 (*ortho*-C); ^{19}F NMR (d_8-THF, 300 K, 100.61 MHz) δ/ppm = 72.8 (d, $^1J_{FP}$ = 710 Hz, 6F, PF_6); ^{31}P{^{1}H} NMR (d_8-THF, 300 K, 121.49 MHz) δ/ppm = −141.6 (sept., $^1J_{FP}$ = 710 Hz, 1P, PF_6).

2.5 X-ray Crystallography

The single crystal X-ray diffraction data were recorded on an Agilent Technologies SuperNova diffractometer or, in case of compounds **2** and **3**, with an Agilent Technologies Gemini Ultra R with Cu K$_\alpha$ radiation (λ = 1.54178 Å). The data for **1-H** were recorded with an Agilent Technologies SuperMova diffractometer with Mo K$_\alpha$ radiation (λ = 0.71073 Å). Either semi-empirical multi-scan absorption corrections[6] or analytical ones[7] were applied to the data. The structures were solved with SHELXS[8] or SIR[9] and least-square refinements on F^2 were carried out with SHELXL.[7]

CCDC 995931-995941 contain the supplementary crystallographic data for this paper. These data can be obtained free of charge from The Cambridge Crystallographic Data Centre via www.ccdc.cam.ac.uk/data_request/cif.

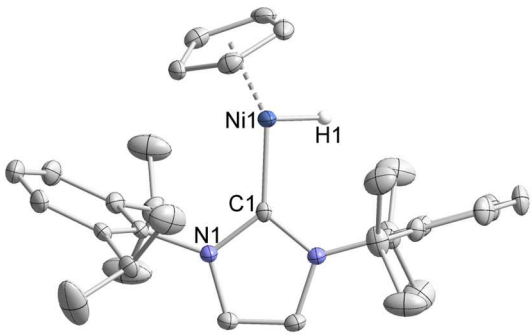

Figure S6. Solid-state molecular structure of **1-H**. Except for H1 the hydrogen atoms are omitted for clarity. Thermal ellipsoids are drawn at 40% level. Selected bond lengths [Å] and angles [°] the analogous bond distances and angles of the second molecule in the asymmetric unit are pointed out in brackets: Ni1-C1 1.849(4) (1.838(4)), (C$_5$H$_5$)$_{centroid}$-Ni1 1.77(1) (1.75(1)), C1-Ni1-(C$_5$H$_5$)$_{centroid}$ 148.3(1) (145.9(1)).

Table S1. Crystallographic data of **1**, **2**, **3**, **5**, **6-S**, **7-S**, **6-Se**, **7-Se**, **6-Te**, **8**, **1-H**, **1-THF**.

Compound	**1**	**2**	**3**
Empirical formula	$C_{32}H_{41}N_2Ni$	$C_{26}H_{29}N_2Ni$	$C_{37}H_{51}N_2Ni$
Formula weight	512.38	428.22	582.50
Temperature [K]	123(1)	123(1)	123(1)
Crystal system	triclinic	orthorhombic	monoclinic
Space group	*P*-1	*Pnma*	$P2_1/n$
a [Å]	9.1771(3)	22.89090(10)	9.23970(10)
b [Å]	9.3242(3)	11.10740(10)	18.6957(2)
c [Å]	18.2253(5)	9.03710(10)	21.5074(2)
α [°]	92.783(2)	90	90
β [°]	90.158(2)	90	93.7790(10)
γ [°]	116.159(3)	90	90
Volume [Å^3]	1397.63(7)	2297.76(3)	3707.17(7)
Z	2	4	4
ρ_{calc} [g/cm^3]	1.218	1.238	1.044
μ [mm^{-1}]	1.146	1.299	0.913
F(000)	550.0	908.0	1260.0
Crystal size [mm^3]	0.4 × 0.2 × 0.1	0.1 × 0.1 × 0.05	0.1 × 0.1 × 0.05
2Θ range for data collection [°]	9.72 to 153.36°	7.724 to 134.068°	8.24 to 134.012°
Index ranges	$-8 \le h \le 11$, $-11 \le k \le 11$, $-22 \le l \le 22$	$-27 \le h \le 27$, $-13 \le k \le 13$, $-10 \le l \le 10$	$-11 \le h \le 10$, $-22 \le k \le 22$, $-21 \le l \le 25$
Reflections collected	14839	49162	19260
Independent reflections	5715[R(int) = 0.0186]	2165 [R_{int} = 0.0377]	6556 [R_{int} = 0.0278]
Data / restraints / parameters	5715/0/325	2165/2/167	6556/6/410
Goodness-of-fit on F^2	1.035	1.120	1.074
Final R indexes [I>=2σ (I)]	0.0293, 0.0737	0.0298, 0.0789	0.0384, 0.1080
Final R indexes [all data]	0.0304, 0.0745	0.0309, 0.0798	0.0427, 0.1121
Largest diff. peak/hole [e Å^{-3}]	0.30/−0.30	0.21/−0.42	0.57/−0.43
CCDC-	995938	995940	995941

Compound	**5**	**6-S**	**7-S**
Empirical formula	$C_{55}H_{75}N_3ONi$	$C_{64}H_{82}N_4Ni_2S_2$	$C_{128}H_{164}N_8Ni_4S_6$
Formula weight	852.89	1088.88	2241.87
Temperature [K]	123(1)	123(1)	123(1)
Crystal system	triclinic	triclinic	Monoclinic
Space group	*P*-1	*P*-1	$P2_1/n$
a [Å]	11.1354(8)	13.0231(5)	16.6760(4)
b [Å]	12.2243(5)	14.2423(6)	18.4118(5)
c [Å]	17.8241(7)	18.1147(5)	38.8467(10)
α [°]	87.524(4)	100.585(3)	90.00
β [°]	85.065(5)	95.676(3)	96.027(2)
γ [°]	87.053(5)	114.757(4)	90.00
Volume [Å^3]	2412.2(2)	2940.41(19)	11861.4(5)
Z	2	2	4
ρ_{calc} [g/cm^3]	1.174	1.230	1.255
μ [mm^{-1}]	0.877	1.766	2.086
F(000)	924.0	1164.0	4784.0
Crystal size [mm^3]	0.3 × 0.15 × 0.1	0.3 × 0.2 × 0.1	0.09 × 0.08 × 0.07
2Θ range for data collection [°]	7.246 to 147.526	7.06 to 147.32	6.64 to 147.52
Index ranges	$-13 \le h \le 13$, $-15 \le k \le 15$, $-22 \le l \le 19$	$-13 \le h \le 16$, $-17 \le k \le 17$, $-22 \le l \le 21$	$-20 \le h \le 18$, $-22 \le k \le 15$, $-47 \le l \le 47$
Reflections collected	21977	21454	47574
Independent reflections	9329 [R_{int} = 0.0504]	11356[R(int) = 0.0211]	22844[R(int) = 0.0291]
Data / restraints / parameters	9329/0/561	11356/0/649	22844/0/1315
Goodness-of-fit on F^2	1.041	1.024	1.010
Final R indexes [I>=2σ (I)]	0.0476, 0.1224	0.0302, 0.0738	0.0367, 0.0903
Final R indexes [all data]	0.0606, 0.1354	0.0368, 0.0782	0.0475, 0.0961
Largest diff. peak/hole [e Å^{-3}]	0.65/−0.35	0.28/−0.32	0.72/−0.42
CCDC-	995931	995932	995935

Compound	**6-Se**	**7-Se**	**6-Te**
Empirical formula	$C_{70}H_{96}N_4Ni_2Se_2$	$C_{64}H_{82}N_4Ni_2Se_3$	$C_{70}H_{96}N_4Ni_2Te_2$
Formula weight	1268.84	1261.63	1366.12
Temperature [K]	123(1)	123(1)	123(1)
Crystal system	monoclinic	monoclinic	monoclinic
Space group	$P2_1/c$	$P2_1/n$	$P2_1/c$
a [Å]	19.5580(3)	16.8208(6)	19.69630(10)
b [Å]	20.1611(2)	18.4669(10)	20.47330(10)
c [Å]	16.7962(2)	39.0547(10)	16.93030(10)
α [°]	90	90	90
β [°]	96.1920(10)	96.196(3)	98.0580(10)
γ [°]	90	90	90
Volume [Å^3]	6584.28(14)	12060.6(8)	6759.71(6)
Z	4	8	4
ρ_{calc} [g/cm^3]	1.280	1.390	1.342
μ [mm^{-1}]	2.282	3.152	7.667
F(000)	2672.0	5216.0	2816.0
Crystal size [mm^3]	0.3 × 0.25 × 0.25	0.2 × 0.2 × 0.1	0.2 × 0.05 × 0.05
2Θ range for data collection [°]	6.32 to 146.96	7.13 to 147.97	6.26 to 147.26
Index ranges	$-23 \le h \le 20$, $-24 \le k \le 21$, $-20 \le l \le 19$	$-20 \le h \le 14$, $-22 \le k \le 20$, $-42 \le l \le 48$	$-24 \le h \le 24$, $-25 \le \le 25$, $-20 \le l \le 17$
Reflections collected	32467	43761	88776
Independent reflections	12810[R(int) = 0.0254]	23312 [R_{int} = 0.0292]	13479 [R_{int} = 0.0472]
Data / restraints / parameters	12810/0/703	23312/0/1315	13479/0/703
Goodness-of-fit on F^2	1.022	1.031	1.037
Final R indexes [I>=2σ (I)]	0.0296, 0.0709	0.0409, 0.0985	0.0277, 0.0717
Final R indexes [all data]	0.0382, 0.0759	0.0495, 0.1040	0.0302, 0.0735
Largest diff. peak/hole [e Å^{-3}]	0.38/−0.58	2.76/−0.71	2.47/−0.75
CCDC-	995933	995936	995934

Compound	**8**	**1-H**	**1-THF**
Empirical formula	$C_{66}H_{86}N_4Ni_2O_{0.5}P_4$	$C_{32}H_{42}N_2Ni$	$C_{36}H_{49}N_2F_6PNiO$
Formula weight	1184.69	513.39	729.45
Temperature [K]	123(1)	123(1)	123(1)
Crystal system	monoclinic	monoclinic	monoclinic
Space group	$P2_1/c$	$P2_1/n$	Cc
a [Å]	13.7371(2)	12.4764(4)	12.7889(2)
b [Å]	23.6940(5)	36.2568(10)	16.8666(3)
c [Å]	19.4754(3)	12.7163(4)	16.4852(3)
α [°]	90.00	90.00	90.00
β [°]	91.093(2)	90.223(3)	94.4860(10)
γ [°]	90.00	90.00	90.00
Volume [Å^3]	6337.83(19)	5752.2(3)	3545.05(11)
Z	4	8	4
ρ_{calc} [g/cm^3]	1.242	1.186	1.367
μ [mm^{-1}]	2.012	0.696	1.754
F(000)	2520.0	2208.0	1536.0
Crystal size [mm^3]	0.3 × 0.07 × 0.04	0.35 × 0.3 × 0.25	0.197 × 0.071 × 0.046
2Θ range for data collection [°]	6.44 to 147.18	6.4 to 52	8.7 to 147.32
Index ranges	$-17 \le h \le 16$, $-25 \le k \le 28$, $-22 \le l \le 24$	$-12 \le h \le 15$, $-44 \le k \le 44$, $-15 \le l \le 13$	$-15 \le h \le 15$, $-20 \le k \le 20$, $-20 \le l \le 20$
Reflections collected	27288	27792	20803
Independent reflections	12211[R(int) = 0.0367]	11247[R(int) = 0.0275]	6714 [R(int) = 0.0307]
Data / restraints / parameters	12211/23/712	11247/0/639	6714/2/424
Goodness-of-fit on F^2	1.017	1.159	1.059
Final R indexes [I>=2σ (I)]	0.0366, 0.0925	0.0627, 0.1742	0.0258, 0.0661
Final R indexes [all data]	0.0465, 0.0995	0.0696, 0.1771	0.0268, 0.0671
Largest diff. peak/hole [e Å^{-3}]	0.36/−0.44	0.63/−0.42	0.23/−0.26
Flack parameter	-	-	−0.007(13)
CCDC-	995937	995939	999501

2.6 EPR Spectroscopy

Experimental X-band EPR spectra were recorded on a Bruker EMX spectrometer (Bruker BioSpin Rheinstetten) equipped with a He temperature control cryostat system (Oxford Instruments). Simulations of the EPR spectra were performed by iteration of the anisotropic g-values and line widths using the EPR simulation program W95EPR developed by Prof. Dr. Frank Neese.

Calculation of the EPR Properties with DFT

The gas phase geometry of **1**, **2** and **3** (using the X-ray crystal structure geometry as a starting point) was optimized with the Turbomole program package[10] coupled to the PQS Baker optimizer[11] via the BOpt package[12] at the ri-DFT[13]/BP86[14] level. We used Grimme's D3 dispersion corrections (disp3)[15] and the def2-TZVP basis set[16] for all atoms. The minimum (no imaginary frequencies) was characterized by calculating the Hessian matrix. The Cartesian coordinates of the optimized geometries are supplied in .xyz format.

EPR parameters[17] were calculated with both the ORCA[18] and the ADF[19] program systems, using the coordinates from the structures optimized in Turbomole as input. In the Orca calculations we used the b3-lyp[20] functional and def2-TZVP basis set. In the ADF calculations we used the BP86 functional with the ZORA/TZP basis sets supplied with the program (all electron, core double zeta, valence triple zeta polarized basis set on all atoms). The EPR g-tensors in ADF were obtained from restricted SPINORBIT ZORA calculations.

Table 2. Experimental[(a)] and DFT calculated [(b)] EPR parameters of [(C_5H_5)Ni(IDipp)] (**1**), [(C_5H_5)Ni(IMes)] (**2**) and (C_5Me_5)Ni(IDipp) (**3**).

1	g_{11} (W) [(d)]	g_{22} (W) [(d)]	g_{33} (W) [(d)]
Exp [(a)]	2.377 (50)	2.306 (19)	2.050 (16)
DFT [(b)]	2.220	2.187	2.078
DFT [(c)]	2.559	2.007	1.930
2			
Exp [(a)]	2.420(37)	2.289(16)	2.039(13)
DFT [(b)]	2.225	2.210	2.076
DFT [(c)]	2.236	2.229	2.071
3			
Exp [(a)]	2.315(22)	2.305(49)	2.064(11)
DFT [(b)]	2.228	2.179	2.087
DFT [(c)]	2.242	2.187	2.090

(a) Obtained by simulation of the experimental spectrum.
(b) Orca, b3-lyp, def2-TZVP.
(c) ADF, BP86, TZ2P.
(d) g-tensor (line width W in MHz).

Cartesian coordinates of [(C_5H_5)Ni(IDipp)] (**1**) optimized with Turbomole at the ri-DFT-D3, BP86, def2-TZVP level

76
Energy = -2862.8786196500

C	8.1629980	1.8209051	4.6447538
C	9.4973894	0.0212958	5.1707102
H	10.1099830	-0.6002987	5.8113760
C	9.1343029	-0.1130336	3.8675043
H	9.3642247	-0.8784003	3.1371932
C	7.3365598	5.3005980	3.7258491
H	8.2387069	5.7405040	3.3131112
C	6.4685895	4.3765785	3.0641519
H	6.6044554	3.9743870	2.0638249
C	5.3882004	4.0555039	3.9540119
H	4.5610708	3.3895469	3.7358988
C	5.6113284	4.7414495	5.1767856
H	4.9818432	4.7025377	6.0608740
C	6.8252631	5.5046401	5.0389918
H	7.2678613	6.1345745	5.8059834
C	7.6978182	1.1984684	2.2877897
C	6.3180207	0.9346225	2.1522657
C	5.7445746	1.1771714	0.8980352
H	4.6821830	0.9916141	0.7450134
C	6.5083506	1.6650986	-0.1625419
H	6.0365130	1.8500375	-1.1289474
C	7.8661946	1.9268901	0.0065625
H	8.4445634	2.3209255	-0.8287281
C	8.4921836	1.7003397	1.2394176
C	8.9476263	1.6899533	6.9704014
C	7.9486273	1.2702701	7.8709303
C	7.9921183	1.7946813	9.1687735
H	7.2326750	1.4983185	9.8936381
C	8.9842319	2.7014534	9.5425988
H	8.9986957	3.1008897	10.5579926
C	9.9516316	3.1076294	8.6244045
H	10.7114847	3.8303387	8.9255131
C	9.9539957	2.6112774	7.3140776
C	5.4927007	0.4418667	3.3350095
H	5.7910541	1.0699106	4.1923568
C	5.8007847	-1.0266277	3.6859937
H	5.5364955	-1.6888784	2.8475052
H	5.2110015	-1.3361107	4.5621934
H	6.8594026	-1.1838457	3.9260870
C	3.9810066	0.6146554	3.1491270
H	3.7138295	1.6363655	2.8477822
H	3.4675689	0.3980569	4.0965647
H	3.5791485	-0.0780741	2.3932376
C	9.9540500	2.0615034	1.4704897
H	10.3643031	1.3477306	2.2019128
C	10.8202571	1.9632513	0.2078845
H	10.7165572	0.9851507	-0.2837210
H	11.8783462	2.1049697	0.4703283
H	10.5632822	2.7423790	-0.5247611
C	10.0541406	3.4642993	2.1011299
H	9.6584137	4.2216088	1.4073444
H	11.1029627	3.7147510	2.3208862
H	9.4729245	3.5280977	3.0320584
C	6.8265084	0.3389402	7.4364950
H	7.1016657	-0.0893389	6.4612634
C	5.5264428	1.1364781	7.2285002
H	5.1810119	1.5786384	8.1754594
H	4.7299912	0.4802431	6.8451856
H	5.6869623	1.9510777	6.5037264
C	6.6208250	-0.8312794	8.4097979
H	7.5524534	-1.3947325	8.5615438
H	5.8609479	-1.5219133	8.0158860
H	6.2705380	-0.4857584	9.3933896
C	10.9724826	3.0965203	6.2945276
H	10.8565724	2.4839123	5.3889429
C	10.6772940	4.5529280	5.8953495
H	9.6552325	4.6391180	5.4939633
H	11.3828039	4.8904225	5.1217005
H	10.7693500	5.2258548	6.7613809
C	12.4166999	2.9273456	6.7917003
H	12.6193462	3.5597040	7.6685702
H	13.1266315	3.2190015	6.0041386
H	12.6242346	1.8849959	7.0735174
N	8.3191025	0.9773495	3.5620277
N	8.9000276	1.1909485	5.6276879
Ni	7.2693903	3.4297180	4.8286251

2.7 Electrochemical Measurements

Conventional cyclic voltammetry (CV) was performed in a pre-dried air-tight single-compartment cell connected to a Metrohm Autolab PGSTAT302N potentiostat. The cell was equipped with a Pt microdisc (0.14 mm^2) working electrode carefully polished with a 25-μm diamond paste, a Pt coil auxiliary electrode and an Ag coil pseudoreference electrode. The solutions of the studied complexes were prepared under an atmosphere of dry argon in THF freshly distilled from Na/benzophenone. The supporting electrolyte, tetrabutylammonium hexafluorophosphate (TBAH, 10^{-1} mol dm^{-3}) was recrystallized twice from absolute ethanol and dried overnight *in vacuo* at 80 ºC. All redox potentials are reported against the ferrocene/ferrocenium (Fc/Fc^+) redox couple used as an internal standard; v = 100 mV s^{-1}.

Controlled-potential electrolyses within the OTTLE cell[21] were carried out using a PA4 potentiostat (Laboratory Devices, Polná, Czech Republic). The concentrations of the dinuclear complexes and TBAH used in these measurements were ca. 5×10^{-4} and 3×10^{-1} mol dm^{-3}, respectively. The UV/Vis spectra were obtained using the Scinco S3100 diode array spectrophotometer. The different redox steps were localized with the aid of the contemporarily recorded thin-layer cyclic voltammograms.

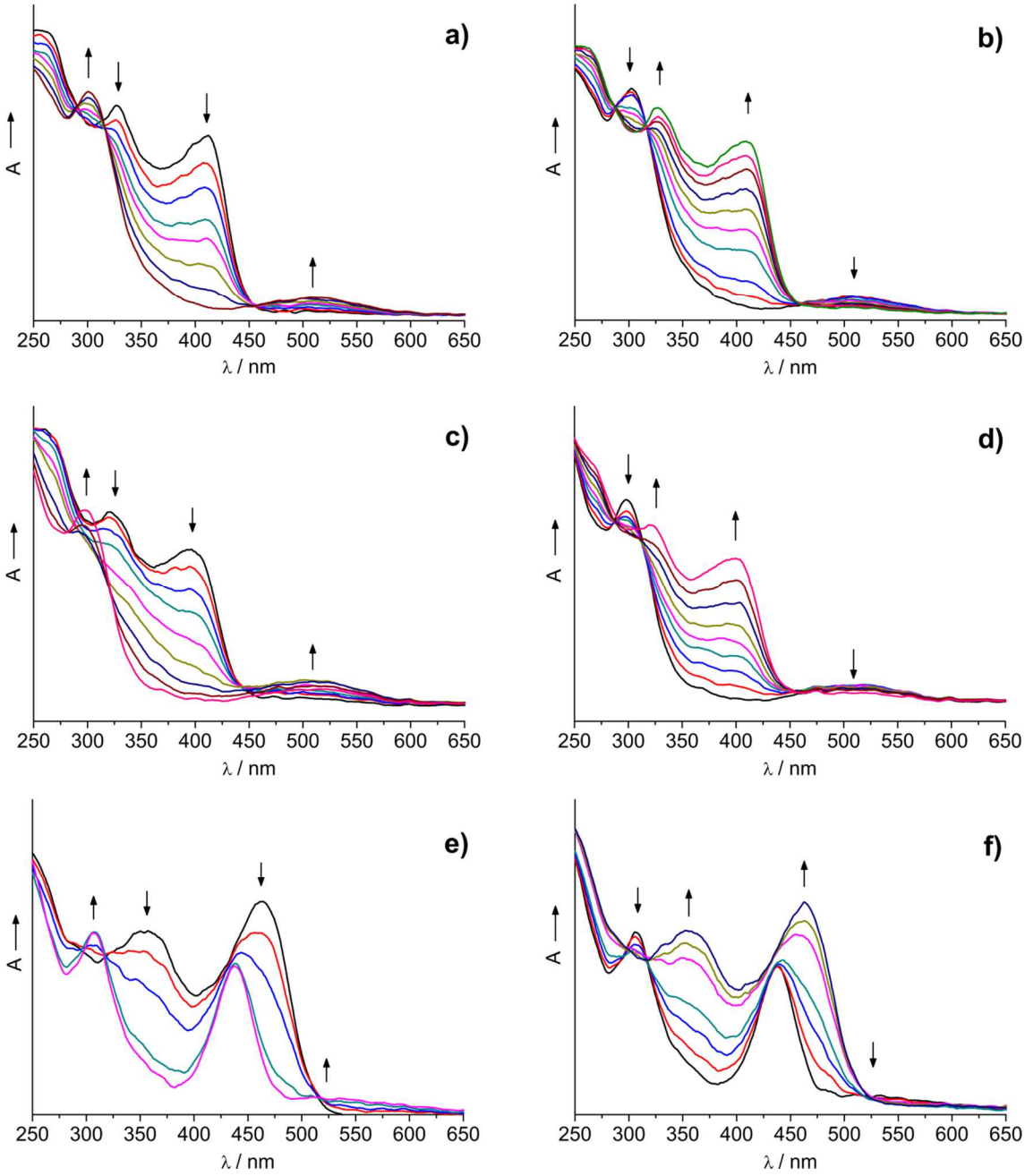

Figure S7: Spectroelectrochemical analysis of compounds **1**−**3**: a) Anodic step **1**→**1**$^+$ monitored in the UV/Vis region; b) reverse cathodic step **1**$^+$→**1**; c) anodic step **2**→**2**$^+$; d) reverse cathodic step **2**$^+$→**2**; e) anodic step **3**→**3**$^+$; f) reverse cathodic step **3**$^+$→**3**. Note the intense absorption band of **3**$^+$ at 435 nm, which is absent in the UV/Vis spectra of the Cp-complexes **1**$^+$ and **2**$^+$.

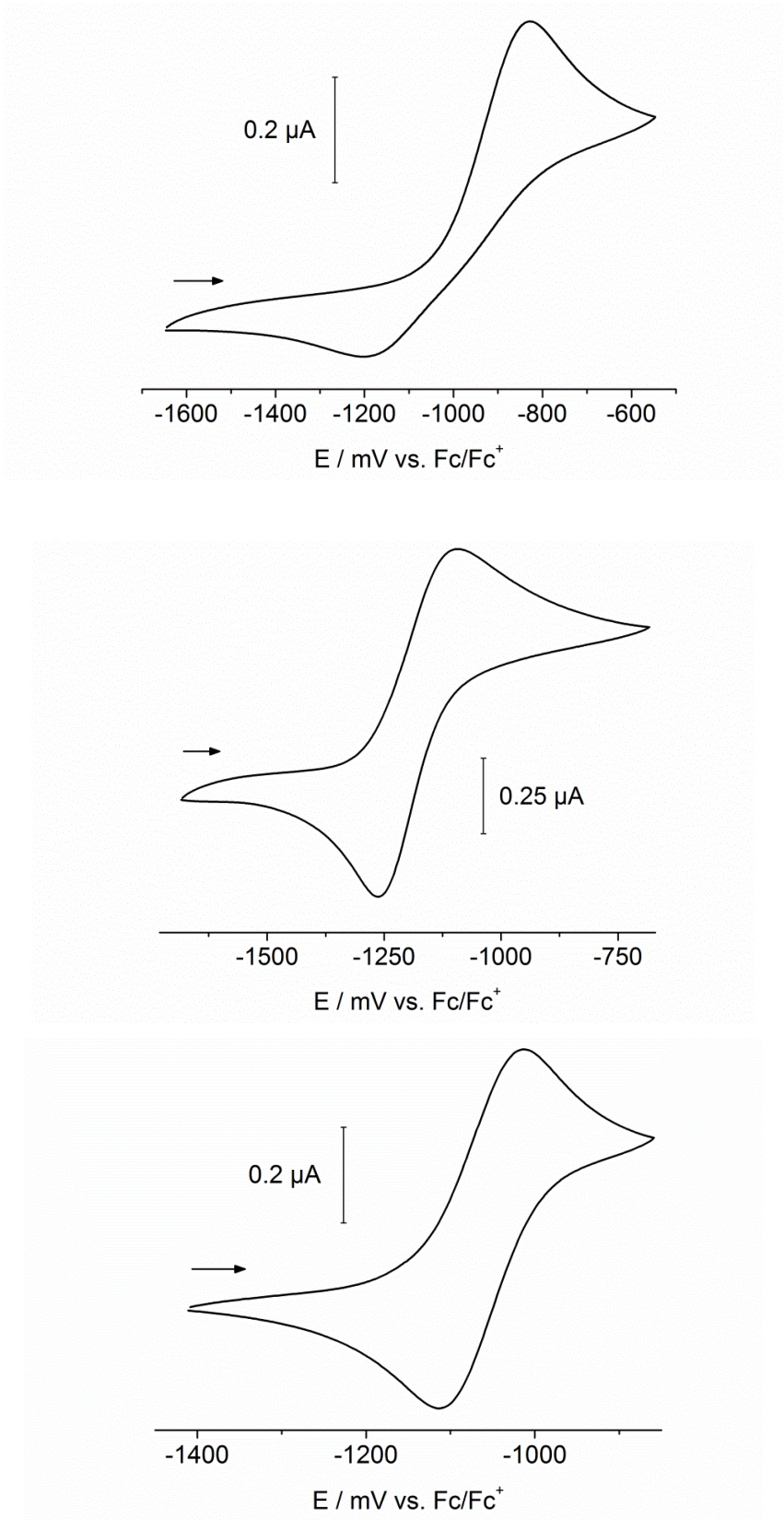

Figure S8: Cyclic voltammograms of compounds **1** (top), **2** (centre), **3** (bottom). Conditions: see above.

References:

1 D. F. Evans, *J. Chem. Soc. Resumed* **1959**, 2003–2005.

2 G. J. P. Britovsek, V. C. Gibson, S. K. Spitzmesser, K. P. Tellmann, A. J. P. White, D. J. Williams, *J. Chem. Soc. Dalton Trans.* **2002**, 1159–1171.

3 S. P. Nolan, **2006**, *US Patent:* 7109348.

4 a) R. A. Kelly, N. M. Scott, S. Díez-González, E. D. Stevens, S. P. Nolan, *Organometallics* **2005**, *24*, 3442–3447; b) O. R. Luca, B. A. Thompson, M. K. Takase, R. H. Crabtree, *J. Organomet. Chem.* **2013**, *730*, 79–80.

5 V. Ritleng, C. Barth, E. Brenner, S. Milosevic, M. J. Chetcuti, *Organometallics* **2008**, *27*, 4223–4228.

6 a) *SCALE3ABS*, *CrysAlis^{Pro}*, Aglient Technologies Inc., Oxford, GB, **2012**; b) G. M. Sheldrick, *SADABS*, Bruker AXS, Madison, USA, **2007**.

7 R. C. Clark, J. S. Reid, *Acta Crystallogr. A* **1995**, *51*, 887–897.

8 G. M. Sheldrick, *Acta Crystallogr. A* **2007**, *64*, 112–122.

9 A. Altomare, M. C. Burla, M. Camalli, G. L. Cascarano, C. Giacovazzo, A. Guagliardi, A. G. Moliterni, G. Polidori, R. Spagna, *J. Appl. Crystallogr.* **1999**, *32*, 115–119.

10 R. Ahlrichs, Turbomole Version 6.5, Theoretical Chemistry Group, University of Karlsruhe.

11 PQS version 2.4, 2001, Parallel Quantum Solutions, Fayettevile, Arkansas (USA); the Baker optimizer is available separately from PQS upon request: I. Baker, *J. Comput. Chem.* **1986**, *7*, 385–395.

12 P. H. M. Budzelaar, *J. Comput. Chem.* **2007**, *28*, 2226–2236.

13 M. Sierka, A. Hogekamp, R. Ahlrichs, *J. Chem. Phys.* **2003**, *118*, 9136.

14 (a) A. D. Becke, *Phys. Rev. A* **1988,** *38*, 3098. (b) J. P. Perdew, *Phys. Rev. B* **1986**, *33*, 8822.

15 S. Grimme, J. Antony, S. Ehrlich, H. J. Krieg, *J. Chem. Phys.* **2010**, *132*, 154104.

16 a) F. Weigend, R. Ahlrichs, *Phys. Chem. Chem. Phys.* **2005**, *7*, 3297–3305; b) F. Weigend, M. Häser, H. Patzelt, R. Ahlrichs, *Chem. Phys. Lett.* **1998**, *294*, 143–152.

17 Lead reference for calculation of g-tensor (Zeeman interactions) parameters: E. van Lenthe, A. van der Avoird, P. E. S Wormer, *J. Chem. Phys.* **1997**, *107*, 2488. Lead reference for calculation of A-tensor (Nuclear magnetic dipole hyperfine interactions) parameters: E. van Lenthe, A. van der Avoird, P. E. S. Wormer, *J. Chem. Phys.* **1998**, *108*, 4783.

18 F. Neese, ORCA – an ab initio, Density Functional and Semiempirical program package, Version 2.9. Max-Planck-Insitut für Bioanorganische Chemie, Mülheim and der Ruhr, **2009**

19 ADF2012 a) E. J. Baerends, D. E. Ellis, P. Ros, *Chem. Phys.* ***1973***, *2*, 41. b) L. Versluis, T. Ziegler, *J. Chem. Phys.* **1988**, *88*, 322. c) G. te Velde, E. J. Baerends, *J. Comput. Phys.* **1992**, *99*, 84. d) C. Fonseca Guerra, J. G. Snijders, G. te Velde, E. J. Baerends, *Theor. Chem. Acc.* **1998**, *99*, 391.

20 a) C. Lee, W. Yang, R. G. Parr, *Phys. Rev. B* **1988**, *37*, 785–789; b) A. D. Becke, *J. Chem. Phys.* **1993**, *98*, 1372–1377; c) A. D. Becke, *J. Chem. Phys.* **1993**, *98*, 5648–5652; d) Calculations were performed using the Turbomole functional "b3-lyp", which is not completely identical to the Gaussian "B3LYP" functional.

21 M. Krejčík, M. Daněk, F. Hartl, *J. Electroanal. Chem.* **1991**, *317*, 179.

3 Half-Sandwich Nickel(I) Complexes of Ring-Expanded N-Heterocyclic Carbenes: A Structural and Quantum Chemical Study[a,b,c]

Stefan Pelties, Michael K. Whittlesey, and Robert Wolf

[a] The experimental part of this work was done at the University of Bath, UK, under the supervision of Prof. Dr. Michael K. Whittlesey

[b] S. Pelties, E. Carter, M. F. Mahon, D. Murphy, M. K. Whittlesey, R. Wolf, manuscript in preparation.

[c] After completion of the experimental part of this work an alternative procedure for the preparation of **1Br** and **2Br**, and their reactivity in Kumada-Tamao-Corriu couplings were described by Buchowicz *et al.* (Ł. Banach, P. A. Guńka, W. Buchowicz, *Dalton Trans.* **2016**, DOI: 10.1039/C5DT04663G)

3.1 Introduction

The chemistry of nickel(I) has undergone a significant resurgence in recent years, taking it from an oxidation state of proposed (but largely unsubstantiated) importance in catalytic cycles[1] to one that can now be more thoroughly investigated in relation to both stoichiometric and catalytic transformations.[2] A significant portion of the very latest work has employed N-heterocyclic carbene (NHC) ligands in efforts to prepare highly reactive two- and three-coordinate Ni(I) species, a number of which are shown in Scheme 1. Thus, use of the N-aryl NHCs IMes (1,3-bis(2,4,6-trimethylphenyl)imidazolin-2-ylidene) and IDipp (1,3-bis(2,6-diisopropylphenyl)-imidazolin-2-ylidene) has allowed the formation of three-coordinate bis-NHC halide complexes (**A**) with applications in catalytic C-C bond formation.[3] In pioneering studies, the Hillhouse group and, more recently, Tilley and coworkers showed that the commonly employed 5-membered imidazolin-2-ylidene ligand IDipp was sufficiently bulky to stabilize even two-coordinate mono-carbene Ni(I) complexes bearing amido, aryl, and, remarkably, even alkyl ancillary ligands (**B**/**C**).[4]

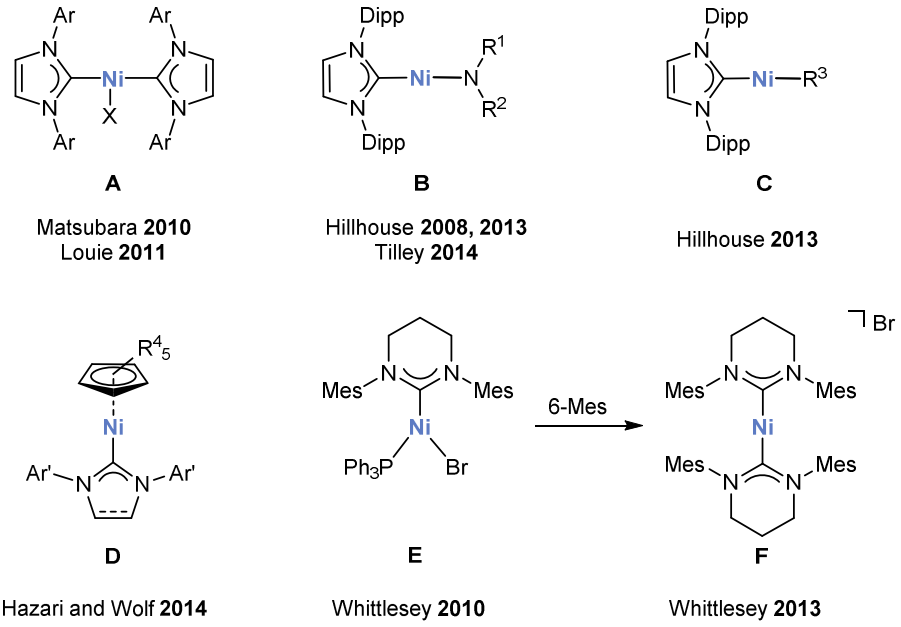

Scheme 1. Selected examples of mononuclear nickel(I) NHC complexes. Ar = Dipp (2,6-*i*Pr$_2$C$_6$H$_2$), X = Cl; Ar = 2,4,6-Mes (Me$_3$C$_6$H$_2$), X = Cl, Br, I; R^1 = R^2 = SiMe$_3$; R^1 = H, R^2 = Dipp, dmp (2,6-Mes-C$_6$H$_3$), dppp (2,6-Dipp-C$_6$H$_3$); R^3 = CH(SiMe$_3$)$_2$, dmp; Ar‘ = Dipp, Mes, R^4 = H; Ar‘ = Dipp, R^4 = Me.

Very recently, the group of Hazari and our group independently prepared a range of [CpNi(NHC)] complexes (**D**, see chapter 2) and indenyl (Ind) analogues again employing IDipp and IMes (as well as the saturated analogue SIDipp) upon reduction of either the half-sandwich precursors [CpNiCl(NHC)] or by reacting Sigman’s dimer [Ni(NHC)(μ-Cl)]$_2$ with NaCp or LiInd, respectively.[5,6] As an alternative to the use of sterically encumbered 5-membered ring NHCs, Whittlesey’s group employed ring-expanded NHCs (RE-NHCs), a generic name for N-

heterocyclic carbene ligands with ring sizes of 6−8,[7] for the synthesis of a range of complexes of the composition [NiBr(RE-NHC)(PPh_3)].[8,9] Treatment of the six-membered N-mesityl derivative **E** with one equivalent of 6-Mes led to formation of the highly unusual two-coordinate Ni(I) salt, [Ni(6-Mes)$_2$]Br (**F**).[10]

An attractive feature of RE-NHCs is that they are open to electronic manipulation through alterations at the backbone ring positions.[11] One particular approach is to incorporate heteroatom substituents, for example in diamidocarbenes (DACs), which contain C=O groups adjacent to the nitrogen atoms.[12] While 6-Mes and 6-MesDAC are essentially isostructural, the electronic properties of the diamidocarbene are altered significantly with enhanced π-acceptor capabilities.[13] Herein, we compare and contrast the impact of the ring-expanded diaminocarbenes 6-Mes and 7-Mes with that of 6-MesDAC on the structural and electronic properties of [CpNi(NHC)] complexes, as well as the reactivity toward white phosphorus (P_4). To this end, we have prepared the three new complexes **1**−**3**, which feature the NHCs 6-Mes, 7-Mes, and 6-MesDAC. The molecular structures of these complexes are reported based on X-ray crystallography, and the electronic structures are analyzed using DFT calculations.

3.2. Results and Discussion

Complexes **1Br–3Br** were synthesized according to Scheme 2 by reacting the ring-expanded NHCs 6-Mes, 7-Mes and 6-MesDAC with an equimolar amount of [CpNiBr(PPh_3)]. ^1H and $^{31}P\{^1H\}$ NMR spectroscopy showed that the phosphine ligand is readily replaced by the σ-donating carbenes within two hours. Complexes **1Br–3Br** are highly soluble in benzene, toluene and tetrahydrofuran, but effectively insoluble in *n*-hexane; they were isolated in moderate yields and characterized by ^1H and $^{13}C\{^1H\}$ NMR spectroscopy, elemental analysis, and single-crystal X-ray diffraction.

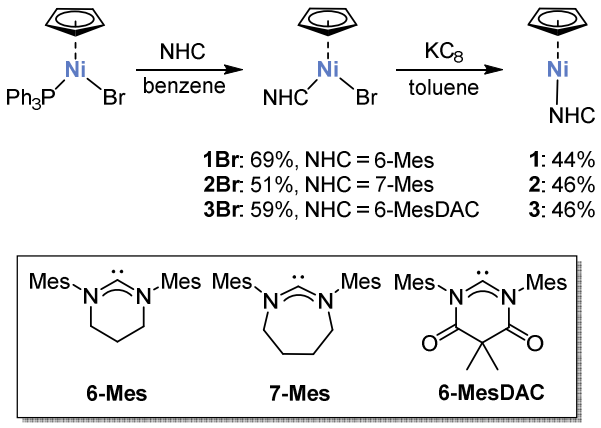

Scheme 2. Preparation of the nickel(II) bromide precursors **1Br–3Br** and their reduction to the nickel(I) compounds **1–3**.

Reduction of **1Br–3Br** with KC_8 in toluene (Scheme 2) afforded the Ni(I) complexes **1–3** in 44–46% yield upon crystallization from toluene at low temperature. Similarly, their nickel(II) bromide precursors **1–3** dissolve well in THF, toluene, benzene, but not in *n*-hexane.

Single-crystal X-ray diffraction revealed coordination of nickel by a Cp ligand and the carbene (Figure 1), and slightly bent structures in agreement with the previously described Ni(I) derivatives of type **D** (see chapter 2), featuring Arduengo type NHCs based on 5-membered rings.[5,6] The Cp ligand in **1–3** shows an η^5-coordination analogous to **D**. In this context, it is noteworthy that complex **3** features disorder of the cyclopentadienyl metal fragment over two similar positions (relative occupancies 58:42) with respect to the NHC ligand (Figure 1, bottom). The Ni(1)-C(1) distance of **3** (1.816(2) Å for the major component and 1.835(2) Å for the minor component of the disordered structure) is slightly shortened compared to the diaminocarbene derivatives **1** and **2** (**1**: 1.87430(9) Å; **2**: 1.87586(9) Å). This is presumably due to enhanced backbonding from the metal to the π-accepting diamidocarbene.

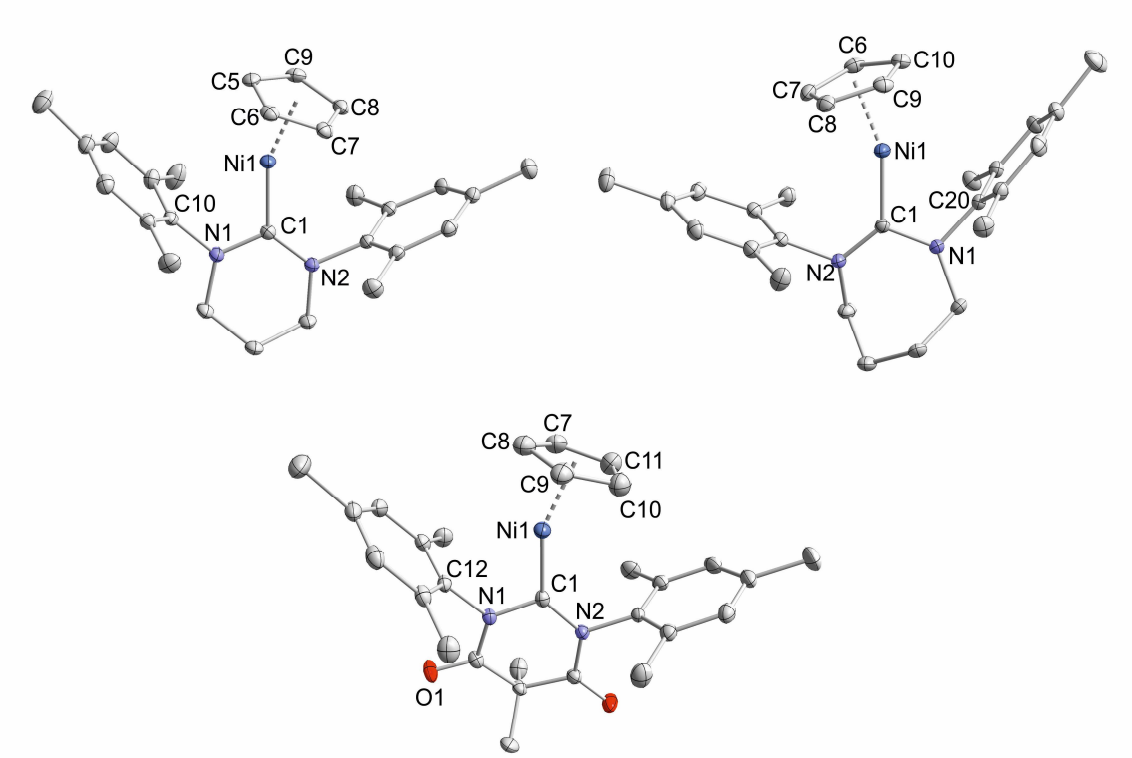

Figure 1. Solid-state molecular structures of [CpNi(6-Mes)] (**1,** left top), [CpNi(7-Mes)] (**2**, right top) and [CpNi(6-MesDAC)] (**3**,bottom). The hydrogen atoms are omitted for clarity. Thermal ellipsoids are drawn at 40% level. Selected bond lengths [Å] and angles [°]: **1**: Ni1−C5 2.11225(9), Ni1−C6 2.13215(8), Ni1−C7 2.17511(6), Ni1−C8 2.19406(7), Ni1−C9 2.17212(8), Ni1−C10 2.77024(7); **2**: Ni1−C6 2.17406(8), Ni1−C7 2.18479(8), Ni1−C8 2.17868(8), Ni1−C9 2.13799(11), Ni1−C10 2.13107(10), Ni1−C20 2.60559(9); **3**: Ni1−C7 2.11(2) (2.19(1)), Ni1−C8 2.085(8) (2.176(6)), Ni1−C9 2.09(2) (2.153(9)), Ni1−C10 2.230(7) (2.095(5)), Ni1−C11 2.26(1) (2.098(6)), Ni1−C12 2.666(2) (2.663(2)); bond lengths and angles of the second, disordered part are given in parenthesis.

The structures of **1–3** are bent with C(1)−Ni−$Cp_{centroid}$ angles (for **1** 159.1481(13)°), for **2** 160.565(3) Å, and for **3** 161.1(3)/160.4(2) Å) significantly larger than in CpNi(IDipp) (**D1)** and CpNi(IMes) (**D2**) (154.3(1) and 152.0(1)° respectively), but smaller than in the pentamethylcyclopentadienyl analogue, [Cp*Ni(IDipp)] (**D3**) (164.8(1)°) (see chapter 2).[5,6] For **D1–D3**, the Ni−C_{ipso} distances were all > 3 Å (**D1**: 3.2438(11), **D2**: 3.40853(3), **D3**: 3.14599(4) Å), which is only slightly smaller than the sum of the van der Waals radii of nickel and carbon (3.67 Å). In contrast, the corresponding distances in **1–3** are significantly smaller (**1**: 2.77024(7); **2**: 2.60559(9); **3**: 2.666(2)/2.663(2) Å), most likely as a result of the increased N-C-N angles of the 6- and 7-membered carbene ligands compared to their 5-membered counterparts.

Table 1. Selected bond lengths [Å] and angles [°].

	1	**2**	**3**[a)]
Ni1−C1	1.87430(9)	1.87586(9)	1.816(2) (1.835(2))
N1−C1	1.35533(3)	1.35821(4)	1.386(2)
N2−C1	1.34984(3)	1.35275(5)	1.379(2)
Ni1−Cp(centr.)	1.78779(9)	1.79507(8)	1.792(4) (1.768(3))
C1−Ni1−Cp(centr.)	159.15(1)	160.565(3)	161.1(3) (160.4(2))
Ni1−C1−N1	114.61(1)	111.006(3)	110.5(1) (133.7(1))
Ni1−C1−N2	128.67(1)	130.849(3)	134.1(1) (110.92(1))
N1−C1−N2	116.69(1)	118.075(3)	115.38(1)

a) bond lengths and angles of the second part of the disordered molecule are given in parenthesis.

The room temperature ^{1}H NMR spectra of **1**–**3** (C_6D_6) showed broad signals in the range of 15.5 to −52.4 ppm, which could partially be assigned based on their intensity and comparison of the ^{1}H NMR patterns of related complexes.[5,9] The η^5-coordinated Cp ligands in **1** and **2** gave rise to low frequency shifted resonances (−47.7 and −52.4 ppm, respectively) similar to those observed in **D1** and **D2** (−40.7 and −38.2 ppm, respectively), whereas in the case of **3**, signals in the range 15.5 to 1.3 ppm were observed (in the range −150 to +150 ppm). Due to partial overlap of the signals further assignments were not possible. Nonetheless, the presence of four signals in case of **1**, five signals for **2**, and four signals for **3** in the ^{1}H NMR spectra indicates high symmetry structures present in solution. The solution magnetic moments (Evans method)[14] of **1** (1.8(1) μ_B), **2** (1.9(1) μ_B), and **3** (1.9(1) μ_B) are consistent with the presence of a single unpaired electron.

Compounds **1** and **2** feature intense absorption maxima in the UV/Vis spectra (342, 368, 418 nm for **1**; 377 and 446 nm for **2**). Similar spectra were observed for **D1**−**D3** (chapter 2, SI), exhibiting yellow to orange colors in solution and the solid-state. In contrast, the UV/Vis spectrum of **3** shows intense absorptions at 313, 442 and 592 nm in agreement with the dark green color of the compound in solution and the solid-state, and moreover, indicating a distinct electronic structure as compared to **1** and **2**.

In order to get further insight into the electronic structure of the nickel(I) radicals **1**–**3,** we performed DFT calculations (B3LYP/def2-TZVP level; see experimental section for details). The optimized structures agree well with those obtained from the X-ray analysis. According to a Löwdin population analysis (reduced atomic orbital populations), the spin density is mainly located on the metal (**1**: 88%, **2**: 93%, and **3**: 94%) and shows a similar asymmetric shape slightly pointing toward one *ipso*-C of the NHC's mesityl substituent for all complexes in agreement with complexes **D**.[5,6] Hazari and coworkers considered a weak interaction between the Ni and one *ipso*-C of the NHC's aryl substituent due to the asymmetric spin density pointing to this carbon atom. However, their NBO analysis did not confirm this assumption.

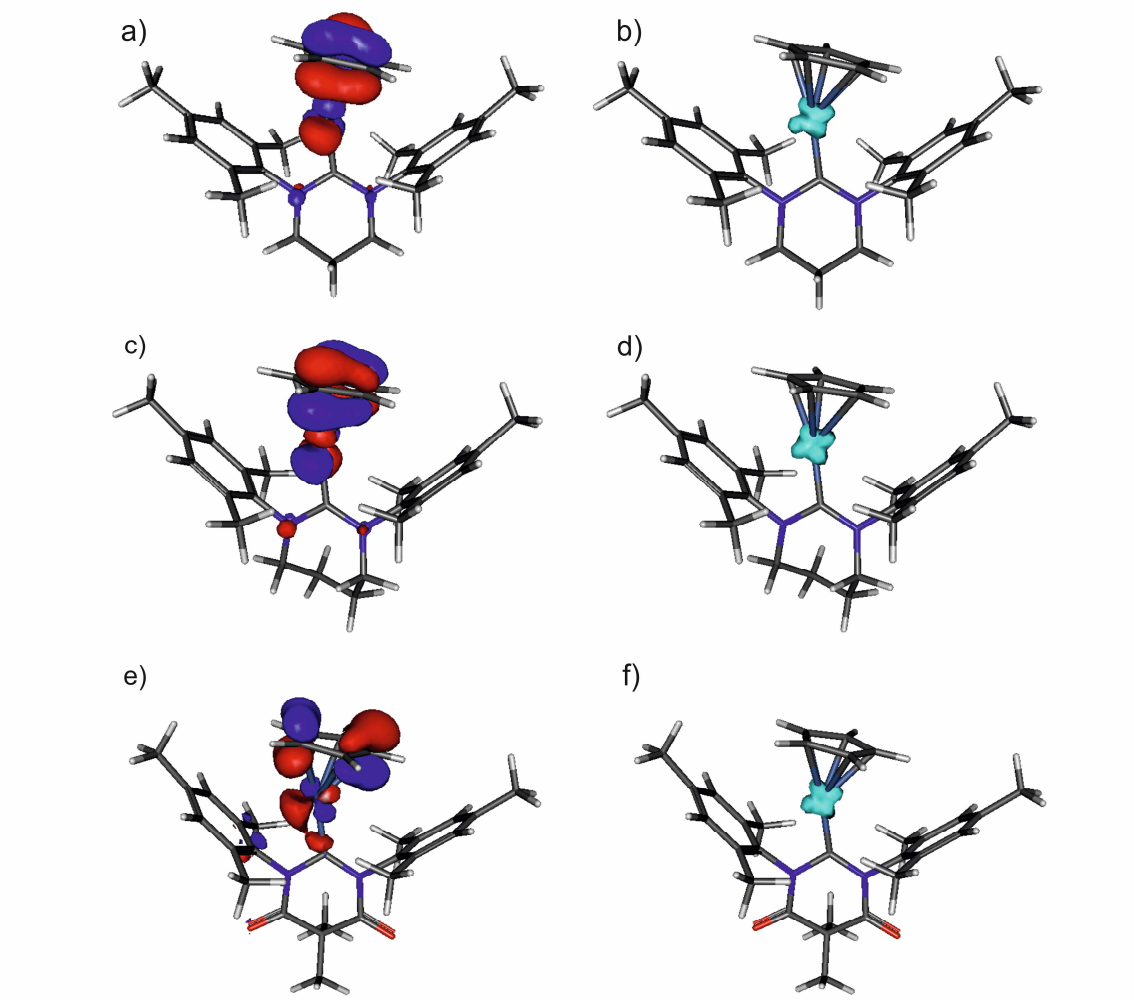

Figure 2. SOMO of complexes **1** (a), **2** (c), and **3** (e) and spin density plots of **1** (b), **2** (d), and **3** (f).

We were interested how the different steric and electronic properties of the RE-NHCs affect the reactivity of the new nickel(I) complexes. As complexes **D1** and **D2** (see chapter 2) react with white phosphorus (P_4) in a very selective fashion to form the dinuclear nickel(II) complexes with bridging "butterfly" P_4 ligands **G1** and **G2** (Scheme 3 in chapter 5), we decided to explore the reaction behavior of **1** – **3** with P_4 in order to probe the effect of the different NHC ligands.[5]

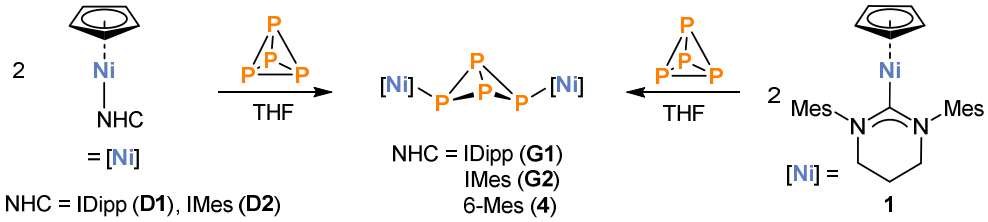

Scheme 2. Comparison of the reactivity toward white phosphorus of **D1** and **D2** with complex **1**.

The reaction of two equivalents of **1** with P_4 led to a main species with two $^{31}P\{^1H\}$ NMR triplets at −312.4 and −56.9 ppm with a $^1J_{PP}$ coupling constant of $^1J_{PP}$ = 193 Hz in the spectrum (Figure 2, top). This pattern indicates the formation of complex [{CpNi(6-Mes)}$_2$(μ-η^1:η^1-P_4)] (**4**),

analogous to **G1** and **G2**. Furthermore, the reaction proceeds instantaneously even at −35 °C in a similar manner as observed for complexes **G1** and **G2**.

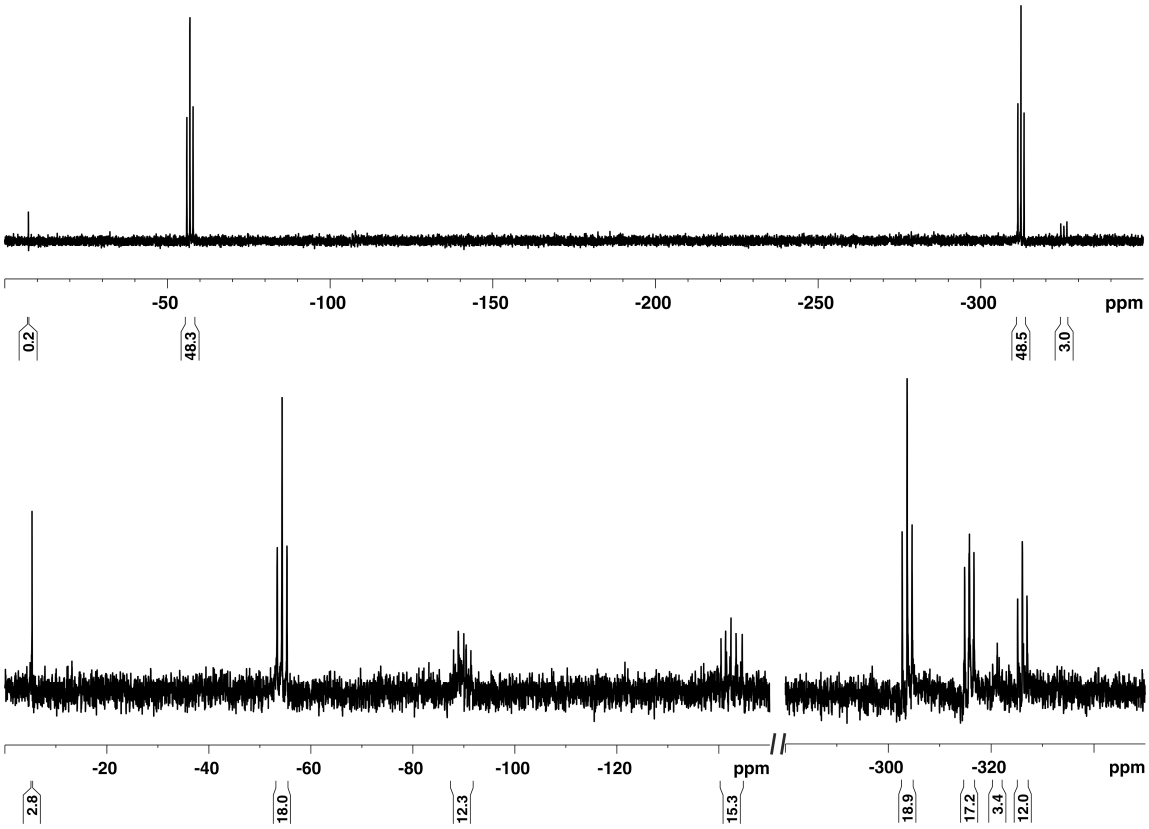

Figure 2. $^{31}P\{^{1}H\}$ NMR spectrum (THF-d_8, 300 K, 200 MHz) of the reaction of **1** with 0.5 equivalent of P_4 (top) and $^{31}P\{^{1}H\}$ NMR spectrum (C_6D_6, 300 K, 200 MHz) of the reaction of **2** with excess P_4 (top).

Interestingly, the $^{31}P\{^{1}H\}$ NMR spectrum of the reaction of **2** with an excess of P_4 showed the presence of a mixture of products, one giving rise to an A_2X_2 spin system (−303.7 (t) and −54.4 (t) ppm in the ratio of 1:1 with a $^{1}J_{PP}$ coupling constant of $^{1}J_{PP}$ = 194 Hz, ca. 37% of the sum of all integrals), which probably corresponds to complex **5**. The four multiplets (poorly resolved) at −326.1, −315.8, −142.2, and −89.6 ppm in an 1:1:1:1 ratio, indicate the presence of another compound with an ABMX spin system. Additional low-intensity signals were observed at −321.2 and −89.6 ppm (Figure 2, bottom), which could not unambiguously be assigned.

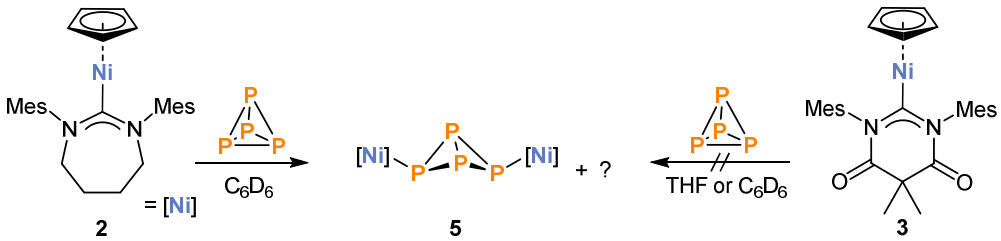

Scheme 3. Reaction of **2** and **3** toward white phosphorus.

In marked contrast, no conversion was observed in either C_6D_6 or THF-d_8 after one day for the reaction of one equivalent of **3** with P_4 (Scheme 3). Heating the solution resulted in partial

decomposition of **3** to unidentified products as indicated by ^{1}H NMR spectroscopy; the ^{31}P{^{1}H} NMR spectrum only showed the signal of free P_4.

3.3 Conclusion

In summary, we described the synthesis of three new cyclopentadienyl nickel(I) NHC complexes **1**–**3**, featuring the ring-expanded carbenes 6-Mes and 7-Mes and the diamidocarbene 6-MesDAC, via the reduction of the corresponding nickel(II) bromides with potassium graphite. Due to the larger N−C−N angle of the carbenes, the molecular structures of **1**–**3** feature slightly increased C(1)−Ni−$Cp_{centroid}$ angles compared to the cyclopentadienyl and indenyl complexes **D**, and smaller angles as against the pentamethylcyclopentadienyl derivative **D3**. Overall, the influence of replacing a five-membered ring (Arduengo) carbene by a ring-expanded NHC or diamidocarbenes on the molecular structure seems to be less than expected: **1**–**3** show a similar structure motif with larger C(1)−Ni−$Cp_{centroid}$ angles in comparison with complexes of type **D**.[5,6] In addition, the electronic structure of compounds **1**–**3** features similar contribution of the metal center against complexes **D**. Nonetheless, complex **3** exhibits a distinct UV/Vis and ^{1}H NMR spectrum as compared to **D1**, **D2**, **D3**, **1,** and **2**. Furthermore, compound **3** showed no reactivity toward P_4 in marked contrast to complexes **D1**, **D2**, **1**, and **2**, which readily react with P_4 even at low temperatures. ^{31}P{^{1}H} NMR spectroscopy indicates the formation of the dinuclear species **4** with a "butterfly"-P_4 ligand in the reaction of **1** with P_4. In contrast, the reaction of **2** with excess P_4 resulted in a mixture of **5** and unidentified products.

These results indicate the presence of a distinct electronic structure of compound **3** in comparison with **1** and **2**. Further investigations by EPR and ENDOR spectroscopy are ongoing to confirm this presumption and get deeper insight into the electronic structure.

3.4 Supporting Information (SI)

3.4.1 General Procedures

All manipulations were performed under an atmosphere of dry argon using standard Schlenk line or glovebox techniques and employing dried and degassed solvents. NMR spectra were recorded on Bruker Avance 500 and 400 spectrometers at 298 K and internally referenced to residual solvent resonances. UV/Vis spectra were recorded on a Varian Cary 50 spectrophotometer. Elemental analyses were determined by Elemental Microanalysis Ltd, Okehampton, Devon, UK. 6-Mes, 7-Mes, 6-MesDAC and CpNiBr(PPh_3) were prepared according to literature procedures.[7a,15]

3.4.2 [CpNiBr(6-Mes)] (1Br)

A benzene solution (3 mL) of 6-Mes (333 mg, 1.04 mmol, 1.05 eq) was added to a benzene solution (3 mL) of [CpNi(PPh_3)Br] (489 mg, 0.990 mmol) and the mixture stirred at room temperature for 2 h. The solvent was removed in vacuum and the residue was washed with hexane (3 x 10 mL) and extracted with toluene (20 mL). After filtration, the solution was concentrated to ca. 5 mL. A purple microcrystalline powder of 1Br formed after adding hexane (15 mL) to the solution. The crystals were isolated and dried *in vacuo*. Yield 356 mg (69%). Single crystals suitable for X-ray diffraction were formed by diffusion of hexane into a concentrated toluene solution of **1Br**. ^{1}H NMR (C_6D_6, 300 K, 400 MHz) δ /ppm = 1.14 (dt, $^3J_{HH}$ = 4.3 Hz, $^1J_{HH}$ = 13.3 Hz, 1H, NCH_2CH_2), 1.64 (m, 1H, NCH_2CH_2), 1.91 (s, 6H, *o*-CH_3), 2.19 (s, 6H, *p*-CH_3), 2.61 (m, 2H, NCH_2CH_2), 2.72 (m, 2H, NCH_2CH_2), 2.79 (s, 6H, *o*-CH), 4.56 (s, 5H, Cp), 6.81 (s, 2H, *m*-CH), 6.99 (s, 2H, *m*-CH); ^{13}C{^{1}H} NMR (C_6D_6, 300 K, 100 MHz) δ/ppm = 18.3 (*o*-CH_3), 21.0 (NCH_2CH_2), 21.1 (*p*-CH_3), 21.1 (*o*-CH_3), 47.0 (NCH_2CH_2), 93.8 (Cp), 128.7 (*m*-CH), 131.1 (*m*-CH), 135.0 (*p*-C), 137.6 (*o*-C), 138.1 (*o*-C), 145.2 (*i*-C), 203.0 (NCN); anal. calcd. (%) for $C_{27}H_{33}BrN_2Ni \cdot 0.25(C_7H_8)$ (547.21): C 63.11, H 6.45, N 5.12; found C 63.16, H 6.37, N 5.12.

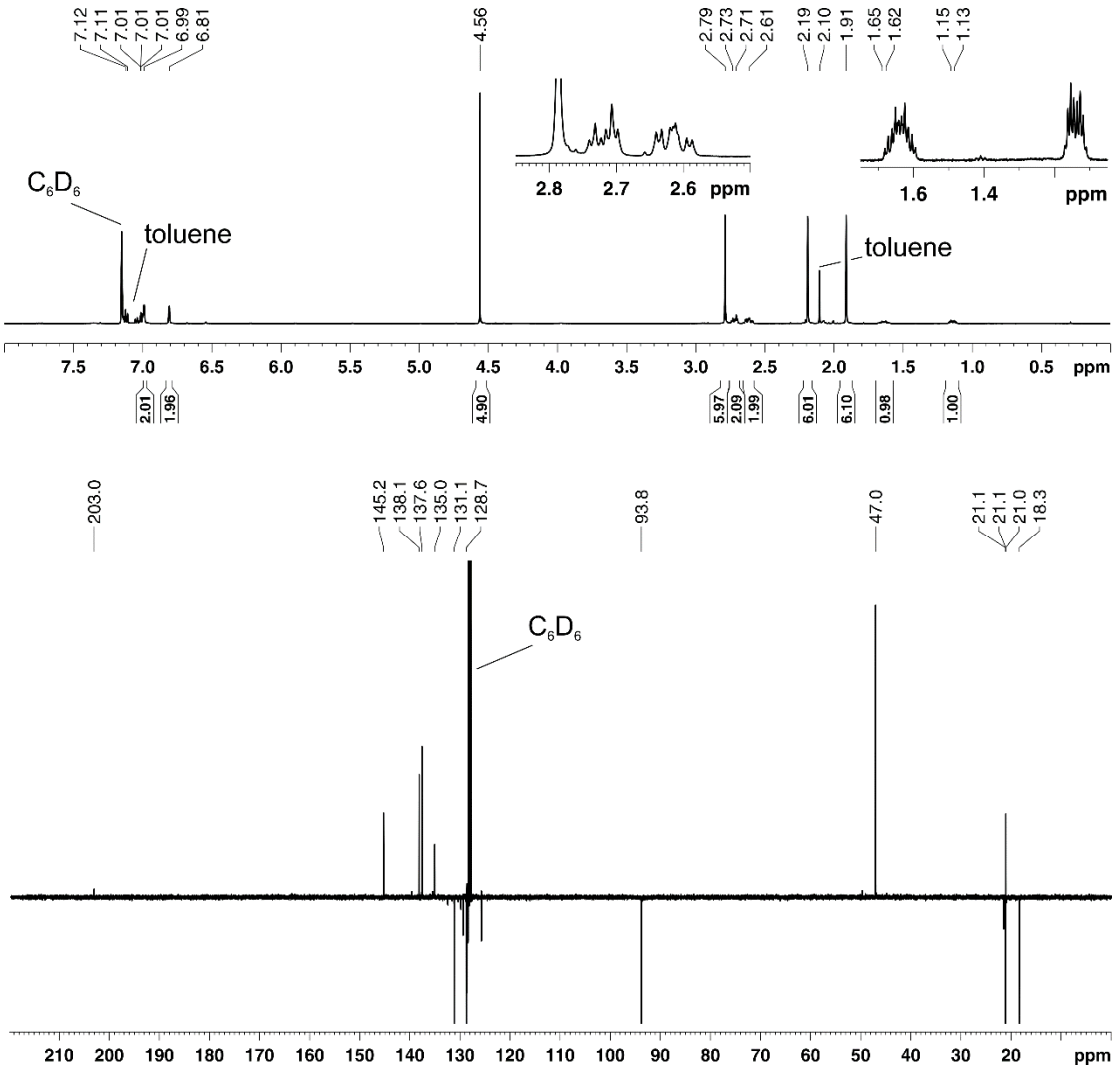

Figure S1. ^{1}H- (top) and ^{13}C{^{1}H} pendant NMR spectrum (bottom) of **1Br** (C_6D_6, 300 K, 400/100 MHz).

3.4.3 [CpNi(6-Mes)] (1)

KC_8 (97.4 mg, 0.720 mmol, 1.1 eq) was added in small portions at −35 °C to a toluene (12 mL) solution of **1Br** (343 g, 0.655 mmol). The reaction mixture was stirred at room temperature for 28 h and then filtered. After concentrating to ca. 5 mL, the filtrate was stored at −30 °C to yield yellow X-ray quality crystals of **1**. Yield 127 mg (44%); ^{1}H NMR (C_6D_6, 300 K, 500 MHz) δ/ppm = −47.7 (br s), −14.7 (br s), 7.5 (br s), 9.3 (br s), 10.8 (br s); effective magnetic moment (C_6D_6) μ_{eff} = 1.8(1) μ_B; UV/Vis (Et_2O, λ_{max} /nm, (ε_{max} /L·mol^{-1}·cm^{-1})): 342 (10600), 368 (11000), 418 (9700); anal. calcd. (%) for $C_{27}H_{33}N_2Ni$ (444.27): C 73.00, H 7.49, N 6.31; found C 72.57, H 7.18, N 6.26.

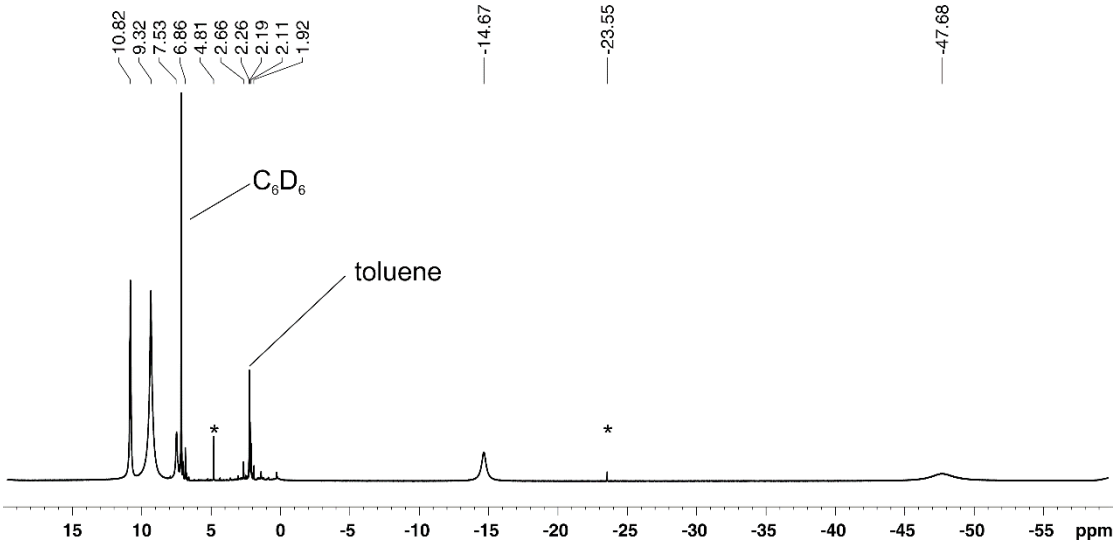

Figure S2. ^{1}H NMR spectrum of **1** (C_6D_6, 300 K, 500 MHz). The signals assigned to the minor by-product [CpNiH(6-Mes)] are labeled with an asterisk.[5]

3.4.4 [CpNiBr(7-Mes)] (2Br)

A toluene (20 mL) solution of 7-Mes (537 mg, 1.60 mmol. 1.04 eq) was added dropwise at −80 °C to a toluene (30 mL) solution of [CpNi(PPh_3)Br] (761 mg, 1.54 mmol), and the mixture stirred at room temperature for 1.5 h. The solvent was removed in vacuum, and the residue washed with hexane (3 x 20 mL). After extraction with toluene (40 mL), the filtrate was concentrated to ca. 15 mL. Violet crystals formed upon cooling to −16 °C. The crystals were washed with pentane (10 mL) and dried under vacuum. Yield 420 mg (51%). Single crystals suitable for X-ray diffraction were isolated from a toluene/hexane solution of 2Br. ^{1}H NMR (C_6D_6, 300 K, 400 MHz) δ/ppm = 1.15 (m, 2H, NCH_2CH_2), 1.88 (m, 2H, NCH_2CH_2), 1.94 (s, 6H, *o*-CH_3), 2.19 (s, 6H, *p*-CH_3), 2.91 (s, 6H, *o*-CH_3), 2.96 (m, 2H, NCH_2CH_2), 3.46 (m, 2H, NCH_2CH_2), 4.52 (s, 5H, Cp), 6.81 (s, 2H, *m*-CH), 7.01 (s, 2H, *m*-CH); ^{13}C{^{1}H} NMR (C_6D_6, 300 K, 100 MHz,) δ/ppm = 19.1 (*o*-MesCH_3), 21.0 (*p*-CH_3), 21.9 (*o*-CH_3), 24.9 (NCH_2CH_2), 54.8 (NCH_2CH_2), 94.0 (Cp), 128.9 (*m*-CH), 131.3 (*m*-CH), 135.0 (*p*-C), 137.3 (*o*-C), 138.2 (*o*-C), 147.1 (*i*-C), 215.7 (NCN); anal. calcd (%) for $C_{28}H_{35}BrN_2Ni$ (538.20): C 62.49, H 6.56, N 5.21; found C 63.24, H 6.40, N 5.25.

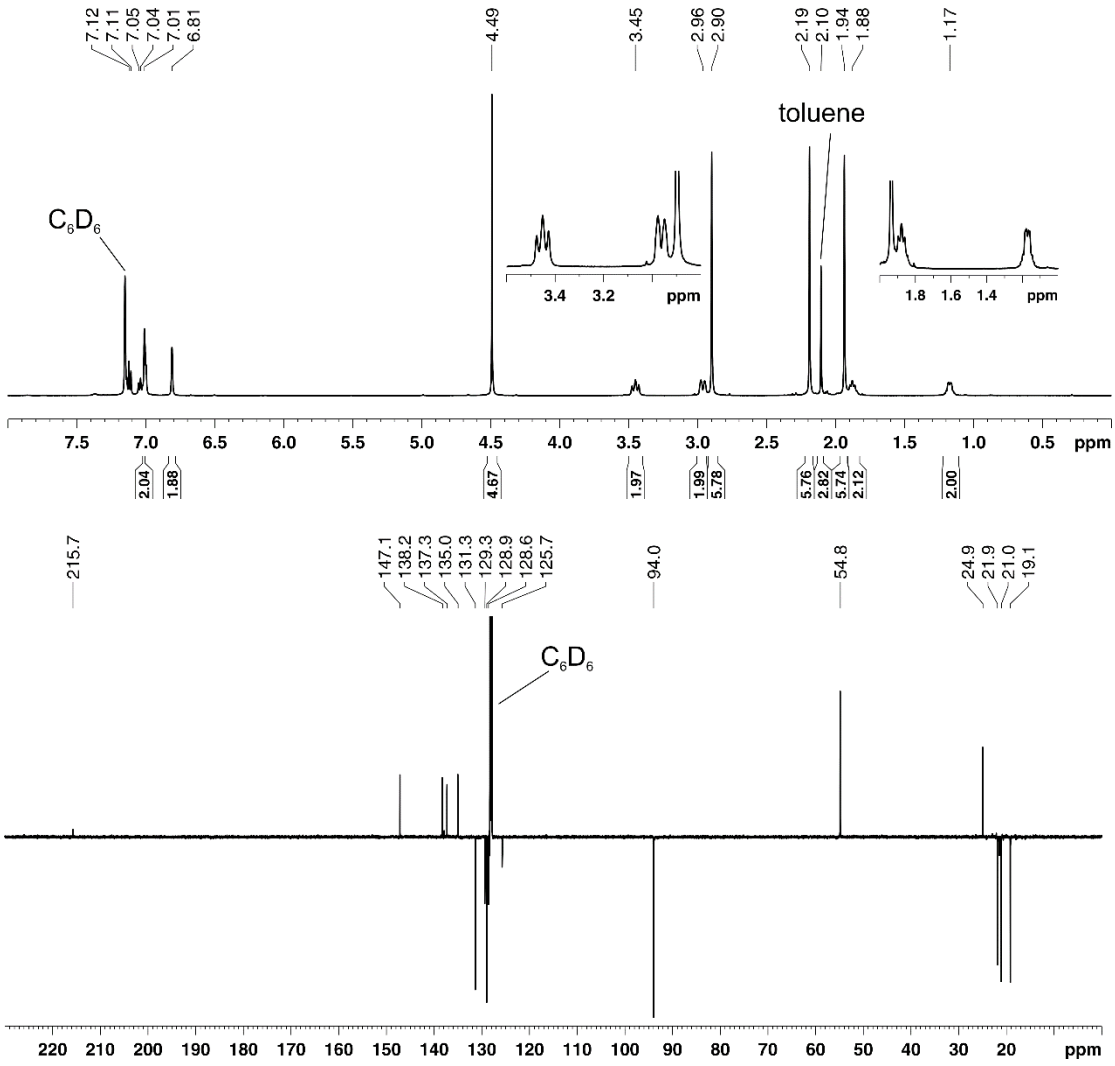

Figure S3. ^{1}H- (top) and ^{13}C{^{1}H} pendant NMR spectrum (bottom) of **2Br** (C_6D_6, 300 K, 400/100 MHz).

3.4.5 [CpNi(7-Mes)] (2)

Compound **2** was prepared by a similar procedure as **1**, using KC_8 (113 mg, 0.836 mmol, 1.1 eq) and a toluene solution(15 mL) of **2Br** (409 mg, 0.760 mmol, 1.0 eq) with stirring for 18 h. After filtration, the filtrate was concentrated to ca. 1 mL and layered with hexane (1.5 mL) to afford yellow, X-ray quality crystals of **2** upon cooling to −35 °C. Yield 156 mg (46%); ^{1}H NMR (C_6D_6, 300 K, 500 MHz) δ/ppm = −52.4 (br s), −7.5 (br s), 4.9 (br s), 11.3 (br s), 12.0 (br s), 15.1 (br s); effective magnetic moment (C_6D_6): μ_{eff} = 1.9(1) μ_B. UV/Vis (Et_2O, λ_{max} /nm, (ε_{max} /L·mol^{-1}·cm^{-1})): 377 (10100), 446 (7100); anal. calcd for $C_{28}H_{35}N_2Ni$ (458.30): C 73.38, H 7.70, N 6.11; found C 72.61, H 7.31, N 5.80.

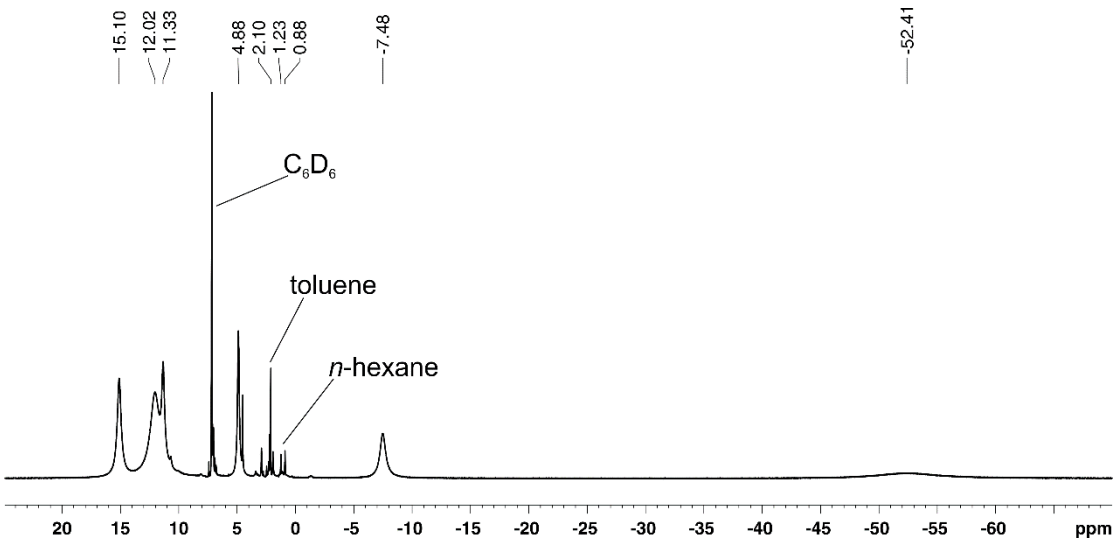

Figure S4. ^{1}H NMR spectrum of **2** (C_6D_6, 300 K, 500 MHz).

3.4.6 [CpNiBr(6-MesDAC)] (3Br)

A benzene solution (30 mL) of 6-MesDAC (990 mg, 2.63 mmol. 1.06 eq) and [CpNi(PPh_3)Br] (1.22 g, 2.48 mmol) was stirred at room temperature for 2 h before being reduced to dryness. The residue was washed with hexane (3 x 20 mL), extracted with toluene (60 mL) and filtered. The filtrate was concentrated to ca. 30 mL and cooled to -30 °C to yield dark brown microcrystals. Yield 913 mg (59%). Single crystals suitable for X-ray diffraction formed upon diffusion of hexane into a concentrated toluene solution of 3Br. ^{1}H NMR (C_6D_6, 300 K, 400 MHz) δ/ppm = 1.41 (s, 3H, C(CH_3)$_2$), 1.60 (s, 3H, C(CH_3)$_2$), 1.76 (s, 6H, *o*-CH_3), 2.12 (s, 6H, *p*-CH_3), 2.76 (s, 6H, *o*-CH_3), 4.53 (s, 5H, Cp), 6.70 (s, 2H, *m*-CH), 6.92 (s, 2H, *m*-CH); ^{13}C{^{1}H} NMR (C_6D_6, 300 K, 100 MHz) δ/ppm = 18.8 (*o*-CH_3), 18.9 (C(*C*H_3)$_2$), 20.9 (*o*-CH_3), 21.0 (*p*-CH_3), 28.5 (C(*C*H_3)$_2$), 51.4 (*C*(CH_3)$_2$), 95.8 (Cp), 129.1 (*m*-CH), 131.1 (*m*-CH), 135.7 (*o*-C), 138.3 (*o*-C), 139.2 (*p*-C), 139.4 (*i*-C), 168.7 (CO), 237.9 (NCN); anal. calcd for $C_{29}H_{33}BrN_2NiO_2$·0.2(C_7H_8) (598.62): C 61.00, H 5.83, N 4.68; found C 61.08, H 5.65, N 4.12.

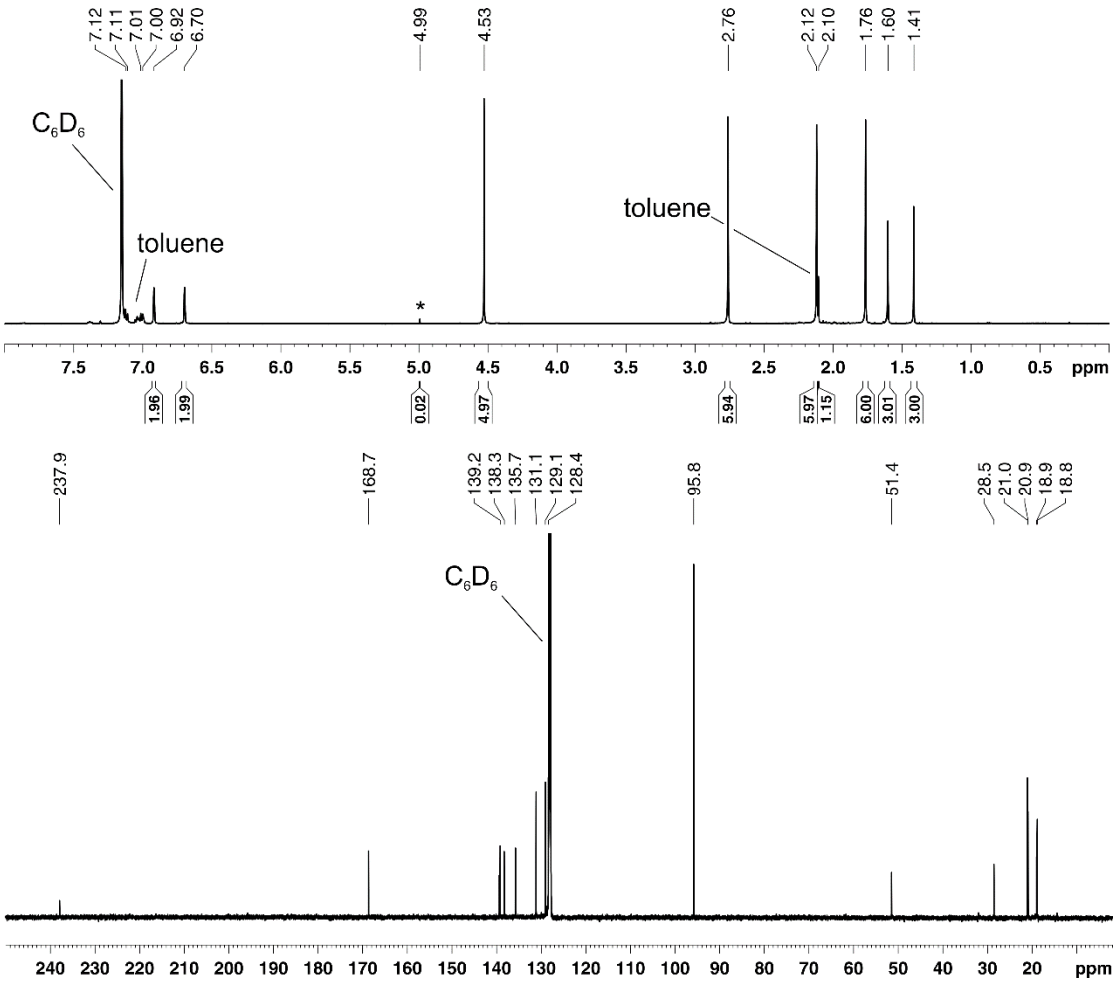

Figure S5. ^{1}H- (top) and ^{13}C{^{1}H} NMR spectrum (bottom) of **3Br** (C_6D_6, 300 K, 400/100 MHz,). Minor signals of [CpNiBr(PPh_3)] are labeled with an asterisk.

3.4.7 [CpNi(6-MesDAC)] (3)

As for **1**, but using KC_8 (47.2 mg, 0.349 mmol, 1.1 eq), a toluene (5 mL) solution of **3Br** (199 g, 0.317 mmol) and stirring at room temperature for 47 h. Dark green crystals of 3 formed after concentrating the filtrate to 3 mL and cooling to −30 °C. Yield 73 mg (46%). X-ray quality crystals were obtained by cooling a concentrated toluene/*n*-hexane solution to −35 °C. ^{1}H NMR (C_6D_6, 300 K, 500 MHz): δ 1.3 (br s), 12.0 (br s), 15.5 (br s); effective magnetic moment (C_6D_6) μ_{eff} = 1.9(1) μ_B. UV/Vis (Et_2O, λ_{max} /nm, (ε_{max} /L·mol^{-1}·cm^{-1})): 313 (10300), 442 (31400), 592 (9300); anal. calcd for $C_{29}H_{33}N_2NiO_2$ (500.29): C 69.62, H 6.65, N 5.60; found: C 69.74, H 6.52, N 5.60.

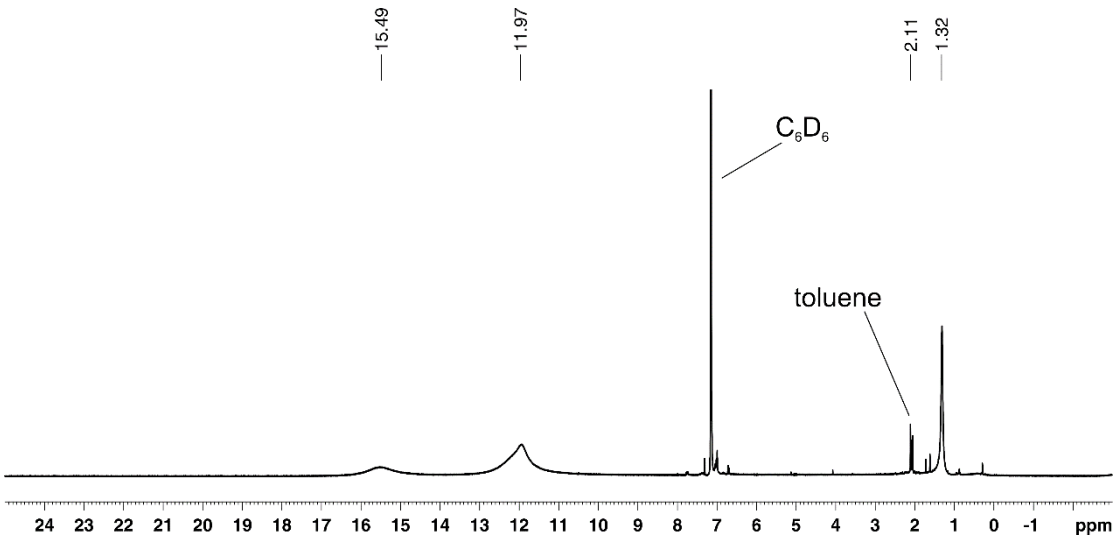

Figure S6. ^{1}H NMR spectrum of **3** (C_6D_6, 300 K, 500 MHz).

3.4.8 X-ray Crystallography

The Data for **1**−**3** and **1Br**−**3Br** (Table S1) were collected using an Agilent SuperNova diffractometer with microfocus Cu K_α radiation (λ = 1.54184 Å). Empical multi-scan[16] were applied to the data. Using Olex2[17], the structures were solved with SHELXT[18] and least-square refinements on F^2 were carried out with SHELXL.[19]

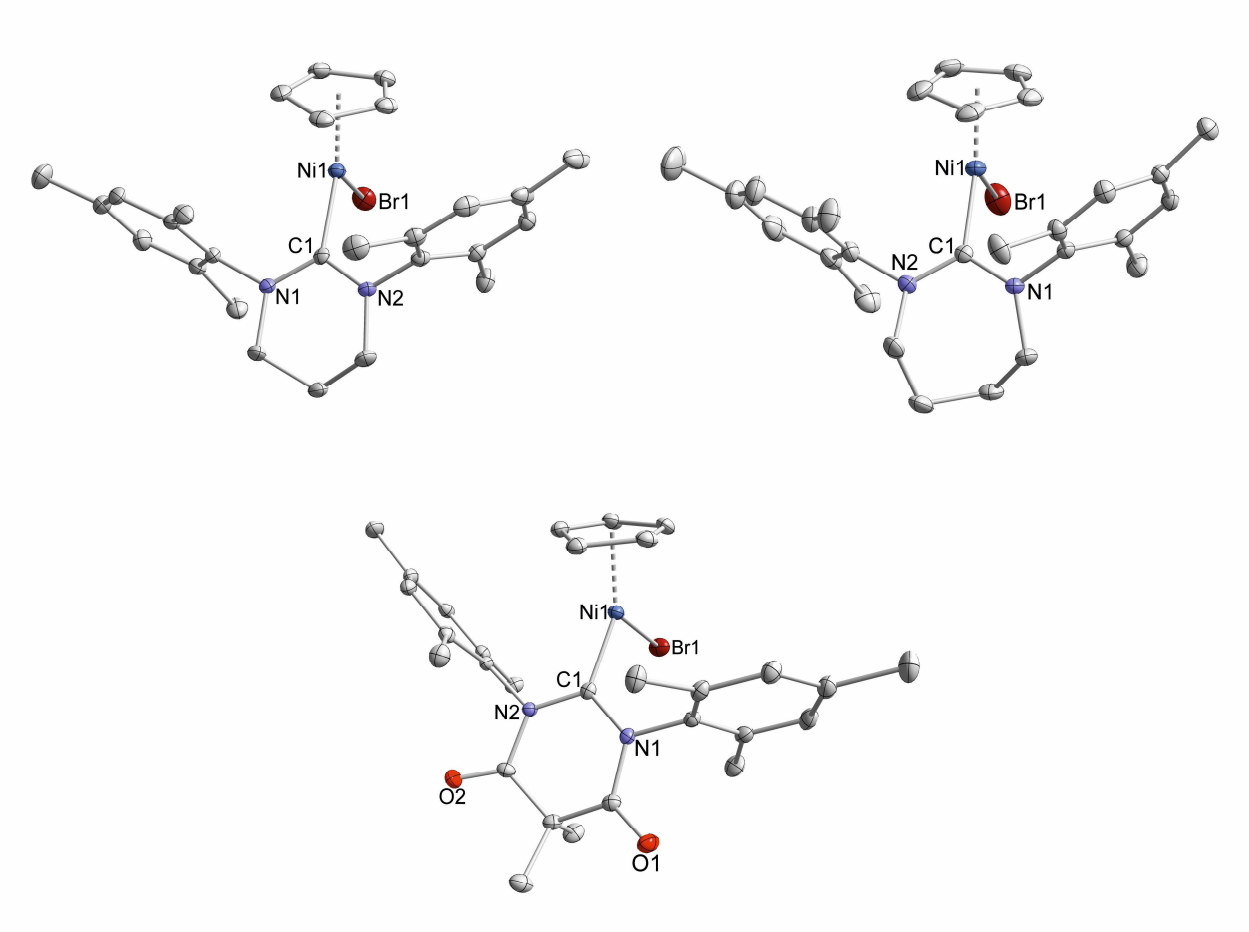

Figure S7. X-ray structures of [CpNiBr(6-Mes)] (**1Br**, top left), [CpNiBr(7-Mes)] (**2Br**, top right) and [CpNiBr(6-MesDAC)] (**3Br**, bottom). Ellipsoids are shown at the 30% level with all hydrogen atoms removed for clarity. Selected bond lengths (Å) and angles (°) for **1Br**: Ni(1)-C(1) 1.90821(1), Ni(1)-Br(1) 2.33480(1), Ni(1)-C(1)-N(1) 122.0964(5), Ni(1)-C(1)-N(2) 120.7691(4). **2Br**: Ni(1)-C(1) 1.900991(9), Ni(1)-Br(1) 2.327934(9), Ni(1)-C(1)-N(1) 119.4368(2), Ni(1)-C(1)-N(2) 121.5945(1). **3Br**: Ni(1)-C(1) 1.87147(3), Ni(1)-Br(1) 2.32581(3), Ni(1)-C(1)-N(1) 121.859(1), Ni(1)-C(1)-N(2) 122.234(1).

Table S1. Crystallographic data of **1**−**3** and **1Br**−**3Br**.

Compound	**1**	**2**	**3**
Empirical formula	$C_{27}H_{33}N_2Ni$	$C_{28}H_{35}N_2Ni$	$C_{29}H_{33}N_2NiO_2$
Formula weight	444.26	458.29	500.28
Temperature [K]	150(1)	150(1)	150(1)
Crystal system	monoclinic	triclinic	orthorhombic
Space group	$P2_1/n$	P-1	$Pbcn$
a [Å]	9.0299(2)	9.0066(3)	26.0692(4)
b [Å]	30.5459(7)	9.4373(3)	9.07493(17)
c [Å]	9.5199(2)	15.9678(5)	21.6239(4)
α [°]	90	100.212(3)	90
β [°]	117.041(3)	93.339(3)	90
γ [°]	90	113.601(3)	90
Volume [Å^3]	2338.79(12)	1211.38(7)	5115.70(16)
Z	4	2	8
ρ_{calc} [g/cm^3]	1.262	1.256	1.299
μ [mm^{-1}]	1.292	1.262	1.305
F(000)	948.0	490.0	2120.0
Crystal size [mm^3]	0.2044 × 0.1321 × 0.0817	0.194 × 0.0941 × 0.0862	0.1192 × 0.0946 × 0.0612
Radiation	CuK$_\alpha$ (λ = 1.54184)	CuK$_\alpha$ (λ = 1.54184)	CuK$_\alpha$ (λ = 1.54184)
2Θ range for data collection [°]	10.828 to 143.898	10.778 to 144.074	8.178 to 143.998
Index ranges	$-10 \le h \le 11$, $-35 \le k \le 37$, $-11 \le l \le 10$	$-11 \le h \le 11$, $-9 \le k \le 11$, $-19 \le l \le 19$	$-24 \le h \le 32$, $-10 \le k \le 11$, $-26 \le l \le 25$
Reflections collected	14915	11545	25391
Independent reflections	4567 [R_{int} = 0.0345, R_{sigma} = 0.0364]	4745 [R_{int} = 0.0210, R_{sigma} = 0.0263]	5016 [R_{int} = 0.0378, R_{sigma} = 0.0264]
Data / restraints / parameters	4567/0/277	4745/0/286	5016/150/369
Goodness-of-fit on F^2	1.036	1.060	1.018
Final R indexes [I>=2σ (I)]	R_1 = 0.0365, wR_2 = 0.0939	R_1 = 0.0358, wR_2 = 0.0929	R_1 = 0.0372, wR_2 = 0.0981
Final R indexes [all data]	R_1 = 0.0409, wR_2 = 0.0979	R_1 = 0.0377, wR_2 = 0.0946	R_1 = 0.0483, wR_2 = 0.1052
Largest diff. peak/hole [e Å^{-3}]	0.58/−0.28	0.79/−0.44	0.31/−0.33

Compound	**1Br**	**2Br**	**3Br**
Empirical formula	$C_{122}H_{148}Br_4N_8Ni_4$	$C_{28}H_{35}BrN_2Ni$	$C_{32.5}H_{37}BrN_2NiO_2$
Formula weight	2280.96	538.20	626.26
Temperature [K]	150(1)	150(1)	123(1)
Crystal system	monoclinic	orthorhombic	monoclinic
Space group	$P2_1/c$	$Pbcn$	$I2/a$
a [Å]	17.20713(12)	9.03948(5)	25.7479(4)
b [Å]	16.17350(11)	17.10755(11)	8.52911(12)
c [Å]	39.3886(3)	32.28154(17)	27.6462(4)
α [°]	90	90	90
β [°]	99.8316(7)	90	104.1525(15)
γ [°]	90	90	90
Volume [Å^3]	10800.84(14)	4992.12(5)	5887.03(15)
Z	4	8	8
ρ_{calc} [g/cm^3]	1.403	1.432	1.413
μ [mm^{-1}]	2.914	3.116	2.780
F(000)	4752.0	2240.0	2600.0
Crystal size [mm^3]	0.1618 × 0.1404 × 0.0799	0.0927 × 0.0817 × 0.0596	0.3973 × 0.1538 × 0.0698
Radiation	CuK_α (λ = 1.54184)	CuK_α (λ = 1.54184)	CuK_α (λ = 1.54184)
2Θ range for data collection [°]	8.144 to 143.944	10.342 to 143.938	7.082 to 147.354
Index ranges	$-16 \le h \le 20$, $-19 \le k \le 19$, $-47 \le l \le 48$	$-11 \le h \le 11$, $-21 \le k \le 19$, $-39 \le l \le 39$	$-31 \le h \le 30$, $-10 \le k \le 7$, $-29 \le l \le 34$
Reflections collected	83250	152563	13703
Independent reflections	21050 [R_{int} = 0.0366, R_{sigma} = 0.0360]	4902 [R_{int} = 0.0339, R_{sigma} = 0.0084]	5732 [R_{int} = 0.0222, R_{sigma} = 0.0240]
Data / restraints / parameters	21050/210/1333	4902/0/295	5732/224/428
Goodness-of-fit on F^2	1.046	1.087	1.071
Final R indexes [I>=2σ (I)]	R_1 = 0.0372, wR_2 = 0.0828	R_1 = 0.0321, wR_2 = 0.0770	R_1 = 0.0272, wR_2 = 0.0687
Final R indexes [all data]	R_1 = 0.0432, wR_2 = 0.0859	R_1 = 0.0331, wR_2 = 0.0777	R_1 = 0.0305, wR_2 = 0.0766
Largest diff. peak/hole [e Å^{-3}]	0.47/−0.68	0.58/−0.61	0.64/−0.35

3.4.5 DFT: Cartesian Coordinates of 1, 2, and 3

The calculations on **1**,**2**, and **3** were performed using the ORCA program package (version 3.0.2.).[20] The B3LYP density functional and the Ahlrichs def2-TZVP basis set were employed for all atoms.[21,22] The RI approximation was used.[23] Ahlrichs Coulomb fitting basis for the TZVP basis for all atoms (TZV/J) and atom-pairwise dispersion correction to the DFT energy with Becke-Johnson damping (d3bj) were applied.[24] The nature of the stationary points were verified by a numerical frequency analysis.

1:
Energy = -2666.344372988211 Hartree

Ni	2.85323933044113	11.38353834187062	3.51813891674195
N	3.70113374842127	10.81480970744743	6.07842249375389
N	5.16684448119229	12.28739882902952	5.08300542416566
C	4.05159198484180	11.53814183304388	4.98982471533825
C	4.41959373518532	10.80613616738935	7.34963606004214
H	5.14350005466533	9.98204170804735	7.37951877956847
H	3.69907316401709	10.62928802871856	8.14932516019543
C	5.12866940478096	12.14026289499887	7.52700895667538
H	4.38445941055771	12.93032864946295	7.65297502851515
H	5.75823285720556	12.12724115871034	8.41775380466504
C	5.97418980455079	12.42854510525461	6.29715163622433
H	6.36732115408170	13.44542352145403	6.32585086633803
H	6.83451143926021	11.74965557920099	6.25924910706667
C	1.42246466697468	10.80950672860242	1.98796276039335
H	0.77569184106160	9.95673435908969	2.12441688861322
C	1.12986130553982	12.14882177147231	2.37718148521945
H	0.22520449676772	12.48642442036128	2.85811991487770
C	2.23271630489301	12.95721344067492	2.00153990688495
H	2.33039914969769	14.01834772523720	2.16670238808858
C	3.19972152504509	12.12289615946274	1.38305636699896
H	4.15897356502498	12.44377089114192	1.01310309190813
C	2.69651930787131	10.79888964162575	1.35782530226955
H	3.19018876788147	9.93840560707989	0.93454991874982
C	2.56835630553591	9.95218372802136	5.89943204689586
C	1.30057661254986	10.39334110274824	6.29873772032015
C	0.20664248786569	9.57284588890455	6.04387775140423
H	-0.78193039649305	9.91252347265821	6.33278421278205
C	0.34557669709897	8.34888707039383	5.39086006433824
C	1.62009232492177	7.93794316919640	5.01544573915511
H	1.74209859152754	6.99524058109731	4.49472200410270
C	2.74584070415782	8.72100644079276	5.25850907912633
C	1.12711642334620	11.75762426050335	6.90865270414488
H	1.75180923365293	11.89714596816121	7.79362209439725
H	0.09024473389592	11.92569186782453	7.19883545766778
H	1.41359840853940	12.52608940484228	6.18689904590499
C	-0.86110417175513	7.50164452148638	5.08472142637542
H	-1.26440318098705	7.03947023269793	5.99028177689400
H	-0.61462647726469	6.70226170090721	4.38602420847740
H	-1.65868609277112	8.10202472568599	4.64249376751152
C	4.10278444789861	8.28835084758441	4.77607797427184
H	4.44689783221330	8.95856082682867	3.98647306375055
H	4.06872278116675	7.27637008933729	4.37341983425193
H	4.84803484916956	8.31774813792066	5.57315793587626
C	5.59936022192196	12.97359204782570	3.89932155823593
C	5.10692518567309	14.25311454125373	3.63894636795833
C	5.45183978302896	14.86389774259994	2.43601273959179
H	5.03643420052553	15.83854911716843	2.20627379282782
C	6.27488365761569	14.23256636430636	1.50857005653142
C	6.77964355836859	12.97241777095935	1.81881532784225
H	7.41429384595060	12.46477767578755	1.10098017642739

C	6.44376580875558	12.31922716526624	2.99980227877172
C	4.16235902329961	14.91353110449617	4.60287635928803
H	3.32367445758877	14.25128890605444	4.82391189991387
H	3.76654622868603	15.84031569825057	4.18777951685542
H	4.65622227478818	15.15129908339143	5.54975454527546
C	6.55512409393863	14.84257250627763	0.16140348188150
H	6.01055349547386	14.30294341795778	-0.61819095881208
H	7.61676367534341	14.78791712408206	-0.08954169450509
H	6.24180318904019	15.88620251723738	0.12062270790341
C	6.88149531549056	10.89984878873744	3.23006604209358
H	7.15396860313013	10.70709617103880	4.26776835329721
H	7.73404733168922	10.64929977407831	2.59934502210420
H	6.06389243546373	10.21962617626152	2.97900554557529

2:
Energy = -2705.637034391495 Hartree

Ni	-0.86303672994093	3.31483254588138	3.61630133845884
N	1.17577368176324	5.12251084396969	3.39077649739676
N	-0.31194251276918	5.81908474370631	5.05218844717771
C	0.02972332911940	4.92705827350968	4.09769865997464
C	-1.58774749193602	5.61014668225753	5.68171017090758
C	1.49741505773664	4.00045819099065	2.54434441058049
C	-2.92493550670683	4.55060592049461	7.36420142758205
H	-2.99518709500927	3.91540253576439	8.24028143052521
C	-1.66554371032980	4.83660267900449	6.84159429505138
C	-2.27160694785098	2.01742452659558	4.89478585656643
H	-2.42502789442931	2.14308187718887	5.95367233143130
C	-2.73549309309548	6.11501469000684	5.06641672557749
C	-1.42237912173976	1.35011422768272	2.87273882584663
H	-0.81530592925481	0.86599114721098	2.12429507741068
C	0.96041070497728	3.92433470896451	1.25297094940652
C	1.97616993834378	6.34820412573372	3.19866083726857
H	2.37203241479607	6.28662540593593	2.18507594255779
H	2.84409235153749	6.35310006560414	3.86756034351975
C	2.49130786251531	1.83267600440070	2.28647142799456
H	3.07076721562970	1.01346222652078	2.69728689563854
C	2.27849650858920	2.96064966483596	3.06790696994987
C	-4.09001311212515	5.00653091047411	6.75483915981966
C	-1.27955489932237	1.21184526993874	4.27942063953690
H	-0.54906542414242	0.60058767743232	4.78523059308353
C	-2.51190721010800	2.23083349512062	2.62063268118988
H	-2.88826146496855	2.51443497714602	1.65046099205994
C	-0.42736154601616	4.24107565846391	7.45023205920461
H	0.10429915883899	3.64651284872529	6.70429631432701
H	-0.67889881347724	3.59207864611489	8.28786055655342
H	0.26284768067923	5.00442550163665	7.81555027937493
C	-3.97312412439181	5.80865118208904	5.62215636284795
H	-4.87029514496867	6.17816087696874	5.13778443947695
C	-3.03069933739302	2.64560788095725	3.87383675532571
H	-3.84728241671500	3.33158649568991	4.02963642766140
C	1.19357354897432	2.76747996158182	0.50918097240979
H	0.73985723933417	2.67967982239232	-0.47135545413678
C	1.93707852080131	1.70699098837231	1.01343132420613
C	0.11224790054615	5.03473293990917	0.69412585952394
H	-0.64700811905686	5.33822455545579	1.41446736038886
H	-0.39402885462816	4.71006405236706	-0.21438752879112
H	0.71162146211939	5.91622153882312	0.44931237608349
C	2.79785226973254	3.02713949990959	4.47580755461786
H	3.25431612529246	3.99212491054231	4.69909285021939
H	3.53793987783296	2.24736818042358	4.65245612592992
H	1.97698295477392	2.88572976552096	5.18302442992077
C	1.17157580660933	7.63607346941115	3.34697885990491
H	0.23622566043512	7.51757589597057	2.79823342446435
H	1.71835591067173	8.44641259252246	2.86012222654454
C	0.62648130487885	6.77153424770199	5.65857458209699
H	1.56669480343360	6.24667592541685	5.84699838225629
H	0.22178475393168	7.05973552983775	6.62681866909211
C	0.88028755913583	8.00702242147357	4.80340632598479

H	1.72595192341755	8.55106346440193	5.23405528128254
H	0.02016352232848	8.67846203754997	4.85153652450643
C	-5.44594881829250	4.57972179554047	7.24788382908820
H	-5.82434876091395	3.75165658628269	6.64199022675863
H	-6.17168928568219	5.39150677654113	7.17551284324172
H	-5.41106459460382	4.23572575023880	8.28262461701838
C	-2.64179498573269	6.89967235470298	3.78731611342342
H	-1.97251884981086	7.75585973044957	3.88312640599376
H	-3.62210548407742	7.26643435537999	3.48357475470252
H	-2.24843471898286	6.26483568852261	2.99028014400936
C	2.11285148589408	0.43490000717526	0.22776951278441
H	3.14891174724039	0.29891426433035	-0.09389851077011
H	1.48379442512765	0.42986145048824	-0.66231939199813
H	1.84363729143420	-0.43185306625330	0.83558318795799

3:
Energy = -2893.040739977326 Hartree

O	9.68473565683584	3.57082250238929	4.93023195970562
O	7.30472673051750	6.78672357109815	7.38471312891074
N	10.03326622018347	3.82257936492834	7.16026796663044
N	8.78068133275408	5.37529580975101	8.37179742057943
C	9.71822419466432	4.36174361137723	8.37577258041669
C	9.49222726719899	4.21645981968341	5.93434021139432
C	8.74098742497773	5.54016530815246	5.91669010639115
C	8.17741802359826	5.95474885898264	7.26755156679828
C	7.62619425707653	5.48891677260425	4.87056765701061
H	8.04902459147925	5.22122159797718	3.90495774195299
H	7.13610562266179	6.45775413600691	4.81048191848914
H	6.87744854141292	4.74157024632726	5.13529935030266
C	9.78394947813994	6.62320794987847	5.53385473150332
H	10.57258274376966	6.70017848037050	6.28299493150094
H	9.28037752957408	7.58620520348385	5.45480662938912
H	10.23518240855107	6.37008352655547	4.57495253165021
C	10.49570346273162	1.95401676285766	11.13561800945084
H	9.92068255274943	1.07516234485675	10.89180966026036
C	11.75581070342210	2.30358096062005	10.58568029825247
H	12.29545410529856	1.74356909355322	9.83992990590373
C	12.16255453702787	3.53517796648466	11.16246360561354
H	13.07652112686828	4.06484202393089	10.94668992125111
C	11.14450098830544	3.95550687350978	12.06073412290120
H	11.14500408695479	4.86044516077087	12.64684043842588
C	10.11319425436137	2.97683019677876	12.04525787895313
H	9.20046812265560	3.01322236577640	12.61789276292481
C	10.94646670452667	2.70043830403781	7.16119009363967
C	12.29695354766566	2.94622818935912	6.93191302489295
C	13.17013918608807	1.86241270882536	6.96061781039193
H	14.22485290959396	2.03439612122004	6.77883243921832
C	12.72104108078691	0.56759845154918	7.21094611427802
C	11.35940887350198	0.36666941530922	7.42074258645986
H	10.99120815511932	-0.63603861232730	7.60426778009046
C	10.45171589159136	1.42105741991140	7.39884428496948
C	12.78974840877744	4.34179415358922	6.66987618946569
H	12.28599665571533	4.78317211948528	5.80841269540101
H	13.86000759153833	4.34499939043571	6.46646632470823
H	12.59935839218694	4.98795193223263	7.53036444716577
C	13.68361737473949	-0.58715932908489	7.27481205009454
H	14.55239820144160	-0.41612583678050	6.63852881010823
H	13.20618927966121	-1.51609277421381	6.96039331121690
H	14.05052347195497	-0.73441340697391	8.29517637239550
C	8.98786265117479	1.19279900558596	7.63566096659145
H	8.65319059797552	1.74514215869568	8.51567852391539
H	8.77954456984235	0.13590154673075	7.79784993127693
H	8.39377886121593	1.53126848528071	6.78412017610372
C	8.40963384737836	5.78380593853379	9.71145414808660
C	7.35937744604505	5.12101425880684	10.35267926562991
C	7.14555524685057	5.39317202554597	11.69914511071565
H	6.35543921001765	4.86505638766281	12.21987731003480
C	7.94809613466793	6.28970792837322	12.40055139263892

C	8.93202221662249	6.98801013521373	11.70660950220727
H	9.54426777569072	7.71091043395602	12.23301125269778
C	9.18124685941273	6.75290043168538	10.35826311575400
C	6.49265198604397	4.14848344628165	9.60756868844060
H	5.87973124485994	4.67639849645320	8.87275471354498
H	5.83130332909031	3.61614933849589	10.28990602124900
H	7.09234857980359	3.41259972364640	9.07064906862834
C	7.79081397246237	6.45842923259813	13.88481549244631
H	8.45977069061481	5.77520728613392	14.41625321285379
H	6.77429393801829	6.23141302678044	14.20838544867681
H	8.04505442381216	7.47031013700838	14.20375214547823
C	10.24077842300559	7.51567590419749	9.61660419678669
H	10.96232007307759	6.83971484153496	9.15485399047649
H	10.78081587087092	8.17980537419828	10.29014952695962
H	9.79128980280113	8.12026442619766	8.82505265276396
Ni	10.26140055998548	3.89804127512272	10.08473277498346

References

1 a) T. T. Tsou, J. K. Kochi, *J. Am. Chem. Soc.* **1979**, *101*, 7547−7560; b) T. T. Tsou, J. K. Kochi, *J. Org. Chem.* **1980**, *45*, 1930−1937.

2 a) D. J. Mindiola, G. L. Hillhouse, *J. Am. Chem. Soc.* **2001**, *123*, 4623−4624; b) R. Melenkivitz, D. J. Mindiola, G. L. Hillhouse, *J. Am. Chem. Soc.* **2002**, *124*, 3846−3847; c) T. J. Anderson, G. D. Jones, D. A. Vicic, *J. Am. Chem. Soc.* **2004**, *126*, 8100−8101; d) Z. Weng, S. Teo, L. L. Koh, T. S. A. Hor, *Angew. Chem. Int. Ed.* **2005**, *44*, 7560−7564; *Angew. Chem.* **2005**, *117*, 7732−7736; e) H.-Y. Wang, X. Meng, G.-X. Jin, *Dalton Trans.* **2006**, 2579−2585; f) M. T. Kieber-Emmons, C. G. Riordan, *Acc. Chem. Res.* **2007**, *40*, 618−625; g) D. Adhikari, S. Mossin, F. Basuli, B. R. Dible, M. Chipara, H. Fan, J. C. Huffman, K. Meyer, D. J. Mindiola, *Inorg. Chem.* **2008**, *47*, 10479−10490; h) B. C. Fullmer, H. Fan, M. Pink, K. G. Caulton, *Inorg. Chem.* **2008**, *47*, 1865−1867; i) M. Ito, T. Matsumoto, K. Tatsumi, *Inorg. Chem.* **2009,** *48*, 2215−2223; j) S. Yao, Y. Xiong, C. Milsmann, E. Bill, S. Pfirrmann, C. Limberg, M. Driess, *Chem. Eur. J.* **2010**, *16*, 436−439; k) C. Jones, C. Schulten, L. Fohlmeister, A. Stasch, K. S. Murray, B. Moubaraki, S. Kohl, M. Z. Ertem, L. Gagliardi, C. J. Cramer, *Chem. Eur. J.* **2011**, *17*, 1294−1303; l) M. Vogt, B. de Bruin, H. Berke, M. Trincado, H. Grützmacher, *Chem. Sci.* **2011**, *2*, 723−727; m) B. Horn, S. Pfirrmann, C. Limberg, C. Herwig, B. Braun, S. Mebs, R. Metzinger, *Z. anorg. allg. Chem.* **2011**, *637*, 1169−1174; n) V. M. Iluc, G. L. Hillhouse, *J. Am. Chem. Soc.* **2010**, *132*, 11890−11892; o) V. M. Iluc, G. L. Hillhouse, *J. Am. Chem. Soc.* **2010**, *132*, 15148−15150; p) Z. Li, Y.-Y. Jiang, Y. Fu, *Chem. Eur. J.* **2012**, *18*, 4345−4357; q) C. Liu, S. Tang, D. Liu, J. Yuan, L. Zheng, L. Meng, A. Lei, *Angew. Chem. Int. Ed.* **2012**, *51*, 3638−3641; *Angew. Chem.* **2012**, *124*, 3698−3701; r) S. L. Yao, M. Driess, *Acc. Chem. Res.* **2012**, *45*, 276−287; s) J. Cornella, E. Gómez-Bengoa, R. Martin, *J. Am. Chem. Soc.* **2013**, *135*, 1997−2009; t) R. Beck, S. A. Johnson, *Organometallics* **2013**, *32*, 2944−2951; u) F. B. Sayyed, Y. Tsuji, S. Sakaki, *Chem. Commun.* **2013**, *49*, 10715−10717; v) B. Horn, C. Limberg, C. Herwig, B. Braun, *Chem. Commun.* **2013**, *49*, 10923−10925; w) M. I. Lipschutz, T. D. Tilley, *Organometallics* **2014**, *33*, 5566−5570; x) L. M. Guard, M. M. Beromi, G. W. Brudvig, N. Hazari, D. J. Vinyard, *Angew. Chem. Int. Ed.* **2015**, *54*, 13352−13356; *Angew. Chem.* **2015**, *127*, 13550−13554; y) M. I. Lipschutz, X. Yang, R. Chatterjee, T. D. Tilley, *J. Am. Chem. Soc.* **2013**, *135*, 15298−15301; z) M. I. Lipschutz, T. D. Tilley, *Angew. Chem. Int. Ed.* **2014**, 53, 7290−7294; *Angew. Chem.* **2014**, *126*, 7418−7422.

3 a) S. Miyazaki, Y. Koga, T. Matsumoto, K. Matsubara, *Chem. Commun.* **2010**, *46*, 1932−1934; b) K. Zhang, M. Conda-Sheridan, S. R. Cooke, J. Louie, *Organometallics* **2011**, *30*, 2546−2552; c) S. Nagao, T. Matsumoto, Y. Koga, K. Matsubara, *Chem. Lett.* **2011**, *40*, 1036−1038.

4 a) C. A. Laskowski, G. L. Hillhouse, *J. Am. Chem. Soc.* **2008**, *130*, 13846−13847; b) C. A. Laskowski, G. R. Morello, C. T. Saouma, T. R. Cundari, G. L. Hillhouse, *Chem. Sci.* **2013**, *4*, 170−174; c) C. A. Laskowski, D. J. Bungum, S. M. Baldwin, S. A. Del Ciello, V. M. Iluc, G. L. Hillhouse, *J. Am. Chem. Soc.* **2013**, *135*, 18272−18275.

5 S. Pelties, D. Herrmann, B. De Bruin, F. Hartl, R. Wolf, *Chem. Commun.* **2014**, *50*, 7014−7016.

6 J. Wu, A. Nova, D. Balcells, G. W. Brudvig, W. Dai, L. M. Guard, N. Hazari, P.-H. Lin, R. Pokhrel, M. K. Takase, *Chem. Eur. J.* **2014**, *20*, 5327−5337.

7 a) M. Iglesias, D. J. Beetstra, J. C. Knight, L.-L. Ooi, A. Stasch, S. Coles, L. Male, M. B. Hursthouse, K. J. Cavell, A. Dervisi, I. A. Fallis, *Organometallics* **2008**, *27*, 3279−3289; b) E. L. Kolychev, I. A. Portnyagin, V. V. Shuntikov, V. N. Khrustalev, M. S. Nechaev, *J. Organomet. Chem.* **2009**, *694*, 2454−2462; c) W. Y. Lu, K. J. Cavell, J. S. Wixey, B. Kariuki, *Organometallics* **2011**, *30*, 5649−5655; d) J. J. Dunsford, K. J. Cavell, B. Kariuki, *Organometallics* **2012**, *31*, 4118−4121; e) J. Li, W. X. Shen, X. R. Li, *Current Organic Chemistry* **2012**, *16*, 2879−2891; f) N. Bramananthan, M. Carmona, J. P. Lowe, M. F. Mahon, R. C. Poulten, M. K. Whittlesey, *Organometallics* **2014**, *33*, 1986−1995; g) N. Phillips, T. Dodson, R. Tirfoin, J. I. Bates, S. Aldridge, *Chem. Eur. J.* **2014**, *20*, 16721−16731.

8 a) C. J. E. Davies, M. J. Page, C. E. Ellul, M. F. Mahon, M. K. Whittlesey, *Chem. Commun.* **2010**, *46*, 5151−5153; b) R. C. Poulten, I. Lopez, A. Llobet, M. F. Mahon, M. K. Whittlesey, *Inorg. Chem.* **2014**, *53*, 7160−7169.

9 M. J. Page, W. Y. Lu, R. C. Poulten, E. Carter, A. G. Algarra, B. M. Kariuki, S. A. Macgregor, M. F. Mahon, K. J. Cavell, D. M. Murphy, M. K. Whittlesey, *Chem. Eur. J.* **2013**, *19*, 2158−2167.

10 R. C. Poulten, M. J. Page, A. G. Algarra, J. J. Le Roy, I. López, E. Carter, A. Llovet, S. A. Macgregor, M. F. Mahon, D. M. Murphy, M. Murugesu, M. K. Whittlesey, *J. Am. Chem. Soc.* **2013**, *135*, 13640−13643.

11 a) P. Bazinet, G. P. A. Yap, D. S. Richeson, *J. Am. Chem. Soc.* **2003**, *125*, 13314−13315; b) C. C. Scarborough, M. J. W. Grady, I. A. Guzei, B. A. Gandhi, E. E. Bunel, S. S. Stahl, *Angew. Chem. Int. Ed.* **2005**, *44*, 5269−5272; *Angew. Chem.* **2005**, *117*, 5403−5406; c) P. Bazinet, T.-G. Ong, J. S. O'Brien, N. Lavoie, E. Bell, G. P. A. Yap, I., Korobkov, D. S. Richeson, *Organometallics* **2007**, *26*, 2885−2895; d) U. Siemeling, C. Färber, M. Leibold, C. Bruhn, P. Mücke, R. F. Winter, B. Sarakar, M. von Hopffgarten, G. Frenking, *Eur. J. Inorg. Chem.* **2009**, 4607−4612; e) M. Iglesias, D. J. Beetstra, K. J. Cavell, A. Dervisi, I. A. Fallis, B. Kariuki, R. W. Harrington, W. Clegg, P. N. Horton, S. J. Coles, M. B. Hursthouse, *Eur. J. Inorg. Chem.* **2010**, 1604−1607; f) P. D. Newman, K. J. Cavell, B.

Kariuki, *Organometallics* **2010**, *29*, 2724−2734; g) U. Siemeling, C. Färber, C. Bruhn, S. Fürmeier, T. Schulz, M. Kurlemann, S. Tripp, *Eur. J. Inorg. Chem.* **2012**, 1413−1422.

12 a) T. W. Hudnall, C. W. Bielawski, *J. Am. Chem. Soc.* **2009**, *131*, 16039−16040; b) V. César, N. Lugan, G. Lavigne, *Eur. J. Inorg. Chem.* **2010**, 361−365; c) T. W. Hudnall, A. G. Tennyson, C. W. Bielawski, *Organometallics* **2010**, *29*, 4569−4578.

13 a) G. A. Blake, J. P. Moerdyk, C. W. Bielawski, *Organometallics* **2012**, *31*, 3373−3378; b) O. Back, M. Henry-Ellinger, C. D. Martin, D. Martin, G. Bertrand, *Angew. Chem. Int. Ed.* **2013**, *52*, 2939−2943; *Angew. Chem.* **2013**, *125*, 3011−3015; c) M. Chen, J. P. Moerdyk, G. A. Blake, C. W. Bielawski, J. K. Lee, *J. Org. Chem.* **2013**, *78*, 10452−10458; d) S. V. C. Vummaleti, D. J. Nelson, A. Poater, A. Gómez-Suárez, D. B. Cordes, A. M. Z. Slawin, S. P. Nolan, L. Cavallo, *Chem. Sci.* **2015**, *6*, 1895−1904.

14 a) D. F. Evans, *J. Chem. Soc.* **1959**, 2003–2005; b) G. J. P. Britovsek, V. C. Gibson, S. K. Spitzmesser, K. P. Tellmann, A. J. P. White, D. J. Williams, *J. Chem. Soc. Dalton Trans.* **2002**, 1159–1171.

15 a) T. W. Hudnall, J. P. Moerdyk, C. W. Bielawski, *Chem. Commun.* 2010, *46*, 4288; b) L. M. Perry, US3476769 (A), **1969**.

16 a) SCALE3ABS, CrysAlisPro, Aglient Technologies Inc., Oxford, GB, **2015**; b) G. M. Sheldrick, SADABS, Bruker AXS, Madison, USA, **2007**.

17 O. V. Dolomanov, L. J. Bourhis, R. J. Gildea, J. A. K. Howard, H. Puschmann, *J. Appl. Cryst.* **2009**, *42*, 339.

18 G. M. Sheldrick, *Acta Cryst. A* **2015**, *71*, 3.

19 G. M. Sheldrick, *Acta Cryst. C* **2015**, *71*, 3.

20 F. Neese, *Wiley Interdiscip. Rev. Comput. Mol. Sci.* **2012**, *2*, 73.

21 a) C. Lee, W. Yang, R. G. Parr, *Phys. Rev. B* **1988**, *37*, 785. b) A. D. Becke, *J. Chem. Phys.* **1993**, *98*, 1372. c) A. D. Becke, *J. Chem. Phys.* **1993**, *98*, 5648.

22 a) A. Schäfer, H. Horn, R. Ahlrichs, *J. Chem. Phys.* **1992**, *97*, 2571, b) F. Weigend, R. Ahlrichs, *Phys. Chem. Chem. Phys.* **2005**, *7*, 3297.

23 a) A. D. Becke, *Phys. Rev. A* **1988**, *38*, 3098, b) J. P. Perdew, *Phys. Rev. B* **1986**, *33*, 8822.

24 a) S. Grimme, S. Ehrlich, L. Goerigk, *J. Comput. Chem.* **2011**, *32*, 1456, b) S. Grimme, J. Antony, S. Ehrlich, H. Krieg, *J. Chem. Phys.* **2010**, *132*, 154104.

4 Formation of Heteronickelacycles through the Reductive Coupling of Phenyl Iso(thio)cyanate[a]

Stefan Pelties and Robert Wolf

[a] S. Pelties, R. Wolf, manuscript in preparation.

4.1 Introduction

In marked contrast to the well-developed chemistry of nickel(II) and nickel(0), well-defined mononuclear nickel(I) complexes are still relatively scarce,[1–3] The nickel(I) NHC complex [(η^5-Cp)Ni(IDipp)] (**A**, Cp = cyclopentadienyl, IDipp = 1,3-bis(2,6-diisopropylphenyl)imidazolin-2-ylidene), recently reported by Hazari and co-workers and by our group (see chapter 2), is a mononuclear 17e compound with pronounced metalloradical character. Complex **A** reacts with the persistent radical TEMPO (TEMPO = 2,2,6,6-tetramethylpiperidine 1-oxyl), forming the square planar nickel(II) complex **B** with a side-on η^2-coordinated TEMPO ligand and a η^1-coordinated Cp ligand (Scheme 1).[3] Furthermore, the metalloradical **A** is capable of reacting with sulfur, grey selenium, grey tellurium, and white phosphorus, giving dinuclear complexes of types **C**−**E**.

Considerung that reductive couplings of unsaturated organyls mediated by nickel(0) complexes have attracted much attention,[4,5] we became interested in examining the reactivity of nickel(I) complex **A**. Here, we describe the reaction behavior of **A** with phenyl isocyanate and phenyl isothiocyanate. We report the synthesis and molecular structure of [(IDipp)NiSC(NPh)N(Ph)CS] (**1**), formed by the reductive dimerization of the PhNCS molecules in the coordination sphere of nickel. In addition, we describe the preparation of [(IDipp)NiN(Ph)C(O)CH_2CH(Ph) (**3**), which was obtained by reacting PhNCO with [(IDipp)Ni(styrene)$_2$] (**F**). The synthesis of complex **3** demonstrates the reductive coupling of PhNCO with styrene in the coordination sphere of nickel.

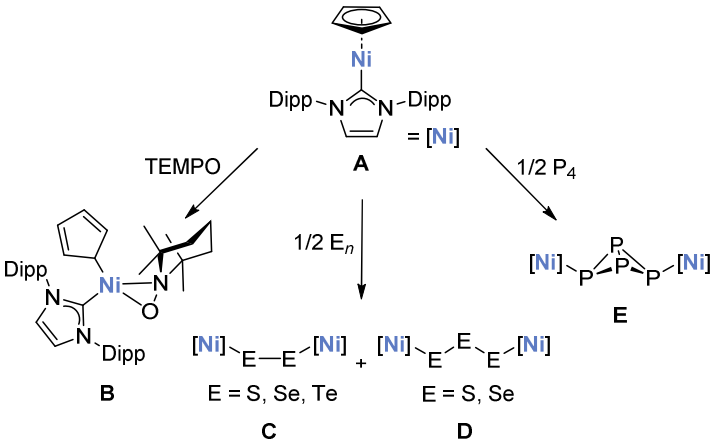

Scheme 1. Reactivity of nickel(I) radical **A**.[3]

4.2 Results and Discussion

The reaction of complex **A** with one equivalent of phenyl isothiocyanate in THF (Scheme 2a) affords complex **1** as a mixture with the known bis(cyclopentadienyl) complex [(η^5-Cp)(η^1-Cp)Ni(IDipp)] (**2**).[6] Complex **2** was identified by X-ray diffraction analysis and ^{1}H NMR spectroscopy. Attempts to separate compounds **1** and **2** by fractional crystallization remained unsuccessful to date.

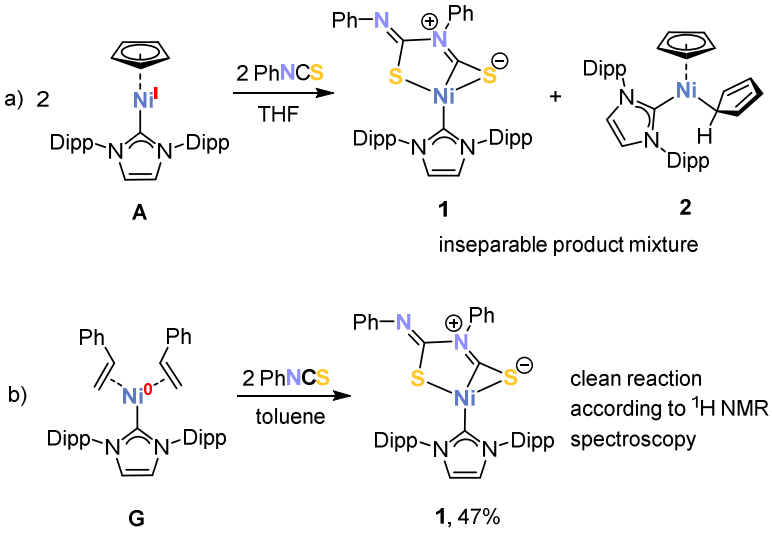

Scheme 2. Synthesis of Complex **1**.

A possible reaction pathway from the nickel(I) complex **A** to **1** and **2** is displayed in Scheme 3. The reaction is likely initiated by phenyl isothiocyanate coordination, which induces a hapticity change of the former η^5-Cp ligand to η^1-coordination forming intermediate **F** (Scheme 2, step i). We could not detect this intermediate spectroscopically, but a similar η^1-Cp complex, [(η^1-Cp)Ni(η^2-TEMPO)(IDipp)] (**B**, Scheme 1), was recently characterized.[3] Subsequent to the formation of the proposed intermediate **F**, a Cp radical may transfer from **F** to another molecule of **A** (Scheme 3, step ii), yielding complex **2** and a zerovalent nickel species that may react with PhNCS to give product **1**.

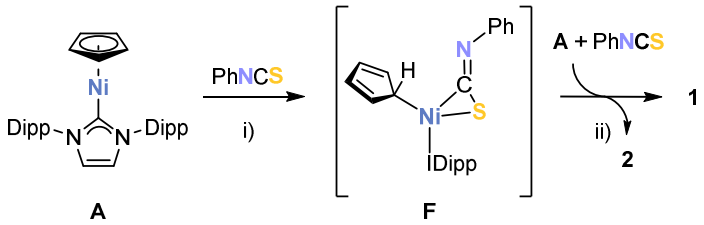

Scheme 3. Proposed Mechanism of Formation of Complex **1** Starting from the Nickel(I) Radical A.

In order to test whether the reaction pathway may involve nickel(0) species, we reacted the nickel(0) complex [(IDipp)Ni(styrene)$_2$] (**G**)[7] with two equivalents PhNCS. ^{1}H NMR monitoring revealed that the reaction proceeds in a clean fashion, allowing complex **1** to be isolated as a pure solid in 47% yield (Scheme 2b).

Orange crystalline **1** is soluble in *n*-hexane, benzene, toluene, diethyl ether, and tetrahydrofuran; the complex was fully characterized by ^{1}H and $^{13}C\{^{1}H\}$ NMR spectroscopy, UV/vis spectroscopy, elemental analysis, and a single crystal X-ray structure analysis (see the SI). The molecular structure of **1** shows that two PhNCS molecules were coupled in the coordination sphere of nickel with the formation of a C–N single bond (C5–N3 1.442(3) Å), resulting in a dianionic $\{SC(NPh)N(Ph)CS\}^{2-}$ ligand, which coordinates to the $[(IDipp)Ni]^{2+}$ fragment (Figure 1). The nickel atom is in a planar environment (sum of angles at Ni1 359.9°) formed by the carbene ligand, an η^1-coordinated thiolate function [C5–S2 1.763(2) Å)] and a side-on η^2-coordinated thiocarbonyl moiety [C4–S1 1.632(2) Å]. While the Ni1–S2 distance [Ni1–S2 2.1780(5)] is comparable to other square planar nickel(II) thiolates,[8] the Ni1–S1 distance [Ni1–S1 2.3012(6)] is slightly longer, consistent with side-on coordination of the thiocarbonyl moiety.

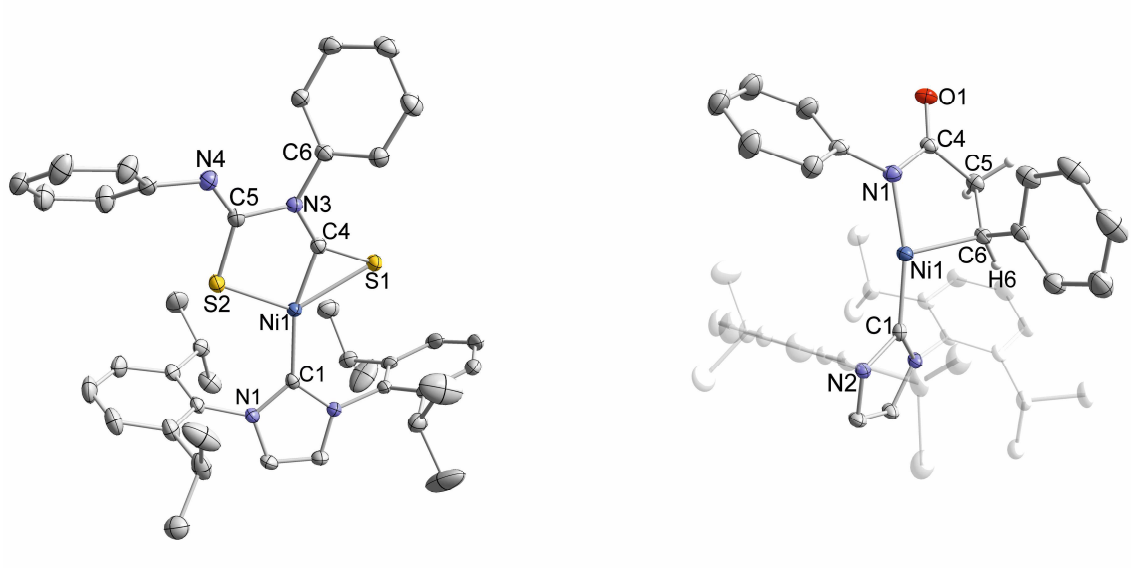

Figure 1. Solid-state molecular structure of [(IDipp)Ni{SC(NPh)N(Ph)CS}] (**1**, left) and [(IDipp)Ni{N(Ph)C(O)CH_2CHPh}] (**3**, right), only the (S)-enantiomer (**(S)-3**) is shown. The hydrogen atoms are omitted for clarity. Thermal ellipsoids are drawn at 40% level. Selected bond length [Å] and angles [°] **1**: Ni1–S1 2.3012(6), Ni1–C4 1.763(2), Ni1–S2 2.1780(5), Ni1–C1 1.954(2), C4–S1 1.632(2), C5–S2 1.763(2), C5–N3 1.442(3), N3–C4 1.328(3), N4–C5 1.268(3), S1–Ni1–C4 44.97(6), C4–Ni1–S2 83.32(6), S2–Ni1–C1 113.69(6), C1–Ni1–S1 117.89(6), C4–N3–C6 124.06(17), C4–N3–C5 112.45(17), C5–N3–C6 122.96(16); **3**: Ni1–N1 1.876(4) [1.878(4)], Ni1–C6 1.945(5) [1.941(5)], Ni1–C1 1.879(4) [1.877(4)], Ni1–H6 2.32(5) [2.35(6)] N1–C4 1.356(6) [1.347(6)], C4–O1 1.227(6) [1.238(6)], C4–C5 1.518(6) [1.515(6)], C5–C6 1.521(7) [1.524(6)], N1–Ni1–C1 164.4(2) [164.6(2)], C1–Ni1–C6 104.0(2) [103.3(2)], N1–Ni1–C6 86.2(2) [86.5(2)].

Furthermore, the N3–C4 bond distance [N3–C4 1.328(3) Å] is longer than the N4–C5 double bond [N4–C5 1.268(3) Å], presumably as a result of π-delocalization over S1, C4, and N3. Numerous π and σ transition metal complexes of organyl isothiocyanates are known,[9] and the insertion of organyl isothiocyanates into transition metal heteroatom bonds is well-documented.[10]

Nonetheless, to our knowledge such a reductive dimerization of phenyl isothiocyanate in the coordination sphere of a transition metal has not been described in the literature.

The ^{1}H NMR spectrum of **1** in C_6D_6 (Figure S1, SI) agrees with the crystallographically-determined structure. Two characteristic doublets at 1.07 and 1.52 ppm are assigned to the methyl groups of the 2,6-diisopropylphenyl (Dipp) substituents; the methine protons give rise to a septet at 2.83 ppm. A singlet at 6.53 ppm is detected for the protons of the imidazolin-2-ylidene backbone. The hydrogen atoms in *meta*- and *para*-position of the Dipp substituent and the ones of the phenyl groups are detected as five overlapping multiplets ranging from 6.75 to 7.37 ppm. The ^{13}C{^{1}H} NMR spectrum features two signals for the C4 and C5 atoms (Figure 1) at 171.4 and 237.8 ppm. The carbene atom is detected at 189.9 ppm. The UV/Vis spectrum of **1** in THF shows two intense absorptions at 284 and 325 nm, as well as two bands in the visual region at 413 nm and 519 nm.

Our results with PhNCS prompted us to investigate the reactivity of **A** toward PhNCO. According to ^{1}H NMR monitoring, several diamagnetic species are formed in this reaction that could not be identified. It is interesting to note, however, that the reaction with [(IDipp)Ni(styrene)$_2$] (**G**) affords complex **3** (Scheme 4a), which results from the coupling of PhNCO and styrene in the coordination sphere of nickel. The complex was isolated in 48% yield as blue crystals from THF/*n*-hexane. Complex **3** was also obtained in a lower yield of 20% when two equivalents of PhNCO were added. Crystalline **3** is only sparingly soluble in non-polar solvents (*n*-hexane, benzene, and toluene), but it dissolves well in THF. According to ^{1}H NMR spectroscopy, the complex slowly decomposes in THF-d_8 over the course of days at room temperature, forming the starting material, [(IDipp)Ni(styrene)$_2$] (**G**) and unidentified species.

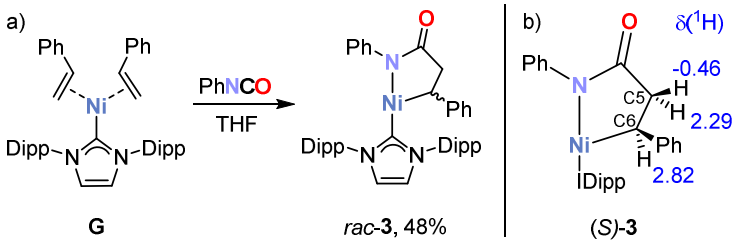

Scheme 4. Synthesis of **3** from [(IDipp)Ni(styrene)$_2$].

Compound **3** crystallizes in the space group $P\bar{1}$ with two crystallographically independent molecules in the asymmetric unit, which represent the (*R*)- and the (*S*)-isomers. The molecular structure of (*S*)-**3** is shown in Figure 2. In contrast to the reaction of [(IDipp)Ni(styrene)$_2$] with phenyl isothiocycanate, one styrene ligand and one phenyl isocyanate molecule underwent a [2+2+1] cycloaddition, forming a γ-lactam-nickelacycle (Figure 2). The nickel(II) atom features a distorted T-shaped environment [C1–Ni1–C6 104.0(2)°, N1–Ni1–C6 86.2(2)°]. The nitrogen atom of the amide function is in a planar environment (Σ_{angles} = 358.8°). No hydrogen atom

appears close enough to the vacant coordination site of the metal atom for an agostic interaction, the closest contact being Ni1–H6 2.32(5) Å (Figure 1, right).

A DFT optimization of the structure of **3** (BP86/def2-TZVP level, see the SI) is in good agreement with the XRD analysis and also indicates the absence of agostic interactions (shortest Ni–H distance: Ni1–H6 2.47 Å). T-shaped nickel(II) complexes, where the metal atom is purely surrounded by σ-donor ligands, should be electronically favored over Y-shaped molecules.[9] Nonetheless, such T-shaped nickel(II) complexes are rare and only three, "true" T-shaped three-coordinate nickel(II) species have been described, where there is no ligand or agostic interaction at the fourth position of the square plane.[3,12]

The ^{1}H NMR spectrum of **3** (THF-d_8, Figure S2, SI) displays one set of signals of the NHC ligand; a doublet at 2.82 ppm may be assigned to CH group adjacent to the nickel atom. An unusual feature of the spectrum is the observation of two doublets of doublets at 2.29 and −0.46 ppm that can be assigned to the diastereotopic CH_2 moiety in the γ-position of the metallacycle (Scheme 4b). It is well known that methylene protons with a *syn* orientation adjacent to organyl substituents can show a significant high-field chemical shift compared to the *anti* hydrogen.[13] Additionally, the magnetic anisotropy effect of the phenyl group attached to C6 could lead to a high-field shift of the proton signal.[14] It is noteworthy that the chemical shift of this multiplet is strongly solvent dependent ($\delta(^{1}H)$ = 0.30 ppm in C_6D_6 vs. −0.46 ppm in THF-d_8). It is conceivable that a C−H agostic interaction may be the cause for the unsual high-field shift.[15] However, this explanation seems unlikely based on the high $^{1}J(^{13}C,^{1}H)$ coupling constant ($^{1}J(^{13}C,^{1}H)$ = 130 Hz), which is in the typical range of sp^3-CH_2 groups, while $^{1}J(^{13}C,^{1}H)$ coupling constants in the range of 75−100 Hz are usually expected for an agostic C−H bond. The UV/Vis spectrum of **3** in THF displays two intense absorptions at 296 and 354 nm, while a broad absorption is detected in the visible at 699 nm.

Metallacycles related to complex **3** were described by the groups of Yamamoto[16] and Hoberg[17] (Figure 2). Yamamoto *et al.* obtained nickel-containing cyclic amides by reacting $Ni(cod)_2$ (cod = 1,5-cyclooctadiene) with mono- and bidentate phosphanes and α,β-unsaturated amides.[16] Cryoscopic molecular weight determinations in benzene indicated that these metallacycles are trimer in solution,[16b] while a single crystal X-ray structure analysis on one of the compounds revealed a tetrameric structure (Figure 3).[16c] The monomers are connected via an interaction of the nickel(II) centers and the amide oxygen atom of another γ-lactam-nickelacycle. Hoberg *et al.* obtained a series of complexes by reacting $Ni(cod)_2$, mono- and bidentate σ-donors, organyl isocyanates with alkenes. The structural composition of these complexes was proven by NMR and IR spectroscopy, but they were not crystallographically characterized at the time. Thus, the degree of association and the coordination number of nickel remains unknown for Hoberg's compounds in case of the monodentate ligands. Nevertheless, it seems likely that these complexes also feature oligomeric or polymeric structures. In contrast, complex **3** is monomeric, presumably

as a consequence of the large steric demand of the Dipp substituents on the carbene, which prevent any further association.

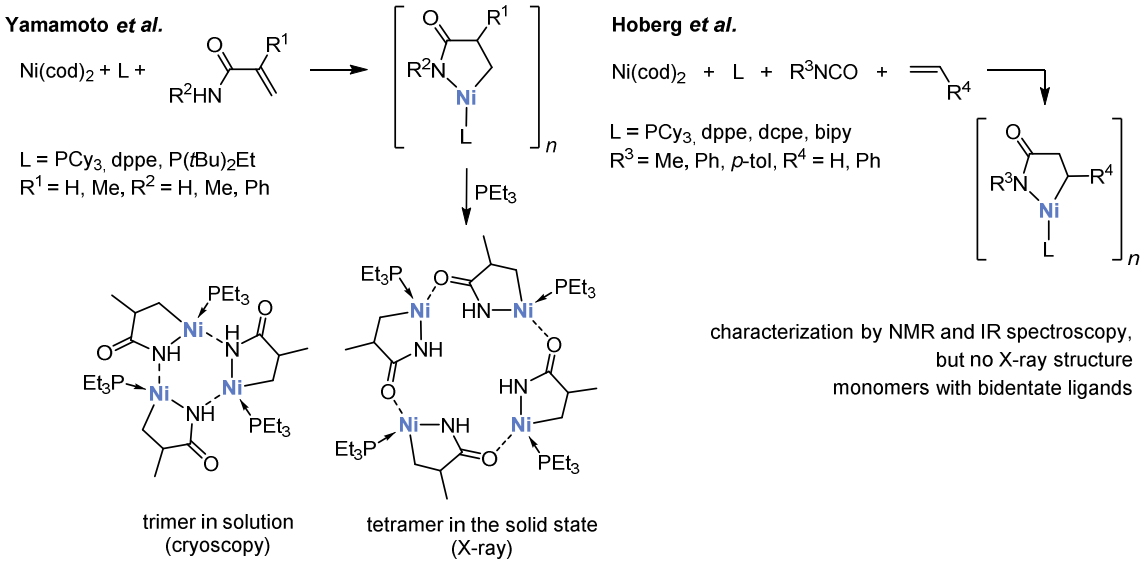

Figure 2. Heteronickelacycles related to **3**.

4.3 Conclusion

In conclusion, we have shown that the reaction of the nickel(I) radical [(η^5-Cp)Ni(IDipp)] (**A**) with one equivalent of PhNCS yields complex [(IDipp)Ni{SC(NPh)N(Ph)CS}] (**1**), which displays the new {SC(NPh)N(Ph)CS}$^{2-}$ dianion derived from the dimerization of phenyl isothiocyanate in the coordination sphere of nickel(II). The nickel(II) complex [(η^5-Cp)(η^1-Cp)Ni(IDipp)] (**2**) is a stoichiometric by-product in the reaction. It seems plausible that the reaction pathway involves transfer of a Cp radical to a second equivalent of complex **A**, resulting in the formation of a reactive intermediate that essentially acts as nickel(0) surrogate. In fact, complex **1** is cleanly produced by reacting the nickel(0) compound [(IDipp)Ni(styrene)$_2$] (**G**) with two equivalents PhNCS. Interestingly, the reaction of **G** with PhNCO afforded the new γ-lactam-nickelacycle [(IDipp)Ni{N(Ph)C(O)CH$_2$CHPh}] (**3**) as a result of the reductive coupling of phenyl isocyanate and a styrene ligand. In the solid state, complex **3** is monomeric and displays a rare T-shaped structure with a three-coordinate nickel atom. The reaction of PhNCO with the nickel(I) complex [(η^5-Cp)Ni(IDipp)] yielded in an inseparable mixture of products, showing that this complex shows a distinct reactivity in this case.

References

1 a) S. Miyazaki, Y. Koga, T. Matsumoto, K. Matsubara, *Chem. Commun.* **2010**, *46*, 1932–1934; b) C. J. E. Davies, M. J. Page, C. E. Ellul, M.F. Mahon, M. K. Whittlesey, *Chem. Commun.* **2010**, *46*, 5151–5153; c) K. Zhang, M. Conda-Sheridan, S. Cooke, J. Louie, *Organometallics* **2011**, *30*, 2546–2552; d) S. Nagao, T. Matsumoto, Y. Koga, K. Matsubara, *Chem. Lett.* **2011**, *40*, 1036–1038; e) C. A. Laskowski, D. J. Bungum, S. M. Baldwin, S. A. Del Ciello, V. M. Iluc, G. L. Hillhouse, *J. Am. Chem. Soc.* **2013**, *135*, 18272–18275; f) M. J. Page, W. Y. Lu, R. C. Poulten, E. Carter, A. G. Algarra, B. M. Kariuki, S. A. Macgregor, M. F. Mahon, K. J. Cavell, D. M. Murphy, M. K. Whittlesey, *Chem. Eur. J.* **2013**, *19*, 2158–2167.

2 B. De Bruin, D. G. H. Hetterscheid, A. J. J. Koekkoek, H. Grützmacher, *Progress in Inorganic Chemistry*, John Wiley & Sons, Inc., **2007**, 247–354.

3 a) C. A. Laskowski, G. L. Hillhouse, *J. Am. Chem. Soc.* **2008**, *130*, 13846–13847; b) C. A. Laskowski, G. R. Morello, C. T. Saouma, T. R. Cundari, G. L. Hillhouse, *Chem. Sci.* **2012**, *4*, 170–174; c) J. Wu, A. Nova, D. Balcells, G. W. Brudvig, W. Dai, L. M. Guard, N. Hazari, P.-H. Lin, R. Pokhrel, M. K. Takase, *Chem. Eur. J.* **2014**, *20*, 5327–5337; d) S. Pelties, D. Herrmann, B. de Bruin, F. Hartl, R. Wolf, *Chem. Commun.* **2014**, *50*, 7014–7016; e) R. C. Poulten, I. López, A. Llobet, M. F. Mahon, M. K. Whittlesey, *Inorg. Chem.* **2014**, *53*, 7160–7169.

4 a) J. Montgomery, *Acc. Chem. Res.* **2000**, *33*, 467–473; b) J. Montgomery, *Angew. Chem. Int. Ed.* **2004**, *43*, 3890–3908; c) M. Jeganmohan, C.-H. Cheng, *Chem. Eur. J.* **2008**, *14*, 10876–10886; d) S. Z. Tasker, E. A. Standley, T. F. Jamison, *Nature* **2014**, *509*, 299–309.

5 a) S. Ogoshi, M. Oka, H. Kurosawa, *J. Am. Chem. Soc.* **2004**, *126*, 11802–11803; b) S. Ogoshi, M. Nagata, H. Kurosawa, *J. Am. Chem. Soc.* **2006**, *128*, 5350–5351; c) S. Ogoshi, H. Ikeda, H. Kurosawa, *Angew. Chem. Int. Ed.* **2007**, *46*, 4930–4932; d) S. Ogoshi, T. Arai, M. Ohashi, H. Kurosawa, *Chem. Commun.* **2008**, *11*, 1347–1349; e) M. Ohashi, M. Ikawa, S. Ogoshi, *Organometallics* **2011**, *30*, 2765–2774; f) Y. Hoshimoto, T. Ohata, M. Ohashi, S. Ogoshi, *Chem. Eur. J.* **2014**, *20*, 4105–4110; g) M. Ohashi, Y. Hoshimoto, S. Ogoshi, *Dalton Trans.* **2015**, *44*, 12060.

6 E. A. Bielinski, W. Dai, L. M. Guard, N. Hazari, M. K. Takase, *Organometallics* **2013**, *32*, 4025–4037.

7 M. J. Iglesias, J. F. Blandez, M. R. Fructos, A. Prieto, E. Álvarez, T. R. Belderrain, M. C. Nicasio, *Organometallics* **2012**, *31*, 6312–6316.

8 T. Schaub, M. Backes, O. Plietzsch, U. Radius, *Dalton Trans.* **2009**, 35, 7071–7079.

9 a) C. Bianchini, D. Masi, C. Mealli, A. Meli, *J. Organomet. Chem.* **1983**, *247*, c29–c31; b) Y.-J. Kim, J.-T. Han, S. Kang, W. S. Han, S. W. Lee, *Dalton Trans.* **2003**, *17*, 3357–3364;

c) S. H. Bertz, Y. Moazami, M. D. Murphy, C. A. Ogle, J. D. Richter, A. A. Thomas, *J. Am. Chem. Soc.* **2010**, *132*, 9549–9551; d) S. H. Bertz, R. A. Hardin, M. D. Murphy, C. A. Ogle, J. D. Richter, A. A. Thomas, *Angew. Chem. Int. Ed.* **2012**, *51*, 2681–2685.

10 a) P. Jernakoff, N. J. Cooper, *J. Am. Chem. Soc.* **1989**, *111*, 7424–7430; b) M. Wang, S. Lu, M. Bei, H. Guo, Z. Jin, *J. Organomet. Chem.* **1993**, *447*, 227–231; c) C. Wycliff, A. G. Samuelson, M. Nethaji, *Inorg. Chem.* **1996**, *35*, 5427–5434; d) L. D. Field, W. J. Shaw, P. Turner, *Organometallics* **2001**, *20*, 3491–3499; e) Q. Shen, H. Li, C. Yao, Y. Yao, L. Zhang, K. Yu, *Organometallics* **2001**, *20*, 3070–3073; f) J. Cámpora, I. Matas, P. Palma, E. Álvarez, C. Graiff, A. Tiripicchio, *Organometallics* **2007**, *26*, 3840–3849; g) K.-E. Lee, X. Chang, Y.-J. Kim, H. S. Huh, S. W. Lee, *Organometallics* **2008**, *27*, 5566–5570.

11 a) Burdett, J. K. *Inorg. Chem.* **1975**, *14*, 375–382; b) S. Komiya, T. A. Albright, H. Roald, J. K. Kochi, *J. Am. Chem. Soc.* **1976**, *98*, 7255–7265.

12 a) M. A. Ortuño, S. Conejero, A. Lledós, *Beilstein J. Org. Chem.* **2013**, *9*, 1352–1382; b) T. Tamaki, M. Nagata, M. Ohashi, S. Ogoshi, *Chem. Eur. J.* **2009**, *15*, 10083–10091.

13 E. D. Mihelich, G. A. Hite, *J. Am. Chem. Soc.* **1992**, *114*, 7318–7319.

14 N. H. Martin, N. W. Allen, E. K. Minga, S. T. Ingrassia, J. D. Brown, *J. Am. Chem. Soc.* **1998**, *120*, 11510–11511.

15 M. Brookhart, M. L. H. Green, *J. Organomet. Chem.* **1983**, *250*, 395–408.

16 a) T. Yamamoto, K. Igarashi, J. Ishizu, A. Yamamoto, *J. Chem. Soc. Chem. Commun.* **1979**, *13*, 554–555; b) T. Yamamoto, K. Igarashi, S. Komiya, A. Yamamoto, *J. Am. Chem. Soc.* **1980**, *102*, 7448–7456; c) T. Yamamoto, K. Sano, K. Osakada, S. Komiya, A. Yamamoto, Y. Kushi, T. Tada, *Organometallics* **1990**, *9*, 2396–2403.

17 a) H. Hoberg, K. Sümmermann, *J. Organomet. Chem.* **1984**, *275*, 239–247; b) H. Hoberg, K. Sümmermann, A. Milchereit, *Angew. Chem. Int. Ed. Engl.* **1985**, *24*, 325–326; c) E. Hernandez, H. Hoberg, *J. Organomet. Chem.* **1986**, *315*, 245–253; d) H. Hoberg, D. Guhl, *J. Organomet. Chem.* **1989**, *375*, 245–257.

4.4 Supporting Information (SI)

4.4.1 General Procedures

All experiments were performed under an atmosphere of dry argon using standard Schlenk techniques or an MBraun UniLab glovebox. Solvents were dried and degassed with an MBraun SPS800 solvent purification system. Tetrahydrofuran and toluene were stored over molecular sieves (3 Å). Diethyl ether and *n*-hexane were stored over a potassium mirror. NMR spectra were recorded on Bruker Avance 300 and Avance 400 spectrometers at 300 K and internally referenced to residual solvent resonances. Melting points were measured on samples in sealed capillaries on a Stuart SMP10 melting point apparatus. UV/Vis spectra were recorded on a Varian Cary 50 spectrophotometer. Elemental analyses were determined by the analytical department of Regensburg University. The starting materials [(C_5H_5)Ni(IDipp)] and [(IDipp)Ni(styrene)$_2$] were prepared according to literature procedures.[1,2] Phenyl isothiocyanate and phenyl isocyanate were purchased from commercial suppliers (PhNCS from ALFA Aesar and PhNCO Sigma Aldrich) and used as received.

4.4.2 Synthesis of [(IDipp)NiSC(NPh)N(Ph)CS] (1)

A solution of phenyl isothiocyanate (58.8 mg, 0.435 mmol, 2.0 eq) in toluene (~2 mL) was added to a solution of [(IDipp)Ni(styrene)$_2$] (142.6 mg, 0.217 mmol, 1.0 eq) in toluene (~7 mL) at room temperature. An immediate color change from yellow to orange was observed. After stirring this solution for two and a half hours the solvent was removed in *vacuo* and the residue was extracted with diethyl ether (5 mL). The filtrate was concentrated to 3 mL. Storage at room temperature for 18 hours afforded orange X-ray quality crystals of 1 (58.9 mg). A second crop of crystalline 1 can be obtained after reducing the volume of the filtrate to 1 mL and storing the solution at −35 °C. Combined yield: 73.0 mg (47%); m.p. >154 °C (decomp. to a black solid); UV/Vis (THF, λ_{max} /nm, (ε_{max} /L·mol^{-1}·cm^{-1})): 284 (22000), 325 (8700), 413 (4100), 519 (2200); elemental analysis calcd. for $C_{42}H_{46}N_4NiS_2$ (*M* = 717.66): C 69.14, H 6.35, N 7.68, found: C 68.47, H 6.43, N 7.58; ^{1}H NMR (C_6D_6, 300 K, 400.13 MHz) δ/ppm = 1.07 (d, $^3J_{HH}$ = 6.9 Hz, 12H, CH(C*H*$_3$)$_2$), 1.52 (d, $^3J_{HH}$ = 6.9 Hz, 12H, CH(C*H*$_3$)$_2$), 2.83 (sept., $^3J_{HH}$ = 6.9 Hz, 4H, C*H*(CH$_3$)$_2$), 6.53 (s, 2H, NC-H), 6.75 − 6.82 (m, 3H, CH$_{Ph}$), 6.99 − 7.04 (m, 3H, CH$_{Ph}$), 7.14 (m, 4H, *meta*-CH$_{Dipp}$), 7.23 − 7.30 (m, 4H, CH$_{Ph}$/*para*-CH$_{Dipp}$), 7.37 (m, 2H, CH$_{Ph}$); ^{13}C{^{1}H} NMR (C_6D_6, 300 K, 100.61 MHz) δ/ppm = 23.9 (CH(*C*H$_3$)$_2$), 25.1 (CH(*C*H$_3$)$_2$), 29.1 ((*C*HCH$_3$)$_2$), 122.9 (Ph), 123.2 (Ph), 123.8 (NCH), 124.3 (Dipp), 126.1 (Ph), 127.4 (Ph), 128.5 (Ph), 130.3 (Dipp), 136.7 (Dipp), 140.6 (Ph), 145.9 (Dipp), 149.7 (Dipp), 171.4 (NCS), 189.8 (N*C*N of IDipp), 237.8 (NCS).

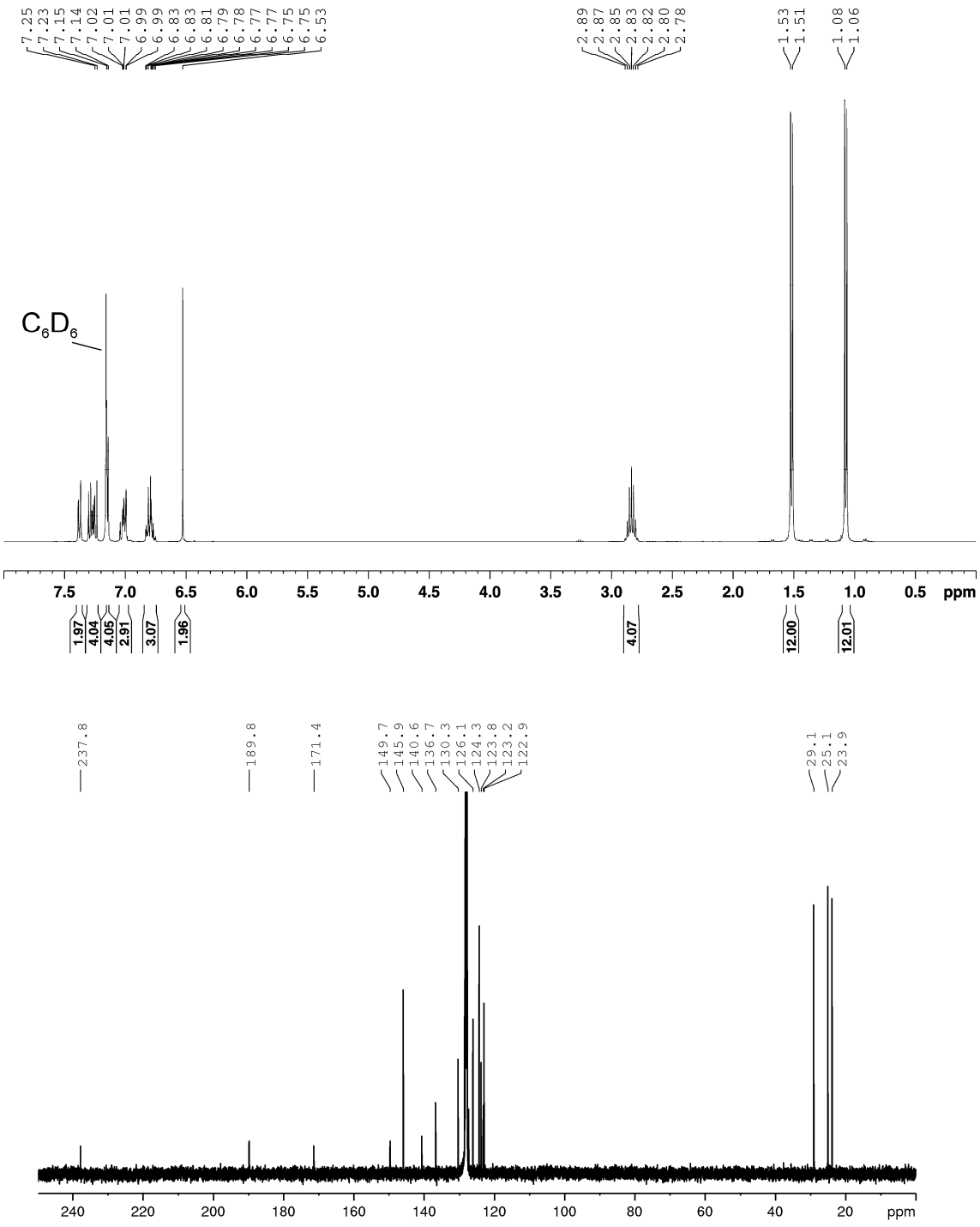

Figure S1. ^{1}H (top) and $^{13}C\{^{1}H\}$ NMR spectra (bottom) of **1** (C_6D_6, 300 K, 400.16/100.61 MHz).

4.4.3 Synthesis of [(IDipp)NiN(Ph)C(O)CH_2CH(Ph) (3)

A solution of phenyl isocyanate (37.9 mg, 0.289 mmol, 1.1 eq) in tetrahydrofuran (1 mL) was added to a solution of [(IDipp)Ni(styrene)$_2$] (189.6 mg, 0.318 mmol, 1.0 eq) in tetrahydrofuran (3 mL) at room temperature. A color change from yellow to blue was observed. After stirring the reaction mixture for two hours at room temperature the solvent was removed and the residue was extracted with tetrahydrofuran (1 mL). Blue X-ray quality crystals formed by diffusion of *n*-hexane into the THF solution of 3. Yield: 93.3 mg (48%); m.p. >170 °C (slow decomp. to a black solid); UV/Vis (THF, λ_{max} /nm, (ε_{max} /L·mol^{-1}·cm^{-1})): 296 (16000), 354 (11400), 699 (1100); elemental analysis calcd. for $C_{42}H_{49}N_3NiO$ (*M* = 670.57): C 75.23, H 7.37, N 6.27, found: C 75.24, H 7.23, N 6.16; ^{1}H NMR (THF-d_8, 300 K, 400.13 MHz) δ/ppm = −0.46 (d, $^3J_{HH}$ = 16.8 Hz, 1H, PhCHCH_2), 0.96 (d, $^3J_{HH}$ = 6.8 Hz, 6H, CH(CH_3)$_2$), 1.17 (d, $^3J_{HH}$ = 6.8 Hz, 6H, CH(CH_3)$_2$), 1.19 (d, $^3J_{HH}$ = 6.8 Hz, 6H, CH(CH_3)$_2$), 1.70 (d, $^3J_{HH}$ = 6.8 Hz, 6H, CH(CH_3)$_2$), 2.29 (dd, $^3J_{HH}$ = 7.7 Hz, $^2J_{HH}$ = 16.8 Hz, 1H, PhCHCH_2), 2.49 (sept., $^3J_{HH}$ = 6.8 Hz, 2H, CH(CH$_3$)$_2$), 2.82 (d, $^3J_{HH}$ = 7.7 Hz, 1H, PhCHCH$_2$), 3.85 (sept., $^3J_{HH}$ = 6.8 Hz, 2H, CH(CH$_3$)$_2$), 6.40 (d, J_{HH} = 7.9 Hz, 2H, *ortho*-CH$_{NPh}$), 6.46 (t, J_{HH} = 7.2 Hz, 1H, *para*-CH$_{NPh}$), 6.57 (t, J_{HH} = 7.6 Hz, 2H, *meta*-CH$_{NPh}$), 6.90 (t, J_{HH} = 7.6 Hz, 2H, *meta*-CH$_{PhCH}$), 7.08 (d, J_{HH} = 7.6 Hz, 2H, *ortho*-CH$_{PhCH}$), 7.15 (t, J_{HH} = 7.4 Hz, 1H, *para*-CH$_{PhCH}$), 7.23 (d, J_{HH} = 7.2 Hz, 2H, *para*-CH$_{Dipp}$), 7.44 (s, 2H, NCH of IDipp), 7.52 (m, 2H, *meta*-CH$_{Dipp}$), 7.53 (m, 2H, *meta*-CH$_{Dipp}$); ^{13}C{^{1}H} NMR (THF-d_8, 300 K, 100.61 MHz) δ/ppm = 14.5 (PhCHCH$_2$), 23.6 (CH(CH$_3$)$_2$), 24.2 (CH(CH$_3$)$_2$), 25.4 (CH(CH$_3$)$_2$), 25.4 (CH(CH$_3$)$_2$), 29.3 (*C*H(CH$_3$)), 30.2 (*C*H(CH$_3$)), 46.6 (PhCH*C*H$_2$), 120.0 (*para*-CH$_{NPh}$), 120.5 (*ortho*-CH$_{NPh}$), 123.4 (*para*-CH$_{PhCH}$), 125.3 (*para*-CH$_{Dipp}$), 125.4 (*meta*-CH$_{Dipp}$), 126.2 (N*C*H of IDipp), 127.1 (*ortho*-CH$_{PhCH}$), 128.3 (*meta*-CH$_{NPh}$), 130.3 (*meta*-CH$_{PhCH}$), 131.1 (*meta*-Ar$_{Dipp}$), 135.5 (Dipp), 146.5 (Dipp), 147.3 (Dipp), 149.1 (*ipso*-C$_{NPh}$), 151.4 (*ipso*-C$_{PhCH}$), 176.2 (C=O), 178.9 (N*C*N of IDipp).

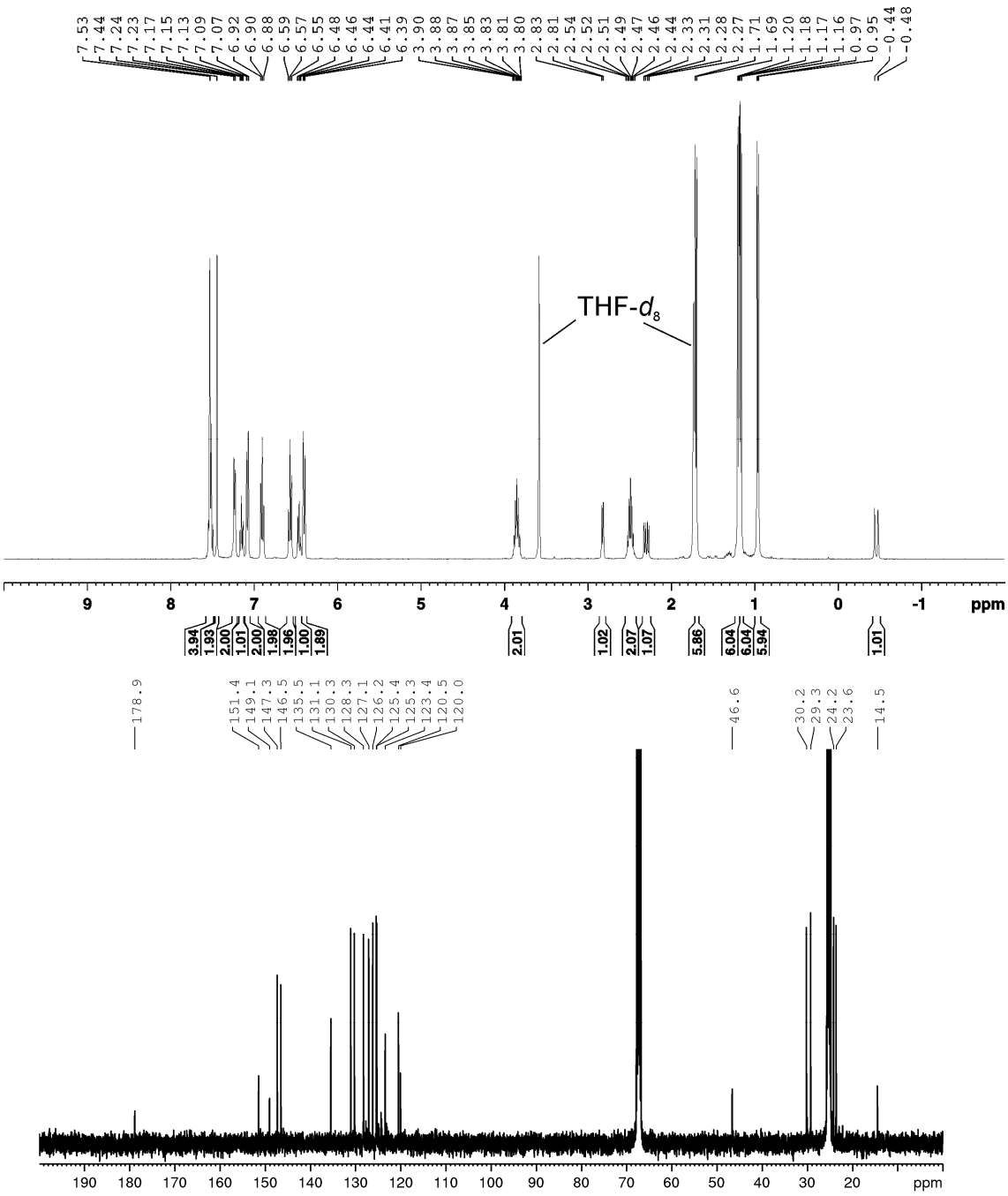

Figure S2. ^{1}H (top) and ^{13}C{^{1}H} NMR spectra (bottom) of **3** (THF-d_8, 300 K, 400.16/100.61 MHz).

4.4.4 X-ray Crystallography

The single crystal X-ray diffraction data (Table S1) were recorded on an Agilent Technologies Gemini Ultra R diffractometer with microfocus Cu K_α radiation (λ = 1.54184 Å). Empical multi-scan[3] and analytical absorption corrections[4] were applied to the data. Using Olex2[5], the structures were solved with SHELXT[6] and least-square refinements on F^2 were carried out with SHELXL.[7]

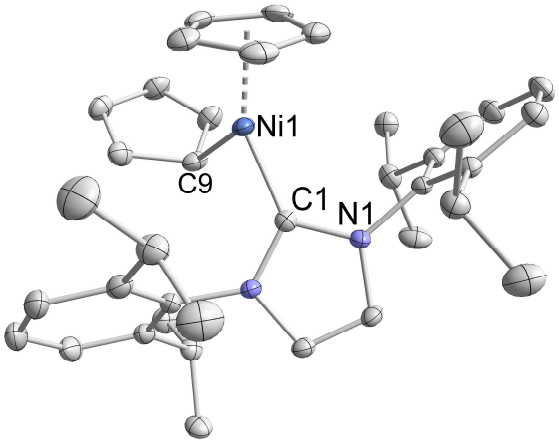

Figure S3. Solid-state molecular structure of [(η^5-Cp)Ni(η^1-Cp)(IDipp)] (**2**). The hydrogen atoms are omitted for clarity. Thermal ellipsoids are drawn at 40% level. Selected bond length [Å] and angles [°]: Ni1-C1 1.881(2), Ni1-C9 2.021(3).

Table S1. Crystallographic data of **1**, **2**, and **3.**

Compound	**1**	**2**	**3**
Empirical formula	$C_{41}H_{46}N_4NiS_2$	$C_{37}H_{46}N_2Ni$	$C_{42}H_{49}N_3NiO$
Formula weight	717.65	577.47	670.55
Temperature [K]	123(1)	123(1)	123(1)
Crystal system	monoclinic	monoclinic	triclinic
Space group	*C*2/*c*	$P2_1/n$	*P*-1
a [Å]	21.2844(3)	10.32832(18)	10.3147(2)
b [Å]	12.13298(17)	19.6066(3)	18.7357(5)
c [Å]	29.3618(3)	15.8877(3)	19.4834(6)
α [°]	90	90	84.582(2)
β [°]	92.0206(12)	98.3793(15)	82.009(2)
γ [°]	90	90	89.3620(18)
Volume [Å^3]	7577.77(17)	3182.98(9)	3711.99(16)
Z	8	4	4
ρ_{calc} [g/cm^3]	1.258	1.205	1.200
μ [mm^{-1}]	2.017	1.063	1.012
F(000)	3040.0	1240.0	1432.0
Crystal size [mm^3]	0.8135 × 0.3574 × 0.1914	0.3672 × 0.3136 × 0.2458	0.4458 × 0.1609 × 0.0796
Radiation	CuK_α (λ = 1.54184)	CuK_α (λ = 1.54184)	CuK_α (λ = 1.54184)
2Θ range for data collection [°]	8.314 to 133.274	7.208 to 133.502	6.908 to 133.442
Index ranges	$-19 \le h \le 25$, $-13 \le k \le 14$, $-34 \le l \le 34$	$-11 \le h \le 12$, $-22 \le k \le 23$, $-18 \le l \le 18$	$-12 \le h \le 12$, $-21 \le k \le 22$, $-23 \le l \le 23$
Reflections collected	23029	15944	47839
Independent reflections	6661 [R_{int} = 0.0418, R_{sigma} = 0.0372]	5595 [R_{int} = 0.0399, R_{sigma} = 0.0372]	13030 [R_{int} = 0.0385, R_{sigma} = 0.0336]
Data / restraints / parameters	6661 / 0 / 441	5595 / 0 / 369	13030 / 0 / 867
Goodness-of-fit on F^2	1.123	1.144	1.114
Final R indexes [I>=2σ (I)]	R_1 = 0.0375, wR_2 = 0.1033	R_1 = 0.0527, wR_2 = 0.1417	R_1 = 0.0647, wR_2 = 0.2327
Final R indexes [all data]	R_1 = 0.0447, wR_2 = 0.1163	R_1 = 0.0555, wR_2 = 0.1438	R_1 = 0.0728, wR_2 = 0.2371
Largest diff. peak/hole [e Å^{-3}]	0.78/−0.52	0.84/−0.59	0.99/−0.53

4.4.5 DFT: Cartesian Coordinates of 3

The calculation on **3** was performed using the ORCA program package (version 3.0.2.).[8] The BP86 density functional and the Ahlrichs def2-TZVP basis set were employed for all atoms.[9,10] The RI approximation was used.[11] Ahlrichs Coulomb fitting basis for the TZVP basis for all atoms (TZV/J) and atom-pairwise dispersion correction to the DFT energy with Becke-Johnson damping (d3bj) were applied.[12] The nature of the stationary point was verified by a numerical frequency analysis.

Energy = -3379.034146552428 Hartree

Ni	5.23959073765144	12.74947840829250	4.94929431415208
O	1.84622870675009	14.77060529769954	4.76864733726782
N	7.81389415910773	11.62977983600131	4.42468245359597
N	8.04170994461066	13.56325605878626	5.36240861577139
N	3.47298590469282	13.11985923506476	4.50953845232663
C	7.08389189057301	12.63373570894096	5.01383917753210
C	2.87036750940787	14.18296809131247	5.12661111997632
C	8.11481522965699	15.23078025768383	7.15923297347658
C	7.19943150817967	10.55908606052867	3.68407330314999
C	7.74266428023072	14.88513061976054	5.84704217644021
C	7.50102600654300	11.98295509885156	1.57234722415304
H	7.91292694232463	12.68066301873331	2.31406474838687
C	4.57281165650217	12.43964679466749	7.50404129313589
C	6.69086170878189	9.44271788575221	4.37636883483057
C	7.11540253944029	10.69888966872769	2.28751814174446
C	4.82044699455288	13.61639942038702	6.64598981466696
C	9.31782257431104	13.13952582227330	4.99049030718781
H	10.19699255537796	13.74251247141709	5.17439893874579
C	8.80664435080948	14.24862504678645	8.08983494942979
H	8.68702082075770	13.24231722423470	7.65947035534995
C	3.67393569625854	14.57647537343726	6.37119547009359
C	7.81215163811479	16.52567401023369	7.60169027231812
H	8.08435774791070	16.82226312037420	8.61486732023461
C	7.07217752323016	15.78089000721312	4.98407152282228
C	3.51733323163787	11.25732629782445	3.01549401335771
H	3.97812459215289	10.68595664479915	3.82684262698008
C	3.11435870090982	12.58726667088188	3.26935264142675
C	9.17356652480029	11.92488239651922	4.39683379598465
H	9.89828578016598	11.25295085667761	3.95507406549095
C	6.58680048691167	9.62328299596880	1.56218598996912
H	6.50513663078691	9.69951071537014	0.47736437747912
C	5.63353096520421	11.89195827243157	8.25591266618659
H	6.63008961747458	12.31934290983892	8.13911960640939
C	6.15736555018494	8.40436580146375	3.60525336361656
H	5.75013523841757	7.52465538237525	4.10124559340095
C	6.70312028794275	9.39662267197817	5.89421177083966
H	6.44768962364540	10.41117442334396	6.24166470134173
C	3.29825430220809	11.85346457939487	7.64420064492542
H	2.46494213559816	12.23686586027508	7.05523062377767
C	3.30749298373779	10.67482864528588	1.76644908092270
H	3.62167820610096	9.64535462337823	1.59759174687360
C	2.68902559696174	11.40159129008664	0.74741861647696
H	2.51401612561663	10.94535051635846	-0.22776369282963
C	3.09536900135167	10.78512094579291	8.51554311422143
H	2.09926647960936	10.34959760155762	8.60945429263715
C	6.77571316428018	17.05279977356522	5.48566544459795
H	6.24429511666402	17.76255013961864	4.85265940856837
C	4.15421186136264	10.27297749964759	9.27318366181544
H	3.98814561794196	9.44237794198045	9.96031824899423
C	6.12964321543261	8.48161690546414	2.21172961278427
H	5.71762077213332	7.65397114919075	1.63221780062170
C	6.25588295100918	12.64734495610116	0.96173412246970

H	5.78901732144895	12.00324225215843	0.20386132597559
H	6.52996038363248	13.59652499213484	0.47889967175822
H	5.49240839677722	12.85222685887398	1.72467226536209
C	2.47924677920042	13.31329241046003	2.23865238802251
H	2.14351438961697	14.32740534258697	2.44280652328760
C	8.18197431130637	14.23834319409138	9.49391831704676
H	8.38981155149322	15.17435556476238	10.03189768700579
H	8.60507554901930	13.41708418252689	10.08980738511979
H	7.09315799443566	14.10557949542581	9.45282054010102
C	5.42917586949381	10.83219491863581	9.13491383820087
H	6.26579679653963	10.44010839228182	9.71612979782513
C	6.72866221089664	15.41503916164454	3.54963553166990
H	6.51637972519532	14.33431397319750	3.53307737567144
C	10.31448690298157	14.54485796251116	8.18042218669856
H	10.79669082753725	14.51876045502588	7.19389637462202
H	10.81583950806920	13.80879258371455	8.82553383925952
H	10.48539722552335	15.54462764042369	8.60627581561728
C	7.14454039532425	17.42614603513003	6.77749884772757
H	6.90171864533552	18.42411536736496	7.14497050293927
C	2.27710705764860	12.71774006411221	0.99604230186186
H	1.78403967253857	13.28848556020367	0.20668522221603
C	8.58830467213496	11.74713452265109	0.51410919085330
H	9.48824753904469	11.29753563248238	0.95748472604305
H	8.87554927068953	12.69859958291703	0.04379445048555
H	8.23394431452371	11.07470430931275	-0.28080903948389
C	5.46463655202440	16.09801622924945	3.02100373103547
H	4.60891111668592	15.93026351329482	3.68824515368400
H	5.20616037587378	15.67620223771642	2.04012404471416
H	5.59786538958154	17.18193972373258	2.88875027980208
C	7.93757650119780	15.67982966457665	2.63562096745346
H	8.19639970167504	16.74947543525370	2.63204462556628
H	7.70888546927959	15.37968664146436	1.60292007903681
H	8.82261542091176	15.11798147331529	2.96609495819440
C	5.65167149819552	8.44914244675050	6.47495811612756
H	4.64820205658949	8.67743252725266	6.09047217686630
H	5.61938363570014	8.56218929157673	7.56550605515130
H	5.88025061718548	7.39541156315292	6.25406441147399
C	8.10146442794863	9.05369445854925	6.43620337087108
H	8.40518584668472	8.04531951523067	6.11652477392491
H	8.09560500125723	9.07662230194820	7.53572647725876
H	8.86172626905432	9.76519034238055	6.08708767669411
H	5.74101053859405	14.12923801461947	6.93747402162162
H	2.98299142320246	14.66038545820293	7.22654284637022
H	4.07457746193161	15.58599570277236	6.19277211213754

References:

1 S. Pelties, D. Herrmann, B. de Bruin, F. Hartl, R. Wolf, *Chem. Commun.* **2014**, *50*, 7014.

2 N. J. Iglesias, J. F. Blandez, M. R. Fructos, A. Prieto, E. Álvarez, T. R. Belderrain, M. C. Nicasio, *Organometallics* **2012**, *31*, 6312–6316.

3 a) SCALE3ABS, CrysAlisPro, Aglient Technologies Inc., Oxford, GB, **2015**; b) G. M. Sheldrick, SADABS, Bruker AXS, Madison, USA, **2007**.

4 R. C. Clark, J. S. Reid, *Acta Cryst. A* **1995**, *51*, 887.

5 O. V. Dolomanov, L. J. Bourhis, R. J. Gildea, J. A. K. Howard, H. Puschmann, *J. Appl. Cryst.* **2009**, *42*, 339.

6 G. M. Sheldrick, *Acta Cryst. A* **2015**, *71*, 3.

7 G. M. Sheldrick, *Acta Cryst. C* **2015**, *71*, 3.

8 F. Neese, *Wiley Interdiscip. Rev. Comput. Mol. Sci.* **2012**, *2*, 73.

9 a) C. Lee, W. Yang, R. G. Parr, *Phys. Rev. B* **1988**, *37*, 785, b) A. D. Becke, *J. Chem. Phys.* **1993**, *98*, 1372, c) A. D. Becke, *J. Chem. Phys.* **1993**, *98*, 5648.

10 a) A. Schäfer, H. Horn, R. Ahlrichs, *J. Chem. Phys.* **1992**, *97*, 2571, b) F. Weigend, R. Ahlrichs, *Phys. Chem. Chem. Phys.* **2005**, *7*, 3297.

11 a) A. D. Becke, *Phys. Rev. A* **1988**, *38*, 3098, b) J. P. Perdew, *Phys. Rev. B* **1986**, *33*, 8822.

12 a) S. Grimme, S. Ehrlich, L. Goerigk, *J. Comput. Chem.* **2011**, *32*, 1456, b) S. Grimme, J. Antony, S. Ehrlich, H. Krieg, *J. Chem. Phys.* **2010**, *132*, 154104.

5 Insertion of Phenyl Isothiocyanate into a P−P Bond of a Nickel-substituted Bicyclo[1.1.0]tetraphosphabutane[a,b]

Stefan Pelties, Andreas W. Ehlers, and Robert Wolf

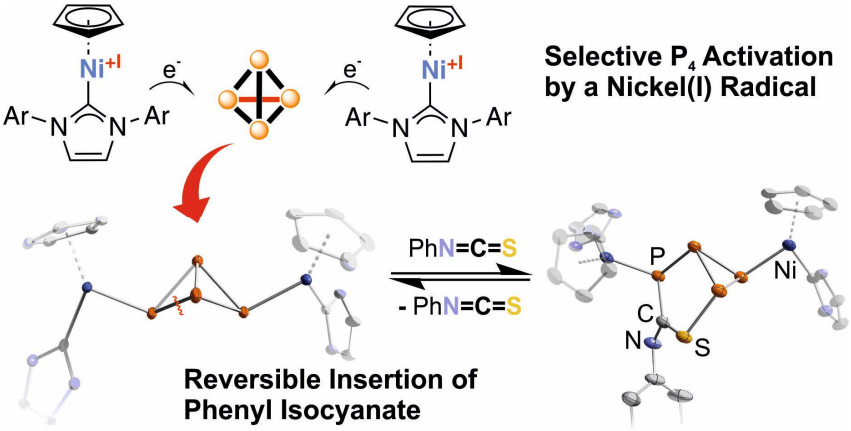

[a] S. Pelties, A. W. Ehlers, R. Wolf, *Chem. Commun.*, in revision.

[b] DFT calculations were performed by Stefan Pelties under supervision of Andreas W. Ehlers.

5.1 Introduction

Developing new, targeted and selective methods for the functionalisation of the P_4 molecule remains a topical challenge despite the extensive research efforts carried out in the past.[1,2] Recent reports have focused on the use of nucleophilic carbanions and carbenes,[3,4] insertion reactions of *p*-block elements, e.g. phosphenium cations[5] and the use of main group element or transition metal-based radicals.[6,7] The latter approach often gives rise to bicyclo[1.1.0]tetraphosphabutanes **A**, which may be seen as potential intermediates on the way to a stepwise P_4 degradation sequence (Scheme 1a). While various "P_4 butterfly" compounds of type **A** are known, it is interesting to note that their reactivity has only been explored to a small extent.[1,6–9]

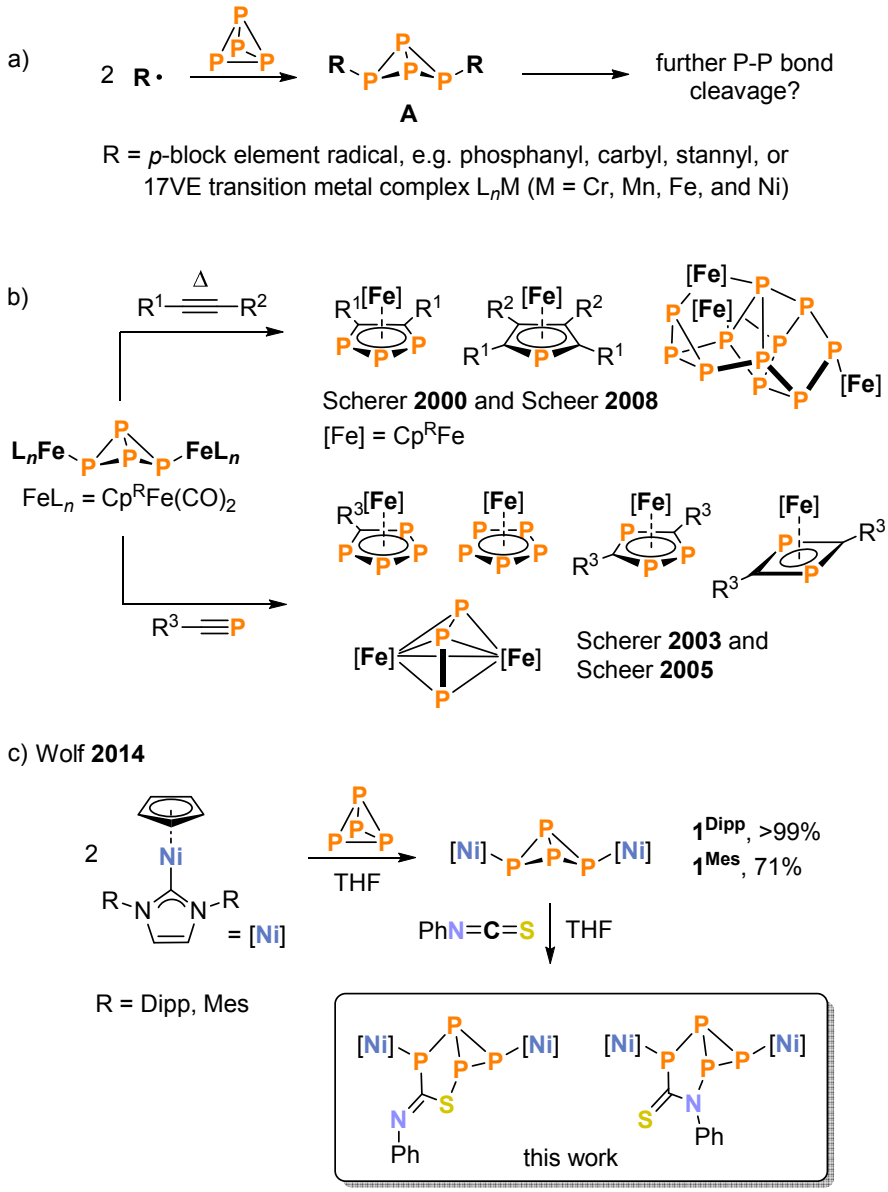

Scheme 1. a) Formation of bicyclo[1.1.0]tetraphosphabutanes amenable for further transformations; b) Selected reactions of iron-substituted bicyclo[1.1.0]tetraphosphabutanes; Cp^R = C_5H_2-1,2,4-*t*Bu_3, C_5H_2-1,2,4-*t*Bu_3, C_9H_5-1,3-*t*Bu_2, $C_5i Pr_5$, R^1 = R^2 = Me, Ph; R^1 = H, R^2 = Ph, *t*Bu, $SiMe_3$, CO_2Me/Et, R^3 = *t*Bu, $C(CH_2)_5$Me; c) synthesis of $\mathbf{1}^{Dipp}$ and $\mathbf{1}^{Mes}$ and reactivity toward phenyl isothiocyanate.[6–10]

Previous studies mainly focused on iron complexes.[1d,7a,c,9−11] As reported by Scherer and Scheer, thermolysis or photolysis of $[(Cp^{R}Fe(CO)_2)_2(\mu\text{-}\eta^1\text{:}\eta^1\text{-}P_4)]$ (Cp^{R} = C_5H_2-1,2,4-*t*Bu_3, C_5H_2-1,2,4-*t*Bu_3, C_9H_5-1,3-*t*Bu_2, and $C_5i Pr_5$) affords mixtures of polyphosphido complexes.[7a,c] Reactions with (phospha)alkynes evoked the P_3/P_1 fragmentation of the bicyclo[1.1.0]tetraphosphabutanediyl fragment, forming phosphide, phospholide, diphosphacyclobutadiene components.[9,10] Further studies revealed that the "P_4 butterfly" may be protonated reversibly and coordinates as a chelate ligand to copper(I).[11]

Here, we disclose a new reaction mode for metal-substituted bicyclo[1.1.0]tetraphosphabutanes. We have found that phenyl isothiocyanate reversibly inserts into a P−P bond of the bicyclo[1.1.0]tetraphosphabutane scaffold of the dinuclear nickel complex $[\{(\eta^5\text{-}Cp)Ni(IMes)\}_2(\mu\text{-}\eta^1\text{:}\eta^1\text{-}P_4)]$ (**1^{Mes}**, Scheme 2b).[7b] This unprecedented reaction affords the isomers **2a** and **2b**, which display a bicyclo[3.1.0]heterohexane skeleton. We describe the single-crystal X-ray structures and $^{31}P\{^1H\}$ NMR data of these new complexes, and analyse the possible nature of additional reaction products using DFT calculations.

5.2. Results and Discussion

We recently synthesised of the first nickel-substituted bicyclo[1.1.0]tetraphosphabutane, [{(η^5-Cp)Ni(IDipp)}$_2$(μ-η^1:η^1-P_4)] (**1^{Dipp}**, IDipp = 1,3-bis(2,6-diisopropylphenyl)imidazolin-2-ylidene).[7b] This complex is formed in a quantitative reaction from two equivalents [(η^5-Cp)Ni(IDipp)] and P_4 (Scheme 1c). Subsequent work showed that the slightly less encumbered mesityl-substituted complex [{(η^5-Cp)Ni(IMes)}$_2$(μ-η^1:η^1-P_4)] (**1^{Mes}**) is obtained in an analogous fashion. **1^{Mes}** was isolated as dark red air-sensitive crystals in 71% yield (Scheme 1c) and shows a better solubility than **1^{Dipp}**, dissolving well in benzene, toluene, diethyl ether and tetrahydrofuran.†

In order to probe the reactivity of **1^{Dipp}** and **1^{Mes}**, we investigated reactions with heteroallenes. ADMX spin systems were observed by ^{31}P NMR spectroscopy with CS_2 (10 equiv.), suggesting insertion into a P−P bond, but these products could not be isolated.§† Isolable products were obtained with phenyl isothiocyanate, however. Monitoring the reaction of **1^{Mes}** and PhNCS in [D_8]THF (Figure 1) revealed that 7 equiv. PhNCS were necessary for full conversion of **1^{Mes}** after four hours.§ Two main products **2a** and **2b** (ADMX spin systems) and one minor species **2c** (A_2MX spin system) were detected (approximate ratio **2a**:**2b**:**2c** 75:20:5). The simultaneous formation of **2a**, **2b** and **2c** commences below 0 °C according to a VT NMR study ([D_8]THF, Figure S8, SI). Prolonged reaction times and heating of the solution resulted in essentially the same product ratio, although the signal to noise ratio of the spectra decreased over time. In contrast, the ^{31}P{^{1}H} NMR spectrum of the reaction of **1^{Dipp}** with a large excess of PhNCS in [D_8]THF after two days at room temperature showed signals of a species similar to **2b** (15%, ADMX spin system), **1^{Dipp}** (50%) and P_4 (35%) (Figure S9, SI).

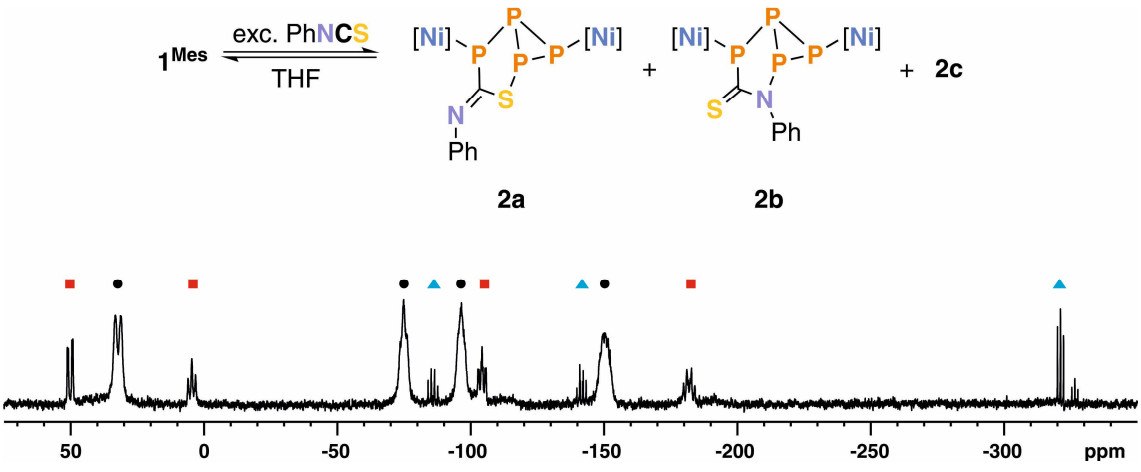

Figure 1. Synthesis of **2a** and **2b** (top), and ^{31}P{^{1}H} NMR spectrum ([D_8]THF) of the reaction of PhNCS and **1^{Mes}** (7:1) at room temperature after four hours; ● = **2a**, ■ = **2b**, ▲ = **2c** (bottom).

Complex **2a** can be isolated as an analytically pure, dark brown solid in 31% yield by crystallising the crude product twice from toluene/*n*-hexane.† Crystallisation of the crude product from diethyl

ether and recrystallization from toluene/*n*-hexane affords pure, crystalline **2b** in 16% isolated yield. Single-crystal XRD for **2a** (Figure 2, left) revealed an unusual nickel-substituted bicyclo[3.1.0]-2-thia-1,4,5,6-tetraphosphahexane moiety (P1–C1 1.860(4) Å, P4–S1 2.1257(13) Å) with an exocyclic imino function. The C1–N1 (1.278(5) Å) and S1–C1 (1.795(5) Å) bonds of **2a** are elongated compared to free aryl isothiocyanates.[12] The P–P distances (2.1818(14) − 2.2222(14) Å) are in the range of single bonds.[7] The five-membered CP_3S heterocycle (P1–P2–P4–S1–C1) is almost flat (Σ_{angles} = 535.8°) and orthogonal (89.60(7)°) to the plane formed by P2, P3, and P4. The scaffold of **2a** is analogous to that of 2,3,4,6-tetra-*tert*-butylbicyclo[3.1.0]hexaphosphane synthesised by Baudler *et al*..[13]

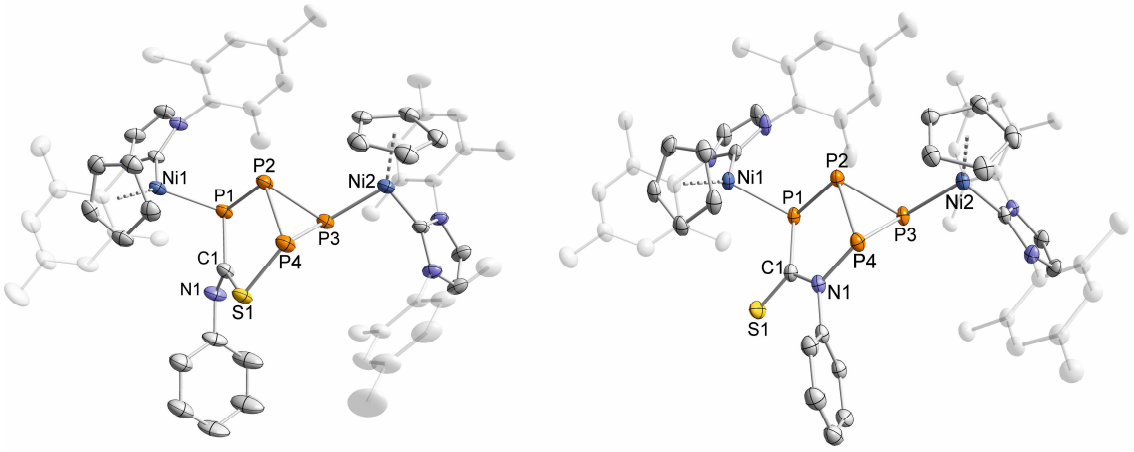

Figure 2. Solid-state molecular structures of **2a** (left) and **2b** (right). The hydrogen atoms are omitted for clarity. Thermal ellipsoids are drawn at 40% level. Selected bond lengths [Å] and angles [°] for **2a**: P1–C1 1.860(4), P4–S1 2.1257(13), P1–P2 2.1818(14), P2–P3 2.2182(15), P2–P4 2.2222(14), P3–P4 2.1935(15), C1–S1 1.794(4), C1–N1 1.278(6), Ni1–P1 2.2036(13), Ni2–P3 2.1906(11), P1–P2–P4 102.89(5), P2–P4–S1 102.86(6), P4–S1–C1 104.82(14), S1–C1–P1 122.3(2), C1–P1–P2 102.88(14), P3–P2–P4 59.20(5), P1–C1–N1 116.4(3), S1–C1–N1 121.3(2); for **2b**: P1–C1 1.828(3), P4–N1 1.785(3), P1–P2 2.2157(11), P2–P4 2.1969(10), P2–P3 2.2233(10), P3–P4 2.206(1), C1–N1 1.359(4), C1–S1 1.678(3), Ni1–P1 2.2188(9), Ni2–P3 2.2192(9), P1–P2–P4 95.28(4), P2–P4–N1 99.75(9), P4–N1–C1 124.9(2), N1–C1–P1 118.6(2), C1–P1–P2 100.48(3), P3–P2–P4 59.88(3), P1–C1–S1 117.68(18), N1–C1–S1 123.6(2).

The molecular structure of the regio isomer **2b** (Figure 2, right) features a flat CNP_3 heterocycle (Σ_{angles} = 539.0°) with a thioketone function (C1–S1 1.678(3) Å) and single bonds between P1–C1 (1.828(3) Å) and P4–N1 (1.785(3) Å). The P–P distances in **2b** (2.1969(10) − 2.2233(10) Å) are similar to those of **2a**. The CNP_3 ring forms an acute dihedral angle of 79.58(5)° with the P2–P3–P4 plane.

The $^{31}P\{^1H\}$ NMR spectrum of **2a** ([D_8]THF, room temperature) features four broad multiplets at −150.1, −96.4, −75.0 and 32.1 ppm consistent with four chemically different P atoms. The signals are broad at room temperature (average half-width τ_{FWHM} = 565 Hz); they become sharper when the temperature is decreased to −80 °C (av. τ_{FWHM} = 35 Hz). Experimental and fitted $^{31}P\{^1H\}$ NMR spectra in [D_8]THF at −80 °C along with the assignment of the chemical shifts and coupling constants are shown in Figure 3. The resonance at −151.8 ppm is assigned to P_A connected to three P atoms based on the observation of three large ^1J(P,P)-coupling constants for

this multiplet ($^1J(P_AP_D)$ = −178 Hz, $^1J(P_AP_M)$ = −185 Hz and $^1J(P_AP_X)$ = −374 Hz). The P atoms coordinated to nickel ($\delta(P_D)$ = −105.5 ppm; $\delta(P_X)$ = 27.8 ppm) show a common large ^2J(P,P) coupling ($^2J(P_D,P_X)$ = 82 Hz), which may arise from an interaction of the lone pairs due to the conformational constraints of the bicyclo[3.1.0]heterohexane skeleton.[13] The signal of P_D shows two typical ^1J couplings to P_A and P_M ($^1J(P_AP_D)$ = −178 Hz and $^1J(P_DP_M)$ = −238 Hz), while P_X is a doublet of doublets due to the presence of one large ^1J coupling constant. The multiplet at −78.0 ppm is assigned to the P atom connected to sulfur (P_M) and features a common coupling constant with P_X ($^2J(P_M,P_X)$ = 9 Hz).

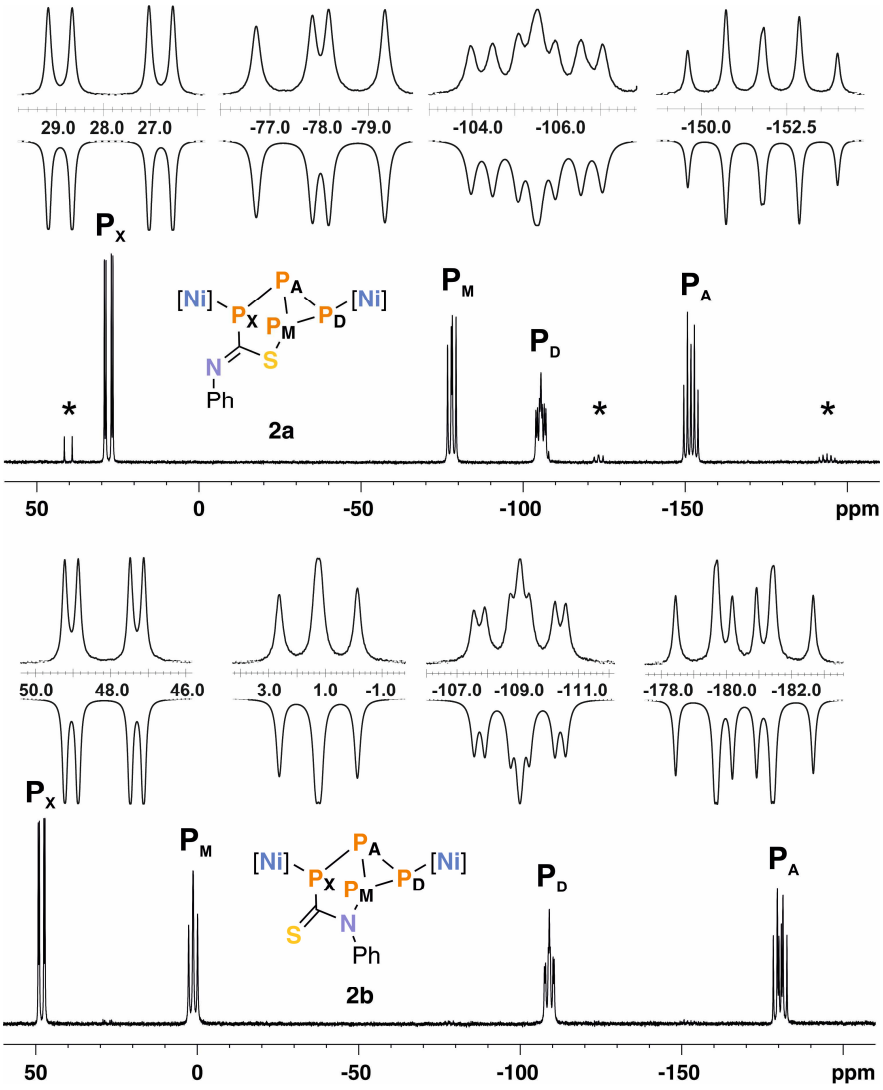

Figure 3. $^{31}P\{^1H\}$ NMR spectra of **2a** (top) and **2b** (bottom, 161.98 MHz, [D8]THF, 193 K); **2a** (ADMX spin system): δ_A = −151.8 ppm, δ_D = −105.5 ppm, δ_M = −78.0 ppm, δ_X = 27.8 ppm, $^1J(P_AP_D)$ = −178 Hz, $^1J(P_AP_M)$ = −185 Hz, $^1J(P_AP_X)$ = −374 Hz, $^1J(P_DP_M)$ = −238 Hz, $^2J(P_DP_X)$ = 82 Hz, $^2J(P_MP_X)$ = 9 Hz; **2b** (ADMX spin system): δ_A = −180.5 ppm, δ_D = −109.1 ppm, δ_M = 1.2 ppm, δ_X = 48.2 ppm, $^1J(P_AP_D)$ = −193 Hz, $^1J(P_AP_M)$ = −209 Hz, $^1J(P_AP_X)$ = −282 Hz, $^1J(P_DP_M)$ = −237 Hz, $^2J(P_DP_X)$ = 57 Hz, $^2J(P_MP_X)$ = 10 Hz; Expansions (inset) show the experimental (up) and fitted spectra (down). The signals assigned to **2b** are labeled with an asterisk.

Complex **2b** gives rise to four slightly broad $^{31}P\{^1H\}$ NMR resonances at −182.1, −104.5, 4.5 and 50.1 ppm in [D8]THF at room temperature. The line width decreased from an average of τ_{FWHM} =

33 Hz at room temperature to τ_{FWHM} = 23 Hz upon cooling to −80 °C. The chemical shifts and coupling constants of **2b** lie in a similar range as observed for **2a** (Figure 3, bottom) in agreement with the similar structure motif. The multiplet for P_A (δ = −180.5 ppm) arises from three distinct ^1J(P,P) couplings ($^1J(P_AP_D)$ = −193 Hz, $^1J(P_AP_M)$ = −209 Hz and $^1J(P_AP_X)$ = −282 Hz). In addition, a characteristic large ^2J(P,P) coupling constant ($^2J(P_DP_X)$ = 57 Hz) was detected for the P atoms P_D and P_X, both of which are connected to nickel atoms.

$^{31}P\{^1H\}$ NMR studies indicate that the formation of **2a**, **2b**, and **2c** is reversible; i.e. the products slowly equilibrate with the starting material $\mathbf{1^{Mes}}$ in solution.† A mixture of **2a** (89%), $\mathbf{1^{Mes}}$ (7%), **2c** (4%) and **2b** (traces) was detected upon storing a [D_8]THF solution of pure **2a** in an NMR tube at room temperature for two days, while a 65:10:5:20 mixture (**2a**:**2b**:**2c**:$\mathbf{1^{Mes}}$) was present after one week.‡ Additional multiplets of unidentified minor species can be observed upon prolonged storage (Figure S11, SI). A similar behaviour was observed for pure **2b** in [D_8]THF (Figure S12). $\mathbf{1^{Mes}}$ was the exclusive component detected by $^{31}P\{^1H\}$ NMR after storing **2b** in [D_8]THF at 60 °C for 20 hours.

DFT calculations (ωB97X-D/6-311G(d,p) level)[14] were performed to gain additional insight into the thermodynamics of the reaction and the unidentified structure of the minor product **2c**. The optimized structures of the truncated model complexes $\mathbf{1^{Ph}}$, $\mathbf{2a^{Ph}}$ and $\mathbf{2b^{Ph}}$, where the Mes substituents were replaced by phenyl groups for computational efficiency, are in good agreement with the experimental structures (Figure 4). The formation of $\mathbf{2a^{Ph}}$ and $\mathbf{2b^{Ph}}$ is exergonic, and the thermodynamic product of the reaction appears to be $\mathbf{2b^{Ph}}$ (−15.2 kcal/mol with respect the starting materials), while $\mathbf{2a^{Ph}}$ (−11.3 kcal/mol) is a kinetic product.

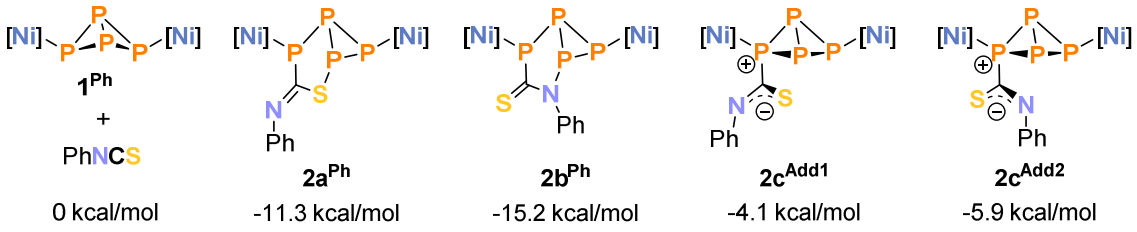

Figure 4. a) Calculated, relative Gibbs free energies (kcal/mol) of $\mathbf{1^{Ph}}$, $\mathbf{2a^{Ph}}$, and $\mathbf{2b^{Ph}}$ and further isomers $\mathbf{2c^{Add1}}$ and $\mathbf{2c^{Add2}}$, which potentially correspond to **2c**. The relative Gibbs free energies refer to $\mathbf{1^{Ph}}$ + PhNCS (kcal/mol).

The NMR spectroscopically detected species **2c** gives rise to an A_2MX spin system in the $^{31}P\{^1H\}$ NMR spectrum (*vide supra*) indicative of an unsymmetrically-substituted "P_4 butterfly" fragment.[3] It is conceivable that adduct complexes $\mathbf{2c^{Add1}}$ and $\mathbf{2c^{Add2}}$ (Figure 4b) represent intermediates on the reaction coordinate from $\mathbf{1^{Mes}}$ and PhNCS to **2a** and **2b**, respectively. However, the transition states connecting $\mathbf{2c^{Add1}}$ with $\mathbf{2a^{Ph}}$, and $\mathbf{2c^{Add2}}$ with $\mathbf{2b^{Ph}}$ possess unrealistically high energies (~50 kcal mol^{-1}), thus indicating that a direct interconversion between these species is unlikely to occur under the reaction conditions.† The formation of Ni−P

insertion products is also conceivable, but the calculated energies of these species were higher than those of **2a** and **2b** (Figure S14).[15]†

5.3 Conclusion

In conclusion, the reaction of $\mathbf{1^{Mes}}$ with PhNCS affords the novel complexes **2a** and **2b** with an unsual bicyclo[3.1.0]heterohexane skeleton. To our knowledge, this represents the first example of a formal cycloaddition of a heteroallene to a bicyclo[1.1.0]tetraphosphabutane. In future work, it will be of interest to investigate whether reactions of cyclopolyphosphanes with polar multiple bonds offer a general route toward "functionalized" polyphosphanes.[15] Efficient preparative methods exist for a range of bicyclo[1.1.0]tetraphosphabutanes,[1,6–9] therefore, such transformations may provide a fruitful avenue to the stepwise and selective degradation of the P_4 molecule.

Notes and References

§Excess PhNCS (7 equiv.) is needed to achieve full conversion of $\mathbf{1^{Mes}}$, while a large amount of $\mathbf{1^{Mes}}$ (55%) remained in the reaction mixture with one equiv. PhNCS after one day ([D_8]THF, Figure S8, SI).

‡The ^{1}H NMR spectrum of a freshly prepared [D_8]THF solution of pure crystals of **2a** stored for one week at room temperature in an Ar-filled glove box also showed a mixture containing **2a**, **2b** and $\mathbf{1^{Mes}}$ in a 94.5:0.5:5 ratio.

1 Reviews: a) B. M. Cossairt, N. A. Piro, C. C. Cummins, *Chem. Rev.* **2010**, *110*, 4164; b) M. Caporali, L. Gonsalvi, A. Rossin, M. Peruzzini, *Chem. Rev.* **2010**, *110*, 4178; c) M. Peruzzini, I. de los Rios, A. Romerosa, F. Vizza, *Eur. J. Inorg. Chem.* **2001**, 593; d) M. Peruzzini, R. R. Abdreimova, Y. Budnikova, A. Romerosa, O. J. Scherer, H. Sitzmann, *J. Organomet. Chem.* **2004**, *689*, 4319; e) M. Peruzzini, L. Gonsalvi, A. Romerosa, *Chem. Soc. Rev.* **2005**, *34*, 1038.

2 Selected publications on transformations of transition metal phosphide complexes derived from P_4 in one step: a) P. Barbaro, C. Bazzicalupi, M. Peruzzini, S. Seniori Costantini, P. Stoppioni, *Angew. Chem. Int. Ed.* **2012**, *51*, 8628; b) E. Mädl, M. V. Butovskii, G. Balázs, E. V. Peresypkina, A. V. Virovets, M. Seidl and M. Scheer, *Angew. Chem. Int. Ed.* **2014**, *53*, 7643.

3 a) W. T. K. Chan, F. García, A. D. Hopkins, L. C. Martin, M. McPartlin, D. S. Wright, *Angew. Chem. Int. Ed.* **2007**, *46*, 3084; b) J. E. Borger, A. W. Ehlers, M. Lutz, J. C. Slootweg, K. Lammertsma, *Angew. Chem. Int. Ed.* **2014**, *53*, 12836; c) M. Arrowsmith, M. S. Hill, A. L. Johnson, G. Kociok-Köhn, M. F. Mahon, *Angew. Chem. Int. Ed.* **2015**, *54*, 7882; d) J. E. Borger, A. W. Ehlers, M. Lutz, J. C. Slootweg, K. Lammertsma, *Angew. Chem. Int. Ed.* **2015**, *55*, 613.

4 a) J. D. Masuda, W. W. Schoeller, B. Donnadieu, G. Bertrand, *Angew. Chem. Int. Ed.* **2007**, *46*, 7052; b) O. Back, G. Kuchenbeiser, B. Donnadieu, G. Bertrand, *Angew. Chem. Int. Ed.* **2009**, *48*, 5530.

5 Selected publications on the insertion of *p*-block elements into the P−P bonds of P_4: a) Y. Xiong, S. Yao, M. Brym, M. Driess, *Angew. Chem. Int. Ed.* **2007**, *46*, 4511; b) J. J. Weigand, M. Holthausen, R. Fröhlich, *Angew. Chem. Int. Ed.* **2009**, *48*, 295; c) M. H. Holthausen, J. J. Weigand, *J. Am. Chem. Soc.* **2009**, *131*, 14210; d) G. Prabusankar, A. Doddi, C. Gemel, M. Winter, R. A. Fischer, *Inorg. Chem.* **2010**, *49*, 7976; e) M. H. Holthausen, J. J. Weigand, *Chem. Soc. Rev.* **2014**, *43*, 6639.

6 a) J.-P. Bezombes, P. B. Hitchcock, M. F. Lappert, J. E. Nycz, *Dalton Trans.* **2004**, 499; b) B. M. Cossairt, C. C. Cummins, *New J. Chem.* **2010**, *34*, 1533; c) S. Khan, R. Michel, J. M. Dieterich, R. A. Mata, H. W. Roesky, J.-P. Demers, A. Lange, D. Stalke,

J. Am. Chem. Soc. **2011**, *133*, 17889; d) N. A. Giffin, A. D. Hendsbee, T. L. Roemmele, M. D. Lumsden, C. C. Pye, J. D. Masuda, *Inorg. Chem.* **2012**, *51*, 11837; e) S. Heinl, S. Reisinger, C. Schwarzmaier, M. Bodensteiner, M. Scheer, *Angew. Chem. Int. Ed.* **2014**, *53*, 7639.

7 a) O. J. Scherer, T. Hilt, G. Wolmershäuser, *Organometallics* **1998**, *17*, 4110; b) S. Pelties, D. Herrmann, B. de Bruin, F. Hartl, R. Wolf, *Chem. Commun.* **2014**, *50*, 7014; c) S. Heinl, M. Scheer, *Chem. Sci.* **2014**, *5*, 3221; d) C. Schwarzmaier, A. Y. Timoshkin, G. Balázs, M. Scheer, *Angew. Chem. Int. Ed.* **2014**, *53*, 9077; e) D. W. Agnew, C. E. Moore, A. L. Rheingold, J. S. Figueroa, *Angew. Chem. Int. Ed.* **2015**, *54*, 12673.

8 Selected main group element-substituted "butterfly P_4" compounds with an E_2P_4 core: a) E. Niecke, R. Rüger, B. Krebs, *Angew. Chem. Int. Ed. Engl.* **1982**, *21*, 544; b) R. Riedel, H.-D. Hausen, E. Fluck, *Angew. Chem. Int. Ed. Engl.* **1985**, *24*, 1056; c) S. L. Hinchley, C. A. Morrison, D. W. H. Rankin, C. L. B. Macdonald, R. J. Wiacek, A. Voigt, A. H. Cowley, M. F. Lappert, G. Gundersen, J. A. C. Clyburne, P. P. Power, *J. Am. Chem. Soc.* **2001**, *123*, 9045.

9 a) O. J. Scherer, T. Hilt, G. Wolmershäuser, *Angew. Chem. Int. Ed.* **2000**, *39*, 1425; b) C. Eichhorn, *PhD thesis*, Kaiserslautern **2003**; c) S. Deng, C. Schwarzmaier, C. Eichhorn, O. J. Scherer, G. Wolmershäuser, M. Zabel, M. Scheer, *Chem. Commun.* **2008**, 4064.

10 M. Scheer, S. Deng, O. J. Scherer, M. Sierka, *Angew. Chem. Int. Ed.* **2005**, *44*, 3755.

11 C. Schwarzmaier, S. Heinl, G. Balázs, M. Scheer, *Angew. Chem. Int. Ed.* **2015**, *54*, 13116.

12 S. Biswas, S. Haldar, P. K. Mandal, K. Goubitz, H. Schenk, R. Dabrowski, *Cryst. Res. Technol.* **2007**, *42*, 1029.

13 a) M. Baudler, Y. Aktalay, K.-F. Tebbe, T. Heinlein, *Angew. Chem. Int. Ed. Engl.* **1981**, *20*, 967; in this context see also: b) M. Baudler, *Angew. Chem. Int. Ed. Engl.* **1982**, *21*, 492.

14 DFT calculations were performed using Gaussian09; see supporting information for further details.

15 Selected examples for the insertion of isothiocyanates into transition metal−phosphorus bonds: a) U. Segerer, E. Hey-Hawkins, *Polyhedron* **1997**, *16*, 2537; b) U. Segerer, J. Sieler, E. Hey-Hawkins, *Organometallics* **2000**, *19*, 2445; c) A. Antiñolo, S. García-Yuste, A. Otero, R. Reguillo-Carmona, *Eur. J. Inorg. Chem.* **2009**, 539; d) W. Yi, J. Zhang, L. Hong, Z. Chen, X. Zhou, *Organometallics* **2011**, *30*, 5809.

16 a) A. R. Jupp and J. M. Goicoechea, *Angew. Chem. Int. Ed.* 2013, **52**, 10064; b) R. S. P. Turbervill, J. M. Goicoechea, *Chem. Commun.* **2012**, *48*, 6100; c) R. S. P. Turbervill,

A. R. Jupp, P. S. B. McCullough, D. Ergöçmen, J. M. Goicoechea, *Organometallics* **2013**, *32*, 2234.

5.4 Supporting Information (SI)

5.4.1 General Procedures

All experiments were performed under an atmosphere of dry argon using standard Schlenk techniques or an MBraun UniLab glovebox. Solvents were dried and degassed with an MBraun SPS800 solvent purification system. Tetrahydrofuran and toluene were stored over molecular sieves (3 Å). Diethyl ether and *n*-hexane were stored over a potassium mirror. NMR spectra were recorded on Bruker Avance 300 and Avance 400 spectrometers at 300 K and internally referenced to residual solvent resonances. Melting points were measured on samples in sealed capillaries on a Stuart SMP10 melting point apparatus. UV/Vis spectra were recorded on a Varian Cary 50 spectrophotometer. Elemental analyses were determined by the analytical department of Regensburg University. Phenyl isothiocyanate was purchased from ALFA Aesar and used as received.

5.4.2 Synthesis of $\mathbf{1^{Mes}}$

P_4 (310.4 mg, 2.505 mmol, 1.0 eq) was added in one portion at −60 °C to a solution of CpNi(IMes) (2.165 g, 5.053 mmol, 2.0 eq). The solution turned immediately dark red. After stirring the solution for 19 h, the solvent was removed in vacuum, and the residue was extracted with toluene (50 mL). Subsequently, the solution was filtered and reduced in volume (45 mL). Dark red crystals of $\mathbf{1^{Mes}}$ formed upon storing the solution at −16 °C for one day. The isolated compound contains one equivalent of toluene per formula unit after drying in high vacuum. Yield 1.932 g (71%); m.p. >158 °C (slow decomp. to a black oil); UV/Vis (THF, λ_{max} /nm, (ε_{max} /L·mol^{-1}·cm^{-1})): 354 (15100), 421 (9600), 515 (9200); elemental analysis calcd. for $C_{54}H_{66}N_4Ni_2P_4{\cdot}C_7H_8$ (*M* = 1104.55): C 66.33, H 6.75, N 5.07, found: C 66.35, H 6.15, N 5.12; ^{1}H NMR ([D$_8$]THF, 300 K, 400.13 MHz) δ /ppm = 2.19 (s, 24H, *ortho*-C*H*$_3$), 2.41 (s, 12H, *para*-C*H*$_3$), 4.31 (s, 10H, Cp), 7.04 (s, 8H, *meta*-CH$_{Dipp}$), 7.10 (s, 4H, NC-H); ^{13}C{^{1}H} NMR ([D$_8$]THF, 300 K, 100.61 MHz) δ /ppm =19.6 (*ortho*-*C*H$_3$), 21.2 (*para*-*C*H$_3$), 90.6 (Cp), 124.3 (NCH), 129.7 (*meta*-C$_{Dipp}$), 136.7 (C$_{Dipp}$), 138.3 (C$_{Dipp}$), 138.8 (C$_{Dipp}$), 182.8 (C$_{Carbene}$); ^{31}P{^{1}H} NMR ([D$_8$]THF, 193 K, 100.61 MHz) δ /ppm = −320.4 (t, $^1J_{PP}$ = −190.5 Hz, 2P), −56.0 (t, $^1J_{PP}$ = −190.5 Hz, 2P).

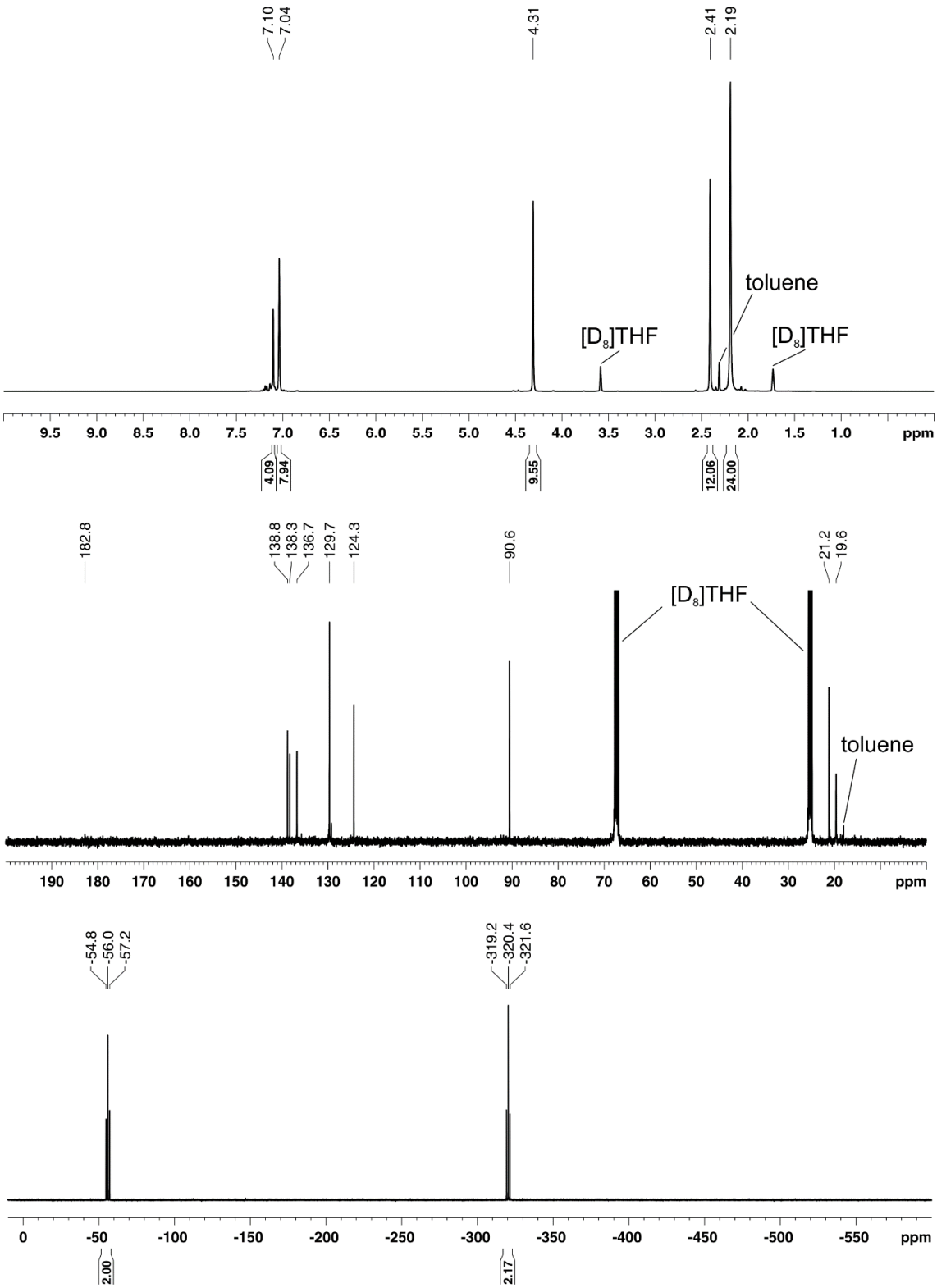

Figure S1. ^{1}H (top), ^{13}C{^{1}H} (middle), and ^{31}P{^{1}H} NMR spectrum (bottom) of **1^{Mes}** (400.16/100.61/161.98 MHz, [D$_8$]THF, 300 K).

5.4.3 Synthesis of 2a

A solution of phenyl isothiocyanate (122 mg, 0.900 mmol, 7.0 eq) in tetrahydrofuran (1.5 mL) was added to a solution of $\mathbf{1^{Mes}}$ (139 mg, 0.129 mmol, 1.0 eq) in tetrahydrofuran (2 mL) at room temperature. After stirring this solution for 4.5 hours the solvent was removed in *vacuo*, and the residue was washed with *n*-hexane (2 mL). The residue was extracted with toluene (1.5 mL) and layered with *n*-hexane (1 mL). Dark brown crystals formed during storage at room temperature after one day. X-ray quality crystals of **2a** were obtained by recrystallization of the crude product from toluene (2 mL) and diffusing *n*-hexane into this solution. The isolated compound contains two equivalents of toluene per formula unit after drying in high vacuum. Yield 54 mg (31%); m.p. >150 °C (slow decomp. to a black solid); UV/Vis (THF, λ_{max} /nm, (ε_{max} /L·mol^{-1}·cm^{-1})): 353sh (21500), 403 (13700), 490 (8000), 565sh (4800); elemental analysis calcd. for $C_{61}H_{71}N_5Ni_2P_4S{\cdot}2C_7H_8$ (M = 1331.90): C 67.63, H 6.58, N 5.26, found: C 67.65, H 5.85, N 5.38; ^{1}H NMR ([D$_8$]THF, 300 K, 400.13 MHz) δ /ppm = 2.12 (s, 6H, *para*-CH$_3$), 2.21 (s, 6H, *para*-CH$_3$), 2.30 (s, 12H, *ortho*-CH$_3$), 2.36 (s, 6H, *ortho*-CH$_3$), 4.29 (s, 5H, Cp), 4.62 (s, 5H, Cp), 6.65 (m, 2H, *meta*-CH$_{Ph}$), 6.92 (m, 1H, *para*-CH$_{Ph}$), 6.97−7.01 (m, 5H, CH$_{Ph/Dipp}$), 7.07−7.14 (m, 3H, CH$_{Ph/Dipp}$), 7.17−7.22 (m, 6H, CH$_{Ph/Dipp}$); ^{1}H NMR ([D$_8$]THF, 193 K, 400.13 MHz) δ /ppm = 1.98 (s, 3H, CH$_3$), 1.99 (s, 3H, CH$_3$), 2.03 (s, 3H, CH$_3$), 2.23 (s, 3H, CH$_3$), 2.24 (s, 3H, CH$_3$), 2.27 (s, 3H, CH$_3$), 2.30 (s, 3H, CH$_3$), 2.39 (s, 6H, CH$_3$), 2.42 (s, 3H, CH$_3$), 2.50 (s, 3H, CH$_3$), 2.61 (s, 3H, CH$_3$), 4.19 (s, 5H, Cp), 4.49 (s, 5H, Cp), 6.65 (s, 1H, CH$_{Ph/Dipp}$), 6.67 (s, 1H, CH$_{Ph/Dipp}$), 6.80 (s, 1H, CH$_{Ph/Dipp}$), 6.98 (t, $^3J_{HH}$ = 7.4 Hz, 1H, CH$_{Ph/Dipp}$), 7.02 (s, 1H, CH$_{Ph/Dipp}$), 7.13 (s, 1H, CH$_{Ph/Dipp}$), 7.15 (m, 2H, CH$_{Ph/Dipp}$), 7.22 (m, 6H, CH$_{Ph/Dipp}$), 7.30 (s, 1H, CH$_{Ph/Dipp}$), 7.39 (s, 1H, CH$_{Ph/Dipp}$), 7.44 (s, 1H, CH$_{Ph/Dipp}$), 7.47 (s, 1H, CH$_{Ph/Dipp}$), 7.51 (s, 1H, CH$_{Ph/Dipp}$), 7.53 (s, 1H, CH$_{Ph/Dipp}$); ^{13}C{^{1}H} NMR ([D$_8$]THF, 300 K, 100.61 MHz) δ /ppm = 19.4 (*ortho*-CH$_3$), 19.4 (*ortho*-CH$_3$), 21.3 (*para*-CH$_3$), 21.4 (*para*-CH$_3$), 91.1 (Cp), 91.6 (Cp), 120.5, 122.6, 124.9, 128.8, 129.7, 129.9, 130.1, 136.5, 138.0, 138.9, 155.8, 156.0, 179.3 (C$_{Carbene}$), 179.4 (C$_{Carbene}$); ^{31}P{^{1}H} NMR ([D$_8$]THF, 300 K, 100.61 MHz) δ /ppm = −150.1 (m, 1P), −96.4 (m, 1P), −75.0 (m, 1P), 32.1 (m, 1P); ^{31}P{^{1}H} NMR ([D$_8$]THF, 193 K, 100.61 MHz) δ /ppm = −151.8 (m, 1P), −105.5 (m, 1P), −78.0 (m, 1P), 27.8 (m, 1P).

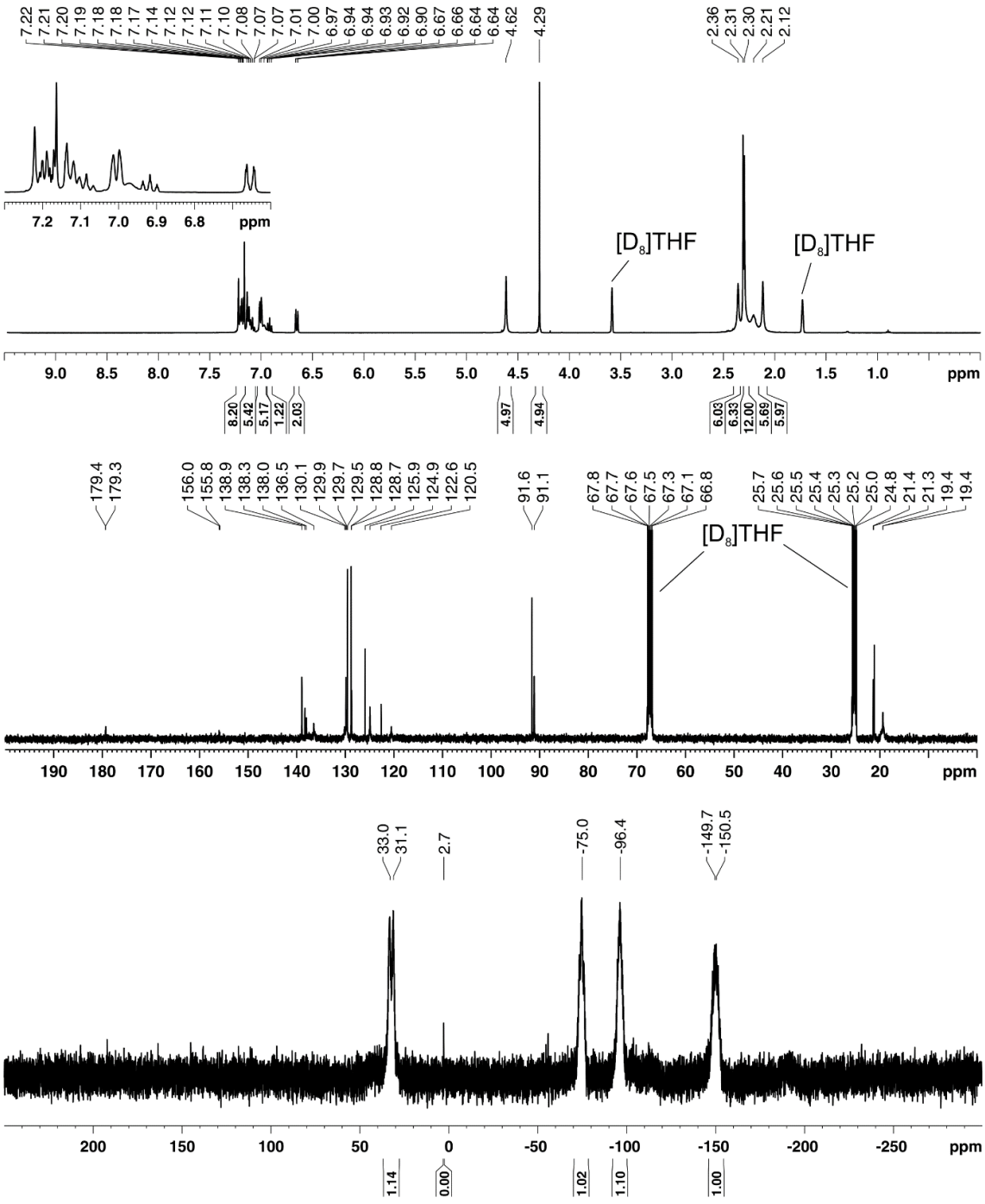

Figure S2. ^{1}H (top), $^{13}C\{^{1}H\}$ (middle), and $^{31}P\{^{1}H\}$ NMR spectrum (bottom) of **2a** (400.16/100.61/161.98 MHz, [D8]THF, 300 K).

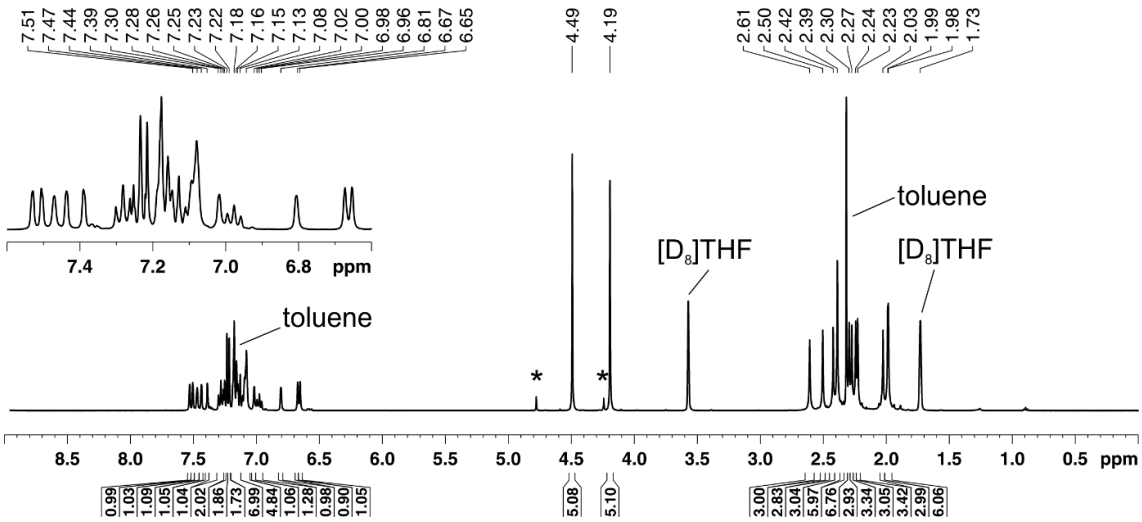

Figure S3. ^{1}H NMR spectrum of **2a** (400.16 MHz, [D$_8$]THF, 193 K). The signals assigned to **2b** are labeled with an asterisk.

5.4.4 Synthesis of 2b

A solution of phenyl isothiocyanate (176 mg, 1.30 mmol, 7.0 eq) in tetrahydrofuran (3 mL) was added to a solution of **1^{Mes}** (201 mg, 0.186 mmol, 1.0 eq) in tetrahydrofuran (2 mL) at room temperature. After stirring this solution for 25 hours the solvent was removed in vacuum, and the residue was washed with *n*-hexane (5 mL). The residue was extracted with diethyl ether (8 mL) and after filtration reduced in volume to 3 mL. Dark yellow crystals formed upon storing this solution at −35 °C for one day. X-ray quality crystals of **2b** were obtained by recrystallizing from toluene (1.5 mL) and diffusing *n*-hexane into this solution. Yield 34 mg (16%); m.p. >170 °C (slow decomp. to a black solid); UV/Vis (THF, λ_{max} /nm, (ε_{max} /L·mol^{-1}·cm^{-1})): 348 (22600), 400 (14400), 503 (7400), 586sh (4600); elemental analysis calcd. for $C_{61}H_{71}N_5NiP_4S$ (M = 1147.62): C 63.84, H 6.24, N 6.10, found: C 63.95, H 6.24, N 6.08; ^{1}H NMR ([D$_8$]THF, 300 K, 400.13 MHz) δ /ppm = 2.13 (s, 6H, *para*-CH$_3$), 2.20 (s, 12H, *ortho*-CH$_3$), 2.30 (s, 6H, *para*-CH$_3$), 2.38 (s, 6H, *ortho*-CH$_3$), 4.18 (s, 5H, Cp), 4.65 (s, 5H, Cp), 6.84 (s, 2H, CH$_{Ph/Dipp}$), 6.97 (s, 2H, CH$_{Ph/Dipp}$), 7.00 (m, 1H, *para*-CH$_{Ph}$), 7.02 (m, 3H, CH$_{Ph/Dipp}$), 7.09 (s, 2H, CH$_{Ph/Dipp}$), 7.14−7.16 (m, 3H, CH$_{Ph/Dipp}$), 7.24−7.27 (m, 4H, CH$_{Ph/Dipp}$); ^{1}H NMR ([D$_8$]THF, 193 K, 400.13 MHz) δ /ppm = 1.90 (s, 3H, CH$_3$), 1.97 (s, 3H, CH$_3$), 2.17 (s, 3H, CH$_3$), 2.23 (s, 9H, CH$_3$), 2.24 (s, 3H, CH$_3$), 2.27 (s, 3H, CH$_3$), 2.36 (s, 3H, CH$_3$), 2.51 (s, 3H, CH$_3$), 2.54 (s, 6H, CH$_3$), 4.10 (s, 5H, Cp), 4.58 (s, 5H, Cp), 6.59 (s, 1H, CH$_{Ph/Dipp}$), 6.73 (s, 1H, CH$_{Ph/Dipp}$), 6.94 (s, 1H, CH$_{Ph/Dipp}$), 6.96 (s, 1H, CH$_{Ph/Dipp}$), 6.99 (s, 2H, NCH), 7.06 (s, 1H, CH$_{Ph/Dipp}$), 7.11 (s, 1H, CH$_{Ph/Dipp}$), 7.22 (d, $^{3}J_{HH}$ = 7.5 Hz, 1H, CH$_{Ph/Dipp}$), 7.30−7.36 (m, 5H, CH$_{Ph/Dipp}$), 7.41 (s, 1H, CH$_{Ph/Dipp}$), 7.49 (s, 1H, CH$_{Ph/Dipp}$), 7.55 (s, 1H, CH$_{Ph/Dipp}$); ^{13}C{^{1}H} NMR ([D$_8$]THF, 300 K, 100.61 MHz) δ /ppm = 19.4 (*ortho*-CH$_3$), 19.7 (*ortho*-CH$_3$), 21.2 (*para*-CH$_3$), 21.2 (*para*-CH$_3$), 90.9 (Cp), 92.5 (Cp), 125.0, 125.3, 126.3, 128.7, 129.7, 129.9, 136.5, 137.1, 137.8, 138.2, 138.9, 139.0, 146.8, 146.9, 178.0 (C$_{Carbene}$), 178.1 (C$_{Carbene}$), 178.6 (NCS); ^{31}P{^{1}H} NMR ([D$_8$]THF, 300 K, 100.61 MHz) δ /ppm =

−182.1 (m, 1P), −104.5 (m, 1P), 4.5 (m, 1P), 50.1 (m, 1P); $^{31}P\{^{1}H\}$ NMR ([D8]THF, 193 K, 100.61 MHz) δ /ppm = −180.5 (m, 1P), −109.1 (m, 1P), 1.2 (m, 1P), 48.2 (m, 1P).

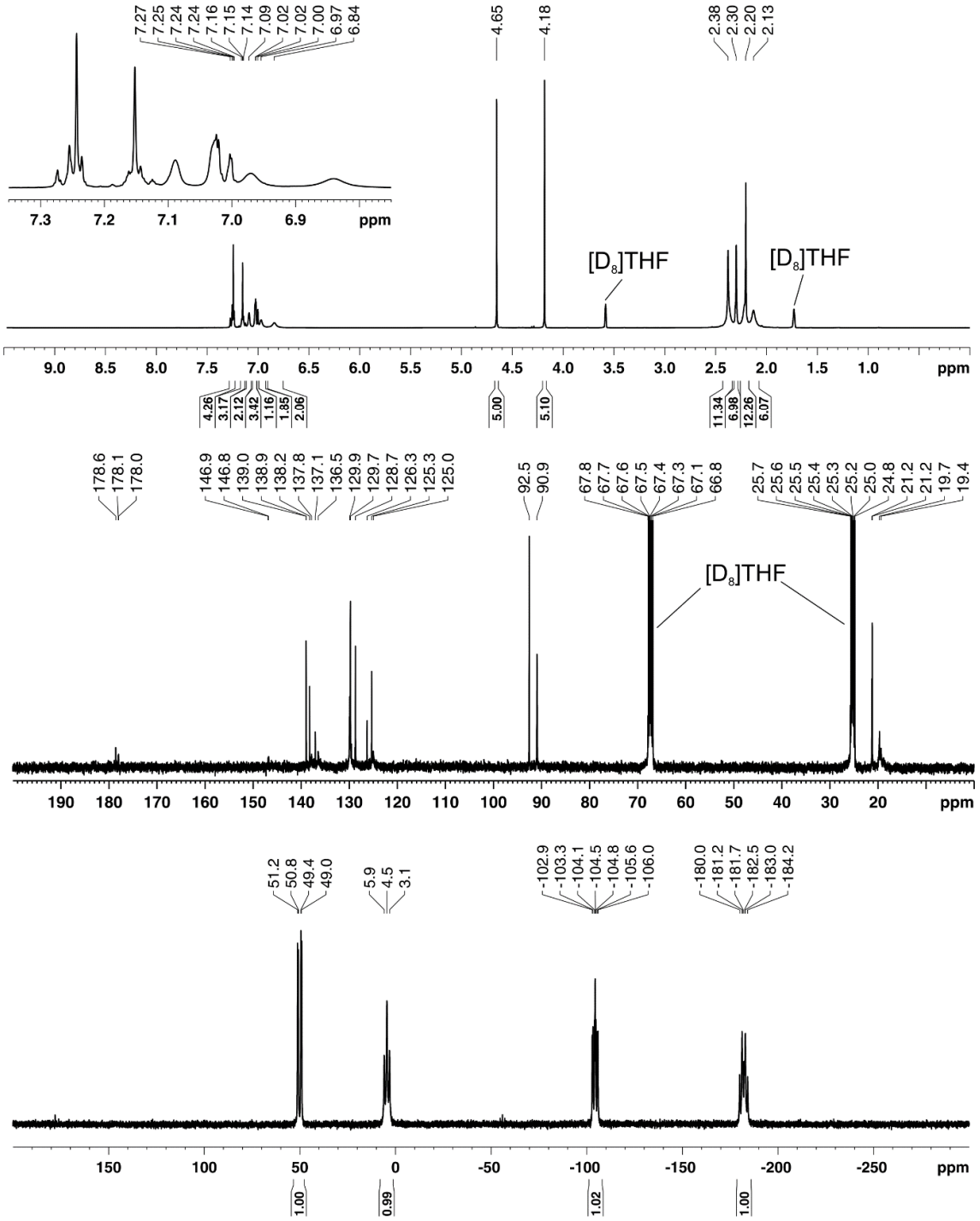

Figure S4. ^{1}H (top), $^{13}C\{^{1}H\}$ (middle), and $^{31}P\{^{1}H\}$ NMR spectrum (bottom) of **2b** (400.16/100.61/161.98 MHz, [D8]THF, 300 K).

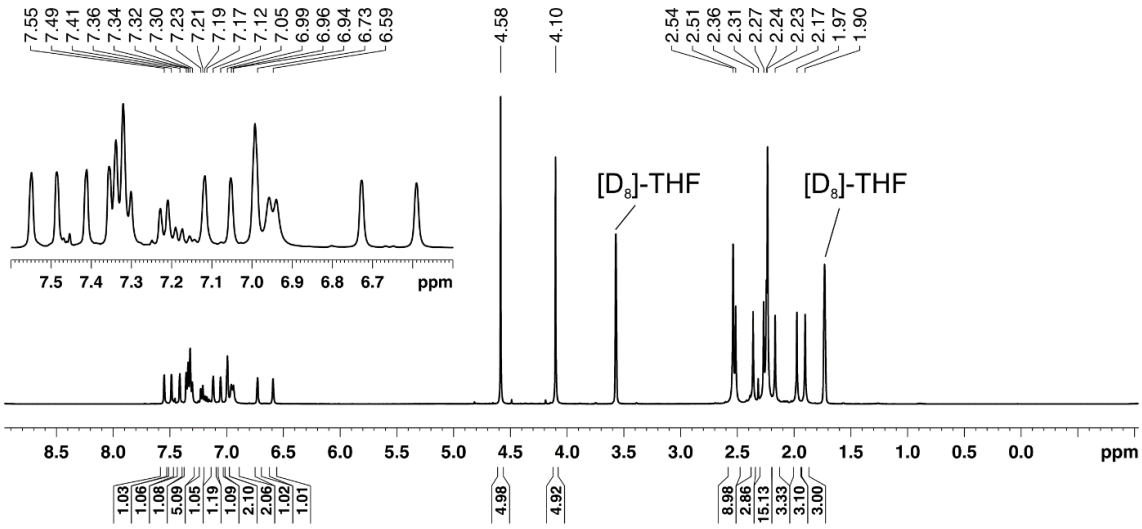

Figure S5. ^{1}H NMR spectrum of **2b** (400.16 MHz, [D$_8$]THF, 193 K).

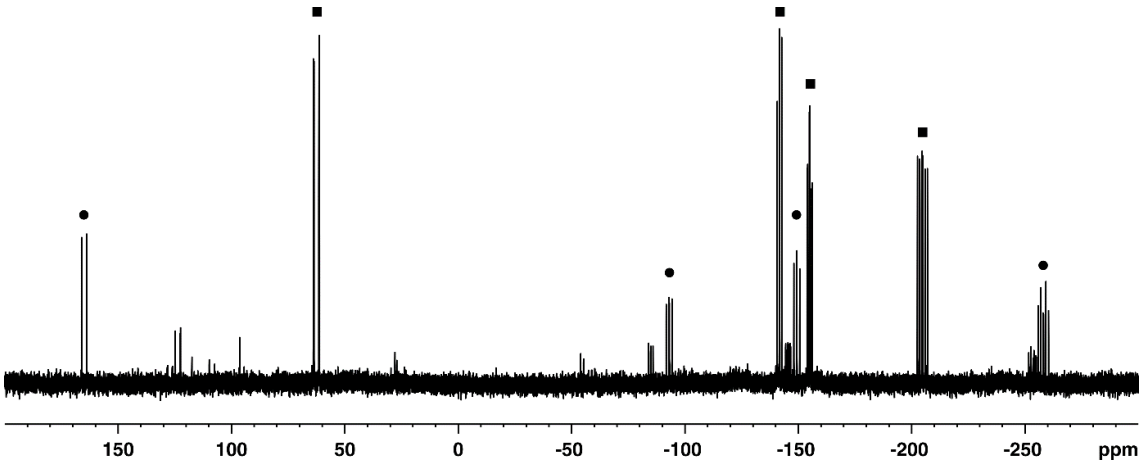

Figure S6. ^{31}P{^{1}H} NMR spectrum (161.98 MHz, THF/C_6D_6-capillary) of the reaction of CS_2 and **1^{Mes}** (10:1) after one hour; ■ = major species, ● = minor species.

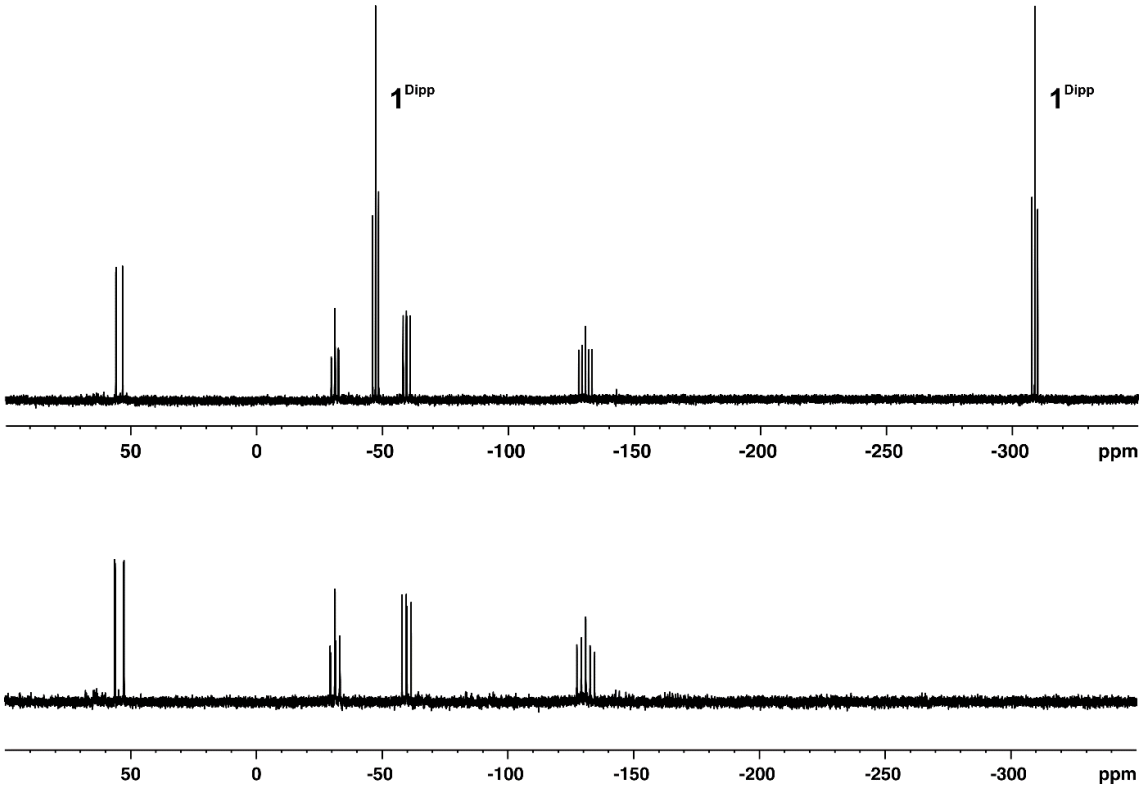

Figure S7. $^{31}P\{^{1}H\}$ NMR spectra (161.98 MHz, THF/C_6D_6-capillary) of the reaction of CS_2 and **1^{Dipp}** (10:1) after 1.5 hours (top) and after one day (bottom, 121.49 MHz).

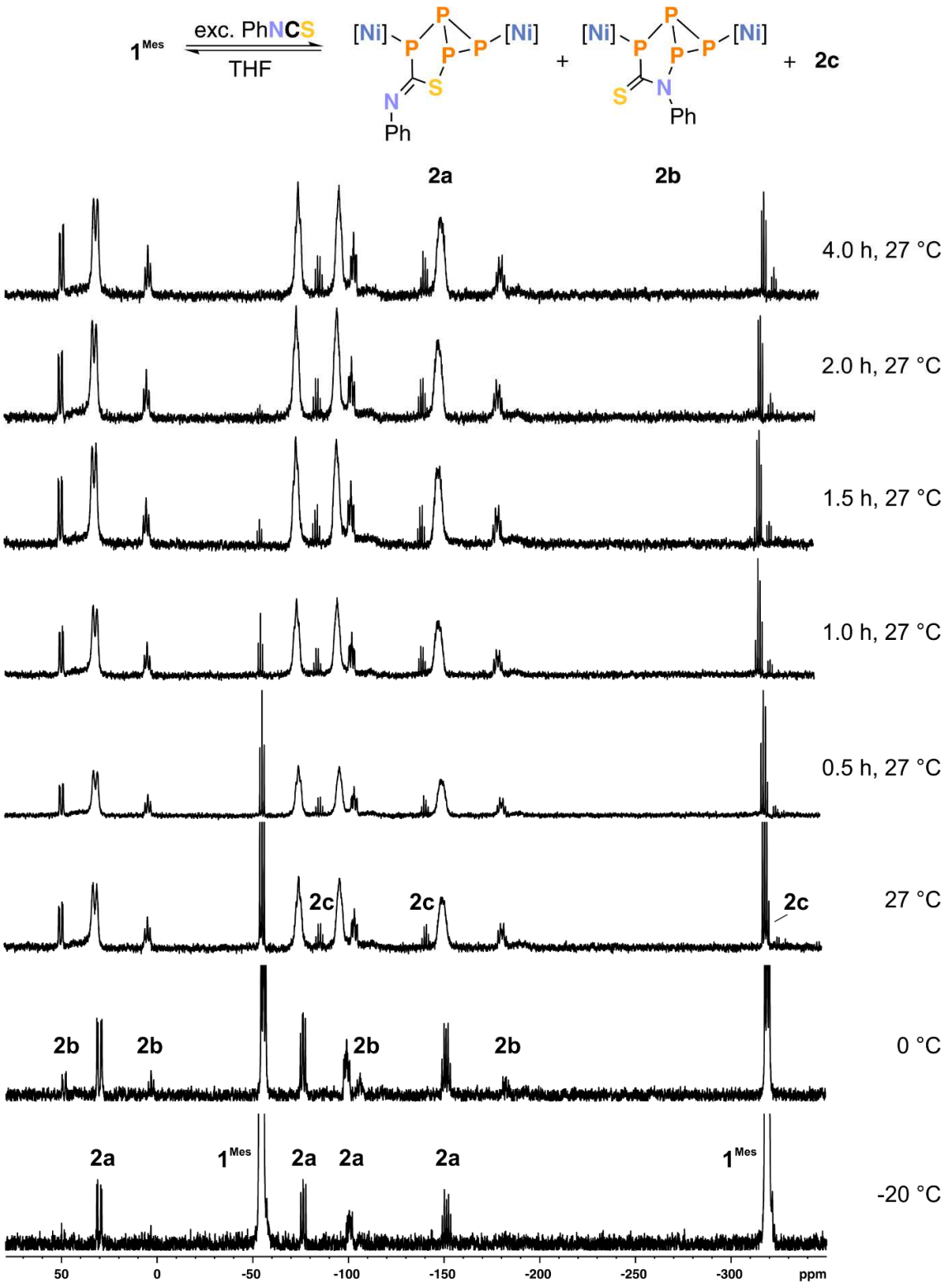

Figure S8. $^{31}P\{^{1}H\}$ NMR monitoring (161.98 MHz, $[D_8]$THF) of the reaction of PhNCS and **1^{Mes}** (7:1) at variable temperatures.

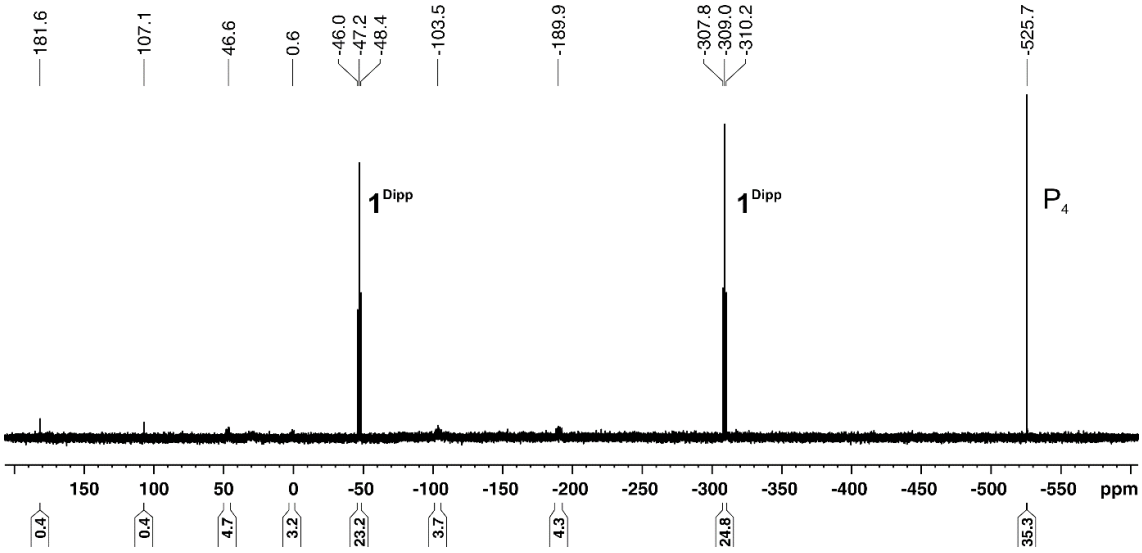

Figure S9. $^{31}P\{^{1}H\}$ NMR spectrum (161.98 MHz, THF/C_6D_6-capillary) of the reaction of PhNCS and $\mathbf{1^{Dipp}}$ (29:1) after two days.

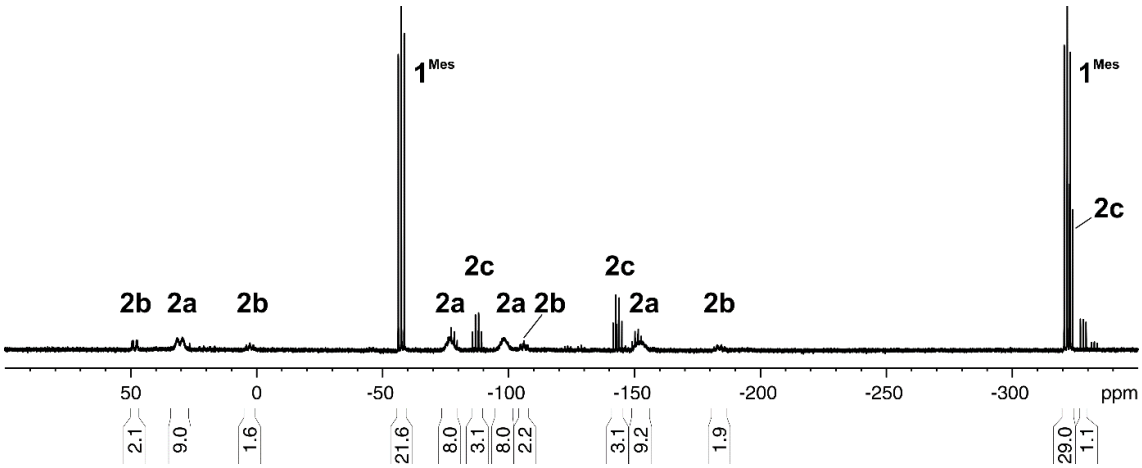

Figure S10. $^{31}P\{^{1}H\}$ NMR spectrum (161.98 MHz, THF/C_6D_6-capillary) of the reaction of PhNCS and $\mathbf{1^{Mes}}$ (1:1) after one day.

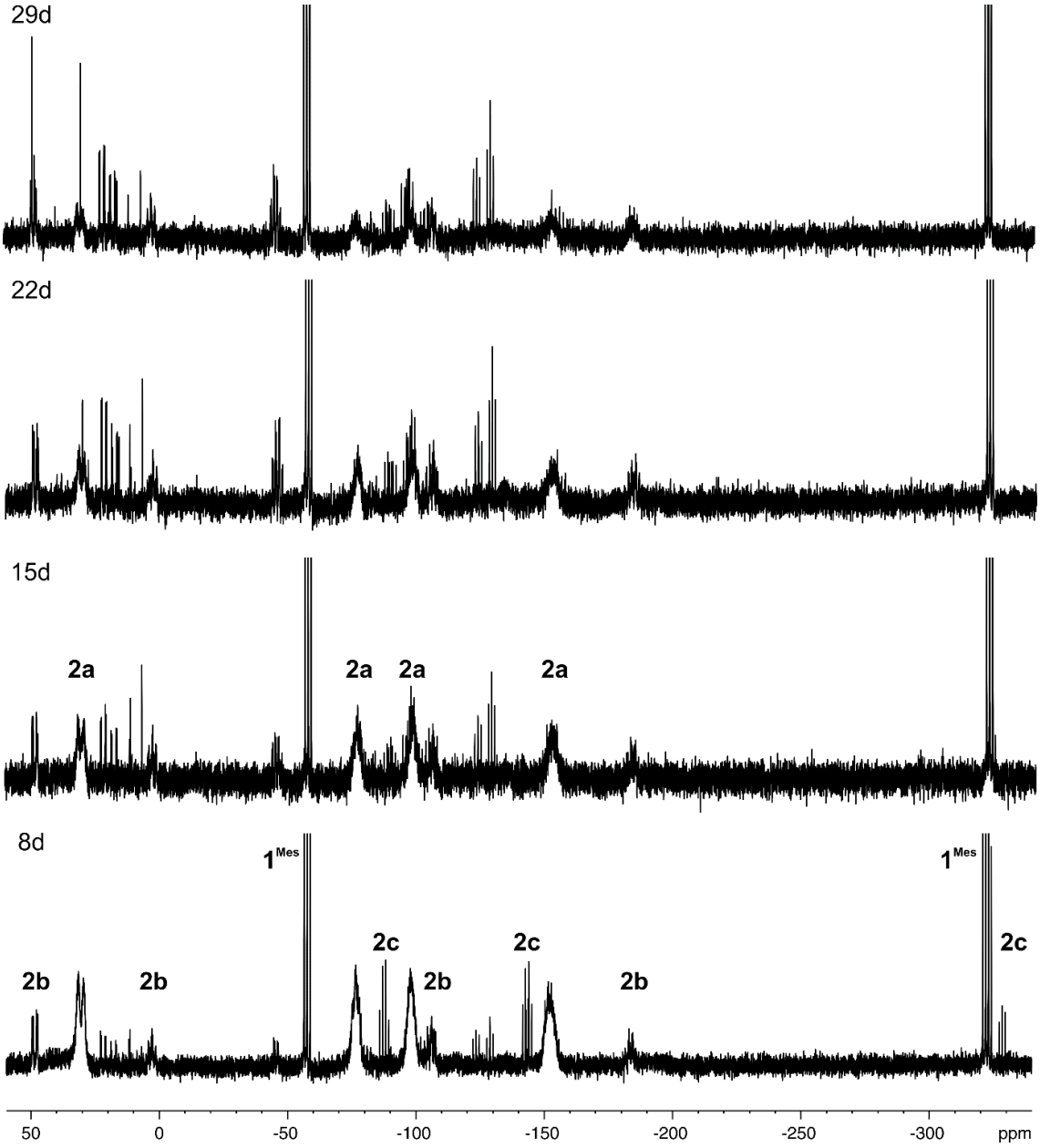

Figure S11. $^{31}P\{^{1}H\}$ NMR monitoring (161.98 MHz, $[D_8]THF$) of a solution of **2a**.

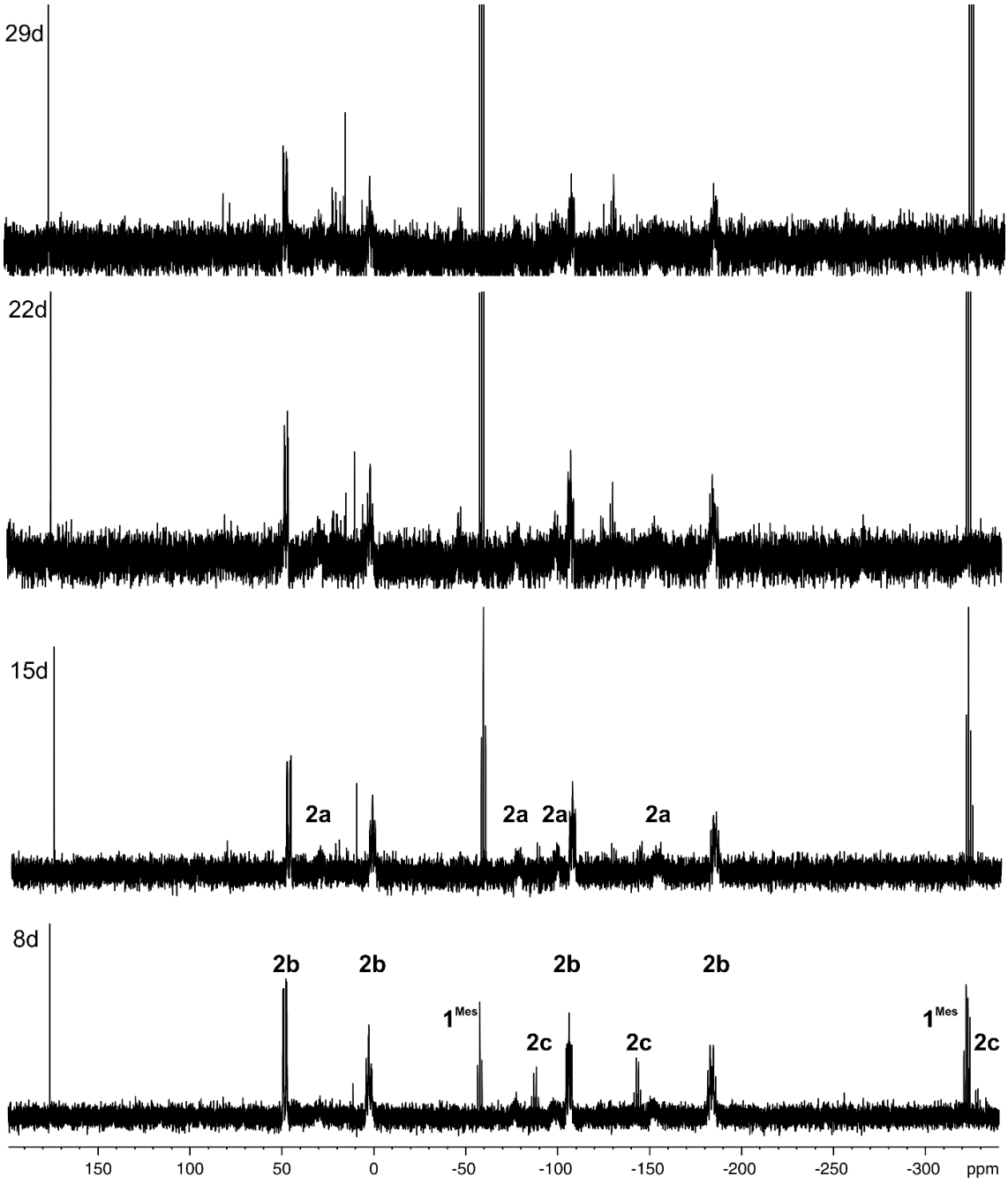

Figure S12. $^{31}P\{^{1}H\}$ NMR monitoring (161.98 MHz, [D_8]THF) of a solution of **2b**.

5.4.5 X-ray Crystallography

The single crystal X-ray diffraction data were recorded on an Agilent Technologies Gemini Ultra R diffractometer and an Agilent Technologies SuperNova in case of **2b** with Cu K_α radiation (λ = 1.54184 Å). Semi-empirical multi-scan absorption corrections[1] and analytical ones[2] were applied to the data. The structures were solved with SHELXT[3] and least-square refinements on F^2 were carried out with SHELXL.[4]

CCDC 1446071-1446073 contain the supplementary crystallographic data for this paper. These data can be obtained free of charge from The Cambridge Crystallographic Data Centre via www.ccdc.cam.ac.uk/data_request/cif.

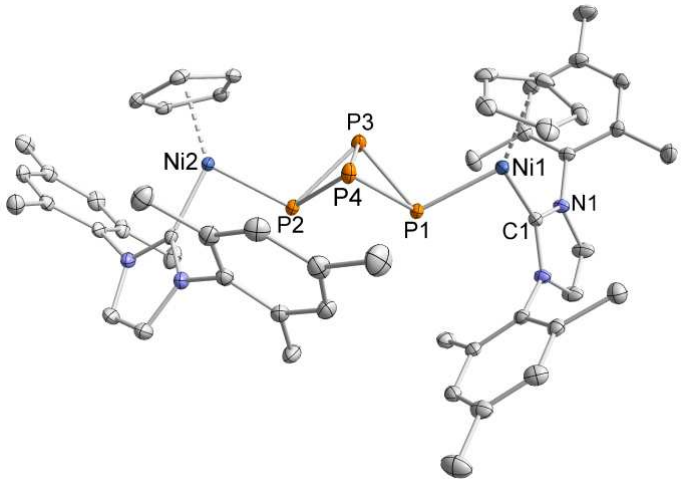

Figure S13. Solid-state molecular structure of [{CpNi(IMes)}$_2$(μ-η^1:η^1-P$_4$)] (**1^{Mes}**). The hydrogen atoms are omitted for clarity. Thermal ellipsoids are drawn at 40% level. Selected bond lengths [Å] and angles [°]: Ni1–P1 2.2207(6), Ni2–P2 2.2177(6), P1–P3 2.2239(7), P1–P4 2.2233(7), P3–P4 2.1681(8), P1–P2 2.9288(7), fold angle (of the planes P1–P3–P4 and P2–P3–P4) 98.07(3), P4–P1–P3 58.36(2), P1–P3–P4 60.81(2), P1–P4–P3 60.83(2).

Table S1. Crystallographic data of **1**, **2**, and **3**.

Compound	**1**	**2a**	**2b**
Empirical formula	$C_{62.5}H_{70}N_4Ni_2P_4$	$C_{76.5}H_{83}N_5Ni_2P_4S$	$C_{73}H_{79}N_5Ni_2P_4S$
Formula weight	1118.52	1345.83	1299.77
Temperature [K]	123(1)	123(1)	123(1)
Crystal system	triclinic	triclinic	triclinic
Space group	*P*-1	*P*-1	*P*-1
a [Å]	12.4093(4)	13.6251(4)	12.4533(2)
b [Å]	13.1987(2)	14.0607(3)	15.5940(3)
c [Å]	18.3557(4)	19.7007(5)	19.3068(3)
α [°]	79.4323(17)	99.8667(19)	104.2274(14)
β [°]	76.229(2)	99.819(2)	103.1281(14)
γ [°]	84.6926(19)	98.0922(19)	106.3708(16)
Volume [Å^3]	2866.71(12)	3607.32(16)	3305.17(10)
Z	2	2	2
ρ_{calc} [g/cm^3]	1.296	1.239	1.306
μ [mm^{-1}]	2.190	2.096	2.269
F(000)	1178.0	1418.0	1368.0
Crystal size [mm^3]	0.332 × 0.182 × 0.168	0.267 × 0.187 × 0.178	0.161 × 0.099 × 0.072
Radiation	CuKα (λ = 1.54184)	CuKα (λ = 1.54184)	CuKα (λ = 1.54184)
2Θ range for data collection [°]	9.13 to 133.45	7.34 to 133.25	6.58 to 146.95
Index ranges	−14 ≤ h ≤ 14, −14 ≤ k ≤ 15, −21 ≤ l ≤ 19	−16 ≤ h ≤ 16, −16 ≤ k ≤ 16, −23 ≤ l ≤ 23	−15 ≤ h ≤ 15, −18 ≤ k ≤ 19, −23 ≤ l ≤ 23
Reflections collected	25046	65571	31085
Independent reflections	10078 [R_{int} = 0.0256, R_{sigma} = 0.0285]	12645 [R_{int} = 0.0489, R_{sigma} = 0.0324]	12849 [R_{int} = 0.0374, R_{sigma} = 0.0442]
Data / restraints / parameters	10078/0/652	12645/4/754	12849/2/742
Goodness-of-fit on F^2	1.030	1.050	1.032
Final R indexes [I>=2σ (I)]	R_1 = 0.0379, wR_2 = 0.0966	R_1 = 0.0753, wR_2 = 0.2095	R_1 = 0.0574, wR_2 = 0.1646
Final R indexes [all data]	R_1 = 0.0426, wR_2 = 0.1006	R_1 = 0.0845, wR_2 = 0.2185	R_1 = 0.0721, wR_2 = 0.1791
Largest diff. peak/hole [e Å^{-3}]	1.14/−0.61	1.49/−0.91	1.05/−0.90

5.4.6 Computational Details

Density functional calculations were performed using Gaussian09, revision D.01[5] at the ωB97X-D level of theory.[6] Geometry optimizations were performed using the 6-311G(d,p)[7] basis set for all atoms. The nature of each stationary point was validated by frequency calculations.

The *Synchronous Transit-Guided Quasi-Newton* (STQN) Method was used for the transition state search.[8] The geometry optimizations of the starting materials and QST2 optimizations were performed at the ωB97X-D[6] level of theory using LANL2DZ[9] for Ni and the 6-31G(d,p)[7] basis set for the C, H, N, P, and S atoms. One imaginary frequency was found for each transition state structure which corresponds to the nuclear motion along the reaction coordinate. Moreover, intrinsic reaction coordinate (IRC) calculations were conducted to confirm the transition states.

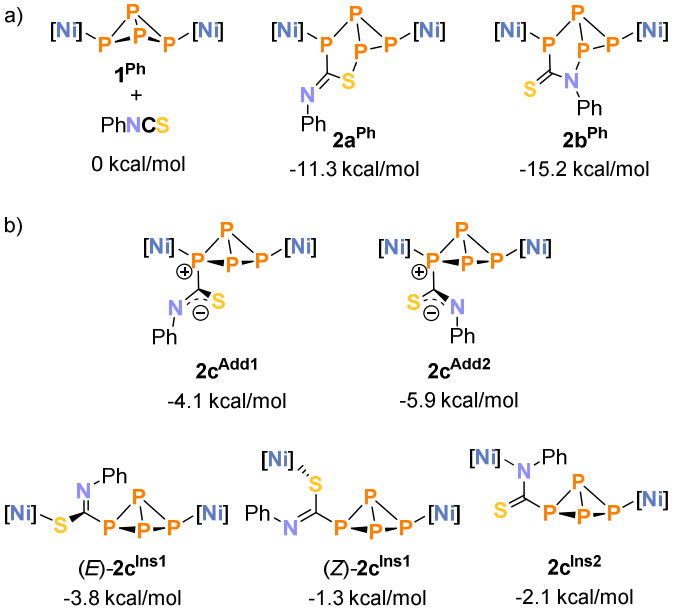

Figure S14. a) Calculated, relative Gibbs free energies (kcal/mol) of $\mathbf{1}^{Ph}$, $\mathbf{2a}^{Ph}$, and $\mathbf{2b}^{Ph}$; b) optimized structures of further isomers which potentially correspond to **2c**, including their relative Gibbs free energies referring to $\mathbf{1}^{Ph}$ + PhNCS (kcal/mol).

$\mathbf{1}^{Ph}$:

electronic energy *E*/ a.u.	−6145.58651995
thermal enthalpy *H*/ a.u.	−6144.889305
total free Gibbs energy at 298 K *G*/ a.u.	−6145.019660

Cartesian Coordinates:

Ni	-3.37594200	-0.31682500	0.57778400	C	-4.00824500	-0.60105900	2.63187600
P	-1.47982800	-0.16526700	-0.57429600	H	-4.04946600	0.16222000	3.39384500
C	-4.04439200	1.08664200	-0.45300200	Ni	3.37647200	0.31719400	0.57834200
C	-3.29108600	-2.30390200	1.26078200	P	1.48019300	0.16725200	-0.57365900
H	-2.64675500	-3.04865300	0.81808600	C	4.04362500	-1.08698300	-0.45245600
C	-5.04243100	-0.92882200	1.70212100	C	2.90944300	1.41261400	2.32473700
H	-6.01634000	-0.46174800	1.65640100	H	1.94026900	1.39134000	2.80052200
C	-4.62930700	-2.04827500	0.92617900	C	4.00909400	0.60289400	2.63180600
H	-5.20617800	-2.53414800	0.15320800	H	4.04984300	-0.15979500	3.39439600
C	-2.90819700	-1.41047700	2.32570100	C	5.04351300	0.92927700	1.70187700
H	-1.93887700	-1.38794700	2.80113700	H	6.01722800	0.46174300	1.65673400

C	3.29297700	2.30501400	1.25921000	C	-2.04858200	3.98315000	0.05842800
H	2.64917600	3.04980400	0.81580600	C	1.22295800	-4.64306600	0.96064700
C	4.63105400	2.04833500	0.92495200	H	5.87605400	-2.20480200	-2.93734700
H	5.20833800	2.53341800	0.15180400	H	0.45721900	-5.31564700	0.59285800
P	0.12837300	-1.08060800	0.67051700	C	1.35809600	-4.41757900	2.32463300
P	-0.12824000	1.08039800	0.67246600	H	4.55026100	-4.15837600	-1.48816800
N	3.85909400	-2.43185100	-0.39219200	H	-8.18629000	-2.17128200	-2.16011700
C	3.01427800	-3.10905700	0.53765300	H	-5.87741600	2.20317600	-2.93799300
C	4.56960100	-3.08740700	-1.38697400	H	4.19116400	3.19876700	-3.33295000
N	-3.86051300	2.43160400	-0.39290800	C	6.24000700	2.82150100	-2.79845700
C	-3.01560300	3.10920900	0.53657400	H	-4.55246400	4.15761700	-1.48920200
C	-4.57132500	3.08665700	-1.38779200	C	-2.32924700	3.53968700	2.78841900
N	4.88870800	-0.92800900	-1.50451900	C	7.14023700	1.90809500	-2.26356100
C	5.35255200	0.34119100	-1.96696100	C	-1.22375300	4.64277300	0.95883100
C	5.22145900	-2.14012800	-2.08579300	H	2.43312100	-3.35634000	3.85256600
N	-4.88937100	0.92708000	-1.50501800	C	-1.35934200	4.41839900	2.32295800
C	-5.35264700	-0.34251100	-1.96695700	H	8.18711500	2.16844300	-2.16093400
C	-5.22276900	2.13895600	-2.08644600	H	-2.43516500	3.35875300	3.85144500
C	-4.44410300	-1.24193100	-2.50771900	H	-0.45764000	5.31475200	0.59072200
C	-6.69583300	-0.66329800	-1.84067500	H	0.69963000	-4.91889200	3.02406900
C	-4.89462700	-2.48787600	-2.91948600	H	1.91802100	-4.11274700	-1.00822200
C	3.16750100	-2.88696100	1.89763400	H	3.92928100	-2.20017400	2.24030400
C	2.04774400	-3.98379800	0.05995600	H	3.39803300	0.96530800	-2.58002300
C	-7.13953800	-1.91046100	-2.26282700	H	7.37845900	-0.05314400	-1.39508600
C	4.44446700	1.24078400	-2.50821100	H	6.58670200	3.79725800	-3.11888000
C	6.69589200	0.66136800	-1.84079600	H	-7.37877000	0.05109300	-1.39534100
C	2.32752800	-3.53811300	2.78965000	H	-6.58501900	-3.79979200	-3.11715500
C	4.89563500	2.48629100	-2.92060000	H	-3.39782600	-0.96592600	-2.57970100
H	-4.18979900	-3.20021200	-3.33146500	H	-0.70084200	4.91998900	3.02216300
C	-6.23883600	-2.82369100	-2.79722500	H	-3.93140600	2.20197900	2.23963800
C	-3.16926600	2.88822100	1.89668100	H	-1.91858500	4.11124300	-1.00981900

PhNCS:

electronic energy *E*/ a.u.	−722.64982621
thermal enthalpy *H*/ a.u.	−722.539229
total free Gibbs energy at 298 K *G*/ a.u.	−722.581603

Cartesian Coordinates:

C	2.05512100	-0.18514500	-0.00017900	H	-0.16800100	1.90721900	-0.00027700
S	3.60154000	0.14662000	0.00002500	C	-2.25288600	1.35708900	0.00008000
N	0.91282700	-0.49904900	-0.00034300	H	-2.60172400	2.38320000	0.00009000
C	-0.44436400	-0.22268900	-0.00013100	C	-3.16721900	0.30944800	0.00027400
C	-0.89051000	1.09996800	-0.00012500	H	-0.98338600	-2.29506200	0.00002600
C	-1.35399500	-1.27757400	0.00004700	C	-2.71401300	-1.00459300	0.00025500
				H	-4.23070500	0.51676400	0.00044000
				H	-3.42341600	-1.82372800	0.00040000

$2a^{Ph}$:

electronic energy *E*/ a.u.	−6868.28335893
thermal enthalpy *H*/ a.u.	−6867.472885
total free Gibbs energy at 298 K *G*/ a.u.	−6867.619246

Cartesian Coordinates:

Ni	-3.78067500	-0.50899400	0.59109300	H	-2.60935900	-3.08751200	0.69076300
P	-1.84788500	0.20373200	-0.25684900	C	-3.26566600	-1.65314300	2.27911700
C	-4.61599600	0.79515100	-0.44845300	H	-2.35195900	-1.52270600	2.83995100
C	-3.41071700	-2.51307100	1.12957900	Ni	3.22953200	-0.84436700	0.93690700

P	1.50866700	-0.39555100	-0.43309700	H	5.68393200	-3.32712800	-2.67227600
C	3.78242700	-2.14329800	-0.28060100	H	2.63811500	-1.75524000	3.62258000
C	2.73637500	0.24185700	2.64698400	H	-1.13803700	-4.72473700	-0.76566700
H	1.75795600	0.65555300	2.83512900	C	-0.31783100	-4.74205800	1.22035800
C	3.20613300	-1.01521800	3.07996800	H	3.58008100	-4.97041600	-1.92581100
C	4.50888500	-1.16287100	2.54616500	H	5.14437500	-2.03130200	2.64907500
C	3.81018400	0.93768100	1.98945500	C	4.90524300	0.07993500	1.93496100
P	-0.22509700	-0.84325800	0.83099300	H	-7.75206300	-3.04681600	-2.93460400
C	1.55554200	1.45185700	-0.47718700	H	-6.30503900	1.76186700	-3.08909300
S	0.57602000	2.48092200	0.64118600	H	5.71272800	2.33231000	-1.91613300
P	-0.90398600	1.17174000	1.47950100	C	7.44763200	1.19261500	-1.33911500
N	3.21220700	-3.34222600	-0.55748700	H	-5.54978900	3.79827400	-1.36683300
C	2.01379100	-3.82375300	0.05176600	C	-3.82662500	3.30868800	3.11593500
C	3.88945100	-4.00296500	-1.57064100	H	-4.73030100	-0.37211300	3.34688100
N	-4.69546800	2.13820300	-0.28561600	C	7.93389400	-0.06057300	-0.98465600
C	-4.07830100	2.86593400	0.77863300	C	-2.49172100	4.50483200	1.50768300
C	-5.38731400	2.73531200	-1.32769500	C	3.66085100	3.96826400	-0.75138600
N	4.83651900	-2.07854300	-1.12932000	C	1.73655400	4.13563800	-2.19176800
C	5.72756300	-0.96469100	-1.21920900	H	0.75209400	-4.62662100	3.07899000
C	4.91680400	-3.20920300	-1.92710600	H	3.73877800	1.93346200	1.57987700
N	-5.28182200	0.56852400	-1.60884000	H	5.85800900	0.27587000	1.46560700
C	-5.41160000	-0.72216300	-2.20571000	C	-2.85170100	4.25583600	2.82614400
C	-5.76158600	1.74568600	-2.16054100	H	8.98331300	-0.19325500	-0.74892700
N	2.38363500	1.97667800	-1.28605600	H	-4.09914700	3.10708700	4.14502100
C	2.57716700	3.36155200	-1.38904000	H	-1.71139700	5.22019900	1.27815300
C	-4.27111500	-1.37817500	-2.64921600	H	4.31553500	3.36113000	-0.13640500
C	-6.66406200	-1.30869800	-2.30489000	C	3.89176700	5.32865700	-0.90732000
C	-4.39316700	-2.64847200	-3.19284000	H	4.73398500	5.78876300	-0.40188100
C	1.97262800	-4.02841000	1.42353900	C	3.05309800	6.09822300	-1.70439500
C	0.90189300	-4.06824900	-0.74287800	H	0.89903700	3.65575500	-2.68483100
C	-6.77795600	-2.57857300	-2.85757800	C	1.97628300	5.49332100	-2.34423900
C	5.22960500	0.27866100	-1.58205700	H	3.23765500	7.15893300	-1.82932900
C	7.07052000	-1.14711400	-0.92070000	H	1.31694500	6.08507900	-2.97015500
C	0.79754700	-4.47979500	2.00656900	H	-2.79305900	3.94896800	-0.55267800
C	6.09984200	1.35911700	-1.63776200	H	-2.35939600	4.78888500	3.63082900
H	-3.50711700	-3.16887400	-3.53657300	H	7.42700300	-2.12574500	-0.61940300
C	-5.64314200	-3.24969400	-3.29675700	H	4.17674200	0.41694900	-1.80158500
C	-4.73637400	-2.44232500	0.69041600	H	-3.30590000	-0.89456300	-2.55314200
C	-4.45018600	2.61244400	2.09045100	H	-5.73376300	-4.24234300	-3.72236900
C	-3.10204400	3.80418800	0.47587800	H	-7.53481000	-0.78249000	-1.93090100
C	-5.39187400	-1.46737300	1.50439600	H	-1.23595900	-5.08746400	1.68103900
H	-6.42258700	-1.15928800	1.39819000	H	2.85336100	-3.82135000	2.01758900
C	-4.50806600	-1.06289800	2.54815600	H	0.94728200	-3.85923100	-1.80509600
H	-5.16338200	-2.94500800	-0.16476000	H	8.12166400	2.04048100	-1.38256100
C	-0.26331800	-4.53966100	-0.15281300	H	-5.20871800	1.86755400	2.29375600

2b^{Ph}:

electronic energy *E*/ a.u.	−6868.29212478
thermal enthalpy *H*/ a.u.	−6867.481530
total free Gibbs energy at 298 K *G*/ a.u.	−6867.625484

Cartesian Coordinates:

Ni	-3.43422700	-0.96413000	0.56412300	C	4.20337100	-1.75476000	-0.09835400
P	-1.69137700	-0.20843500	-0.60927500	C	2.76079800	1.22733900	2.00075200
C	-4.51440900	0.31980900	-0.26405600	H	1.73317700	1.55136400	2.05621200
C	-2.83481600	-2.93944800	0.95960300	C	3.34059200	0.20220500	2.77299200
H	-2.04872600	-3.41944700	0.39766500	C	4.67616200	0.06530700	2.31888000
C	-2.62458300	-2.12749700	2.13356500	C	3.78250600	1.83222500	1.18500700
H	-1.66235200	-1.93552200	2.58452600	P	0.10399600	-0.83743000	0.53549700
Ni	3.44814700	-0.22513500	0.66506700	C	1.40459900	1.43650900	-1.11260500
P	1.76185500	-0.34119500	-0.83522300	S	2.29849400	2.25830500	-2.26492700

P	-0.68408600	1.20462600	0.75301800	H	5.39492300	-0.66252500	2.66849100
N	3.79133800	-3.04499300	-0.03221700	C	4.96611700	1.13148100	1.39605600
C	2.62716800	-3.49401300	0.66229100	H	-7.73357300	-3.69578500	-2.30077300
C	4.61463500	-3.87820000	-0.77424900	H	-6.70515700	1.19098100	-2.54651000
N	-4.70274900	1.64088200	-0.01967500	H	5.71280900	2.33790800	-2.74304300
C	-4.02124100	2.40487600	0.97636500	C	7.53210400	1.61201700	-1.84151600
C	-5.61398200	2.19480200	-0.90582100	H	-5.89295400	3.23274000	-0.85709100
N	5.30576500	-1.80440700	-0.88536900	C	-3.31772100	2.71371700	3.24137800
C	6.07773500	-0.65765000	-1.24688400	H	-4.05606200	-1.04380400	3.43549900
C	5.57209300	-3.09636200	-1.30750600	C	8.13889900	0.55845100	-1.16639300
N	-5.33318600	0.06635200	-1.31728000	C	-2.68952800	4.31096600	1.55455600
C	-5.46994200	-1.21523600	-1.93377800	C	-0.66652000	3.86786400	-1.52257300
C	-6.01490100	1.20198300	-1.72114400	C	0.73961900	4.33361200	0.38037700
N	0.44250500	2.02815200	-0.35830800	H	1.27268400	-3.54695400	3.75447500
C	0.17547000	3.42898500	-0.50867400	H	3.62852900	2.63823100	0.48241300
C	-4.39152500	-1.76607900	-2.61203200	H	5.91051300	1.29930400	0.90004600
C	-6.67266200	-1.89611600	-1.81848800	C	-2.65533900	3.87875100	2.87385700
C	-4.52360300	-3.02809500	-3.17378900	H	9.17684100	0.63095700	-0.86304300
C	2.51550800	-3.28667000	2.02952200	H	-3.29249400	2.37461100	4.27034500
C	1.62393900	-4.13860500	-0.04862600	H	-2.15601800	5.20355800	1.25177900
C	-6.79864800	-3.15551200	-2.39109400	H	-1.08154300	3.13913700	-2.20928000
C	5.46654300	0.37723600	-1.93822400	C	-0.93703400	5.22293100	-1.65087700
C	7.40851900	-0.58278100	-0.85945500	H	-1.58255500	5.56977400	-2.45029100
C	1.37537500	-3.72162700	2.69008900	C	-0.37106500	6.13609200	-0.76649200
C	6.19917800	1.51949600	-2.22597600	H	1.39817100	3.96883400	1.16047300
H	-3.68325600	-3.46921800	-3.69631800	C	0.46768700	5.68934400	0.24801500
C	-5.72316900	-3.72324100	-3.06370400	H	-0.57562800	7.19528900	-0.87553900
C	-4.20748400	-2.98104200	0.68744000	H	0.91537200	6.39766800	0.93595100
C	-4.01342400	1.97549700	2.29476900	H	-3.35702000	3.87443500	-0.44042600
C	-3.37121100	3.57094000	0.59925500	H	-2.10341500	4.44561000	3.61430800
C	-4.83794500	-2.10439200	1.61872300	H	7.85488400	-1.39791800	-0.30100400
H	-5.89650000	-1.88823400	1.65503100	H	4.42494300	0.30852900	-2.22929400
C	-3.86942600	-1.66416500	2.57235300	H	-3.46064100	-1.21434200	-2.67774100
H	-4.68874000	-3.48413800	-0.13799200	H	-5.82062400	-4.70881500	-3.50394700
C	0.49790500	-4.59034500	0.62579200	H	-7.49196700	-1.44882600	-1.26739700
H	6.40186700	-3.32593500	-1.95293300	H	-0.52666200	-4.70498100	2.50745100
H	2.82928600	-0.42171700	3.48990800	H	3.31242200	-2.77777100	2.55618000
H	-0.29033700	-5.09232300	0.07684600	H	1.71930000	-4.25823400	-1.12143500
C	0.36864900	-4.37730000	1.99224100	H	8.09911000	2.50840800	-2.06510000
H	4.44250400	-4.93830400	-0.83911400	H	-4.53825100	1.06882800	2.56245500

2c^{Add1}:

electronic energy *E*/ a.u.	−6868.27270590
thermal enthalpy *H*/ a.u.	−6867.461964
total free Gibbs energy at 298 K *G*/ a.u.	−6867.607822

Cartesian Coordinates:

Ni	-3.65574100	-0.88429700	-0.84699800	C	3.32877800	-3.08761200	-0.91019700
P	-1.66471200	-0.20921400	-0.15391700	P	-0.26358600	-0.15779600	-1.87812000
C	-4.20924800	-0.67710200	0.92603800	C	1.16274100	0.51236800	1.18026200
C	-3.79421700	-0.39327700	-2.90317300	S	1.23427900	-0.38351200	2.63506400
H	-3.22571400	0.39710500	-3.37005700	P	-0.34639100	-1.95207000	-0.53448000
C	-3.33813100	-1.75129400	-2.72694000	N	3.52366700	1.93875300	-1.30244500
H	-2.38631800	-2.13681800	-3.06247100	C	2.55566400	2.11916900	-2.33856900
Ni	3.26260300	-0.98553000	-1.09687600	C	4.19893000	2.99361600	-0.71643200
P	1.27979400	-0.51747200	-0.36345100	N	-3.92872200	-1.43368400	2.01165000
C	3.87350400	0.75928200	-0.73861200	C	-3.06932500	-2.57858500	1.99410700
C	2.91292800	-2.71288000	-2.24467000	C	-4.48782600	-0.89861800	3.16005600
H	1.95922000	-2.95649700	-2.68953800	N	4.79330500	1.09701900	0.19452600
C	3.95800500	-2.00847800	-2.85114400	C	5.48815200	0.16529000	1.03143600
C	4.97359800	-1.84569200	-1.85754900	C	5.00460500	2.46336400	0.22337000

N	-4.96813300	0.33351300	1.41662100	C	6.83716400	-1.66510800	2.59361600
C	-5.43838100	1.42128600	0.62027900	H	-4.35886400	-1.36196800	4.12243800
C	-5.14915100	0.21382000	2.78574900	C	-2.62257600	-4.82557800	1.30757800
N	1.13125600	1.77067300	0.92384200	H	-4.32417200	-3.53142300	-1.83775500
C	0.93386100	2.70890400	1.94587400	C	7.48986300	-1.05273700	1.52860000
C	-4.51411100	2.29815600	0.06825300	C	-0.97877900	-3.58865100	2.56476800
C	-6.79734100	1.56502100	0.38613900	C	1.91492600	3.65593700	2.23635600
C	-4.96361200	3.32771900	-0.74518200	C	-0.29750000	2.78110100	2.60618700
C	2.74494200	1.50733300	-3.56912300	H	1.94065600	1.22105800	-5.53473700
C	1.45351600	2.92619100	-2.09336000	H	2.72392800	-3.63678300	-0.20428900
C	-7.23969600	2.60435400	-0.42315700	H	5.20646300	-2.69457300	0.20382200
C	4.82785300	-0.42516800	2.09689500	C	-1.37733100	-4.75462900	1.92354800
C	6.81298700	-0.13179200	0.74073300	H	8.52283000	-1.29502300	1.30832900
C	1.80707900	1.70339200	-4.57379200	H	-2.92686800	-5.73099500	0.79572200
C	5.51273200	-1.35033500	2.87486000	H	0.00636000	-3.50368400	3.00671900
H	-4.24847800	4.01271000	-1.18465700	H	2.86750700	3.59265700	1.72282900
C	-6.32374400	3.48097400	-0.99231100	C	1.67531500	4.65026700	3.17754800
C	-5.07749500	-0.28962500	-2.36006000	H	2.45132300	5.37489300	3.40189300
C	-3.47793400	-3.73308700	1.34152500	C	0.45108800	4.72195000	3.82917900
C	-1.82667700	-2.48914600	2.60207900	H	-1.05049600	2.03776800	2.36862300
C	-5.39061100	-1.55988100	-1.77974800	C	-0.53303400	3.78142500	3.53539600
H	-6.30785300	-1.79635800	-1.25912200	H	0.26400400	5.50031100	4.56035000
C	-4.35792700	-2.48581800	-2.10219200	H	-1.49245400	3.82669900	4.04035700
H	-5.68447900	0.60189600	-2.30285300	H	-1.49224200	-1.55670800	3.04283700
C	0.53082000	3.12795300	-3.11096300	H	-0.70769600	-5.60621200	1.88601800
H	5.69237900	2.91676100	0.91539600	H	7.29702800	0.34423200	-0.10475100
H	3.96420800	-1.59660700	-3.84834400	H	3.78639700	-0.19078600	2.30217600
H	-0.34091500	3.74388600	-2.92448100	H	-3.45811000	2.15572800	0.26856500
C	0.70489800	2.51880300	-4.34791200	H	-6.67058900	4.28524500	-1.63069600
H	4.03709300	4.01135400	-1.02506900	H	-7.49451100	0.85458300	0.81521200
H	5.90742800	-1.31991100	-1.99555600	H	-0.02757600	2.66723400	-5.13276400
C	4.62273700	-2.60771000	-0.69971900	H	3.61693700	0.88504200	-3.72641500
H	-8.29931900	2.72247100	-0.61647900	H	1.29992300	3.32606100	-1.09893900
H	-5.71323900	0.93337400	3.35301000	H	7.36487900	-2.38761500	3.20571500
H	4.99969800	-1.82354800	3.70368600	H	-4.44738700	-3.75905700	0.85913000

2c^{Add2}:

electronic energy *E*/ a.u.	−6868.27571923
thermal enthalpy *H*/ a.u.	−6867.465505
total free Gibbs energy at 298 K *G*/ a.u.	−6867.610695

Cartesian Coordinates:

Ni	3.64477900	0.54681800	-1.12046200	C	-1.50524400	-3.05328700	1.75884500
P	1.48815300	0.76933500	-0.75352700	C	-3.37052200	-2.05445200	3.03176500
C	3.83750600	0.57796700	0.74317000	N	3.48955700	1.55158300	1.62203000
C	3.88197000	-0.41904400	-2.99786700	C	2.95504500	2.83080200	1.25300900
H	3.17120400	-1.11850600	-3.41340900	C	3.71355700	1.15753500	2.92866500
C	3.81900300	1.01616800	-3.14020600	N	-4.40397700	-1.07799800	1.37227900
H	3.06343000	1.55477700	-3.69195700	C	-5.34130100	-0.26191600	0.66240800
Ni	-2.93813100	-1.66114900	-1.03363700	C	-4.43045600	-1.27882100	2.73964800
P	-1.20769000	-0.39768700	-0.72409900	N	4.30402600	-0.42205600	1.53357500
C	-3.34462100	-1.69728500	0.80310500	C	4.82814900	-1.65722600	1.04024800
C	-2.59050200	-2.50116800	-2.93851500	C	4.23316700	-0.08450700	2.87599500
H	-1.60947300	-2.66585400	-3.35895000	N	-1.72686900	2.12904100	-0.47955200
C	-3.34844400	-3.41546400	-2.20204300	C	-1.96354600	3.44397100	-0.06604200
C	-4.53386500	-2.72908100	-1.78410100	C	3.95982100	-2.66361200	0.64514200
C	-3.35274900	-1.27855600	-3.06422500	C	6.20307200	-1.81992800	0.94760000
P	0.74610400	-1.30340100	-0.47486000	C	4.47874900	-3.84245700	0.12757900
C	-1.44815200	1.14474500	0.29997400	C	-1.41107500	-4.15112200	0.91605100
S	-1.35003700	0.92460900	1.99667100	C	-0.43235000	-2.65994900	2.54886200
P	0.25728000	-0.17446500	-2.34555400	C	6.71593200	-3.00539900	0.43711600
N	-2.72539600	-2.31621500	1.83567400	C	-4.93917900	0.97845100	0.19133300

C	-6.62761900	-0.73542800	0.44524500	C	-1.57522600	4.43816900	-0.97416800
C	-0.22168600	-4.86559300	0.86160100	C	-2.57543700	3.83689800	1.13183600
C	-5.83771800	1.75091000	-0.53104700	H	-0.13986300	-5.71884300	0.19864900
H	3.80156800	-4.62088700	-0.20440900	H	-3.01889000	-0.38992100	-3.57862100
C	5.85420800	-4.01440200	0.02170700	H	-5.35936100	-0.71223100	-2.30401200
C	5.00383200	-0.73231800	-2.22818900	C	1.91074200	5.25751800	0.46524200
C	3.73358900	3.68637500	0.48778600	H	-8.52811300	-0.31677300	-0.45494900
C	1.66436300	3.16856800	1.63532100	H	3.79555800	5.57534100	-0.52246200
C	5.60295400	0.50700700	-1.83334100	H	0.12799700	4.65281900	1.50587000
H	6.48421700	0.60262200	-1.21502200	H	-1.11360200	4.11795400	-1.90083100
C	4.93069900	1.57663100	-2.48701800	C	-1.75074500	5.78051300	-0.68322500
H	5.31782900	-1.71656600	-1.91428400	H	-1.42551900	6.53180600	-1.39512600
C	0.74521400	-3.39398900	2.50245400	C	-2.34984200	6.16443800	0.51407200
H	-5.18458600	-0.83564100	3.36556500	H	-2.87049600	3.08632900	1.85151300
H	-3.07059400	-4.42591700	-1.94538600	C	-2.76921200	5.18645600	1.40723400
H	1.58999800	-3.08676400	3.10822300	H	-2.49546000	7.21448900	0.74223300
C	0.85319000	-4.49411600	1.66013800	H	-3.24328800	5.47318600	2.34010900
H	-3.01166200	-2.44740400	3.96634400	H	1.04226500	2.45730000	2.16885800
H	-5.31825700	-3.15096500	-1.17223400	H	1.48656600	6.20075800	0.14073000
C	-4.57820100	-1.44888900	-2.41323300	H	-6.91220300	-1.71178000	0.82105300
H	7.78809100	-3.13549700	0.35032100	H	-3.93001800	1.32123000	0.37287800
H	4.55519800	-0.75863500	3.65031200	H	2.88986900	-2.51003800	0.71158800
H	-5.51986900	2.71550100	-0.90846700	H	6.25653000	-4.93281600	-0.38977100
C	-7.12671600	1.28542000	-0.76556200	H	6.85810800	-1.01241500	1.25344700
H	3.48563500	1.80144600	3.75997100	H	1.78027700	-5.05491200	1.62061600
C	3.20137200	4.90476500	0.08759100	H	-2.26483900	-4.43531800	0.31493800
H	5.17119000	2.62625500	-2.41609900	H	-0.51289400	-1.75810600	3.14335300
C	-7.52344800	0.04646100	-0.27308400	H	-7.82520200	1.88936900	-1.33322700
C	1.14693000	4.39495600	1.24204900	H	4.73274400	3.38463800	0.19768600

(*E*)-2c^{Ins1}:

electronic energy *E*/ a.u.	−6868.27175336
thermal enthalpy *H*/ a.u.	−6867.461189
total free Gibbs energy at 298 K *G*/ a.u.	−6867.607389

Cartesian Coordinates:

Ni	-4.29601900	0.13388600	-0.68372200	C	4.96607800	1.42009700	-2.27712300
P	-2.80699400	0.91889900	0.77604700	N	-6.18304800	-0.50979700	1.38571900
C	-5.05453200	-0.85530400	0.71467500	C	-6.94048300	0.66913000	1.10778700
C	-4.43577700	1.62664600	-2.18545400	C	-6.50010100	-1.43472500	2.36646700
H	-4.19267900	2.66492100	-2.01711800	N	2.49803700	1.56029500	0.19342200
C	-3.49306500	0.60428300	-2.56935600	C	2.15089000	2.90588300	0.02089700
H	-2.44236600	0.76843700	-2.75734700	C	-6.36099400	1.91303000	1.31476700
Ni	4.30255300	-1.38179200	0.60868400	C	-8.22564400	0.54764900	0.60056100
P	0.03759800	1.12241100	1.52202600	C	-7.08146000	3.05370400	0.99159000
C	4.38987700	-0.25181300	-0.87201400	C	3.07197800	-2.63852800	-2.49802600
C	4.49011400	-3.11002300	1.79102300	C	1.35064800	-0.95141800	-2.30793800
H	3.64094700	-3.62463900	2.21636700	C	-8.94344900	1.69558300	0.28844400
C	5.08585400	-3.37970500	0.54878400	C	5.59174300	1.71837900	1.16578700
C	6.08489200	-2.38472000	0.36144700	C	7.45437500	1.37374800	-0.33928800
C	5.23480100	-2.06133500	2.44658800	C	2.10034700	-3.59860000	-2.74115900
P	-1.03424700	1.65782200	-0.36536000	C	6.47172700	2.17284700	2.13695500
C	1.75850900	0.73388700	0.82897900	H	-6.63185900	4.02817700	1.13945100
S	2.24494400	-0.89406800	1.23412800	C	-8.36915400	2.94687600	0.47706500
P	-1.08267100	-0.40344200	0.37698900	C	-5.69627900	1.03561500	-2.06665500
N	3.68397800	-0.33596000	-2.02019900	C	-3.34811300	-3.22339400	-0.34446500
C	2.68545700	-1.32354300	-2.28285000	C	-2.54314100	-3.00476000	1.92332700
C	4.00868500	0.69475700	-2.88663700	C	-5.52561700	-0.36590300	-2.29477800
N	-4.67604800	-2.01950600	1.30032400	H	-6.31422900	-1.10416500	-2.25436100
C	-3.50919800	-2.76800800	0.95515700	C	-4.18408400	-0.60774200	-2.70976800
C	-5.54675100	-2.38395200	2.31548300	H	-6.61183300	1.52323500	-1.76675800
N	5.20038900	0.81566900	-1.05456600	C	0.38353000	-1.91708800	-2.55145100
C	6.09547500	1.31886600	-0.06449700	H	5.48325700	2.31371100	-2.57955000

H	4.76676000	-4.11690600	-0.17158600	H	-2.04895800	-4.24979300	-1.70081900
H	-0.66369900	-1.63940400	-2.52881600	H	-0.61021300	-3.84024000	2.31529400
C	0.75822600	-3.23626200	-2.77186200	H	2.10911500	2.75266300	-2.11171700
H	3.53457800	0.80241800	-3.84648800	C	1.71461600	4.76708700	-1.45529600
H	6.71627200	-2.28036500	-0.50963400	H	1.58482300	5.15180900	-2.46112500
C	6.23868400	-1.64154200	1.58420300	C	1.58796100	5.62057500	-0.36393600
H	-9.94472000	1.60979900	-0.11688300	H	2.17093700	3.37368700	2.11491900
H	-7.35797900	-1.31885600	3.00556300	C	1.75370200	5.11424400	0.91892800
H	6.08699500	2.48361800	3.10115100	H	1.36740100	6.67108900	-0.51381700
C	7.83691700	2.23051900	1.87730800	H	1.66281800	5.77039400	1.77766200
H	-5.40557100	-3.28425200	2.88757000	H	-2.67292300	-2.60424300	2.92204800
C	-2.18644300	-3.90252100	-0.68345100	H	-0.28191200	-4.62807500	-0.00731700
H	-3.76062300	-1.55633500	-3.00241500	H	7.82312200	1.03706300	-1.30173700
C	8.32727700	1.83550600	0.63825100	H	4.52311700	1.66089400	1.33161200
C	-1.38655700	-3.68989000	1.57541600	H	-5.35388700	1.97474100	1.71083200
C	2.00469300	3.42450500	-1.26780500	H	-8.92558900	3.84134900	0.22213600
C	2.03529600	3.76891300	1.11397600	H	-8.64629900	-0.43686500	0.43092900
H	2.39078300	-4.62927000	-2.90919800	H	0.00201700	-3.98934600	-2.96230500
H	5.00555600	-1.64859400	3.41719400	H	4.12367200	-2.89531800	-2.46353100
H	6.94615700	-0.84346200	1.75221400	H	1.07348700	0.07366100	-2.09011800
C	-1.20264700	-4.12952100	0.27069600	H	8.52047100	2.58403100	2.64064300
H	9.39090400	1.87671100	0.43466300	H	-4.12153900	-3.02828500	-1.07558200

(*Z*)-2c^{Ins1}:

electronic energy *E*/ a.u.	−6868.27110289
thermal enthalpy *H*/ a.u.	−6867.460233
total free Gibbs energy at 298 K *G*/ a.u.	−6867.603407

Cartesian Coordinates:

Ni	-3.83961900	-0.12536400	0.66984900	C	4.01579700	-0.62619500	-2.90291200
P	-2.63099800	-0.73992200	-1.10118900	C	-6.17801300	-1.43585800	-1.41239500
C	-4.77282800	1.14874700	-0.32810300	C	-7.92010500	-0.35369000	-0.13215800
C	-3.12293800	-1.57978800	1.96353800	C	-6.86717000	-2.63677700	-1.31792900
H	-2.35223300	-2.28694000	1.69576800	C	1.56337600	-3.19426800	1.82030100
C	-2.89607200	-0.32035800	2.60261500	C	1.74927900	-3.48751500	-0.57318600
H	-1.93276800	0.10310200	2.84760500	C	-8.60806100	-1.55754400	-0.05234800
Ni	2.50350900	0.40879300	1.04354100	C	5.65461700	1.32409400	0.00011500
P	0.06307300	-0.83018600	-2.33921000	C	6.49370300	0.58062600	2.14545300
C	3.71438800	-1.00169700	0.76981700	C	0.35883500	-3.88187600	1.81032500
C	0.83340700	1.33518900	2.01887700	C	6.29873500	2.53968100	0.18177800
H	-0.09987700	1.48647200	1.49965800	H	-6.45194200	-3.52506200	-1.77892600
C	1.19483200	0.20956000	2.75287500	C	-8.07897700	-2.70040300	-0.63959000
C	2.58051300	0.36602100	3.09005200	C	-4.52726500	-1.80386400	1.86295000
C	1.95592000	2.24269000	1.99059300	C	-2.75853400	3.10379700	0.94673600
P	-0.60182800	-0.95008100	-0.23182900	C	-2.68955300	3.88270500	-1.33671700
C	1.83775900	-0.26331400	-2.09253500	C	-5.15606900	-0.62721100	2.28436700
S	2.25497400	1.12293500	-1.05819200	H	-6.21946100	-0.43776200	2.28335200
P	-1.05604200	0.83890900	-1.36111000	C	-4.14755500	0.28718600	2.75493100
N	3.51306100	-2.33501100	0.65080200	H	-5.00788400	-2.67329900	1.44090200
C	2.24357100	-2.99879900	0.62616300	C	0.54628800	-4.18307400	-0.57339100
C	4.71226600	-3.03087800	0.65497000	H	6.76044500	-2.20757600	0.78348100
N	-4.51350500	2.45066500	-0.62437100	H	0.58839700	-0.66786600	2.91477700
C	-3.30757300	3.15692700	-0.32569500	H	0.13813400	-4.54261500	-1.50989700
C	-5.55828000	3.02471900	-1.33417400	C	-0.14782100	-4.37810400	0.61365600
N	5.06350600	-0.88083800	0.83533100	H	4.74575700	-4.10228800	0.56152900
C	5.75401000	0.36048800	0.99148700	H	3.17466200	-0.34354900	3.64943400
C	5.68894600	-2.11176000	0.77115300	C	3.00538000	1.68221600	2.72085600
N	-5.99959000	0.93400700	-0.87358900	H	-9.55181500	-1.60374600	0.47814400
C	-6.70883800	-0.30496100	-0.80818900	H	-7.45227200	2.08610900	-1.97857800
C	-6.49491700	2.07213600	-1.48769600	H	6.21845300	3.30107100	-0.58488100
N	2.64790300	-0.92836600	-2.82138900	C	7.03946000	2.77886600	1.33368800

H	-5.53670100	4.05437200	-1.64505800	C	6.75871900	-0.12006600	-3.14962500
C	-1.56532200	3.76678400	1.20001300	H	3.74168400	1.28408000	-3.83776600
H	-4.34690800	1.25692800	3.18726100	C	5.82726500	0.80413100	-3.61362700
C	7.14250000	1.79722400	2.31289500	H	7.82017000	0.07804000	-3.24219700
C	-1.50205700	4.54867000	-1.07216500	H	6.16304000	1.72882900	-4.07042000
C	4.95128200	-1.56511000	-2.47383600	H	-3.10937800	3.88261000	-2.33586300
C	4.46793100	0.56019100	-3.48935400	H	0.00803100	4.98313400	0.39024600
H	-0.18538700	-4.02763000	2.73616400	H	6.53913400	-0.18600200	2.91083500
H	1.96979400	3.19053400	1.47276200	H	5.06076000	1.12721300	-0.88358700
H	3.99067500	2.09934000	2.86508000	H	-5.22756100	-1.37556400	-1.92993000
C	-0.93246300	4.48292800	0.19266100	H	-8.61129900	-3.64177900	-0.56832200
H	7.71566200	1.98176700	3.21395500	H	-8.30631300	0.54123800	0.34277100
H	-1.12390100	3.71275900	2.18818400	H	-1.09412000	-4.90642800	0.60503700
H	-1.00444200	5.09069300	-1.86707900	H	1.97949600	-2.80179500	2.74028900
H	4.60134100	-2.49796700	-2.04833700	H	2.27551500	-3.28372300	-1.49863200
C	6.31143900	-1.30546400	-2.58125300	H	7.53802400	3.73170800	1.47001200
H	7.02470100	-2.04289900	-2.22837500	H	-3.25969000	2.54554200	1.72343000

2c^{Ins2}:

electronic energy *E*/ a.u.	−6868.26931825
thermal enthalpy *H*/ a.u.	−6867.458543
total free Gibbs energy at 298 K *G*/ a.u.	−6867.604613

Cartesian Coordinates:

Ni	4.58429300	0.41151500	-1.01595200	C	8.89300500	-2.05900100	-0.46661800
P	2.88055500	-0.48946400	0.09621400	C	-4.95344000	2.51385500	-1.66182300
C	5.36949700	0.79508200	0.63563900	C	-7.23836800	2.49599800	-0.86568500
C	4.53312900	-0.55958500	-2.89429600	C	-4.09696800	-2.81418000	3.73515100
H	4.05769600	-1.51566600	-3.05353900	C	-5.39309800	3.02675400	-2.87489900
C	3.86926400	0.71965300	-2.97110500	H	6.25349400	-4.18826000	-0.39721500
H	2.82716800	0.86890300	-3.21242000	C	8.15237500	-3.21718100	-0.66960800
Ni	-4.49419500	-0.78717100	-0.54625000	C	5.87894900	-0.33853400	-2.58361500
P	0.01505300	-0.57331000	0.59779700	C	4.10168000	3.60763700	0.32385600
C	-4.84483600	0.51949900	0.75902000	C	3.09295600	2.84133800	2.38170200
C	-4.98459500	-2.73095900	-1.41323100	C	6.03248300	1.06542300	-2.37373500
H	-4.37866800	-3.61544300	-1.28675900	H	6.95466700	1.55704300	-2.09675000
C	-6.04381400	-2.33484400	-0.60862700	C	4.81344300	1.72232700	-2.71745300
C	-6.46027900	-1.04294400	-1.07997300	H	6.63886200	-1.09070800	-2.43253900
C	-4.79193900	-1.73372900	-2.44025400	C	-2.06778200	-1.52534000	3.90956600
P	1.16123100	-0.69687600	-1.30152300	H	-5.94366200	3.40986500	1.82794300
C	-1.69573400	0.02069200	0.03500500	H	-6.42422000	-2.84967800	0.26026400
S	-2.00701700	1.67845700	0.19454400	H	-1.03566500	-1.43357000	4.22483600
P	1.31598300	1.09532300	-0.05354200	C	-2.78558700	-2.68471100	4.18038900
N	-4.59859100	0.46223600	2.08661800	H	-4.83994400	1.77704300	3.77779000
C	-3.97146500	-0.62501500	2.77048600	H	-7.26184800	-0.45274500	-0.66053400
C	-4.98543500	1.62990900	2.72216200	C	-5.76794200	-0.74540000	-2.29060600
N	5.10584400	1.76302800	1.54911700	H	9.91933900	-2.00015000	-0.80932000
C	4.08717700	2.75533800	1.41716800	H	7.52793000	0.16921000	3.02705600
C	5.93484000	1.65784300	2.65504600	H	-4.67130300	3.23417900	-3.65628400
N	-5.45395700	1.71719200	0.58557500	C	-6.74477800	3.27267500	-3.08863200
C	-5.88605700	2.24996300	-0.66880600	H	5.87350600	2.34841400	3.47788700
C	-5.52739300	2.41917900	1.77640500	C	3.09231000	4.54994600	0.18657400
N	6.38518600	0.09095500	1.19756400	H	4.63115900	2.78590200	-2.71305300
C	6.99425500	-1.04701700	0.58638600	C	-7.66744700	3.00980200	-2.08283300
C	6.74505200	0.60602600	2.43194400	C	2.09295300	3.79379900	2.24116500
N	-2.58319400	-0.90250600	-0.28657900	C	-1.60866800	-2.64053900	-1.70284300
C	-2.11349600	-2.24385600	-0.46753300	C	-2.23761700	-3.17709800	0.55571700
C	6.24614000	-2.20081600	0.39780200	H	-4.65298500	-3.72251500	3.93557100
C	8.31179000	-0.96456700	0.16116000	H	-4.03548600	-1.77773000	-3.20896300
C	6.83221700	-3.28656800	-0.23669200	H	-5.89990000	0.13707500	-2.89666700
C	-4.69630100	-1.78087400	3.02619200	C	2.08939700	4.64452600	1.14296700
C	-2.66181700	-0.48516600	3.20691400	H	-8.72230400	3.19591400	-2.24688500

H	3.08679400	5.20821800	-0.67403500	H	1.29304600	5.36910000	1.02385200
H	1.29747800	3.84785700	2.97422800	H	-7.94697000	2.26925800	-0.07658300
H	-1.51958600	-1.90390700	-2.49273800	H	-3.90632200	2.30653000	-1.46564800
C	-1.23004200	-3.95942800	-1.91027000	H	5.21510100	-2.22922100	0.73162700
H	-0.83265800	-4.25779900	-2.87388800	H	8.60390700	-4.06739000	-1.16751100
C	-1.35636300	-4.89277900	-0.88760900	H	8.86280700	-0.04160800	0.30098300
H	-2.64415500	-2.86074300	1.50575600	H	-2.31685100	-3.49622800	4.72477400
C	-1.85844900	-4.49523900	0.34657000	H	-5.71369400	-1.86271600	2.66333400
H	-1.06381400	-5.92362600	-1.05162500	H	-2.11582200	0.41822700	2.96032700
H	-1.95565900	-5.21503600	1.15192600	H	-7.08096200	3.67099600	-4.03910900
H	3.08052600	2.13615100	3.20463100	H	4.88992700	3.51512400	-0.41150100

TS 2c^{Add1} → 2a^{Ph}:

electronic energy *E*/ a.u.	−4189.65803101
thermal enthalpy *H*/ a.u.	−4188.844993
total free Gibbs energy at 298 K *G*/ a.u.	−4188.989059

Cartesian Coordinates:

Ni	-3.64408300	-0.74265300	-0.15846800	C	-7.54371100	0.65543900	-3.26941200
P	-1.96837900	0.47471800	-1.04612500	C	-5.43363200	-2.01833000	-0.60389200
C	-4.27243400	0.85754500	0.61589000	C	-2.87597900	-0.22466300	3.13749900
C	-4.44414200	-2.31755400	-1.53818100	C	-1.84305300	1.96231000	2.99133600
H	-4.50923000	-2.18251900	-2.60850400	C	-4.89444100	-2.27090500	0.71388600
C	-3.26856900	-2.71592600	-0.80931500	H	-5.43916100	-2.14712400	1.64139200
H	-2.33473500	-3.03891000	-1.24885200	C	-3.59283400	-2.79475400	0.57408400
Ni	2.90111000	-0.76740000	0.66285900	H	-6.41540700	-1.61578100	-0.81410800
P	1.57875200	0.02391500	-0.98971000	C	-0.31646300	-4.96709300	-0.79552000
C	3.54686500	-2.12827900	-0.47995400	H	5.73449900	-3.34034600	-2.59940600
C	2.40571100	0.43746700	2.35814300	H	1.91866700	-1.51426400	3.30719300
H	1.47859800	0.98756300	2.42696000	H	-0.99141300	-5.44946600	-1.49475800
C	2.64879700	-0.86336800	2.84703400	C	-0.67929300	-4.82686800	0.54108900
C	3.96401300	-1.20502300	2.43985800	H	3.55697100	-4.98079300	-2.09992800
C	3.63766500	0.97804500	1.83190100	H	4.46048100	-2.15160400	2.61340300
P	-0.40637800	-1.09429200	-1.36308300	C	4.59969100	-0.02293700	1.88904700
C	1.56829200	1.85629500	-0.73603400	H	-9.24226700	0.71356200	-1.94571200
S	0.35314300	2.47846700	0.35905400	H	-6.22991100	3.49312100	0.67012400
P	-0.45450500	0.03370100	0.47954400	H	5.81519100	2.32763400	-1.79951400
N	3.00463100	-3.32808700	-0.81794400	C	7.44949000	1.10231000	-1.10032800
C	1.75513800	-3.83607000	-0.34955300	H	-4.43142900	3.32010700	2.77805400
C	3.80932300	-4.00211400	-1.72744000	C	-1.86493000	-0.63724500	3.99669300
N	-3.87761000	1.50785600	1.74138200	H	-2.91491400	-3.07514200	1.36776000
C	-2.84943700	1.07176700	2.63278300	C	7.84985300	-0.18064600	-0.73296500
C	-4.60613200	2.67331900	1.93436900	C	-0.84287000	1.54247300	3.86254200
N	4.70056100	-2.07166500	-1.19153800	C	3.97650500	4.24210200	-0.48141800
C	5.62888700	-0.98194500	-1.17403800	C	1.86196400	4.80278000	-1.49734500
C	4.87660500	-3.21191400	-1.96036600	H	-0.09666200	-4.06441100	2.46929300
N	-5.26969700	1.63786400	0.12000300	H	3.74123900	1.96213400	1.39683200
C	-6.03729100	1.32837300	-1.04471500	H	5.61234700	0.03153800	1.51437600
C	-5.48731300	2.75242400	0.91633600	C	-0.84862200	0.24319800	4.36104400
N	2.55774200	2.46147300	-1.28933900	H	8.86992900	-0.36511500	-0.41231100
C	2.77722600	3.83105100	-1.07509100	H	-1.87493900	-1.65010500	4.38647000
C	-5.40334400	1.16391800	-2.27135600	H	-0.04435900	2.22804300	4.12499400
C	-7.41440400	1.17552500	-0.91854000	H	4.68784900	3.48628300	-0.16149800
C	-6.16490800	0.81914400	-3.38255200	C	4.24582200	5.59397500	-0.29554600
C	1.40927200	-3.70315100	0.98991700	H	5.17535300	5.89519400	0.17904500
C	0.89648200	-4.46166800	-1.24926000	C	3.33319700	6.55691400	-0.71803100
C	-8.16887600	0.84101600	-2.03920200	H	0.93410600	4.48405700	-1.95983800
C	5.21769500	0.29166600	-1.55082100	C	2.14442700	6.15237600	-1.32187800
C	6.93674500	-1.22999300	-0.76756200	H	3.54526000	7.61233100	-0.57835700
C	0.18090300	-4.18557600	1.42726900	H	1.42554600	6.89493700	-1.65584800
C	6.13825300	1.33357600	-1.50898100	H	-1.81519000	2.95582400	2.55587900
H	-5.67604400	0.68183200	-4.34127800	H	-0.05706700	-0.08294300	5.02796400

H	7.22557800	-2.23148500	-0.46310300	H	-1.63610400	-5.20643200	0.88377700
H	4.19301500	0.48612000	-1.84932800	H	2.09310400	-3.21145000	1.66929200
H	-4.32874200	1.29341100	-2.34333600	H	1.15632000	-4.52000800	-2.30099900
H	-8.13128300	0.38559500	-4.14101000	H	8.16182700	1.92048900	-1.07000400
H	-7.88287200	1.29518600	0.05341000	H	-3.66981200	-0.89770300	2.83779200

TS 2c^{Add2} → 2b^{Ph}:

electronic energy *E*/ a.u.	− 4189.66462650
thermal enthalpy *H*/ a.u.	− 4188.844993
total free Gibbs energy at 298 K *G*/ a.u.	− 4188.989059

Cartesian Coordinates:

Ni	-3.25989000	-0.61145000	0.57323400	H	-5.41163700	-2.31617400	1.44057600
P	-1.67892600	0.54096700	-0.54874200	C	-4.44283300	-0.56444900	2.46312600
C	-4.35966700	-0.46805600	-0.93253600	H	-2.94343100	-3.38399000	1.37760000
C	-2.32914200	-1.44389000	2.29841600	C	0.32532300	-4.45963600	1.11665400
H	-1.25751600	-1.54466400	2.39239600	H	5.92275900	-3.30266800	-2.02367800
C	-3.10052900	-0.31066200	2.75012900	H	5.20157300	-0.63240900	2.95671700
H	-2.69004000	0.58907000	3.18675400	H	-0.41367500	-5.13496100	0.69776000
Ni	3.44054700	0.05284400	0.79123300	C	0.13977300	-3.92447000	2.38751600
P	1.75842900	0.32262300	-0.67205300	H	3.97676600	-4.78009600	-0.71804900
C	3.99718000	-1.57756300	-0.00680600	H	6.24060400	0.96112100	1.03878200
C	3.43101200	0.72066200	2.87622300	C	4.32471200	2.05527300	1.18628700
H	2.74757500	0.30581000	3.60342000	H	-5.17772600	-5.93836600	-0.90442600
C	4.69298000	0.20993300	2.50501200	H	-5.94480800	-1.66409000	-3.54230600
C	5.27092400	1.08863600	1.49978000	H	5.67337700	2.45842500	-2.67115900
C	3.14411800	1.77321200	1.96945600	C	7.50036000	1.47830000	-2.05809900
P	-0.11158600	-1.04780700	-0.47833100	H	-6.37949900	1.03353900	-3.02912700
C	1.44473300	2.13512100	-0.90967600	C	-5.53527000	3.41433200	0.98092700
S	2.34773000	3.00164800	-2.03849700	H	-5.27393500	0.10546600	2.63046600
P	-0.01297300	0.65313000	0.88717400	C	8.05659800	0.32614300	-1.50628400
N	3.49991900	-2.83791900	0.10751100	C	-3.88684200	4.05716800	-0.66400800
C	2.36921100	-3.21486100	0.89460100	C	-0.14261000	4.76635200	-0.79982700
C	4.20722500	-3.72827000	-0.68984700	C	-0.70011800	3.96001000	1.40751400
N	-5.03495600	0.61135900	-1.39274900	H	0.93328900	-2.60909200	3.89474200
C	-4.93890000	1.90685400	-0.78517700	H	2.22989200	2.35015100	1.93255400
C	-5.78156600	0.29704500	-2.51820000	H	4.38888000	2.80702200	0.41197800
N	5.02106900	-1.70235900	-0.88888400	C	-4.62681200	4.34358500	0.47941900
C	5.86080000	-0.62693800	-1.32206000	H	9.12856100	0.25365500	-1.35436800
C	5.16517400	-3.01336400	-1.31434300	H	-6.11074100	3.63860700	1.87329300
N	-4.70011500	-1.46662300	-1.78606600	H	-3.15460400	4.76818900	-1.02945700
C	-4.18714400	-2.79545700	-1.67186200	H	0.33572000	4.61673000	-1.75846100
C	-5.57477600	-1.01585200	-2.76513100	C	-0.78703100	5.96422900	-0.50534900
N	0.54261800	2.50681200	-0.00833400	H	-0.81161900	6.74779200	-1.25723400
C	-0.07757900	3.75209700	0.16685900	C	-1.38926600	6.17074900	0.73407000
C	-2.82573500	-3.00905900	-1.85396200	H	-0.65820900	3.17235400	2.15393400
C	-5.04211900	-3.83970100	-1.33728900	C	-1.34865100	5.15537600	1.68705800
C	-2.30973900	-4.28776900	-1.67884300	H	-1.88069200	7.11353100	0.95503400
C	2.20224100	-2.68671900	2.17009600	H	-1.81742400	5.29614200	2.65646200
C	1.43780800	-4.10244300	0.36277500	H	-3.44686500	2.57868300	-2.17419100
C	-4.51875600	-5.11917400	-1.17270000	H	-4.47818600	5.29098700	0.98706800
C	5.29575000	0.50744000	-1.89306900	H	7.65049200	-1.62160400	-0.66514000
C	7.23516000	-0.73214000	-1.12916300	H	4.22313900	0.58810600	-2.03425700
C	1.07746600	-3.03670500	2.90799100	H	-2.17882500	-2.17626100	-2.10686600
C	6.12364100	1.56603600	-2.24959700	H	-2.74842500	-6.34056200	-1.20131900
H	-1.24481300	-4.45013600	-1.80848800	H	-6.09887300	-3.64363500	-1.18543500
C	-3.15345200	-5.34253800	-1.33696700	H	-0.74348400	-4.18172100	2.96282400
C	-3.21470600	-2.42893500	1.80667600	H	2.93740300	-1.99453400	2.56111200
C	-5.69176300	2.18468400	0.34953600	H	1.55882300	-4.47464200	-0.64945100
C	-4.04602500	2.83557100	-1.30799300	H	8.14196700	2.30763900	-2.33801700
C	-4.50766700	-1.84429700	1.80403000	H	-6.37271700	1.43341800	0.73552100

References

1 a) SCALE3ABS, CrysAlisPro, Aglient Technologies Inc., Oxford, UK, **2015**; b) G. M. Sheldrick, SADABS, Bruker AXS, Madison, USA, **2007**.

2 a) R. C. Clark, J. S. Reid, *Acta Crystallogr. A* **1995**, *51*, 887; b) CrysAlisPro, Agilent Technologies Inc., Oxford, UK, 2015.

3 G. M. Sheldrick, *Acta Crystallogr. Sect. Found. Adv.* **2015**, *71*, 3.

4 G. M. Sheldrick, *Acta Crystallogr. A* **2008**, *64*, 112.

5 Gaussian 09, Revision D.01, M. J. Frisch, G. W. Trucks, H. B. Schlegel, G. E. Scuseria, M. A. Robb, J. R. Cheeseman, G. Scalmani, V. Barone, B. Mennucci, G. A. Petersson, H. Nakatsuji, M. Caricato, X. Li, H. P. Hratchian, A. F. Izmaylov, J. Bloino, G. Zheng, J. L. Sonnenberg, M. Hada, M. Ehara, K. Toyota, R. Fukuda, J. Hasegawa, M. Ishida, T. Nakajima, Y. Honda, O. Kitao, H. Nakai, T. Vreven, J. A. Montgomery, Jr., J. E. Peralta, F. Ogliaro, M. Bearpark, J. J. Heyd, E. Brothers, K. N. Kudin, V. N. Staroverov, T. Keith, R. Kobayashi, J. Normand, K. Raghavachari, A. Rendell, J. C. Burant, S. S. Iyengar, J. Tomasi, M. Cossi, N. Rega, J. M. Millam, M. Klene, J. E. Knox, J. B. Cross, V. Bakken, C. Adamo, J. Jaramillo, R. Gomperts, R. E. Stratmann, O. Yazyev, A. J. Austin, R. Cammi, C. Pomelli, J. W. Ochterski, R. L. Martin, K. Morokuma, V. G. Zakrzewski, G. A. Voth, P. Salvador, J. J. Dannenberg, S. Dapprich, A. D. Daniels, O. Farkas, J. B. Foresman, J. V. Ortiz, J. Cioslowski, D. J. Fox, Gaussian, Inc., Wallingford CT, 2013.

6 J.–Da. Chai, M. Head-Gordon, *Phys. Chem. Chem. Phys.* **2008**, *10*, 6615−6620.

7 a) R. Ditchfield, W. J. Hehre, J. A. Pople, *J. Chem. Phys.* **1971**, *54*, 724−728; b) W. J. Hehre, R. Ditchfield, J. A. Pople, *J. Chem. Phys.* **1972**, *56*, 2257−2261; c) P. C. Hariharan, J. A. Pople, *Theor. Chem. Acc.* **1973**, *28*, 213−222; d) P. C. Hariharan, J. A. Pople, *Mol. Phys.* **1974**, *27*, 209−214; e) M. S. Gordon, *Chem. Phys. Lett.* **1980**, *76*, 163−168; f) M. M. Francl, W. J. Pietro, W. J. Hehre, J. S. Binkley, D. J. DeFrees, J. A. Pople, M. S. Gordon, *J. Chem. Phys.* **1982**, *77*, 3654−3665; g) R. C. Binning Jr., L. A. Curtiss, *J. Comp. Chem.* **1990**, *11*, 1206−1216; h) J.-P. Blaudeau, M. P. McGrath, L. A. Curtiss, L. Radom, *J. Chem. Phys.* **1997**, *107*, 5016−5021; i) V. A. Rassolov, J. A. Pople, M. A. Ratner, T. L. Windus, *J. Chem. Phys.* **1998**, *109*, 1223−1229; j) V. A. Rassolov, M. A. Ratner, J. A. Pople, P. C. Redfern, L. A. Curtiss, *J. Comp. Chem.* **2001**, *22*, 976−984; k) T. Clark, J. Chandrasekhar, G. W. Spitznagel, P. v. R. Schleyer, *J. Comp. Chem.* **1983**, *4*, 294−301.

8 a) C. Peng and H. B. Schlegel, *Israel J. of Chem.* **1993**, *33*, 449; b) C. Peng, P. Y. Ayala, H. B. Schlegel, M. J. Frisch, *J. Comp. Chem.* **1996**, ***17***, 49.

9 a) P. J. Hay, W. R. Wadt, *J. Chem. Phys.* **1985**, *82*, 270−283; b) P. J. Hay, W. R. Wadt, *J. Chem. Phys.* **1985**, *82*, 299−310.

6 Synthesis and Structural Characterization of Iron(II), Cobalt(II), and Nickel(II) Complexes of a Cyclic (Alkyl)(amino)carbene[a]

Stefan Pelties and Robert Wolf

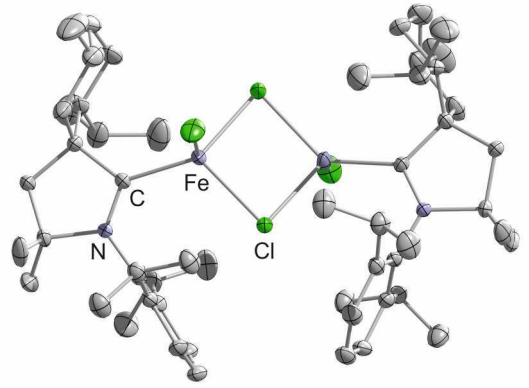

[a] Reproduced with permission from S. Pelties, R. Wolf, *Z. Anorg. Allg. Chem.* **2013**, *639*, 2581−2585.

6.1 Introduction

N-heterocyclic carbene (NHC) complexes of late transition metals are attracting tremendous interest in organometallic chemistry due to their widespread applications in homogeneous catalysis.[1] Furthermore, the strong electron-donating properties and the adjustable steric demand of NHCs enable the stabilization of unusual coordination environments.[2] While many past efforts have been devoted to the second and third row metals, first row metal NHC complexes are increasingly attracting attention. A number of recent reports describe the synthesis of imidazolin-2-ylidene and imidazolidin-2-ylidene complexes with the iron group metals.[3,4] In addition, NHCs have recently been shown to mediate the formation of unprecedented metal-metal bonded iron clusters via the NHC-induced aggregation of bis(cyclooctatetraene)iron [$Fe(cot)_2$].[5]

In 2005, Bertrand and co-workers introduced cyclic (alkyl)(amino)carbenes (CAACs, Figure 1) as a new type of carbene ligand with flexible steric properties and a higher σ-donating character compared to the well-established cyclic diaminocarbenes.[6] A selection of known CAACs is displayed in Figure 1. These have been used for the activation of small molecules such as CO, H_2, NH_3 and P_4, and the synthesis of novel transition metal catalysts.[6,7] Complexes of cyclic (alkyl)(amino)carbenes with palladium(II), ruthenium(II), rhodium(I), iridium(I), and gold(I) and even gold(0) have been reported, showing their aptitude as ligands for electron-rich, noble metals.[8]

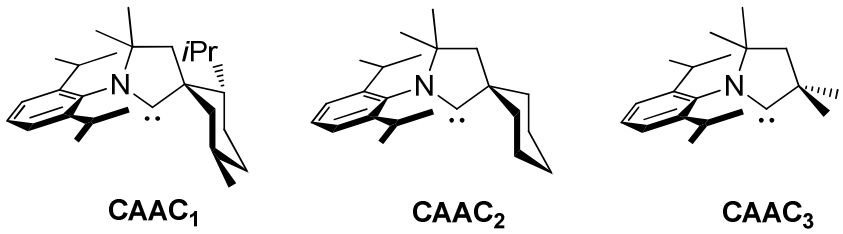

Figure 1. Examples of CAACs with varying steric properties.[6,7]

However, there is still a paucity of first-row metal complexes. A dinuclear copper(I) hydride complex [Cu(μ-H)($CAAC_1$)]$_2$ was prepared by Bertrand *et al.*, while Roesky *et al.* very recently described the synthesis of manganese(II) and zinc(II) chloride adducts [$MCl_2(CAAC_3)$] (M = Mn, Zn) and remarkable two-coordinate bis(carbene) compounds [$M(CAAC_3)_2$], with manganese and zinc in the formal oxidation state zero.[9,10] The latter complexes are particularly noteworthy. According to DFT calculations, [$Zn(CAAC_3)_2$] shows significant singlet biradicaloid character. It reacts with CO_2 to form the adduct $CAAC{\cdot}CO_2$ under mild conditions. In a similar vein, [$Mn(CAAC_3)_2$] is able to add H_2 to the carbene carbon atoms as a consequence of the pronounced radical character of the carbene ligands, thereby forming a two-coordinate mangneses(II) bis(alkyl) complex.

We recently reported on the chemistry of ruthenium(II) NHC complexes.[11] In the context of our on-going investigations of low-valent 3d metal polyarene metalates and polyhydrides,[12] we

became interested in using carbenes as supporting ligands for 3d metal complexes. Here, we report the synthesis and structural characterization of novel iron, cobalt and nickel complexes with the sterically demanding, menthyl-substituted cyclic (alkyl)(amino)carbene ligand $CAAC_1$.

6.2 Results and Discussion

[FeCl(μ-Cl)(CAAC$_1$)]$_2$ (**1**), [CoBr(μ-Br)(CAAC$_1$)]$_2$ (**2**), and [NiBr(μ-Br)(CAAC$_1$)]$_2$ (**3**) are accessible according to Scheme 1 by reacting one equivalent of Bertrand's bulky menthyl- and diisopropylphenyl-substituted CAAC$_1$ with one equiv. of $FeCl_2(thf)_{1.5}$, $CoBr_2$, and $NiBr_2(dme)$ in THF. Yellow **1**, blue **2**, and green **3** crystallized in moderate yields of 20–50% from toluene/*n*-hexane mixtures. The isolated crystals dissolve well in dry THF, but are poorly soluble in *n*-hexane, diethyl ether, benzene, and toluene. The compounds are highly air-sensitive, but appear to be stable at ambient temperature for weeks when stored as solids under an inert atmosphere.

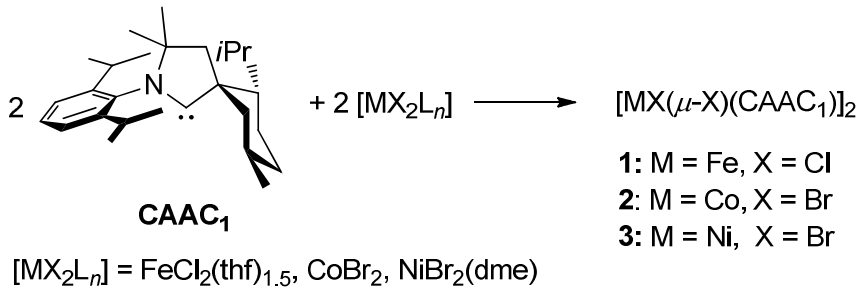

Scheme 1. Synthesis of CAAC complexes **1**–**3**.

Single-crystal X-ray structure determinations of **1**–**3** revealed dimeric halide-bridged structures (Figure 2), in which two MX$_2$(CAAC$_1$) fragments are associated through bridging chloride or bromide ligands. Complexes **1** and **3** are isomorphous and crystallized in the tetragonal crystal system in the chiral space group $P4_22_12_1$ with four molecules in the unit cell. Each molecule resides on a crystallographic 4_2 screw axis. Complex **2** crystallized as a toluene solvate in space group $P2_1$ with two molecules in the unit cell. Each molecule resides on a general position. Both halves of the molecule show practically identical bond lengths and angles. A noteworthy difference between the structures of **1** and **3** on the one hand, and that of **2** on the other hand, is the relative orientation of the substituents on the two carbene ligands. Identical substituents are located on the same side of the molecule in **1** and **3**, but they show opposite orientations in **2**. The observation of such "pseudo-rotamers" in the solid-state structures of **1**–**3** may presumably be attributed to crystal packing forces, since we expect the relative energies between the different conformations in the dimers **1**–**3** to be low. Note that **2** crystallized in a different crystal system than **1** and **3** due to the presence of solvent molecules in the lattice (Table 2).

Important bond lengths and angles of **1**–**3** are summarized in Table 1. In each structure, the metal atoms are surrounded by three halide ligands and one CAAC ligand in a distorted tetrahedral fashion. The metal carbon distances are similar in the structures of **1** and **2**, but they are about 0.1 Å shorter in the structure of **3** in agreement with the smaller atomic radius of nickel. The nickel bromine distances are also slightly shorter by about 0.05 Å in **3** compared to the cobalt bromine bonds in **2**. As expected, the metal halide distances to the terminal halide ligands Cl1 and Br1 are

substantially shorter than those of the bridging halides. The metal-metal distances are large for all three structures (**1**: Fe1–Fe1' 3.318(1) Å, **2**: Co1–Co2: 3.581(1) Å, **3**: Ni1–Ni1' 3.366(1) Å), which indicates that there is no significant metal-metal bonding.

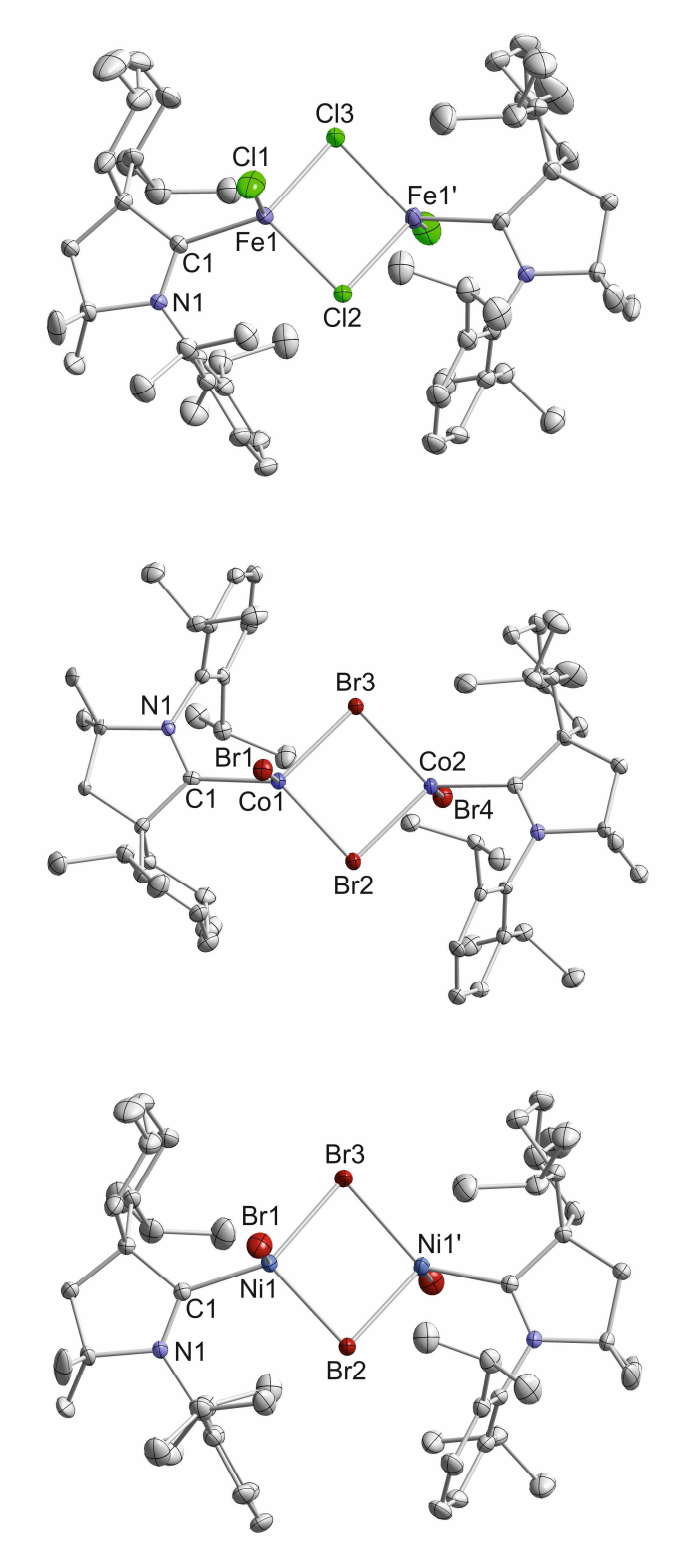

Figure 2. Solid-state molecular structures of complexes [FeCl(μ-Cl)(CAAC$_1$)]$_2$ (**1**, top), [CoBr(μ-Br)(CAAC$_1$)]$_2$ (**2**, middle), and [NiBr(μ-Br)(CAAC$_1$)]$_2$ (**3**, bottom). The hydrogen atoms are omitted for clarity. Thermal ellipsoids are drawn at 40% level.

The structures of **1**–**3** are similar to those of the related diaminocarbene complexes [FeCl(μ-Cl)(IDipp)]$_2$ and [CoX(μ-X)(IDipp)]$_2$ (X = Cl, Br, I, IDipp = 1,3-bis(2,6-diisopropylphenyl)imidazolin-2-ylidene), which were recently described by the groups of Tonzetich and Matsubara.[3a,b] Inspection of the key structural parameters indicates that the substitution of the CAAC by the NHC apparently does not exert a large effect on the molecular structures of the iron and cobalt complexes. In contrast, the structure of the nickel complex **3** is markedly different from its IDipp analogue [NiCl(μ-Cl)(IDipp)]$_2$, which was reported by Hillhouse *et al.*[3c] The solid state structure of the latter complex displays two distorted *square planar* nickel(II) centers. Nonetheless, [NiCl(μ-Cl)(IDipp)]$_2$ is paramagnetic in deuterated toluene with an effective magnetic moment of 2.6 μ_B per Ni atom. This high magnetic moment agrees with the formation of a tetrahedral structure in solution.[13]

Table 1. Selected bond lengths [Å] and angles [°] of **1**–**3**.

	1	**2**[a]	**3**
	M = Fe1, X = Cl	M = Co1, Co2, X = Br	M = Ni, X = Br
M–C1	2.094(3)	2.073(4), 2.097(4)[b]	1.989(2)
M–X1	2.237(1)	2.378(1), 2.391(1)	2.349(1)
M–X2	2.358(1)	2.500(1), 2.501(1)	2.424(1)
M–X3	2.397(1)	2.502(2), 2.485(1)	2.486(1)
C1–M–X1	109.7(1)	101.6(1), 109.6(1)	101.4(1)
C1–M–X2	113.3(1)	126.1(1), 121.7(1)	112.3(1)
C1–M–X3	128.5(1)	122.3(1), 122.4(1)	136.9(1)
X1–M–X2	110.6(1)	110.6, 104.5(1)	105.6(1)
M–X2–M'	89.4(1)	91.5(1)[c]	87.9(1)
M–X3–M'	87.6(1)	91.8(1)[d]	85.2(1)

[a] The first value in this column refers to M = Co1, the second value refers to M = Co2; [b] Co2–C28; [c] Co1–Br2–Co2; [e] Co1–Br3–Co2.

Complexes **1**–**3** are paramagnetic, and their ^{1}H NMR spectra ([D$_8$]THF) accordingly exhibit broad peaks in a wide range from approximately −30 to +46 ppm (see the experimental section), that are difficult to assign to invidual groups or molecular fragments. The determination of the effective magnetic moments of **1**–**3** indicates a high-spin configuration. The solution magnetic moments observed in [D$_8$]THF using the Evans method are 6.0(1) μ_B/Fe atom for **1**, 4.7(1) μ_B/Co for **2**, and 4.3(1) μ_B/ Ni for **3**. Very similar magnetic moments were determined in CD_2Cl_2 (6.2(1) μ_B/Fe atom for **1**, 4.9 μ_B/Co for **2**, and 4.6(1) μ_B/Ni for **3**). These experimental values are significantly higher than the expected spin-only values of 4.90, 3.87 μ_B and 2.83 μ_B, for systems

with four, three and two unpaired electrons per metal center, respectively. High magnetic moments have been observed for several other iron(II) and cobalt(II) carbene and phosphane complexes with a distorted tetrahedral geometry, e.g. $[FeCl(\mu\text{-}Cl)(IDipp)]_2$ (μ_{eff} = 5.2(1) μ_B/Fe),[3a] $[FeCl(\mu\text{-}Cl)(IMes)]_2$ (4.6(1) μ_B/Fe),[3a] $[FeCl_2(IMes)_2]$ (5.2(1) μ_B),[3a] $[FeCl_2(IEtPh^*)_2]$ (IEtPh* = 1,3-bis((*R*)-1'-phenylethyl)-imidazolin-2-ylidene),[4k,] [Fe-Cl_2(C⌒C)] (5.2–5.6 μ_B, L = various chelating dicarbene ligands),[4g,l] $[CoX(\mu\text{-}X)(IDipp)]_2$ (X = Cl, Br, I; 4.03, 4.06, and 4.27 μ_B/Co), $[CoX_2(IDipp)(py)]$ (X = Cl, Br, I; μ_{eff} = 4.72, 4.43, and 4.35 μ_B/Co),[3b] and $[FeCl_2((P⌒P)]$ (5.1–5.5 μ_B; P⌒P = various chelating diphosphine ligands).[14] A likely reason for these deviations from spin-only magnetism is the effect of unquenched orbital momentum.[15]

The UV-vis spectrum of **1** recorded in THF shows a weak absorption maximum in the visible region at 406 nm, which is in accord with the yellow color of the complex. The UV-vis spectra of **2** and **3** show three similar, weak absorptions in the visible range at 602, 668sh and 711 nm for **2**, and 617, 644sh and 709sh nm for **3**. These bands may tentatively be assigned to d-d transitions. Interestingly, the UV/vis spectrum of the related (diamino)carbene complex $[CoBr(\mu\text{-}Br)(IDipp)]_2$ shows a similar UV/vis spectrum as **2** with three bands at 600, 685 and 720sh nm,[3b] which might indicate that both complexes have a similar structure in solution as well as in the solid state.

6.3 Conclusion

New cyclic (alkyl)(amino)carbene complexes of iron(II), cobalt(II) and nickel(II) have been prepared by reacting Bertrand's $CAAC_1$ with divalent iron, cobalt and nickel halides. The resulting complexes $[FeCl(\mu\text{-}Cl)(CAAC_1)]_2$ (**1**), $[CoBr(\mu\text{-}Br)(CAAC_1)]_2$ (**2**), and $[NiBr(\mu\text{-}Br)(CAAC_1)]_2$ (**3**) are paramagnetic and very air-sensitive, but appear to be thermally stable under an inert atmosphere. X-ray crystal structure analyses revealed dimeric halide-bridged structures with distorted tetrahedrally coordinated metal centers. Similar structures were previously obtained with the related diisopropylphenyl-substituted (diamino)carbene IDipp.[3] The isolation and structural characterization of **1**–**3** augurs well for the future development of a more extensive coordination chemistry of the cyclic (alkyl)(amino)carbenes with these and other first row transition metals, which may eventually lead to novel applications in catalysis and small molecule activation.

6.4 Supporting Information (SI)

6.4.1 General Procedures

All experiments were performed in an MBraun UniLab glovebox under an atmosphere of dry argon. Solvents were purified, dried, and degassed with an MBraun SPS800 solvent purification system. NMR spectra were recorded on Bruker Avance 300 and Avance 400 spectrometers at 300 K and internally referenced to residual solvent resonances.[16,17] Melting points were measured on samples in sealed capillaries on a Stuart SMP10 melting point apparatus. UV/Vis spectra were recorded on a Varian Cary 50 spectrometer. Elemental analyses for **1** and **2** were determined by the analytical department of Regensburg University. The elemental analysis of **3** was obtained by Medac Ltd., Chobham Surrey, UK. The starting materials $FeCl_2(thf)_{1.5}$, $NiBr_2(dme)$, and $CAAC_1$ were prepared according to literature procedures.[6,18,19] $CoBr_2$ was purchased from Aldrich and used as received.

6.4.2 Synthesis of $[FeCl(\mu\text{-}Cl)(CAAC_1)]_2$ (1)

A solution of $CAAC_1$ (50 mg, 0.13 mmol) in THF (3 mL) was added dropwise to a suspension of $FeCl_2(thf)_{1.5}$ (30 mg, 0.13 mmol) in THF (2 mL) at room temperature. The resulting yellow solution was stirred for two hours. After removing the solvent, the crude product was extracted with toluene (~3 mL). Yellow crystals suitable for X-ray crystallography were obtained by slow diffusion of *n*-hexane into this solution. The isolated crystals were dried in *vacuo*. Yield: 32 mg (48%); m.p. >145 °C (slow decomp. to a dark oil); UV/Vis (THF, λ_{max} /nm (ε_{max} /L·mol^{-1}·cm^{-1})): 402 (446); Effective magnetic moment ([D$_8$]THF): μ_{eff} = 6.0(1) μ_B/Fe; Elemental analysis calcd for $C_{54}H_{86}N_2Cl_4Fe_2$ (M = 1016.78): C 63.79, H 8.53, N 2.76, found: C 63.29, H 8.61, N 2.83; ^{1}H NMR (400.13 MHz, [D$_8$]THF, 300 K): δ/ppm = −11.3 (br s), 0.0 to 1.2 (overlapping m), 2.2 (m), 3.0 (br s), 6.3 to 7.1 (m), 8.3 (br s), 8.8 (br s), 10.5 (br s), 13.9 (br s), 13.9 (br s), 14.7 (br s), 27.2 (br s), 34 (br s), 45 (br s).

6.4.3 Synthesis of $[CoBr(\mu\text{-}Br)(CAAC_1)]_2$ (2)

An analogous procedure as for the synthesis of **1** was applied, using $CAAC_1$ (43 mg, 0.11 mmol) and $CoBr_2$ (25 mg, 0.11 mmol). X-ray quality crystals of **1** were obtained by slow diffusion of *n*-hexane into a toluene solution of the raw product. The crystals were dried in *vacuo*. The pure compound contains one molecule of toluene per formula unit after drying under vacuum. Yield 37 mg (51%); m.p. >219 °C (slow decomp. to a dark green oil); UV/Vis (THF, λ_{max} /nm (ε_{max} /L·mol^{-1}·cm^{-1})): 602 (237), 668sh (362), 711 (495); Effective magnetic moment ([D$_8$]THF): μ_{eff} = 4.7(1) μ_B/Co; Elemental analysis calcd for $C_{54}H_{86}N_2Br_4Co_2{\cdot}C_7H_8$ (M = 1292.92): C 56.67, H 7.33, N 2.76, found: C 56.41, H 7.26, N 2.10; ^{1}H NMR (400.13 MHz, [D$_8$]THF, 300 K): δ/ppm = −32 (br s), −28 (br s), −20.4 (br s), −15.7 (br s), −11.3 (br s), −10.5 (br s), −7.53 (s), −5.8 to −4.8 (m), −3.6 (br s), −2.52 (s), −2.25 (s), −1.95 (s), −1.50 (s), −0.05 (m), 0.0 to 0.2 (m), 0.50

(s), 0.7 to 1.3 (m), 1.56 (s), 2.28 (s, toluene), 5.0 (br s), 6.3 (m), 6.50 (m), 7.06 to 7.19 (m, toluene), 7.6 (br s), 10.9 (br s), 12.2 (br s), 13.2 (br s), 16.4 (br s), 16.6 (br s), 18.8 (br s), 20.7 (br s), 25.6 (br s), 29.7 (br s), 46 (br s).

6.4.4 Synthesis of [NiBr(μ-Br)($CAAC_1$)]$_2$ (3)

An analogous procedure as for the synthesis of **1** was applied, using $CAAC_1$ (52 mg, 0.13 mmol) and $NiBr_2$(dme) (50 mg, 0.13 mmol). X-ray quality crystals of the product were obtained by slow diffusion of *n*-hexane into a toluene solution of the raw product. Yield 19 mg (19%); m.p. >140 °C (slow decomp. to a dark solid); UV/Vis (THF, λ_{max} /nm (ε_{max} /L·mol^{-1}·cm^{-1})): 617 (51), 644sh (47), 709sh (15); Effective magnetic moment ([D$_8$]THF): μ_{eff} = 4.3(1) μ_B/Ni; Elemental analysis calcd for $C_{54}H_{86}N_2Br_4Ni_2$ (*M* = 1200.3): C 54.04, H 7.22, N 2.33, found: C 52.45, H 7.29, N 2.50; elemental analyses on independent samples reproducibly gave similarly low carbon values; ^{1}H NMR (400.13 MHz, [D$_8$]THF, 300 K): δ/ppm = −23 (br s), −21 (br s), −19 (br s), −14 (br s), −10 (br s), −4.2 (br s), −2.9 (br s), −1.7 to −1.3 (m), 0.90 – 1.57 (m), 1.81 to 1.98 (m), 2.28 (s, toluene), 2.49 (m), 2.98 to 3.27 (m), 3.71 – 4.09 (m), 4.35 (br s), 4.73 (m), 5.22 (br s), 7.06 to 7.19 (overlapping br s, toluene), 7.30 (m), 7.94 to 8.06 (m), 8.72 (br s), 10.10 (s), 11 (br s), 13 (br s), 14 (br s), 16 (br s), 18 (br s), 21 (br s), 29 (br s), 30 (br s), 44 (br s).

6.4.5 X-ray Crystallography

The single crystal X-ray diffraction data were recorded with an Agilent Technologies SuperNova diffractometer with Cu Kα radiation (λ = 1.54178 Å). Either semi-empirical multi-scan absorption corrections[20] or analytical ones[21] were applied to the data. The structures were solved by SHELXS[22] or SIR[23] and least-square refinements on F^2 were carried out with SHELXL.[21] Crystal and structure refinement data are given in Table 2. CCDC-952884 (**1**), -952885 (**2**·toluene), and -952886 (**3**) contain the supplementary crystallographic data for this paper. These data can be obtained free of charge from The Cambridge Crystallographic Data Centre via www.ccdc.cam.ac.uk/data_re-quest/cif.

Table 2. Crystal and structure refinement data for **1**–**3**.

	1	**2**·C_7H_8	**3**
Empirical Formula	$C_{54}H_{86}N_2Cl_4Fe_2$	$C_{61}H_{94}Br_4Co_2N_2$	$C_{54}H_{86}N_2Br_4Ni_2$
Crystal system	tetragonal	monoclinic	tetragonal
Space group	$P4_22_12$	$P2_1$	$P4_22_12$
Z	4	2	4
Temperature [K]	123.0(1)	123.0(2)	123.0(1)
ρ_{calc} [g/cm^3]	1.193	1.428	1.399
a [Å]	16.361(5)	10.1582(1)	16.3839(1)
b [Å]	16.361(5)	18.3224(2)	16.3839(1)
c [Å]	21.156(5)	16.3399(2)	21.2235(3)
α [°]	90	90	90
β [°]	90	98.652(1)	90
γ [°]	90	90	90
Volume [Å^3]	5663(3)	3006(1)	5697.1(1)
μ [mm^{-1}]	6.090	7.709	4.351
2Θ Range /°	7.64 − 147.4	7.3 − 147.94	6.82 − 147.46
Independent Reflections	5507 [R(int) = 0.0941]	10100 [R(int) = 0.0248]	5468 [R(int) = 0.0262]
Parameters	281	641	281
GooF	0.993	0.833	1.032
R_1 [I > 2σ(I)]	0.0469	0.0254	0.0241
wR_2 (all data)	0.1075	0.0453	0.0584
Largest diff. peak/hole [e Å^{-3}]	0.48/−0.65	0.53/−0.43	0.54/−0.40
Flack parameter	−0.009(5)	−0.017(4)	−0.020(15)

References

1 a) W. A. Herrmann, *Angew. Chem.* **2002**, *114*, 1342–1363, *Angew. Chem. Int. Ed.* **2002**, *41*, 1290–1309; b) E. A. B. Kantchev, C. J. O'Brien, M. G. Organ, *Angew. Chem.* **2007**, *119*, 2824–2870, *Angew. Chem. Int. Ed.* **2007**, *46*, 2768–2813; c) S. Würtz, F. Glorius, *Acc. Chem. Res.* **2008**, *41*, 1523–1533; d) G. C. Vougioukalakis, R. H. Grubbs, *Chem. Rev.* **2010**, *110*, 1746–1787; e) S. Díez-González, N. Marion, S. P. Nolan, *Chem. Rev.* **2009**, *109*, 3612–3676; f) T. Hatakeyama, S. Hashimoto, K. Ishizuka, M. Nakamura, *J. Am. Chem. Soc.* **2009**, *131*, 11949–11963.

2 a) D. Bourissou, O. Guerret, F. P. Gabbaï, G. Bertrand, *Chem. Rev.* **2000**, *100*, 39–92; b) T. Weskamp, V. P. W. Böhm, W. A. Herrmann, *J. Organomet. Chem.* **2000**, *600*, 12–22; c) S. T. Liddle, I. S. Edworthy, P. L. Arnold, *Chem. Soc. Rev.* **2007**, 1732; d) F. E. Hahn, M. C. Jahnke, *Angew. Chem.* **2008**, *120*, 3166–3216, *Angew. Chem. Int. Ed.* **2008**, *47*, 3122–3172; e) R. Wolf, W. Uhl, *Angew. Chem.* **2009**, *121*, 6905–6907, *Angew. Chem. Int. Ed.* **2009**, *48*, 6774-6776; f) P. L. Arnold I. J. Casely, *Chem. Rev.* **2009**, 109, 3599; g) M. Melaimi, M. Soleilhavoup, G. Bertrand, *Angew. Chem.* **2010**, *122*, 8992–9032, *Angew. Chem. Int. Ed.* **2010**, *49*, 8810–8849; h) W. Kirmse, *Angew. Chem.* **2010**, *122*, 8980–8983, *Angew. Chem. Int. Ed.* **2010**, *49*, 8798–8801; i) T. Dröge, F. Glorius, *Angew. Chem.* **2010**, *122*, 7094–7107, *Angew. Chem. Int. Ed.* **2010**, *49*, 6940–6952.

3 IDipp complexes with Fe, Co and Ni: a) J. A. Przyojski, H. D. Arman, Z. J. Tonzetich, *Organometallics* **2012**, *31*, 3264–3271; b) K. Matsubara, T. Sueyasu, M. Esaki, A. Kumamoto, S. Nagao, H. Yamamoto, Y. Koga, S. Kawata, T. Matsumoto, *Eur. J. Inorg. Chem.* **2012**, 3079–3086; c) C. A. Laskowski, G. L. Hillhouse, *Organometallics* **2009**, *28*, 6114–6120.

4 Selected key examples with other NHC ligands: a) B. R. Dible, M. S. Sigman, A. M. Arif, *Inorg. Chem.* **2005**, *44*, 3774–3776; b) T. Schaub, U. Radius, *Chem. Eur. J.* **2005**, *11*, 5024–5030; c) Y. Ohki, T. Hatanaka, K. Tatsumi, *J. Am. Chem. Soc.* **2008**, *130*, 17174–17186; d) C. J. E. Davies, M. J. Page, C. E. Ellul, M. F. Mahon, M. K. Whittlesey, *Chem. Commun.* **2010**, *46*, 5151–5153; e) R. A. Layfield, J. J. W. McDouall, M. Scheer, C. Schwarzmaier, F. Tuna, *Chem. Commun.* **2011**, *47*, 10623–10625; f) A. A. Danopoulos, P. Braunstein, N. Stylianides, M. Wesolek, *Organometallics* **2011**, *30*, 6514–6517; g) S. Meyer, C. M. Orben, S. Demeshko, S. Dechert, F. Meyer, *Organometallics* **2011**, *30*, 6692-6702; h) C. A. Laskowski, A. J. M. Miller, G. L. Hillhouse, T. R. Cundari, *J. Am. Chem. Soc.* **2011**, *133*, 771–773; i) M. J. Ingleson, R. A. Layfield, *Chem. Commun.* **2012**, *48*, 3579–3589; j) T. Zell, P. Fischer, D. Schmidt, U. Radius, *Organometallics* **2012**, *31*, 5065–5073; k) T. Hashimoto, S. Urban, R. Hoshino, Y. Ohki, K. Tatsumi, F. Glorius, *Organometallics* **2012**, *31*, 4474-4479; l) C. Grohmann, T. Hashimoto, R. Fröhlich, Y. Ohki, K. Tatsumi, F.

Glorius, *Organometallics* **2012**, *31*, 8047-8050; m) X. Wang, Z. Mo, J. Xiao, L. Deng, *Inorg. Chem.* **2013**, *52*, 59–65; n) J. A. Przyojski, H. D. Arman, Z. J. Tonzetich, *Organometallics* **2013**, *32*, 723–732; o) S. Meyer, I. Klawitter, S. Demeshko, E. Bill, F. Meyer, *Angew. Chem.* **2013**, *125*, 935-939, *Angew. Chem. Int. Ed.* **2013**, *52*, 901-905; p) M. J. Page, W. Y. Lu, R. C. Poulten, E. Carter, A. G. Algarra, B. M. Kariuki, S. A. Macgregor, M. F. Mahon, K. J. Cavell, D. M. Murphy, M. K. Whittlesey, *Chem. Eur. J.* **2013**, *19*, 2158–2167.

5 a) V. Lavallo, R. H. Grubbs, *Science* **2009**, *326*, 559–562; b) V. Lavallo, A. El-Batta, G. Bertrand, R. H. Grubbs, *Angew. Chem.* **2011**, *123*, 282–285, *Angew. Chem. Int. Ed.* **2011**, *50*, 268–271.

6 a) V. Lavallo, Y. Canac, C. Präsang, B. Donnadieu, G. Bertrand, *Angew. Chem.* **2005**, *117*, 5851–5855, *Angew. Chem. Int. Ed.* **2005**, *44*, 5705–5709; b) R. Jazzar, R. D. Dewhurst, J.-B. Bourg, B. Donnadieu, Y. Canac, G. Bertrand, *Angew. Chem.* **2007**, *119*, 2957–2960, *Angew. Chem. Int. Ed.* **2007**, *46*, 2899–2902; c) R. Jazzar, J.-B. Bourg, R. D. Dewhurst, B. Donnadieu, G. Bertrand, *J. Organomet. Chem.* **2007**, *72*, 3492–3499.

7 a) V. Lavallo, Y. Canac, B. Donnadieu, W. W. Schoeller, G. Bertrand, *Angew. Chem.* **2006**, *118*, 3568–3571, *Angew. Chem. Int. Ed.* **2006**, *45*, 3488–3491; b) G. D. Frey, V. Lavallo, B. Donnadieu, W. W. Schoeller, G. Bertrand, *Science* **2007**, *316*, 439–441; c) J. D. Masuda, W. W. Schoeller, B. Donnadieu, G. Bertrand, *Angew. Chem.* **2007**, *119*, 7182–7185, *Angew. Chem. Int. Ed.* **2007**, *46*, 7052–7055; d) D. Martin, M. Soleilhavoup, G. Bertrand, *Chem. Sci.* **2011**, *2*, 389–399.

8 a) V. Lavallo, Y. Canac, A. DeHope, B. Donnadieu, G. Bertrand, *Angew. Chem.* **2005**, *117*, 7402–7405, *Angew. Chem. Int. Ed.* **2005**, *44*, 7236–7239; b) G. Bertrand, V. Lavallo, Y. Canac, **2006**, U.S. Patent WO2006138166 (A2); c) D. R. Anderson, T. Ung, G. Mkrtumyan, G. Bertrand, R. H. Grubbs, Y. Schrodi, *Organometallics* **2008**, *27*, 563–566; d) G. D. Frey, R. D. Dewhurst, S. Kousar, B. Donnadieu, G. Bertrand, *J. Organomet. Chem.* **2008**, *693*, 1674–1682; e) X. Zeng, G. D. Frey, S. Kousar, G. Bertrand, *Chem. Eur. J.* **2009**, *15*, 3056–3060; f) X. Zeng, G. D. Frey, R. Kinjo, B. Donnadieu, G. Bertrand, *J. Am. Chem. Soc.* **2009**, *131*, 8690–8696; g) D. S. Weinberger, M. Melaimi, C. E. Moore, A. L. Rheingold, G. Frenking, P. Jerabek, G. Bertrand, *Angew. Chem.* **2013**, *125*, 9134–9137, *Angew. Chem. Int. Ed.* **2013**, *52*, 8964–8967.

9 G. D. Frey, B. Donnadieu, M. Soleilhavoup, G. Bertrand, *Chem. Asian J.* **2011**, *6*, 402–405.

10 a) A. P. Singh, P. P. Samuel, H. W. Roesky, M. C. Schwarzer, G. Frenking, N. S. Sidhu, B. Dittrich, *J. Am. Chem. Soc.* **2013**, *135*, 7324–7329; A. P. Singh, P. P. Samuel, H. W. Roesky, M. C. Schwarzer, G. Frenking, N. S. Sidhu, B. Dittrich, *J. Am. Chem. Soc.* **2013**, *135*, 7324–7329; b) P. P. Samuel, K. C. Mondal, H. W. Roesky, M. Hermann, G. Frenking,

S. Demeshko, F. Meyer, A. C. Stückl, J. H. Christian, N. S. Dalal, L. Ungur, L. F. Chibotaru, K. Pröpper, A. Meents, B. Dittrich, *Angew. Chem. Int. Ed.* DOI: 10.1002/ange.201304642.

11 a) R. Wolf, M. Plois, A. Hepp, *Eur. J. Inorg. Chem.* **2010**, 918–925; b) R. Wolf, M. Plois, *Eur. J. Inorg. Chem.* **2010**, 4419–4422.

12 a) E.-M. Schnöckelborg, J. J. Weigand, R. Wolf, *Angew. Chem.* **2011**, *123*, 6787–6790, *Angew. Chem. Int. Ed.* **2011**, *50*, 6657–6660; b) E.-M. Schnöckelborg, M. M. Khusniyarov, B. de Bruin, F. Hartl, T. Langer, M. Eul, S. Schulz, R. Pöttgen, R. Wolf, *Inorg. Chem.* **2012**, *51*, 6719–6730; d) M. Plois, T. Wiegand, R. Wolf, *Organometallics* **2012**, *31*, 8469–8477; d) M. Plois, W. Hujo, S. Grimme, C. Schwickert, E. Bill, B. de Bruin, R. Pöttgen, R. Wolf, *Angew. Chem.* **2013**, *125*, 1352–1357, *Angew. Chem. Int. Ed.* **2013**, *52*, 1314–1318.

13 G. N. La Mar, E. O. Sherman, *J. Am. Chem. Soc.* **1970**, *92*, 2691–2699.

14 a) W. A. Baker Jr., P. M. Lutz, *Inorg. Chim. Acta* **1976**, *16*, 5–8; b) T. Hatakeyama, T. Hashimoto, Y. Kondo, Y. Fujiwara, H. Seike, H. Takaya, Y. Tamada, T. Ono, M. Nakamura, *J. Am. Chem. Soc.* **2010**, *132*, 10674–10676.

15 a) P.-H. Lin, N. C. Smythe, S. I. Gorelsky, S. Maguire, N. J. Henson, I. Korobkov, B. L. Scott, J. C. Gordon, R. T. Baker, M. Murugesu, *J. Am. Chem. Soc.* **2011**, *133*, 15806-15809; b) S. A. Sulway, D. Collison, J. J. W. McDouall, F. Tuna, R. A. Layfield, *Inorg. Chem.* **2011**, *50*, 2521-2526.

16 D. F. Evans, *J. Chem. Soc.* **1959**, 2003–2005.

17 G. J. P. Britovsek, V. C. Gibson, S. K. Spitzmesser, K. P. Tellmann, A. J. P. White, D. J. Williams, *J. Chem. Soc. Dalton Trans.* **2002**, 1159–1171.

18 R. J. Kern, *J. Inorg. Nucl. Chem.* **1962**, *24*, 1105–1109.

19 L. G. L. Ward, J. R. Pipal, *Inorg. Synth.* **2007**, 154–164.

20 a) *SCALE3ABS*, *CrysAlis*^{Pro}, Aglient Technologies Inc., Oxford, GB, **2012**; b) G. M. Sheldrick, *SADABS*, Bruker AXS, Madison, USA, **2007**.

21 R. C. Clark, J. S. Reid, *Acta Crystallogr. A* **1995**, *51*, 887–897.

22 G. M. Sheldrick, *Acta Crystallogr. A* **2007**, *64*, 112–122.

23 A. Altomare, M. C. Burla, M. Camalli, G. L. Cascarano, C. Giacovazzo, A. Guagliardi, A. G. Moliterni, G. Polidori, R. Spagna, *J. Appl. Crystallogr.* **1999**, *32*, 115–119.

7 Preparation of a Trigonal Planar Manganese(II) Amido Complex Supported by an N-Heterocyclic Carbene[a,b]

Stefan Pelties and Robert Wolf

[a] Unpublished results

[b] After completion of the experimental work on this chapter, the synthesis of **1** and the related complex $[MnCl(\mu\text{-}Cl)(IMes)]_2$ (IMes = 1,3-bis(2,4,6-trimethylphenyl)imidazolin-2-ylidene) were described by Tonzetich *et al.* together with a series of dimeric alkyl and aryl manganese(II) NHC complexes (M. H. Al-Afyouni, V. M. Krishnan, H. D. Arman, Z. J. Tonzetich, *Organometallics* **2015**, *34*, 5088–5094).

7.1 Introduction

Low-coordinate organomanganese(II) complexes are of interest because of their unusual and notoriously different reactivity compared to other 3d metals.[1,2] However, divalent manganese hydrocarbyls are rather scarce among 3d metals, probably due to the lability of the manganese(II)−carbon bond as a result of its high ionic character.[1] The paucity of manganese NHC (N-heterocyclic carbene) complexes with oxidation states other than +I is particularly salient. Besides the rather limited number of publications regarding Mn(III), Mn(IV), and Mn(V) NHC complexes[3,4,5], also only very few publications deal with manganese(II) carbene complexes so far.[6,7,8,9] In these examples, most manganese centers exhibit a coordination number of four and higher.[6] Respective low-coordinate manganese(II) compounds (coordination number of two and three) are extremely rare.[7,8,9]

The first three-coordinate NHC-stabilized manganese(II) complexes of type **A** were reported by the group of Mulvey and Robertson in 2011. They prepared complexes **A** by reacting two-coordinate manganese alkyls [Mn{$CH_x(SiMe_3)_{3-x}$}$_2$] (x = 0, 1) with the free carbene IDipp (1,3-bis(2,6-diisopropylphenyl)imidazolin-2-ylidene, Scheme 1).[7]

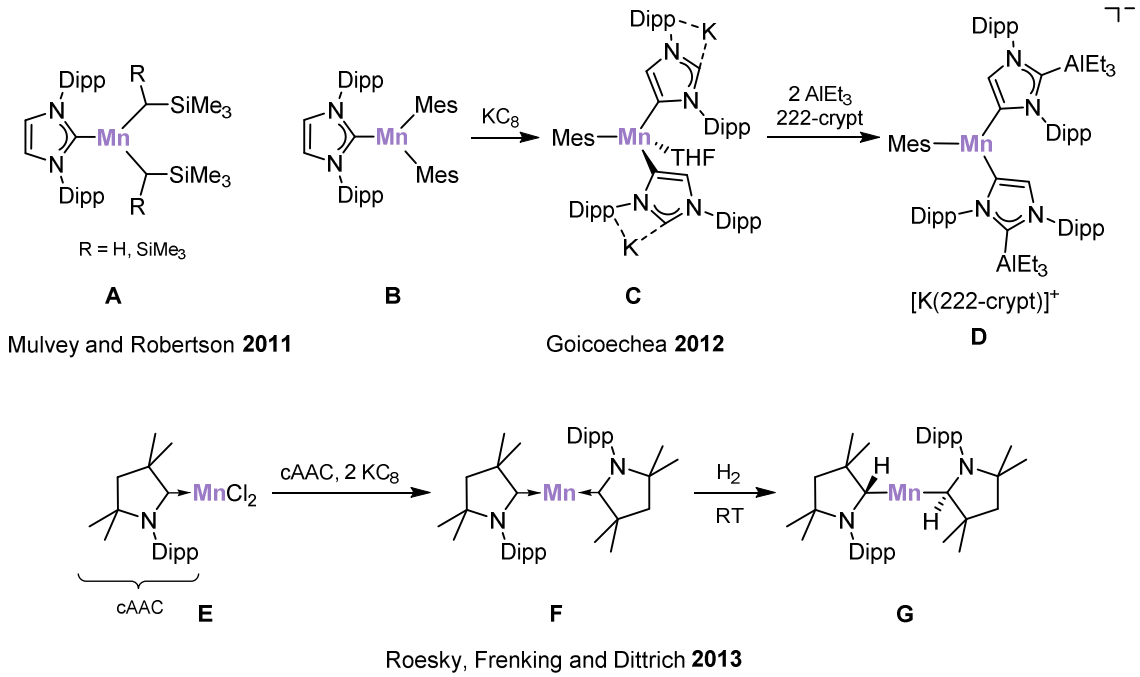

Scheme 1. Known two- and three-coordinate NHC-stabilized manganese(II) complexes and their reactivity.[7,8,9]

In 2012, Goicoechea and coworkers synthesized the three-coordinate complex **B** by converting $Mn_3(Mes)_6$ with three equivalents of IDipp.[8] Remarkably, they obtained **C**, the first manganese complex with an abnormal carbene ligand, upon reduction of **B** with potassium graphite. Strong evidence of the dicarbenic nature came from the reaction of **C** with 2,2,2-crypt (4,7,13,16,21,24-

hexaoxa-1,10-diazabicyclo[8,8,8]hexacosane) and subsequent addition of two equivalents of the Lewis acid $AlEt_3$, which yielded complex **D**.

Very recently, the group of Roesky, Frenking, and Dittrich described the preparation of the two-coordinate complex **F** with a formal Mn(0) center in the reaction of the Mn(II) precursor **E** with an equimolar amount of a CAAC (= cyclic alkyl(amino)carbene) and two equivalents of KC_8.[9] DFT studies, EPR, and magnetic measurements revealed that **F** features a quartet ground state with antiferromagnetic coupling between a Mn(I) atom with a low spin d^6 configuration (S = 2) and a radical (S = 1/2) delocalized over the two carbene atoms. Interestingly, complex **F** is able to cleave dihydrogen under very mild condition, yielding the manganese(II) dialkyl **G**.

The described compounds impressively illustrate the potential of low-coordinate manganese(II) NHC complexes to undergo unusual reactivity. In the course of our investigations toward the synthesis of low-coordinate transition metal carbene complexes,[10] we became interested in preparing low-coordinate NHC-stabilized manganese(II) complexes. Here, we report a convenient gram scale synthesis for the NHC-stabilized manganese(II) chloride **1** and investigate its ability to function as a precursor for low-coordinate NHC-stabilized manganese(II) compounds. Complex **1** possesses a dimeric halide-bridged structure in the solid state, but X-ray diffraction analysis on **1-THF** further indicates the presence of monomers in THF solutions. The labile nature of the manganese(II)-carbon bond is demonstrated by the reaction of **1** with four equivalents of MeMgI. In this case, the NHC and the chloride atom of **1** are transferred to magnesium, resulting in the formation of $[(IDipp)MgMeCl]_2$ (**2**). Finally, we report that dimeric **1** reacts with four equivalents of $LiN(SiMe_3)_2$ to afford the unique trigonal planar amide $[(IDipp)MgMeCl]_2$ (**3**).

7.2 Results and Discussion

Compound **1** is readily accessible on a gram scale upon converting IDipp with an equimolar amount of manganese(II) chloride in tetrahydrofuran at room temperature (Scheme 2). Interestingly, after removal of the solvent from the reaction mixture and drying the crude product in *vacuo* for a few minutes colorless crystals of the monomeric complex **1-THF** were isolated from toluene indicating the presence of monomers in THF solutions of **1**. If crystals of **1-THF** or the crude product were dried for longer than one hour in *vacuo* only colorless crystals of **1** were obtained from toluene crystallization. Compound **1** is oxygen and moisture sensitive, but thermally stable, and dissolves in benzene, toluene, and tetrahydrofuran. The complex was characterized by ^{1}H NMR spectroscopy, elemental analysis, single crystal X-ray diffraction, and its solution magnetic moment.

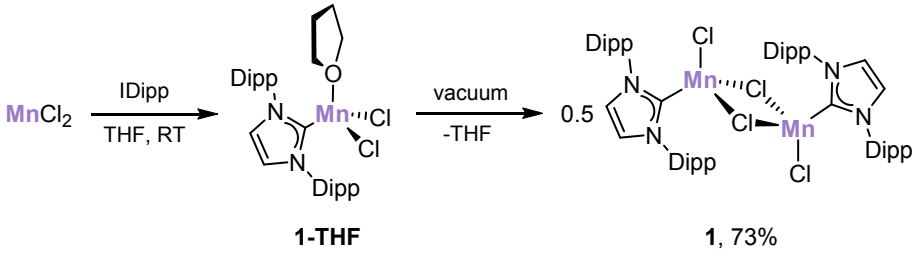

1-THF **1**, 73%

Scheme 2. Synthesis of [MnCl(μ-Cl)(IDipp)]$_2$ (**1**).

The molecular structure of monomer **1-THF** obtained by X-ray crystallography (Figure 1, left) revealed a distorted tetrahedral complex with two terminal chloride ligands and a coordinating tetrahydrofuran molecule.[11] The Mn1-C1 bond lengths in **1-THF** (2.187(8) Å) is only slightly shorter in comparison with the related tetrahedral complexes [(NHC)$_2$MnX$_2$] (2.204(4) − 2.219(3) Å; X = Cl, I; NHC = [C(Me)N(*i*Pr)]$_2$C).[6b,c] Also the manganese distances to the terminal chlorides in **1-THF** (2.306(3) and 2.298(3) Å) are only slightly shorter as against the complex [(NHC)$_2$MnCl$_2$] (2.354(1)− 2.358(1) Å).[6b,c]

Complex **1** crystallizes as a chloride-bridged dimer with pseudo-tetrahedral coordinated manganese atoms (Figure 1, right). Two MnCl$_2$(IDipp) fragments are related by an inversion center, which resides between the manganese atoms. The structure of **1** is related to complexes [FeCl(μ-Cl)(IDipp)]$_2$ and [CoX(μ-X)(IDipp)]$_2$ (X = Cl, Br, I) synthesized by the groups of Tonzetich and Matsubara.[12] The Mn1-C1 bond lengths in **1** (2.182(3) Å) are identical with the ones in **1-THF**, and the distances to the terminal chlorides **1** (2.3052(9) Å) are also in a similar range. Compared to the corresponding distances in [FeCl(μ-Cl)(IDipp)]$_2$ and [CoCl(μ-Cl)(IDipp)]$_2$ (Fe−$C_{Carbene}$ = 2.090(2) Å, Fe−$Cl_{terminal}$ = 2.2419(7) Å, Co−$C_{Carbene}$ = 2.0298(13) Å, Co−$Cl_{terminal}$ = 2.2238(4) Å) the bond lengths in **1** are elongated due to the larger ion radius of the high spin d^5 center. As one would expect, the Mn−$Cl_{terminal}$ bond lengths are shorter (0.12 Å) than the Mn−$Cl_{bridging}$ distances.

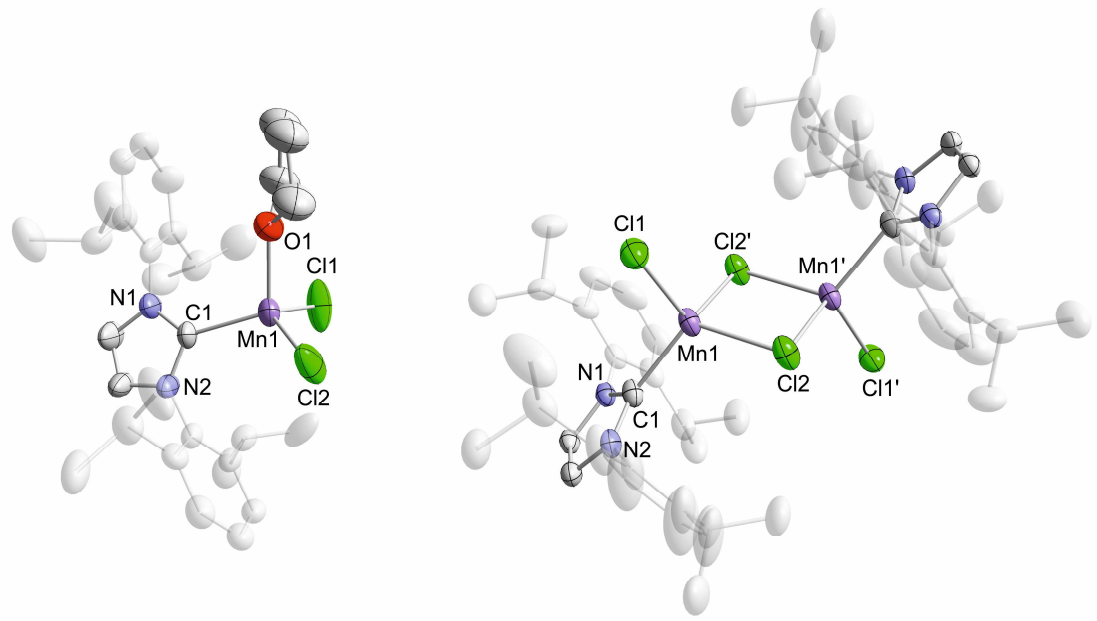

Figure 1. Solid-state molecular structure of [$MnCl_2$(thf)(IDipp)] (**1-THF**, left) and [MnCl(μ-Cl)(IDipp)]$_2$ (**1**, right). The hydrogen atoms are omitted for clarity. Thermal ellipsoids are drawn at 40% level. Selected bond lengths [Å] and angles [°] **1-THF**: Mn1−C1 2.187(8), Mn1−Cl1 2.306(3), Mn1−Cl2 2.298(3), Mn1−O1 2.132(7), C1−Mn1−Cl1 108.6(3), C1−Mn1−Cl2 116.5(2), C1−Mn1−O1 109.7(3), Cl1−Mn1−Cl2 116.67(15); **1**: Mn1−C1 2.182(3), Mn1−Cl1 2.3052(9), Mn1−Cl2 2.4273(8), Mn1−Cl2’ 2.4252(9), C1−Mn1−Cl1 111.35(8), C1−Mn1−Cl2 114.66(8), C1−Mn1−Cl2’ 116.75(8), Cl1−Mn1−Cl2 109.32(4), Mn1−Cl2−Mn1’ 86.42(3), Mn1−Mn1’ 3.3223(10).

Due to the large metal-metal distance of 3.3223(10) Å any significant bonding interactions can be excluded.

The ^{1}H NMR spectrum of **1** (room temperature, C_6D_6) shows only very broad signals in the range of 1.9 to 8.7 ppm. The magnetic moment determined by the Evans method in C_6D_6 of μ_{eff} = 5.8(1) μ_B (per manganese center) agrees with a high spin d^5 configuration with no deviation from the spin only value for five unpaired electrons per metal ion.[13]

We were interested in utilizing **1** as starting material for the preparation of low-coordinate NHC manganese(II) complexes and therefore turned to the investigation of salt metathesis reactions with s-block alkyls and amides. No defined products were obtained with *i*PrMgCl. The reaction of **1** with four equivalents of MeMgI in tetrahydrofuran gave the dinuclear methyl magnesium complex **2** as yellowish crystals (Scheme 3). The yield of **2** could not be determined due to rapid decomposition of these crystals to unidentifiable products even at lower temperatures. Thus, a complete characterization of **2** was not possible.

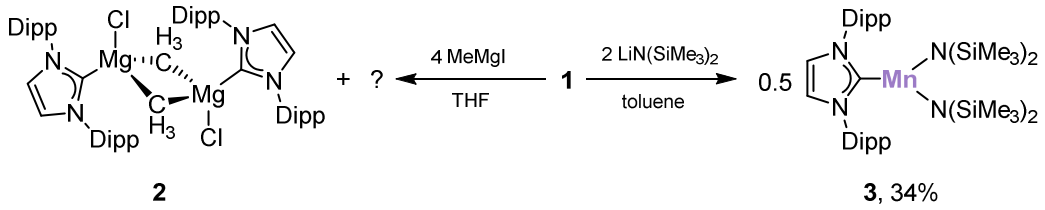

2 **3**, 34%

Scheme 3. Reactivity of **1**.

The X-ray diffraction analysis on a single crystal of **2** revealed a centrosymmetric dinuclear methyl-bridged magnesium complex with a distorted tetrahedral environment (Figure 2, left). Interestingly, the magnesium atoms are coordinated by the NHC and a chloride atom, which have been transferred from the manganese complex **1** demonstrating the lability of the manganese(II)−carbon bond. The Mg1−C1 (2.228(2) Å) and Mg1−Cl1 (2.3701(9) Å) bond distances in **2** compare well to other reported Mg(II) carbene complexes.[14] Moreover, the Mg_2Me_2 core exhibits a short Mg−Mg' distance of 2.7362(13) Å, which is a typical feature for this type of unit.[15]

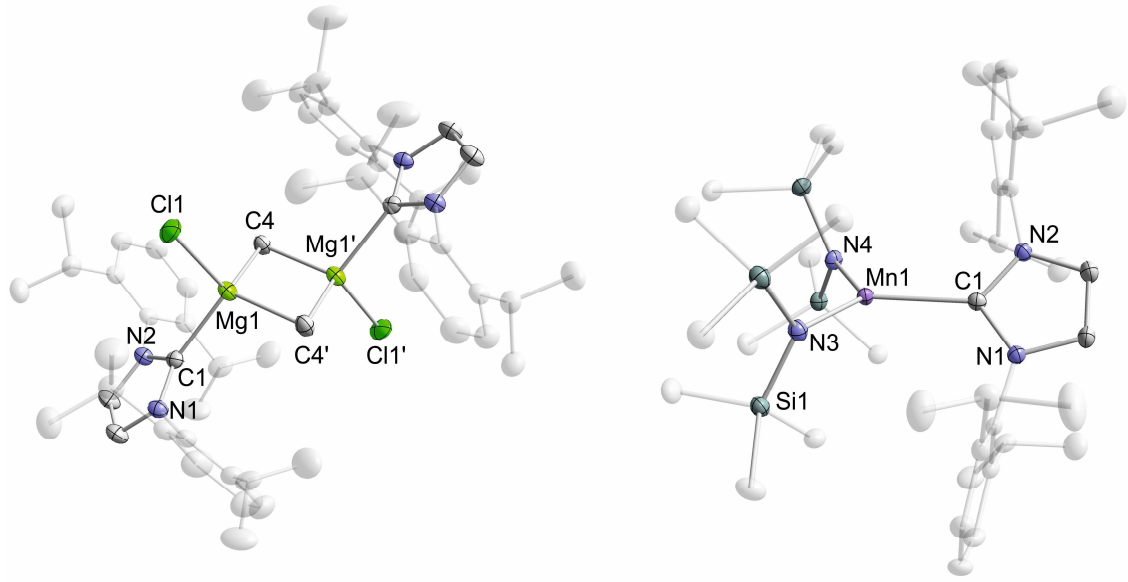

Figure 2. Solid-state molecular structure of $[(IDipp)MgMeCl]_2$ (**2**, left) and $[(IDipp)Mn\{N(SiMe_3)_2\}_2]$ (**3**, right). The hydrogen atoms are omitted for clarity. Thermal ellipsoids are drawn at 40% level. Selected bond lengths [Å] and angles [°] $[(IDipp)MgMeCl]_2$: Mg1−C1 2.228(2), Mg1−Cl1 2.3701(9), Mg1−C4 2.262(2), Mg1−C4' 2.262(2), Mg1−Mg1' 2.7362(13), C1−Mg1−Cl1 108.24(6), C1−Mg1−C4 111.03(8)), C1−Mg1−C4' 110.65(8), C4−Mg1−C4' 105.35(7), Mg1−C4−Mg1' 74.65(7), Mg1−C4'−Mg1' 74.65(7), **2**: Mn1−C1 2.254(2), Mn1−N3 2.0491(19), Mn1−N4 2.0589(18), C1−Mn1−N3 117.75(8), C1−Mn1−N4 119.87(8), N3−Mn1−N4 122.33(8).

In contrast, the low-coordinate complex **3** was isolated from the reaction of **1** with four equivalents of lithium hexamethyldisilazide. (Scheme 3). The compound was obtained in modest yield (34%) by crystallization from toluene. Complex **3** shows a similar solubility as **1** and is extremely oxygen and moisture sensitive.

The molecular structure of **3** shows the formation of a slightly distorted trigonal planar (Σ_{angles} = 359.95°) complex bearing the NHC and two amido ligands. The Mn1−C1 bond length (2.254(2) Å) is elongated by 0.07 Å compared to the starting material **1** (Figure 2). In comparison with the $Mn-N_{terminal}$ distances in the related manganese(II) amides $[Mn\{N(SiMe_3)_2\}\{\mu\text{-}N(SiMe_3)_2\}]_2$ (1.994 Å), $[(thf)Li(\mu\text{-}N(SiMe_3)_2)_2Mn\{N(SiMe_3)_2\}]$ (2.023(3) Å), and $[Mn\{N(SiMe_3)_2\}_2(thf)_2]$ (2.033(5) Å) the corresponding bond lengths in **3** are longer by 0.02 − 0.07 Å (2.0491(19) – 2.0589(18) Å).[16] Very recently, Braunstein and coworkers isolated the isostructural complex $[(IDipp)Co\{N(SiMe_3)_2\}_2]$ and related complexes in the reaction of $[Co\{N(SiMe_3)_2\}_2]$ with IDipp.[17] According to the smaller ion radius of cobalt(II) (d^7 high spin) compared to manganese(II) the Co complexes feature shorter $Co-C_{Carbene}$ (2.119(3) Å) and Co−N (1.958(3) and 1.966(2) Å) bond length.

The coordinatively and electronically unsaturated complex **3** features Mn1−H28B and Mn1−H39A bond lengths of 2.62(4) and 2.68(3) Å, respectively, which indicate the presence of anagostic interactions of the methyl C−H groups of the amide and the manganese atom as illustrated in Figure 3.[18]

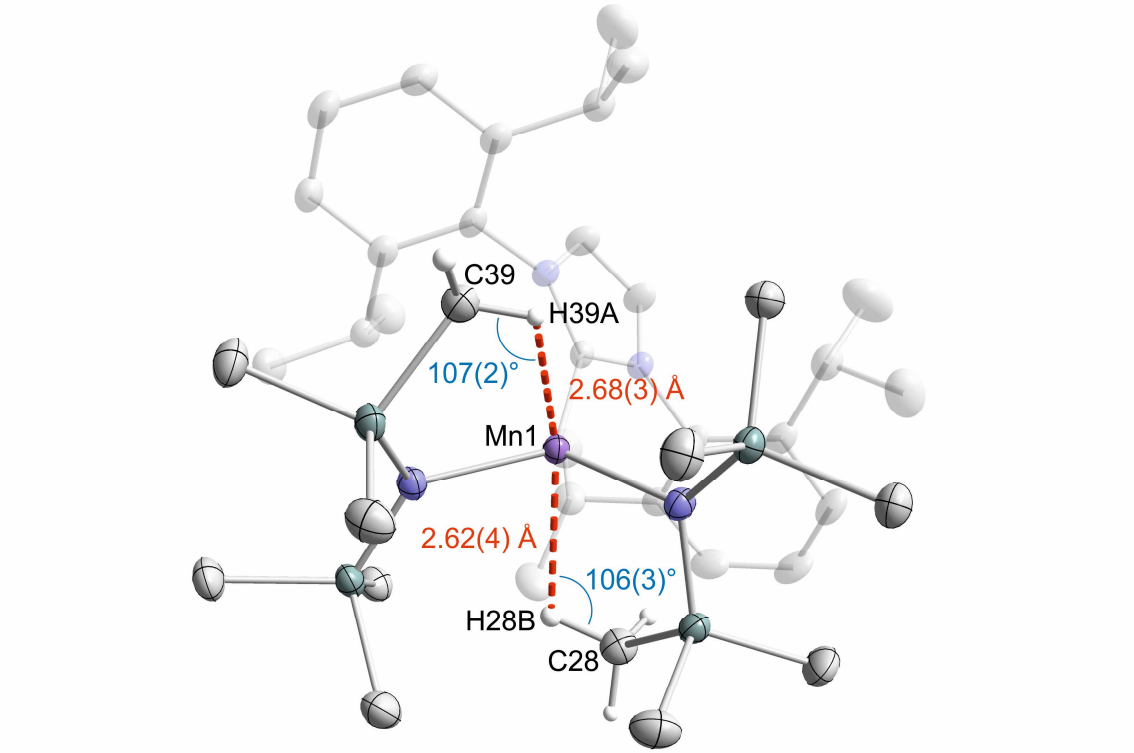

Figure 3. Illustration of the possible anagostic interaction in the molecular structure of **3** with highlighted Mn−H distances (red) and Mn−H−C angles (blue).

All hydrogen atoms in **3** were located in the Fourier difference map and refined freely. Besides these weak electrostatic interactions no other interactions with the metal center were detected in the molecular structure of **3**. Compley **3** represents a rare example of a three-coordinate NHC-stabilized manganese(II) complex.

The ^{1}H NMR spectrum of **3** at room temperature (C_6D_6) shows only broad signals in the range of 1.3 to 8.5 ppm similar to **1**. The solution magnetic moment (Evans' method) of μ_{eff} = 5.8(1) μ_B is very close to the expected spin-only value for a high spin d^5 center.

7.3 Conclusion

In summary, we described the gram scale synthesis of the NHC-stabilized manganese(II) chloride **1** from commercially available starting materials and investigated its ability as precursor for low-coordinate manganese(II) NHC complexes. Our results reproduce the work of Tonzetich *et al.*, who independently reported the preparation of **1** in 2015.[b] The single crystal X-ray analysis of **1-THF** indicate the dissociation of the dimer **1** in tetrahydrofuran solutions. In addition, XRD analysis of the dinuclear compound [(IDipp)MgMeCl]$_2$ (**2**) showed that the IDipp and the chloride ligands were transferred from manganese in **1** to the magnesium atom, demonstrating the lability of the manganese(II)−carbon bond in **1** as a result of the reaction of **1** with four equivalents of MeMgI. The monomeric amide **3** was isolated in modest yield by reacting **1** with four equivalents lithium hexamethyldisilazide. Compound **3** features a trigonal planar coordination environment and represents a rare example of a three-coordinate NHC-stabilized manganese(II) complex. Solution magnetic moments showed the presence of d^5 high spin manganese(II) centers in **1** and **3**.

7.4 Supporting Information (SI)

7.4.1 General Procedures

All experiments were performed under an atmosphere of dry argon using standard Schlenk techniques or an MBraun UniLab glovebox. Solvents were dried and degassed with an MBraun SPS800 solvent purification system. Tetrahydrofuran and toluene were further dried by storing the solvent over molecular sieves (3 Å). *N*-pentane was distilled from Na/benzophenone and further dried over molecular sieves (3 Å). NMR spectra were recorded on a Bruker Avance 400 spectrometers at 300 K and internally referenced to residual solvent resonances. Melting points were measured on samples in sealed capillaries on a Stuart SMP10 melting point apparatus. Elemental analyses were determined by the analytical department of Regensburg University. The starting material 1,3-bis-(2,6-diisopropylphenyl)imidazolin-2-ylidene was prepared according to literature procedure. Manganese(II) chloride and lithium hexamethyldisilazide were purchased from Sigma Aldrich and used as received.

7.4.2 Synthesis of [MnCl(μ-Cl)(IDipp)]$_2$ (1)

Manganese(II) chloride (557 mg, 4.43 mmol, 1.0 eq) and 1,3-bis-(2,6-diisopropylphenyl)-imidazolin-2-ylidene) (1.72 g, 4.43 mmol, 1.0 eq) were dissolved in tetrahydrofuran (50 mL) and the mixture was stirred for 21 hours. The solvent was removed in *vacuo* and the residue extracted with toluene (30 mL). After filtration the solution was reduced in volume to 25 mL. Colorless, X-ray quality crystals of **1** were formed after storing the solution at −30 °C and subsequently washed with *n*-pentane (5 mL). Yield: 1.66 g (73%); m.p. >248 °C (decomp. to a yellowish grey oil); elemental analysis calcd. for $C_{27}H_{36}N_2MnCl_2$ (M = 514.44): C 63.04, H 7.05, N 5.45, found: C 63.10, H 6.97, N 5.33; ^{1}H NMR (C_6D_6, 300 K, 400.13 MHz): δ /ppm = 1.9 (br s), 5.6 (br s), 8.7 (br s); effective magnetic moment: μ_{eff} = 5.8(1) μ_B.

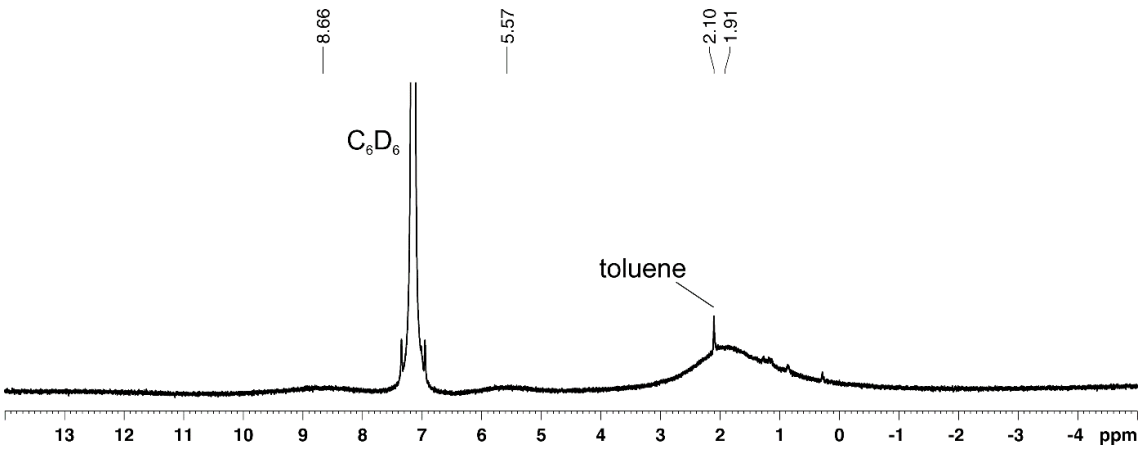

Figure S1. ^{1}H NMR spectrum of **1** (400.16 MHz, C_6D_6, 300 K).

7.4.3 Synthesis of [(IDipp)Mn{N(SiMe$_3$)$_2$}$_2$] (3)

A solution of lithium hexamethyldisilazide (403 mg, 2.41 mmol, 2.0 eq) in toluene (35 mL) was added to a solution of **1** (620 mg, 1.20 mmol, 1.0 eq) in toluene (5 mL) at room temperature. After stirring the reaction mixture for three hours at room temperature a colorless precipate was observed and the suspension was filtered. The solution was slightly reduced to 35 mL and filtered again in order to remove LiCl entirely. Afterwards the solution is concentrated to 12 mL. By storing the solution at −35 °C colorless, X-ray quality crystals (216 mg) of **3** were formed and washed with *n*-hexane (2 mL). The solution was further concentrated and stored at −35 °C to yield another crop of crystals, which were washed with *n*-hexane (1 mL). Overall yield: 313 mg (34%); m.p. >171 °C (decomp. to a yellow oil); elemental analysis calcd. for $C_{39}H_{72}N_4MnSi_4$ (M = 764.31): C 61.29, H 9.50, N 7.33, found: C 61.64, H 9.36, N 7.12; ^{1}H NMR (C_6D_6, 300 K, 400.13 MHz) δ /ppm = 1.3 (br s), 6.6 (br s), 8.5 (br s); effective magnetic moment: μ_{eff} = 5.8(1) μ_B.

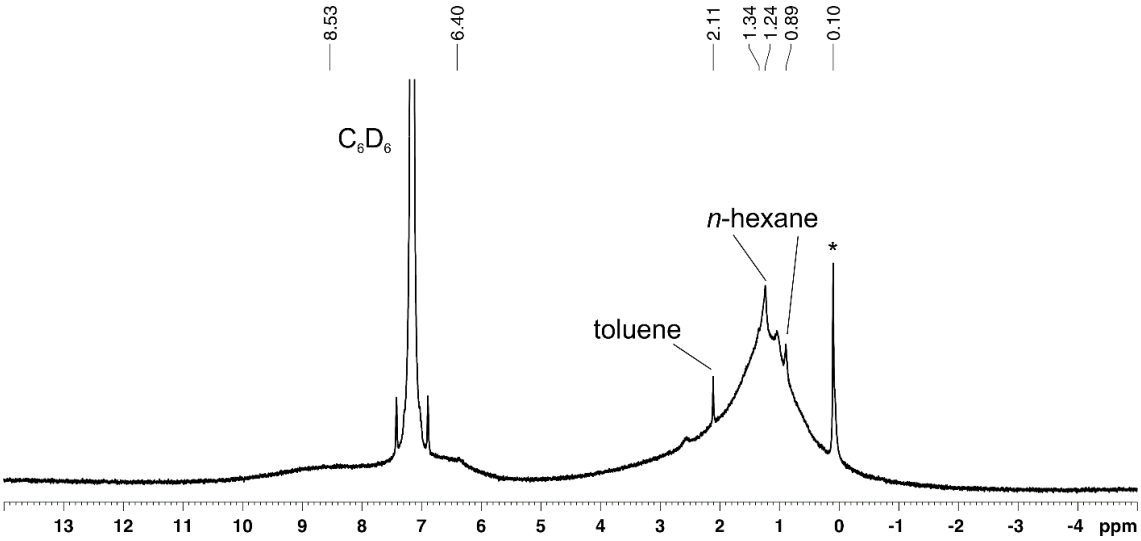

Figure S2. ^{1}H NMR spectrum of **3** (400.16 MHz, C_6D_6, 300 K). Minor amounts of HN(SiMe$_3$)$_2$ are labeled with an asterisk.

7.4.4 X-ray Crystallography

The single crystal X-ray diffraction data were recorded on an Agilent Technologies Gemini Ultra R diffractometer in case of **1** and **2**, and an Agilent Technologies SuperNova in case of **1-THF** and **3** with Cu K_α radiation (λ = 1.54184 Å). Semi-empirical multi-scan absorption corrections[16] and analytical ones[20] were applied to the data. The structures were solved with SHELXT[21] and least-square refinements on F^2 were carried out with SHELXL.[21]

Table S1. Crystallographic data of **1-THF**−**3**.

Compound	**1-THF**	**1**	**2**	**3**
Empirical formula	$C_{38}H_{52}Cl_2MnN_2O$	$C_{37.5}H_{48}Cl_2MnN_2$	$C_{28}H_{39}ClMgN_2$	$C_{39}H_{72}MnN_4Si_4$
Formula weight	678.65	652.62	463.37	764.30
Temperature [K]	123(1)	123(1)	123(1)	123(1)
Crystal system	orthorhombic	monoclinic	monoclinic	triclinic
Space group	$P2_12_12_1$	$P2_1/c$	$P2_1/n$	P-1
a [Å]	12.8489(13)	13.20707(17)	12.44207(14)	11.2591(6)
b [Å]	16.0783(11)	16.3993(2)	14.29553(18)	11.8980(5)
c [Å]	18.2755(13)	16.8217(2)	16.3144(2)	19.1006(8)
α [°]	90	90	90	83.979(4)
β [°]	90	91.7138(11)	94.6791(11)	79.894(4)
γ [°]	90	90	90	63.325(5)
Volume [Å^3]	3775.5(5)	3641.72(8)	2892.10(6)	2249.9(2)
Z	4	4	4	2
ρ_{calc} [g/cm^3]	1.194	1.190	1.064	1.128
μ [mm^{-1}]	4.363	4.485	1.485	3.620
F(000)	1444.0	1384.0	1000.0	830.0
Crystal size [mm^3]	0.3586 × 0.2153 × 0.2058	0.3045 × 0.2221 × 0.2157	0.4353 × 0.2336 × 0.2231	0.3342 × 0.2633 × 0.146
Radiation	CuKα (λ = 1.54184)	CuKα (λ = 1.54184)	CuKα (λ = 1.54184)	CuKα (λ = 1.54184)
2Θ range for data collection [°]	8.41 to 148.31	6.70 to 133.45	8.24 to 133.43	8.32 to 147.44
Index ranges	−12 ≤ h ≤ 15, −18 ≤ k ≤ 19, −15 ≤ l ≤ 22	−15 ≤ h ≤ 15, −18 ≤ k ≤ 19, −19 ≤ l ≤ 20	−14 ≤ h ≤ 13, −16 ≤ k ≤ 15, −19 ≤ l ≤ 14	−9 ≤ h ≤ 13, −14 ≤ k ≤ 14, −22 ≤ l ≤ 23
Reflections collected	8378	30162	17902	19269
Independent reflections	6017 [R_{int} = 0.0504, R_{sigma} = 0.0721]	6394 [R_{int} = 0.0330, R_{sigma} = 0.0250]	5078 [R_{int} = 0.0242, R_{sigma} = 0.0196]	8704 [R_{int} = 0.0220, R_{sigma} = 0.0265]
Data/restraints/parameters	6017/96/446	6394/163/445	5078/0/309	8704/0/453
Goodness-of-fit on F^2	1.034	1.045	1.168	1.092
Final R indexes [I>=2σ (I)]	R_1 = 0.0891, wR_2 = 0.2319	R_1 = 0.0547, wR_2 = 0.1539	R_1 = 0.0507, wR_2 = 0.1453	R1 = 0.0389, wR2 = 0.1131
Final R indexes [all data]	R_1 = 0.1046, wR_2 = 0.2502	R_1 = 0.0612, wR_2 = 0.1644	R_1 = 0.0528, wR_2 = 0.1468	R1 = 0.0415, wR2 = 0.1148
Largest diff. peak/hole [e Å^{-3}]	0.46/−0.58	0.68/−0.50	0.53/−0.33	0.74/−0.35
Flack parameter	0.060(11)	-	-	-

References

1 Reviews: a) S. J. Hock, L.-A. Schaper, W. A. Herrmann, F. E. Kühn, *Chem. Soc. Rev.* **2013**, *42*, 5073–5089; b) R. A. Layfield, *Chem. Soc. Rev.* **2008**, *37*, 1098–1107.

2 Selected publications: a) H. Mutoh, S. Masuda, *J. Chem. Soc., Dalton Trans.* **2002**, 1875–1881; b) L. K. Engerer, C. N. Carlson, T. P. Hanusa, W. W. Brennessel, V. G. Young, *Organometallics* **2012**, *31*, 6131–6138.

3 Manganese(III) NHC complexes: a) S. Bellemin-Laponnaz, R. Welter, L. Brelot, S. Dagorne, *J. Organomet. Chem.* **2009**, *694*, 604–606; b) T. Yagyu, K. Yano, T. Kimata, K. Jitsukawa, *Organometallics* **2009**, *28*, 2342–2344.

4 Manganese(IV) NHC complex: A. P. Forshaw, R. P. Bontchev, J. M. Smith, *Inorg. Chem.* **2007**, *46*, 3792–3794.

5 Manganese(III), (IV) and (V) NHC complexes: H. Kropp, A. E. King, M. M. Khusniyarov, F. W. Heinemann, K. M. Lancaster, S. DeBeer, E. Bill, K. Meyer, *J. Am. Chem. Soc.* **2012**, *134*, 15538–15544.

6 Manganese(II) NHC complexes with a coordination number of four and higher: a) C. D. Abernethy, A. H. Cowley, R. A. Jones, C. L. B. Macdonald, P. Shukla, L. K. Thompson, *Organometallics* **2001**, *20*, 3629–3631; b) J. Chai, H. Zhu, K. Most, H. W. Roesky, D. Vidovic, H.-G. Schmidt, M. Noltemeyer, *Eur. J. Inorg. Chem.* **2003**, *2003*, 4332–4337; c) J. Chai, H. Zhu, Y. Peng, H. W. Roesky, S. Singh, H.-G. Schmidt, M. Noltemeyer, *Eur. J. Inorg. Chem.* **2004**, *2004*, 2673–2677; d) D. Pugh, J. A. Wright, S. Freeman, A. A. Danopoulos, *Dalton Trans.* **2006**, 775–782; e) J. M. Smith, J. R. Long, *Inorg. Chem.* **2010**, *49*, 11223–11230;

7 A. R. Kennedy, J. Klett, R. E. Mulvey, S. D. Robertson, *Eur. J. Inorg. Chem.* **2011**, *2011*, 4675–4679.

8 R. A. Musgrave, R. S. P. Turbervill, M. Irwin, J. M. Goicoechea, *Angew. Chem.* **2012**, *124*, 10990–10993, *Angew. Chem. Int. Ed.* **2012**, *51*, 10832–10835.

9 P. P. Samuel, K. C. Mondal, H. W. Roesky, M. Hermann, G. Frenking, S. Demeshko, F. Meyer, A. C. Stückl, J. H. Christian, N. S. Dalal, L. Ungur, L. Chibotaru, K. Prçpper, A. Meents, B. Dittrich, *Angew. Chem.* **2013**, *125*, 12033–12037, *Angew. Chem. Int. Ed.* **2013**, *52*, 11817–11821.

10 S. Pelties, D. Herrmann, B. de Bruin, F. Hartl, R. Wolf, *Chem. Commun.* **2014**, *50*, 7014–7016.

11 An isostructural iron complex [(IDipp)$FeCl_2$(thf)] has been described earlier by our group, see: M. Plois, *diploma thesis* **2010**, WWU Münster.

12 Related Fe and Co complexes: a) J. A. Przyojski, H. D. Arman, Z. J. Tonzetich, *Organometallics* **2012**, *31*, 3264–3271; b) K. Matsubara, T. Sueyasu, M. Esaki, A. Kumamoto, S. Nagao, H. Yamamoto, Y. Koga, S. Kawata, T. Matsumoto, *Eur. J. Inorg. Chem.* **2012**,

2012, 3079–3086; c) K. Matsubara, A. Kumamoto, H. Yamamoto, Y. Koga, S. Kawata, *J. Organomet. Chem.* **2013**, *727*, 44–49.

13 a) D. F. Evans, *J. Chem. Soc.* **1959**, 2003–2005; b) G. J. P. Britovsek, V. C. Gibson, S. K. Spitzmesser, K. P. Tellmann, A. J. P. White, D. J. Williams, *J. Chem. Soc. Dalton Trans.* **2002**, 1159–1171.

14 Selected publications on magnesium(II) NHC complexes: a) A. J. Arduengo, F. Davidson, R. Krafczyk, W. J. Marshall, M. Tamm, *Organometallics* **1998**, *17*, 3375–3382; b) M. Arrowsmith, M. S. Hill, D. J. MacDougall, M. F. Mahon, *Angew. Chem.* **2009**, *121*, 4073–4076, *Angew. Chem. Int. Ed.* **2009**, *48*, 4013–4016; c) A. R. Kennedy, R. E. Mulvey, S. D. Robertson, *Dalton Trans.* **2010**, *39*, 9091–9099.

15 Selected publications on methyl-bridged magnesium(II) dimers: a) A. D. Pajerski, M. Parvez, H. G. Richey, *J. Am. Chem. Soc.* **1988**, *110*, 2660–2662; b) P. J. Bailey, R. A. Coxall, C. M. Dick, S. Fabre, S. Parsons, L. J. Yellowlees, *Chem. Commun.* **2005**, 4563–4565; c) O. Michel, C. Meermann, K. W. Törnroos, R. Anwander, *Organometallics* **2009**, *28*, 4783–4790.

16 a) D. C. Bradley, M. B. Hursthouse, K. M. A. Malik, R. Möseler, *Transition Met. Chem.* **1978**, *3*, 253–254; b) B. D. Murray, P. P. Power, *Inorg. Chem.* **1984**, *23*, 4584–4588; c) D. C. Bradley, M. B. Hursthouse, A. A. Ibrahim, K. M. A. Malik, M. Motevalli, R. Möseler, H. Powell, J. D. Runnacles, A. C. Sullivan, *Polyhedron* **1990**, *9*, 2959–2964.

17 A. Massard, P. Braunstein, A. A. Danopoulos, S. Choua, P. Rabu, *Organometallics* **2015**, *34*, 2429–2438.

18 a) W. I. Sundquist, D. P. Bancroft, S. J. Lippard, *J. Am. Chem. Soc.* **1990**, *112*, 1590–1596; b) W. Yao, O. Eisenstein, R. H. Crabtree, *Inorg. Chimica Acta* **1997**, *254*, 105–111; c) Y. Zhang, J. C. Lewis, R. G. Bergman, J. A. Ellman, E. Oldfield, *Organometallics* **2006**, *25*, 3515–3519.

19 a) SCALE3ABS, CrysAlisPro, Aglient Technologies Inc., Oxford, UK, 2015; b) G. M. Sheldrick, SADABS, Bruker AXS, Madison, USA, 2007.

20 a) R. C. Clark, J. S. Reid, *Acta Crystallogr. A* **1995**, *51*, 887; b) CrysAlisPro, Agilent Technologies Inc., Oxford, UK, 2015.

21 G. M. Sheldrick, *Acta Crystallogr. Sect. Found. Adv.* **2015**, *71*, 3.

22 G. M. Sheldrick, *Acta Crystallogr. A* **2008**, *64*, 112.

8 Synthesis and Reactivity Studies of a Heteroleptic α-Diimine Cobalt Anion[a,b]

Stefan Pelties, Dirk Herrmann, Thomas Maier, and Robert Wolf

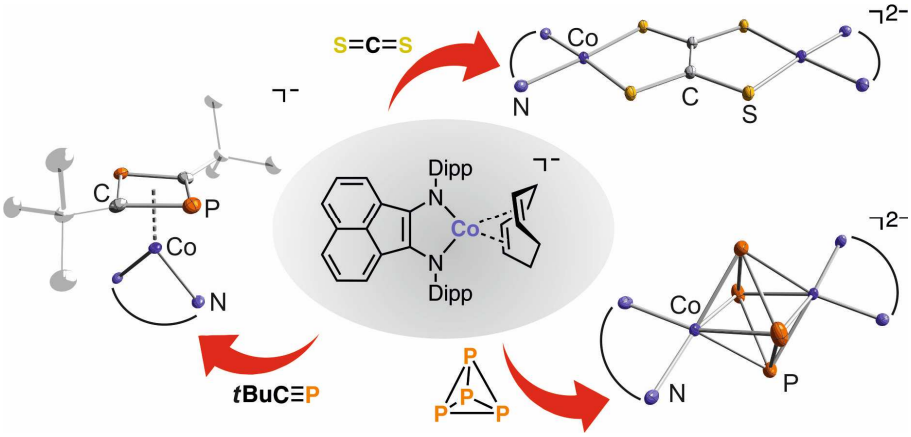

[a] S. Pelties, D. Herrmann, T. Maier, R. Wolf, manuscript in preparation.

[b] Dirk Herrmann carried out the electrochemical measurements (Figures 4, S10–S12). Thomas Maier prepared compound **5** as part of his MSc thesis.

8.1 Introduction

Low-valent cobalt complexes with labile ligands are potentially useful for the activation of small molecules, as catalysts and as sources for cobalt anions, but due to the paucity of appropriate compounds they have only rarely been applied in this regard.[1–4] Heteroleptic complexes with both labile and non-labile ligands are particularly promising in this context. Based on their good π-accepting properties α-diimines can exhibit substantial redox-active character, and therefore they are predestined as electron reservoirs in low-valent 3d metal complexes. Besides profound experimental and theoretical studies on the redox-active nature of formally low-valent homoleptic transition metal complexes rather little is known about corresponding heteroleptic α-diimine complexes.[5] Uhlig *et al.* reported on the synthesis of anionic complexes **B** and **C** by reacting Jonas' bis(cod)cobaltate (**A**, cod = 1,5-cyclooctadiene) with appropriate α-diimines and 2,2'-bipyridine, but these compounds were only characterised by elemental analysis and their magnetic moments (Chart 1).[1,2] By reacting [K([18]crown-6)][Co(η^4-$C_{10}H_8$)(cod)] with 2,2'-bipyridine the group of Ellis obtained complex **C**, which was structurally characterised.[3] Very recently, the group of Yang described the synthesis of two dianionic cobalt complexes (**D** and **E**) by reducing the neutral complex [{CMeN(2,6-*i*$Pr_2C_6H_3$)}$_2$Co]$_2$ with sodium metal in presence of pyrene, and investigated their electronic configuration by X-ray diffraction analysis, EPR spectroscopy, magnetic susceptibility measurement as well as DFT studies.[6]

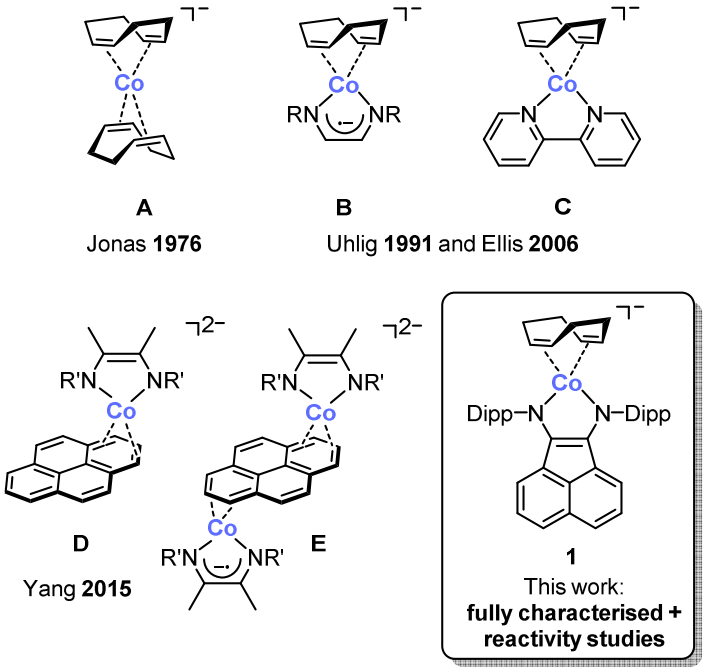

Chart 1 Jonas's $[Co(1,5\text{-cod})]^-$ (**A**) and known heteroleptic α-diimine cobalt anions (**B**–**E**). R = *p*-tolyl, 2,6-diisopropylphenyl (Dipp), R' = Dipp.[1–3,6]

However, besides the synthesis and characterisation of these complexes no attempts to explore the general reactivity of anionic α-diimine cobalt complexes have been made so far.

Here, we report the preparation of the new complex [K(OEt_2)][Co(BIAN)(cod)] (**1**, Fig. 1b), bearing the redox-active BIAN ligand (bis(2,6-diisopropylphenylimino)acenaphthene), as well as its reactivity toward carbon disulfide, *tert*-butylphosphaalkyne and white phosphorus for the first time. In the reaction with carbon disulfide and *tert*-butylphosphaalkyne the dinuclear dianion **2** bearing a bridging ethylene tetrathiolate ligand and the monomeric complex **3** with a terminal 1,3-diphosphacyclobutadiene, respectively, are formed upon dimerisation of the substrates in the coordination sphere of the metal. Moreover, complex **1** activates P_4 selectively under mild conditions, affording the new Co_2P_4 dianion **4**. Tetraphosphide **4** features five redox-active entities (2x BIAN, 2x Co, 1x P_4), including an uncommon rectangular P_4 fragment. Preparative oxidation of **4** yields monoanion **5**, which is the first example of a 3d metal complex with a cyclo-P_4^{4-} ligand.

8.2 Results and Discussion

8.2.1 Synthesis and Characterisation of 1

[K(Et$_2$O)][Co(BIAN)(cod)] (**1**) is readily accessible on a gram scale by reacting BIAN with [K(thf)$_{0.2}$][Co(cod)$_2$] in THF at room temperature (Scheme 1). Monitoring by ^{1}H NMR spectroscopy revealed a selective reaction course for the formation of **1**. Compound **1** was isolated as a highly oxygen and moisture sensitive black solid by crystallisation from diethyl ether in 71% yield. The compound dissolves poorly in non-polar solvents such as *n*-hexane, benzene and toluene, but it is soluble in diethyl ether as well as THF.

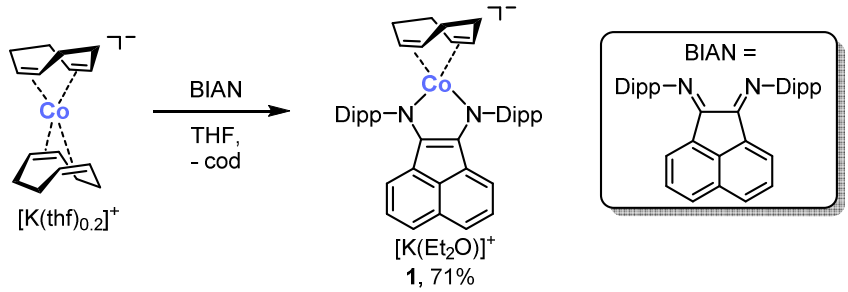

Scheme 1 Synthesis of **1**.

The single crystal X-ray analysis of **1** revealed a slightly distorted square planar coordination environment for cobalt with a twist angle of 17.6° (Figure 1a). Compared to the starting material **A** the Co−C bond lengths (2.012(2) − 2.050(2) Å) and the C−C double bond lengths of the cod ligand (1.390(4) − 1.396(3) Å) in **1** are in a similar range.[1] As illustrated in Figure 1b BIAN ligands feature characteristic structural parameters, which can be often used for the evaluation of the oxidation levels (closed-shell neutral form (BIAN), open-shell π-radical monoanion (BIAN$^-$) and closed-shell dianion (BIAN^{2-})).[5,7,8,9] The C1−N1 (1.380(3) Å), C2−N2 (1.382(3) Å) and C1−C2 (1.383(3) Å) bond lengths in **1** clearly indicate a BIAN^{2-} ligand, which leaves a formal oxidation state of +I for the cobalt atom. The closed-shell dianion (BIAN^{2-}) is more frequently observed in formally low-valent complexes of more electropositive elements such as Mg or Al but expected for an electron-rich metal centre.[9] In contrast, the isoelectronic complex [Ni(BIAN)(cod)] synthesised by Stephan *et al.* features considerably shorter C−N (1.324 − 1.336 Å) and longer C−C bond distances (1.426 − 1.428 Å) which is presumably due to the higher effective nuclear charge of nickel compared to cobalt.[10] The potassium cation is in contact with the anion via an η^4-interaction with the α-diimine unit and additional coordination by two THF molecules (Figure 1a).

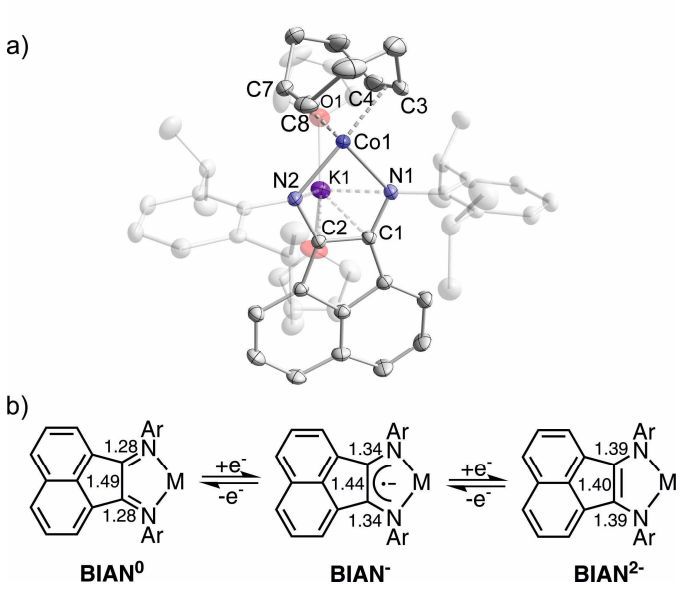

Figure 1 a) solid-state molecular structure of $[K(thf)_2][Co(BIAN)(cod)]$ (**1**). The hydrogen atoms are omitted for clarity. Thermal ellipsoids are drawn at 40% level. Selected bond lengths [Å] and angles [°]: Co1−C3 2.029(2), Co1−C4 2.028(2), Co1−C7 2.050(2), Co1−C8 2.012(2), Co1−N1 1.953(2), Co1−N2 1.936(2), C1−N1 1.380(3), C2−N2 1.382(2), C1−C2 1.383(3), C3−C4 1.390(4), C7−C8 1.396(3), N1−Co1−N2 84.14(7). b) Average C−N and C−C bond lengths of different oxidation states of known BIAN complexes.[5,7,8,9]

Compound **1** is diamagnetic in agreement with a square planar Co(I) centre and the closed-shell $BIAN^{2-}$ dianion. However, the ^{1}H NMR spectrum of **1** features slightly broadened multiplets (Figure S1). A variable temperature ^{1}H NMR experiment of **1** showed that the methine protons of the cod ligand give rise to a multiplet with a half-width of τ_{FWHM}(cod-CH) = 23 Hz at room temperature (THF-d_8, Figure S2). Warming the solution to 50 °C resulted in a decrease of the half-width to τ_{FWHM}(cod-CH) = 12 Hz (Figure S2). In contrast, the half-width of the signal of the methyl hydrogen nuclei (Dipp substituent, $\tau_{FWHM}(CH(CH_3)_2)$ = 12 Hz) did not change upon warming from room temperature to 50 °C. In this context it is worth mentioning that Jonas and Ellis also reported broad ^{1}H NMR signals for the related cobaltates $[Li(thf)_2][Co(1,5\text{-cod})_2]$ and $[K([18]crown\text{-}6)][Co(\eta^4\text{-}C_4H_6)_2]$.[1,3] The ^{1}H and $^{13}C\{^1H\}$ NMR data of compound **1** show one set of BIAN signals, which is in accord with the molecular structure derived by the single crystal X-ray diffraction analysis. The cod ligand in **1** gives rise to three multiplets in the ^{1}H NMR spectrum at 1.12 (CH_2), 2.33 (CH_2) and 2.91 (CH) ppm. The latter signal is significantly upfield shifted. Ellis *et al.* presumed an interaction of the electron-rich metal centre with the coordinated 1,5-cod as cause for this phenomenon in the anion $[Co(cod)_2]^-$.[3] The $^{13}C\{^1H\}$ NMR spectrum features two signals for the carbon nuclei of the cod ligand at 32.6 (CH_2) and 64.1 ppm (CH).

8.2.2 Reactivity Studies of 1 with Carbon Disulfide and *tert*-Butylphosphalkyne

In order to probe the reactivity of the novel cobalt anion we reacted **1** with electrophilic molecules. The 1:1 reaction of **1** with carbon disulfide at room temperature in THF gave complex **2** as a dark purple, almost black solid in moderate yield by crystallisation from THF/diethyl ether (Scheme 2). Compound **2** is sparingly soluble in THF and acetonitrile, but soluble in DMF.

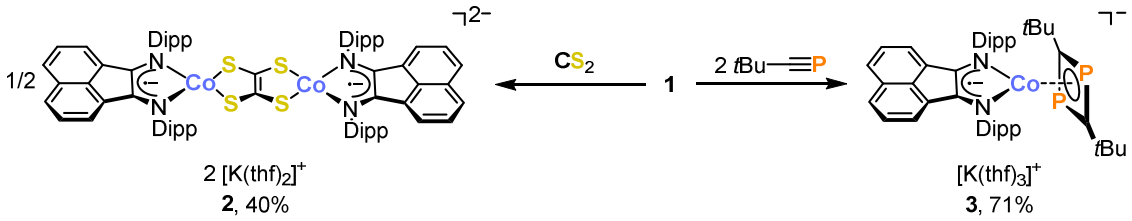

Scheme 2 Reactivity of **1** toward carbon disulfide and *tert*-butylphosphaalkyne.

The molecular structure of **2** shows two (BIAN)Co fragments bridged by a $C_2S_4^{4-}$ unit as an outcome of the reductive head-to-head dimerization of CS_2 (Figure 2, left).[11] The two halves of the planar molecule are related by an inversion centre located at the centroid between C3−C3', and both cobalt centres possess a square planar coordination environment. Compared to the starting material **1** the Co−N bond lengths are shortened by about 0.03 Å. The bridging ligand features C−S single bonds (C3−S1 1.756(2) and C3−S2 1.756(2) Å) and a C=C double bond (C3−C3' 1.348(3) Å), which are diagnostic for an ethylene tetrathiolate ligand.[11] The potassium ions in **2** show an η^3-interaction with the bridging ligand and are coordinated by two DME molecules. The metric parameters of the BIAN ligand (C1−N1 1.332(2), C2−N2 1.332(2), C1−C2 1.418(2) Å) indicate the presence of a monoanionic π-radical resulting in a formal oxidation state of +II for the cobalt centres.

Compound **2** is diamagnetic probably due to a strong antiferromagnetic coupling between the monoanionic BIAN ligands and the Co centres. The ^{1}H and ^{13}C{^{1}H} NMR spectra in DMF-d_7 of complex **2** feature one signal set for the BIAN ligand and the C_2S_4 moiety in agreement with its symmetric structure. However, the assignment of the quaternary carbon nuclei was not possible due to the low solubility of **2**.

The reaction of **1** with two equivalents of *tert*-butylphosphaalkyne afforded complex **3** in a very selective fashion according to ^{1}H NMR monitoring (Scheme 2). Compound **3** was obtained as a dark turquoise, almost black solid in 71% isolated yield by crystallisation from THF/*n*-hexane. The isolated crystals are soluble in diethyl ether, THF and acetonitrile.

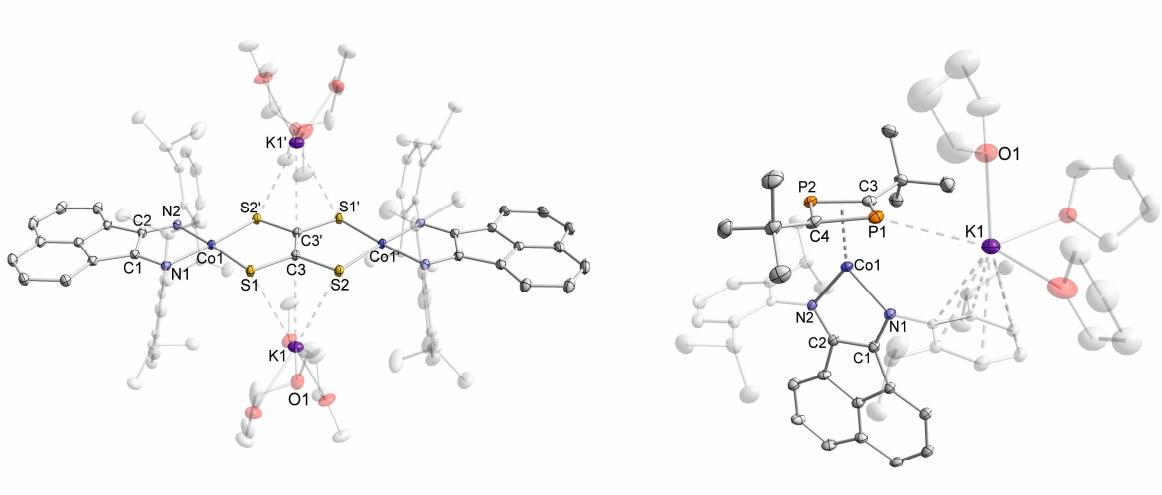

Figure 2 Solid-state molecular structure of $[K(dme)_2]_2[\{(BIAN)Co\}_2(\mu\text{-}C_2S_4)]$ (**2**, left), $[K(thf)_3][(BIAN)Co(P_2C_2tBu_2)]$ (**3**, right). The hydrogen atoms are omitted for clarity. Thermal ellipsoids are drawn at 40% level. Selected bond lengths [Å] and angles [°] **2**: Co1−S1 2.1682(4), Co1−S2' 2.1786(5), Co1−N1 1.911(1), Co1−N2 1.914(1), C3−S1 1.756(2), C3−S2 1.756(2), C3−C3' 1.348(3), C1−N1 1.332(2), C2−N2 1.332(2), C1−C2 1.418(2), S1−C3−S2 120.70(9), S2−C3−C3' 119.8(2), S1−C3−C3' 119.5(2), N1−Co1−N2 83.34(6), **3**: Co1−P1 2.2673(13) (2.261(1)), Co1−P2 2.268(1) (2.274(1)), Co1−C3 2.096(4) (2.103(5)), Co1−C4 2.106(4) (2.098(4)), Co1−N1 1.929(3) (1.923(4)), Co1−N2 1.909(4) (1.912(4)), C1−N1 1.358(6) (1.363(6)), C2−N2 1.351(5) (1.354(6)), C1−C2 1.398(6) (1.393(6)), P1−C3 1.803(5) (1.788(5)), P2−C4 1.802(4) (1.788(5)), P1−C3−P2 98.3(2) (98.5(2)), C3−P2−C4 81.4(2) (81.4(2)), N1−Co1−N2 84.3(2) (84.5(2)).

The molecular structure of **3** reveals that the labile cod ligand has been replaced by an η^4-coordinated 1,3-diphosphacyclobutadiene ligand as a result of the cyclodimerisation of the substrate in the coordination sphere of cobalt (Figure 2, right). Two similar but crystallographically independent molecules are present in the asymmetric unit. The P−C bond lengths (1.786(5) − 1.803(5) Å) of the P_2C_2 ring in **3** are similar and characteristic for 1,3-disphosphacyclobutadienes coordinated to 3d metals.[12–15] Also, the metal−carbon (2.096(4) − 2.106(4) Å) and metal−phosphorus distances (2.261(1) − 2.274(1) Å) compare well to related neutral and anionic cobalt 1,3-disphosphacyclobutadiene complexes.[12,13,15] The C−N (1.351(5) − 1.363(6) Å)) and C−C (C1−C2 (1.398(6) and (1.393(6) Å) bond lengths of the α-diimine are typical for an open-shell monoanion. Again, the potassium cation interacts with the anion, featuring an η^1-coordination by one phosphorus atom (3.357(2) and 3.395(2) Å) of the P_2C_2 ring and an arene η^6-interaction (C−C distances range from 3.184(5) to 3.374(5) Å) of the Dipp group.

Neutral, heteroleptic transition metal complexes with terminal η^4-1,3-disphosphacyclobutadiene ligands are well-known,[12–14] however, the only known anionic transition metal complexes of this type, $[n\text{-}Bu_4N][(\eta^5\text{-}C_2B_9H_{11})Rh(\eta^4\text{-}C_2P_2tBu_2)]$ and $[K([18]crown\text{-}6)(thf)_2][Cp^*Fe(\eta^4\text{-}C_2P_2tBu_2)]$, were synthesised by Stone *et al.* and recently by our group.[16] Thus, **3** represents a rare example of a heteroleptic transition metal anion with a terminal η^4-1,3-disphosphacyclobutadiene ligand and the first cobalt complex of this type.

The ^{1}H NMR spectrum in THF-d_8 of compound **3** shows one singlet at 0.93 ppm for the *t*Bu groups at room temperature. In the ^{31}P{^{1}H} NMR spectrum one singlet at 1.8 ppm was observed in agreement with a symmetric structure present in solution.

8.2.3 Selective P_4 Activation by 1

Transition metal-mediated transformations of white phosphorus (P_4) may open new avenues to the efficient and environmentally benign synthesis of organophosphorus compounds.[17] Despite much research in this area, many established P_4 activation protocols suffer from low selectivities.

In the past, transition metal polyphosphide anions have been prepared by reaction of alkali metal polyphosphides, e.g. K_3P_7, with transition metal complexes[18] or by reducing neutral polyphosphido complexes with alkali metals.[19,20] Anionic transition metalates have rarely been used for the synthesis of polyphosphide anions *directly* from P_4 (Chart 2).[21–23] Ellis et al. obtained the intriguing sandwich complex **F** by reacting $[Ti(C_{10}H_8)_3]^{2-}$ ($C_{10}H_8$ = naphthalene) with P_4.[21] Cummins et al. prepared the $(ArO)_3NbP_3^-$ anion **G** (Ar = 2,6-*i*$Pr_2C_6H_3$) by reacting $[NbCl_2(OAr)_3(thf)]$ with Na/Hg and P_4.[22] Compound **G** was subsequently used as a P_3^{3-} transfer agent, producing unique EP_3 molecules (E = As, Sb). Using a similar approach as Ellis, our group described the synthesis of complexes **H** and **I** by reacting $[Cp^*Fe(C_{10}H_8)]^-$ with P_4.[23] The distinct molecular structures of **H** and **I** illustrate the potential complexity of such seemingly simple transformations.

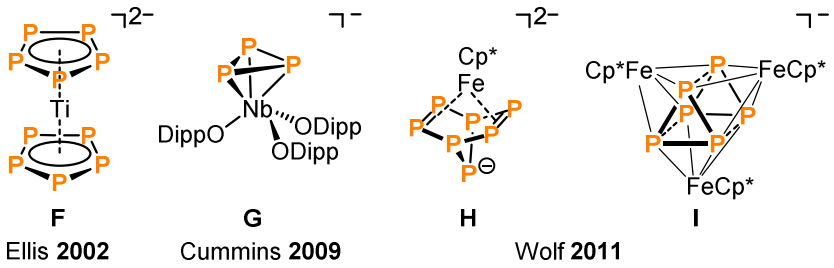

Chart 2. Anionic transition metal phosphides directly obtained by P_4 activation.

We envisioned that the use of **1** for the activation of white phosphorus should result in the formation of an anionic cobalt phosphide, which is potentially useful as starting material for further functionalisation with electrophilic substrates. The reaction of **1** with white phosphorus in THF at room temperature very selectively (according to ^{1}H and ^{31}P{^{1}H} NMR spectroscopy) yielded the dinuclear complex $[K(thf)]_2[\{(BIAN)Co\}_2(\mu\text{-}\eta^4\text{:}\eta^4\text{-}P_4)]$ (**4**) (Scheme 3). Complex **4** was isolated as a black solid in 61% yield and is only barely soluble in THF and acetonitrile, but dissolves well in DMF.

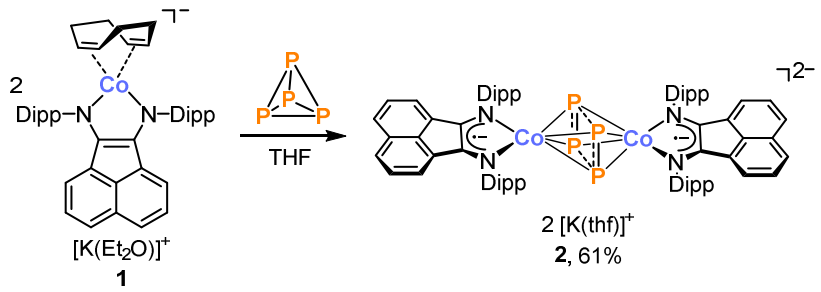

Scheme 3. Selective P_4 activation by anion **1**.

The X-ray diffraction analysis shows an unprecedented dianionic and highly symmetric inverted sandwich cobalt complex featuring a rectangular cyclo-P_4 ligand (Figure 3). Indeed, the two halves of the molecule are related by an inversion centre located at the centroid of the P_4-rectangle. Due to the Co1−Co1' distance of 3.27325(3) Å any significant interaction between the metal centres can be excluded. The characteristic bond parameters of the BIAN ligand (C1−N1 1.34769(2), C2−N2 1.34279(2) and C1−C2 1.40378(2) Å) indicate the presence of an open-shell π-radical monoanion. While P1−P2 (2.161(1) Å) lies in the range observed for aromatic P_4^{2-} anions (cf. P−P 2.146(1) and 2.1484(9) Å in Korber's tetraphosphide $Cs_2P_4 \cdot 2NH_3$),[24,25] P1−P2' (2.500(1) Å) is longer than a typical P−P single bond,[19b,26] but shorter than a van der Waals-contact.[27]

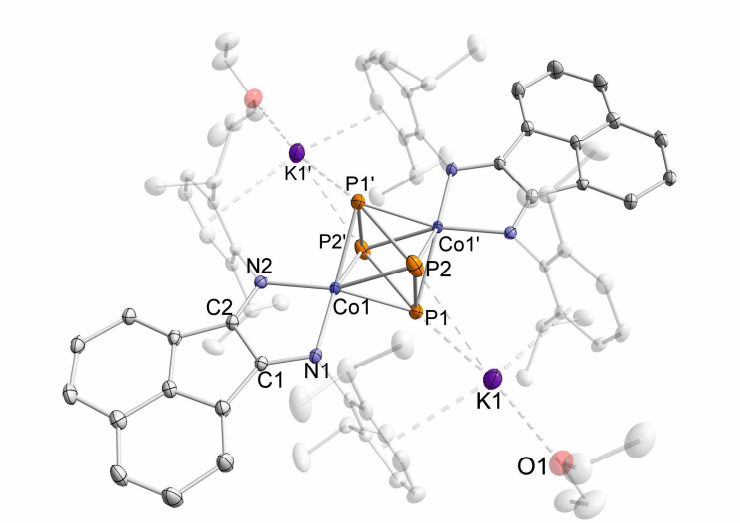

Figure 3 Solid-state molecular structure of $[K(OEt_2)]_2[\{(BIAN)Co\}_2(\mu\text{-}\eta^4\text{:}\eta^4\text{-}P_4)]$ (**4**). The hydrogen atoms are omitted for clarity. Thermal ellipsoids are drawn at 40% level. Selected bond lengths [Å] and angles [°]: Co1−Co1' 3.2733(9), P1−P2 2.161(1), P1−P2' 2.500(1), Co1−P1 2.3209(9), Co1−P2 2.3342(9), Co1−P1' 2.3195(9), Co1−P2' 2.3285(9), Co1−N1 1.930(2), Co1−N2 1.932(2), C1−N1 1.348(2), C2−N2 1.343(4), C1−C2 1.404(4), P1−P2−P1' 89.45(4), P2−P1'−P2' 90.55(4), N1−Co1−N2 83.32(9).

These structural parameters indicate that the structure of the P_4 moiety may be viewed as an intermediate of two resonance structures comprising two P_2^{2-} dianions (**I**, Figure 5a) and a P_4^{4-} unit (**II**, *vide infra*).

The $^{31}P\{^{1}H\}$ NMR spectrum of **4** in DMF-d_7 shows one singlet at −45.9 ppm for the P_4 ligand, which is consistent with its highly symmetric molecular structure. The $^{13}C\{^{1}H\}$ NMR spectrum (DMF-d_7) of **4** in gives rise to broad and overlapping signals for the aromatic carbon nuclei of the Dipp and BIAN units. In addition, one quaternary carbon atom of the BIAN ligand was not detected probably due to the broad and overlapping signals (Fig. S5).

8.2.4 UV-Vis and NIR Spectrocopy

Compounds **1**−**4** feature intense colours in solution and are almost black in the solid-state. The UV-Vis spectrum of **1** in THF shows one intense absorption at 289 nm, as well as two bands in the visual region at 441 and 663 nm (Figure S7). Interestingly, the latter absorption maximum is shifted to 485 nm in the UV-Vis spectrum of **1** in diethyl ether, which is indicative for positive solvatochromism,[28] a phenomenon typically observed for unsymmetrical ligand-to-ligand charge transfer (LL'CT) complexes.[29,30] Unsymmetrical LL'CT complexes are characterised by an electron-rich donor ligand and an electron accepting ligand, both possessing extended π-systems. Ideally these complexes are square planar resulting in an intensification of the electron transition between the coplanar ligands. In case of complex **1**, the donating ligand is probably the dianionic BIAN ligand and accordingly cod the acceptor.

By contrast, complexes **2**−**4** possess broad and medium intense bands in the visible and NIR range (Figure S8 and S9), which are indicative for radical anionic α-diimine ligands in agreement with the results of the X-ray diffraction analysis.

Compound **2** features absorption maxima at 346, 463, 507 and 687 nm in the UV-Vis spectrum (THF, Figure S8, bottom). In addition, intense and broad bands were detected in the near-infrared region at 940, 1056 and 1258 nm. These low energy transitions are indicative for the delocalisation of the π-systems of the BIAN and the ethylene tetrathiolate ligands over the two halves of the completely planar molecule and a strong mixing of the metal d-orbitals resulting in so-called mixed-metal-ligand-to-ligand charge transfers (MMLL'CT). Heyduk and coworkers recently reported the synthesis of square planar nickel(II) LL'CT complexes bearing 2,2'-bipyridine and catecholate or azanidophenolate ligands with similar broad near-IR bands compared to **2**.[29] Furthermore, complex **2** shows no solvatochromism probably due to the highly symmetrical structure. The UV-Vis spectra of **3** and **4** in THF feature intense absorptions at 294, 388, 605 as well as 738 nm (Figure S9, top), and in case of **4** at 345 and 585 nm (Figure S9, bottom).

8.2.5 Cyclic Voltammetry

The electrochemical properties of compounds **1**−**4** were investigated by cyclic voltammetry. All potentials given are referenced to the $[Cp_2Fe]^{+/0}$ (Fc) couple. The cyclic voltammogram (CV, Figure S10) of **1** in THF/$[Bu_4N][PF_6]$ shows one quasi-reversible one-electron oxidation process at $E_{1/2}$ = −1.72 V, which indicates that **1** is a strong reductand. A very broad, irreversible oxidation wave was detected at E_{pa} = −0.1 V and secondary processes at $E_{1/2}$ = −2.0 V were also observed. In contrast, complex **2** features four reversible one-electron oxidation processes at $E_{1/2}$ = −1.60, −1.03, −0.44 and +0.08 V (THF, Figure 4, top). Halve-wave potentials of $E_{1/2}$ = −1.35, −0.88, −0.79 and +0.02 V were found in acetonitrile with the second and third oxidation waves partially overlapping (Figure S11).

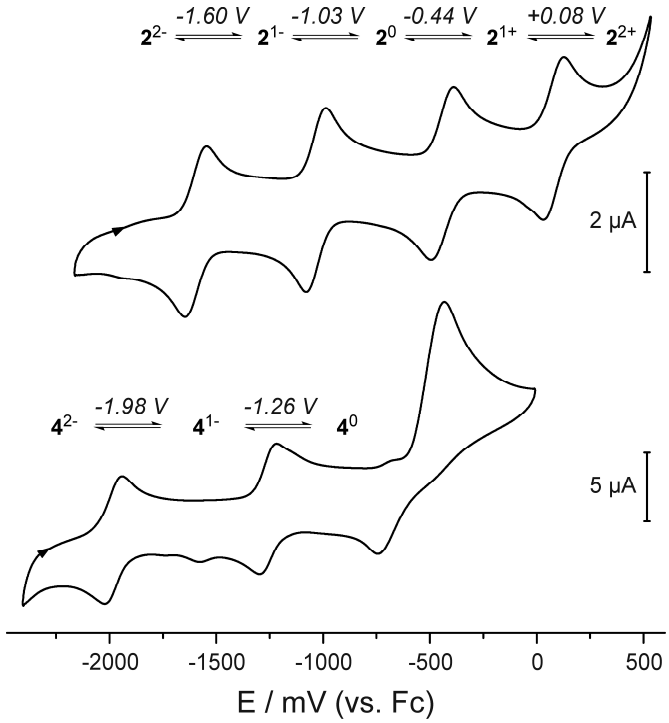

Figure 4 Cyclic voltammograms of **2** (top) and **4** (bottom) in THF/$[Bu_4N][PF_6]$ with a platinum disc working electrode, a platinum wire as counter electrode and a silver wire as pseudoreference electrode. v = 100 mV s^{-1}.

The CV of compound **3** in THF shows a quasi-reversible oxidation at −1.25 V, a reversible oxidation at −0.67 V (Figure S12) and an irreversible oxidation process at E_{pa} = –0.74 V. In addition, secondary processes were observed at $E_{1/2}$ = −1.05 V, along with an irreversible reduction at E_{pc} = −1.57 V.

The cyclic voltammogram of **4** (THF/$[Bu_4N][PF_6]$) features two reversible one-electron oxidation processes at $E_{1/2}$ = −1.98 V and −1.26 V, and an irreversible two-electron oxidation at E_{pa} = –0.43 V (Figure 4, bottom). Additional weak irreversible processes at E_{pa} = −0.66 V and E_{pc} = −1.58 V presumably arise from secondary redox processes derived from the irreversible oxidation products.

8.2.6 Chemical Oxidation of the Dianion 4

Stimulated by the promising CV data of **4**, we synthesised the monoanion $[K(OEt_2)][\{(BIAN)Co\}_2(\mu\text{-}\eta^4\text{:}\eta^4\text{-}P_4)]$ (**5**) by reacting **4** with one equivalent of $[Cp_2Fe]BAr^F{}_4$ in THF (Scheme 4).

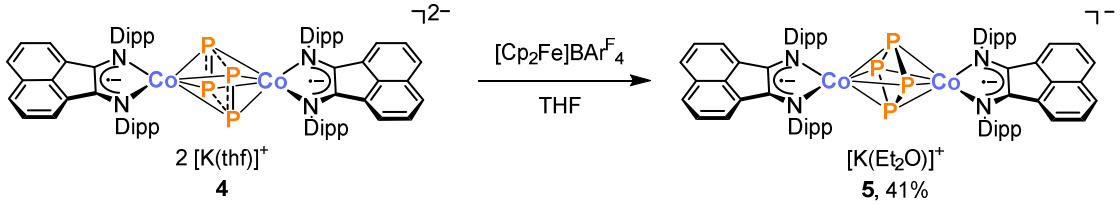

Scheme 4. Chemical oxidation of dianion **4**.

Single-crystal XRD (Figure 5) confirmed the presence of monoanionic $BIAN^-$ anions (C1−N1 1.32(1), C2−N2 1.32(1) and C1−C2 1.44(1) Å) with little back bonding of the metal.[8] Compared to **4**, the Co−Co distance is increased by 0.2 Å. The potassium ion is disordered over two positions and shows the same ligand environment as in **4**. The structure of the central P_4 moiety is distinct from **4** and shows a slightly rhombic arrangement (P1−P2−P1' 86.8(1) and P2−P1'−P2' 93.2(1) Å) with P−P single bonds (2.224(4) − 2.226(4) Å). In addition, the P_4 fragment is rotated about the Co-Co axis by 45° as against in **4**. These structural data indicate that **5** represents the first example of a 3d metal complex bearing a cyclo-P_4^{4-} ligand (resonance structure **II**, Figure 6d), a framework that was previously only observed for a few Zr, Nb and Ta complexes.

Complex **5** is paramagnetic and gives rise to broad ^{1}H NMR signals in the range −0.9 to 19.3 ppm, which could not unambiguously be assigned due to overlap of compound and solvent signals. Nonetheless, the presence of seven signals in the ^{1}H NMR spectrum indicates a highly symmetric structure in solution in agreement with the single-crystal X-ray structure. The solution magnetic moment (Evans method, THF-d_8) of 2.0(1) μ_B indicates the presence of one unpaired electron per molecule.

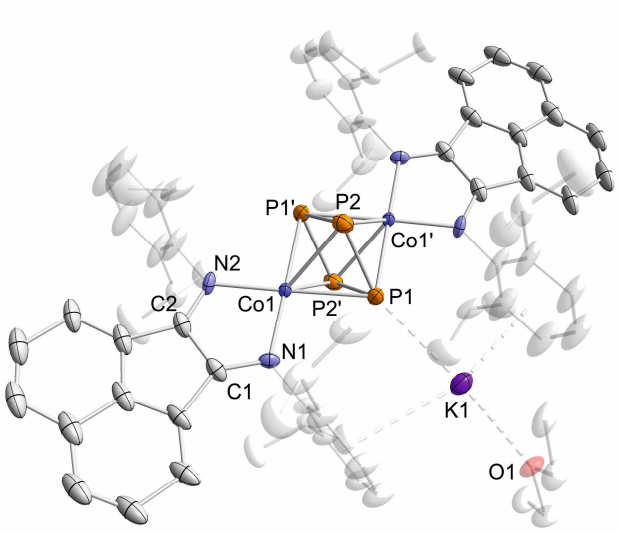

Figure 5. Solid-state molecular structure [K(OEt$_2$)][{(BIAN)Co}$_2$(μ-η^4:η^4-P$_4$)] (**5**). The hydrogen atoms are omitted for clarity. Thermal ellipsoids are drawn at 40% level. Selected bond lengths [Å] and angles [°]: Co1−Co1' 3.469(3), P1−P2 2.224(4), P1−P2' 2.226(4), Co1−P1 2.309(3), Co1−P2 2.367(3), Co1−P1' 2.315(3), Co1−P2' 2.375(3), Co1−N1 1.938(7), Co1−N2 1.919(7), C1−N1 1.32(1), C2−N2 1.32(1), C1−C2 1.44(1), P1−P2−P1' 86.8(1), P2−P1'−P2' 93.2(1), N1−Co1−N2 82. 2(3).

It is illuminating to compare the molecular structures of **4** and **5** with the recently reported anions [{(nacnac)Co}$_2$(μ-η^4:η^4-P$_4$)]$^-$ (**K**) and [{(nacnac)Fe}$_2$(μ-η^2:η^2-P$_2$)$_2$]$^-$ (**M**), prepared by Driess *et al.* by one-electron reduction of the neutral precursors **J** and **L** (Figure 6b).[20] Complex **J** features an unusual *neutral* cyclo-P$_4$ ligand (Figure 6, **IV**), which transforms into a cyclo-P$_4^{2-}$ *dianion* (**III**) upon one-electron reduction of the complex. By contrast, neutral **L** and the corresponding monoanion **M** feature identical the Fe$_2$P$_4$ cores with non-interacting P$_2^{2-}$ units (Figure 6, **I**). Very recently, the group of Scheer also reported on the related neutral species [{(nacnac)Fe}$_2$(μ-η^4:η^4-P$_4$)] (**N**, Figure 6c) and [{(nacnac)Fe}$_4$(μ_4-η^2:η^2:η^2:η^2-P$_8$)] (**O**).[31] They compared the steric influence of different nacnac ligands in the reactions of complexes of type [(nacnac)Fe(toluene)] with P$_4$. While Complex **N** shows also a cyclo-P$_4^{2-}$ *dianion* (**III**) with very similar P−P bond lengths as **K**, compound **O** features a realgar-type P$_8$ ligand by use of sterically less demanding 2,6-dimethylphenyl groups at the N atoms of the ligand.

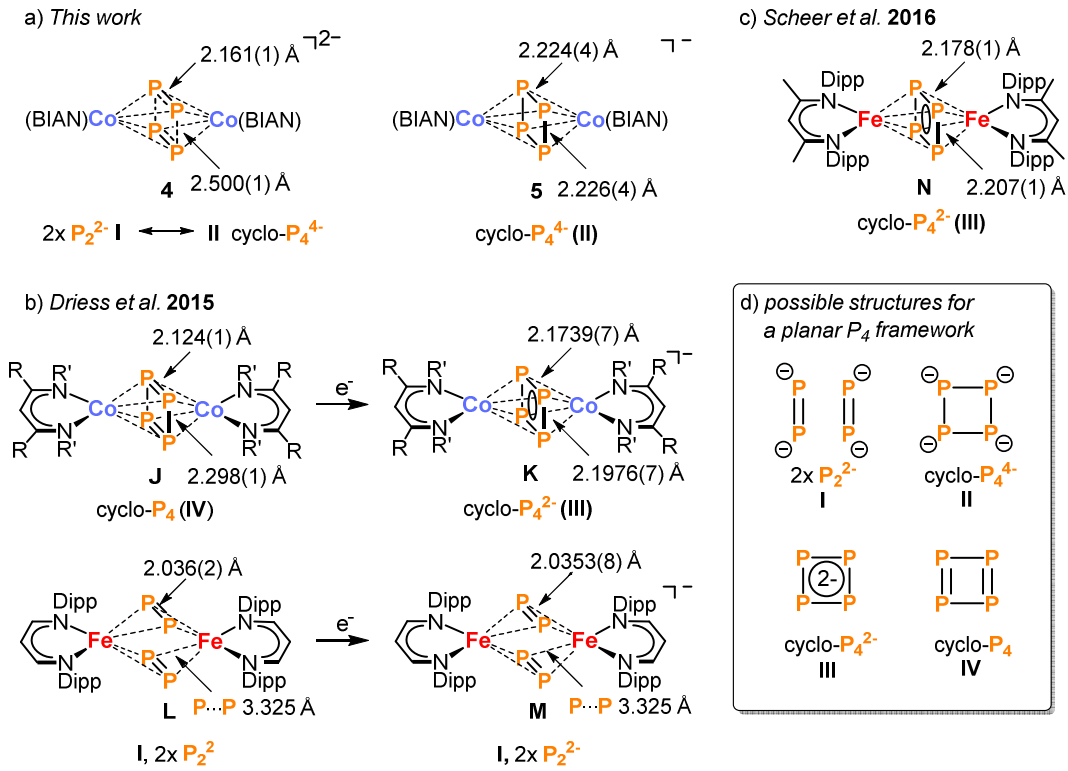

Figure 6. a) Structural data of **4** and **5** containing redox-active $BIAN^{-}$ ligand. b) and c) structural data of $nacnac^{-}$ compexes **J**−**N** prepared by Driess *et al.* and Scheer *et al.*. For **J** and **K**: R = H ; R' = Dipp; for a related complex with similar bond parameters also presented by Driess *et al.*: R = Me; R' = 2,6-EtC_6H_3.[20,31] d) Schematic representation of possible structures for a planar P_4 framework.

The central P_4 moiety of **4** (Figure 6a) is distinct from **F** – **N** and may be viewed as a "snapshot" on the way from two separated P_2^{2-} units (**I**, Figure 6d) to a P_4^{4-} ring (**II**). The rectangular cyclo-P_4^{4-} fragment of **4** rearranges to a slightly rhombic cyclo-P_4^{4-} unit in **5** upon oxidation **4** → **5**. Apparently, the more electron-rich nature of the (BIAN)Co unit of **5** compared to the (nacnac)Co fragment in the isoelectronic complex **K** leads to a higher degree of reduction of the P_4 framework. A similar redox neutral rearrangement was observed by Roesky *et al.* for the reduction of the cyclopentadienylcobalt complex $[(Cp'''Co)_2(\mu,\eta^2{:}\eta^2\text{-}P_2)_2]$ (Cp''' = 1,2,4-*t*$Bu_3C_5H_2$) with samarocenes. In this case, an acyclic P_4^{4-} entity was observed.[32] Previous reports on neutral cyclopentadienyl complexes $Cp^R{}_2M_2P_4$ (Cp^R = substituted cyclopentadienyl ligand, M = Fe and Co) further illustrate the remarkable structural flexibility of the P_4 unit in this type of dinuclear complex.[27,32,33]

8.3 Conclusion

In summary, the new BIAN cobalt complex **1** is accessible from $[Co(cod)_2]^-$ via straightforward substitution of one cod ligand. The dinuclear complex **2** with a bridging ethylene tetrathiolate ligand was accessed by the reductive dimerisation of carbon disufide with **1**. The reaction of **1** with two equivalents of *tert*-butylphosphaalkyne afforded complex **3** bearing an η^4-1,3-disphosphacyclobutadiene ligand. Activation of P_4 gave the dianionic complex **4**, which features an unusual rectangular P_4^{4-} framework. Oxidation of **4** afforded monoanionic **5** with a rare rhombic cyclo-P_4^{4-} ligand. The use of a redox-active dimine ligand appears crucial for achieving a high degree of P_4 reduction. Subsequent reactions could lead to the functionalisation of the P_4 moiety in the coordination sphere of the cobalt centres. This aspect of the reactivity of phosphide anions **4** and **5** is an attractive target for future investigations. The reactivity of **1** and related complexes with other small molecules as well as potential catalytic applications appears to be another worthwhile target for future studies.[34,35]

References

1 a) K. Jonas, R. Mynott, C. Krüger, J. C. Sekutowski, Y.-H. Tsay, *Angew. Chem.* **1976**, *88*, 808*; Angew. Chem. Int. Ed. Engl.* **1976**, *15*, 767; b) K. Jonas, US patent 4169845, **1979**.

2 M. Döring, E. Uhlig, T. Taldbach, *Z. Anorg. Allg. Chem.* **1991**, *600*, 163.

3 a) W. W. Brennessel, V. G. Young, J. E. Ellis, *Angew. Chem.* **2006**, *45*, 7268*; Angew. Chem. Int. Ed.* **2006**, *45*, 7268; b) W. W. Brennessel, J. E. Ellis, *Inorg. Chem.* **2012**, *51*, 9076.

4 D. Gärtner, A. Welther, B. R. Rad, R. Wolf, A. Jacobi von Wangelin, *Angew. Chem.* **2014**, *126*, 3796*; Angew. Chem. Int. Ed.* **2014**, *53*, 3722.

5 Selected publications: a) M. M. Khusniyarov, T. Weyhermüller, E. Bill, K. Wieghardt, *Angew. Chem.* **2008**, *120*, 1248*; Angew. Chem. Int. Ed.* **2008**, *47*, 1228; b) N. Muresan, C. C. Lu, M. Ghosh, J. C. Peters, M. Abe, L. M. Henling, T. Weyhermöller, E. Bill, K. Wieghardt, *Inorg. Chem.* **2008**, *47*, 4579; c) M. M. Khusniyarov, T. Weyhermüller, E. Bill, K. Wieghardt, *J. Am. Chem. Soc.* **2009**, *131*, 1208.

6 X. Wang, Y. Zhao, S. Gong, B. Liu, Q.-S. Li, J.-H. Su, B. Wu, X.-J. Yang, *Chem. Eur. J.* **2015**, *21*, 13302.

7 Selected publications on complexes with $^{Ar}BIAN^{0}$ ligands: a) D. P. Gates, S. A. Svejda, E. Oñate, C. M. Killian, L. K. Johnson, P. S. White, M. Brookhart, *Macromolecules* **2000**, *33*, 2320; b) J. O. Liimatta, B. Löfgren, M. Miettinen, M. Ahlgren, M. Haukka, T. T. Pakkanen, *J. Polym. Sci. A Polym. Chem.* **2001**, *39*, 1426; c) A. Paulovicova, U. El-Ayaan, K. Shibayama, T. Morita, Y. Fukuda, *Eur. J. Inorg. Chem.* **2001**, 2641; d) C. Fliedel, V. Rosa, C. I. M. Santos, P. J. Gonzalez, R. M. Almeida, C. S. B. Gomes, P. T. Gomes, M. A. N. D. A. Lemos, G. Aullón, R. Welter, T. Avilés, *Dalton Trans.* **2014**, *43*, 13041; e) T. Vaidya, K. Klimovica, A. M. LaPointe, I. Keresztes, E. B. Lobkovsky, O. Daugulis, G. W. Coates, *J. Am. Chem. Soc.* **2014**, *136*, 7213.

8 Selected publications on complexes with $^{Ar}BIAN^{-}$ ligands: a) I. L. Fedushkin, A. A. Skatova, V. A. Chudakova, V. K. Cherkasov, S. Dechert, H. Schumann, *Russ. Chem. Bull.* **2004**, *53*, 2142; b) I. L. Fedushkin, A. A. Skatova, S. Y. Ketkov, O. V. Eremenko, A. V. Piskunov, G. K. Fukin, *Angew. Chem.* **2007**, *119*, 4380*; Angew. Chem. Int. Ed.* **2007**, *46*, 4302; c) M. M. Khusniyarov, K. Harms, O. Burghaus, J. Sundermeyer, *Eur. J. Inorg. Chem.* **2006**, 2985; d) M. A. Ogienko, N. A. Pushkarevsky, A. I. Smolentsev, V. A. Nadolinny, S. Y. Ketkov, S. N. Konchenko, *Organometallics* **2014**, *33*, 2713; e) P. Mondal, H. Agarwala, R. D. Jana, S. Plebst, A. Grupp, F. Ehret, S. M. Mobin, W. Kaim, G. K. Lahiri, *Inorg. Chem.* **2014**, *53*, 7389.

9 Selected publications on complexes with $^{Ar}BIAN^{2-}$ ligands: a) I. L. Fedushkin, A. A. Skatova, V. A. Chudakova, G. K. Fukin, S. Dechert, H. Schumann, *Eur. J. Inorg. Chem.* **2003**, 3336; b) I. L. Fedushkin, A. N. Lukoyanov, A. N. Tishkina, M. O. Maslov, S. Y. Ketkov, M. Hummert, *Organometallics* **2011**, *30*, 3628; d) I. L. Fedushkin, V. G. Sokolov, A. V. Piskunov, V. M. Makarov, E. V. Baranov, G. A. Abakumov, *Chem. Commun.* **2014**, *50*, 10108; e) H. Tsurugi, T. Saito, H. Tanahashi, J. Arnold, K. Mashima, *J. Am. Chem. Soc.* **2011**, *133*, 18673.

10 M. J. Sgro, D. W. Stephan, *Dalton Trans.* **2010**, *39*, 5786.

11 Selected examples for the reductive head-to-head dimerisation of CS_2 mediated by transition metal complexes: a) P. V. Broadhurst, B. F. G. Johnson, J. Lewis, P. R. Raithby, *J. Chem. Soc., Chem. Commun.* **1982**, 140; b) J. J. Maj, A. D. Rae, L. F. Dahl, *J. Am. Chem. Soc.* **1982**, *104*, 4278; c) H. A. Harris, A. D. Rae, L. F. Dahl, *J. Am. Chem. Soc.* **1987**, *109*, 4739; d) C. Bianchini, C. Mealli, A. Meli, M. Sabat, P. Zanello, *J. Am. Chem. Soc.* **1987**, *109*, 185.

12 a) M. Regitz, *Chem. Rev.* **1990**, *90*, 191; b) A. C. Gaumont, J. Denis, *Chem. Rev.* **1994**, *94*, 1413; c) J. F. Nixon, *Coord. Chem. Rev.* **1995**, *145*, 201; d) K. B. Dillon, F. Mathey, J. F. Nixon, Phosphorus: The Carbon Copy, Wiley, Chichester, **1998**; e) F. Mathey, *Angew. Chem.* **2003**, *115*, 1616−1643*; Angew. Chem. Int. Ed.* **2003**, *42*, 1578; f) A. Chirila, R. Wolf, J. C. Slootweg, K. Lammertsma, *Coord. Chem. Rev.* **2014**, *270–271*, 57.

13 Neutral, heteroleptic cobalt complexes with terminal η^4-1,3-disphosphacyclobutadiene ligands: a) P. Binger, R. Milczarek, R. Mynott, M. Regitz, W. Rösch, *Angew. Chem.* **1986**, *98*, 640*; Angew. Chem. Int. Ed. Engl.* **1986**, *25*, 644; b) P. B. Hitchcock, M. J. Maah, J. F. Nixon, *J. Chem. Soc., Chem. Commun.* **1986**, 737; c) P. Binger, R. Milczarek, R. Mynott, M. Regitz, *J. Organomet. Chem.* **1987**, *323*, C35; d) P. Binger, R. Milczarek, K. Mynott, C. Kruger, Y.H. Tsay, E. Raabe, M. Regitz, *Chem. Ber.* **1988**, *121*, 637; e) J. J. Schneider, U. Denninger, O. Heinemann, C. Krüger, *Angew. Chem.* **1995**, *107*, 631*; Angew. Chem. Int. Ed. Engl.* **1995**, *34*, 592–595; f) E.-M. Rummel, M. Eckhardt, M. Bodensteiner, E. V. Peresypkina, M. Scheer, *Eur. J. Inorg. Chem.* **2014**, 1625.

14 Neutral, heteroleptic transition metal complexes with terminal η^4-1,3-disphosphacyclobutadiene ligands**:** a) M. Driess, D. Hu, H. Pritzkow, H. Schäufele, U. Zenneck, M. Regitz, W. Rösch, *J. Organomet. Chem.* **1987**, *334*, C35; b) P. Binger, B. Biedenbach, R. Mynott, C. Krüger, P. Betz, M. Regitz, *Angew. Chem.* **1988**, *100*, 1219*; Angew. Chem. Int. Ed. Engl.* ***1988***, *27*, 1157; c) P. Kramkowski, M. Scheer, *Eur. J. Inorg. Chem.* **2000**, 1869; d) P. Binger, B. Biedenbach, R. Schneider, M. Regitz, *Synthesis* **1989**, 960; e) F. G. N. Cloke, K. R. Flower, P. B. Hitchcock, J. F. Nixon, *J.*

Chem. Soc., Chem. Commun. **1994**, 489; f) D. Böhm, F. Knoch, S. Kummer, U. Schmidt, U. Zenneck, *Angew. Chem.* **1995**, *107*, 251*; Angew. Chem. Int. Ed. Engl.* **1995**, *34*, 198; g) P. Binger, G. Glaser, S. Albus, C. Krüger, *Chem. Ber.* **1995**, *128*, 1261; h) G. Brauers, M. Green, C. Jones, J. F. Nixon, *J. Chem. Soc., Chem. Commun.* **1995**, 1125; i) J. Grobe, D. Le Van, F. Immel, M. Hegemann, B. Krebs, M. Läge, *Z. Anorg. Allg. Chem.* **1996**, *622*, 24; j) F. G. N. Cloke, P. B. Hitchcock, J. F. Nixon, D. M. Vickers, *J. Organomet. Chem.* **2001**, *635*, 212; k) D. Himmel, M. Seitz, M. Scheer, *Z. Anorg. Allg. Chem.* **2004**, *630*, 1220.

15 Homoleptic transition metal anions with η^4-1,3-disphosphacyclobutadiene ligands: a) R. Wolf, A. W. Ehlers, J. C. Slootweg, M. Lutz, D. Gudat, M. Hunger, A. L. Spek, K. Lammertsma, *Angew. Chem.* **2008**, *120*, 4660*; Angew. Chem. Int. Ed.* **2008**, *47*, 4584; b) R. Wolf, J. C. Slootweg, A. W. Ehlers, F. Hartl, B. de Bruin, M. Lutz, A. L. Spek, K. Lammertsma, *Angew. Chem.* **2009**, *121*, 3150*; Angew. Chem. Int. Ed.* **2009**, *48*, 3104; c) R. Wolf, A. W. Ehlers, M. M. Khusniyarov, F. Hartl, B. de Bruin, G. J. Long, F. Grandjean, F. M. Schappacher, R. Pöttgen, J. C. Slootweg, M. Lutz, A. L. Spek, K. Lammertsma, *Chem. Eur. J.* **2010**, *16*, 14322.

16 a) H. F. Dare, J. A. K. Howard, M. U. Pilotti, F. Stone, A. Gordon, J. Szameitat, *J. Chem.Soc., Chem. Commun.* **1989**, 1409; b) H. F. Dare, J. A. K. Howard, M. U. Pilotti, F. Stone, A. Gordon, J. Szameitat, *J. Chem.Soc., Dalton Trans.* **1990**, 2263; c) R. Wolf, E.-M. Schnöckelborg, *Chem. Commun.* **2010**, *46*, 2832.

17 Reviews: a) B. M. Cossairt, N. A. Piro, C. C. Cummins, *Chem. Rev.* **2010**, *110*, 4164; b) M. Caporali, L. Gonsalvi, A. Rossin, M. Peruzzini, *Chem. Rev.* **2010**, *110*, 4178; c) J. S. Figueroa, C. C. Cummins, *Dalton Trans.* **2006**, 2161; d) M. Peruzzini, L. Gonsalvi, A. Romerosa, *Chem. Soc. Rev.* **2005**, *34*, 1038; e) M. Peruzzini, R. Abdreimova, Y. Budnikova, A. Romerosa, O. J. Scherer, H. Sitzmann, *J. Organomet. Chem.* **2004**, *689*, 4319.

18 Selected examples: a) S. Charles, B. W. Eichhorn, A. L. Rheingold, S. G. Bott, *J. Am. Chem. Soc.* **1994**, *116*, 8077; b) S. Charles, J. C. Fettinger, S. G. Bott, B. W. Eichhorn, *J. Am. Chem. Soc.* **1996**, *118*, 4713; c) C. M. Knapp, J. S. Large, N. H. Rees, J. M. Goicoechea, *Chem. Commun.* **2011**, *47*, 4111.

19 Selected examples: a) J. S. Figueroa, C. C. Cummins, *J. Am. Chem. Soc.* **2004**, *126*, 13916; b) W. W. Seidel, O. T. Summerscales, B. O. Patrick, M. D. Fryzuk, *Angew. Chem.* **2009**, *121*, 121; *Angew. Chem. Int. Ed.* **2009**, *48*, 115; d) M. V. Butovskiy, G. Balázs, M. Bodensteiner, E. V. Peresypkina, A. V. Virovets, J. Sutter, M. Scheer, *Angew. Chem.* **2013**, *125*, 3045; *Angew. Chem. Int. Ed.* **2013**, *52*, 2972, e) T. Li, M. T. Gamer, M. Scheer, S. N. Konchenko, P. W. Roesky, *Chem. Commun.* **2013**, *49*, 2183–2185.

20 S. Yao, N. Lindenmaier, Y. Xiong, S. Inoue, T. Szilvási, M. Adelhardt, J. Sutter, K. Meyer, M. Driess, *Angew. Chem.* **2015**, *127*, 1266; *Angew. Chem. Int. Ed.* **2015**, *54*, 1250; b) S. Yao, T. Szilvási, N. Lindenmaier, Y. Xiong, S. Inoue, M. Adelhardt, J. Sutter, K. Meyer, M. Driess, *Chem. Commun.* **2015**, *51*, 6153.

21 E. Urnėžius, W. W. Brennessel, C. J. Cramer, J. E. Ellis, P. von R. Schleyer, *Science* **2002**, *295*, 832.

22 B. M. Cossairt, M.-C. Diawara, C. C. Cummins, *Science* **2009**, *323*, 602

23 E.-M. Schnöckelborg, J. J. Weigand, R. Wolf, *Angew. Chem.* **2011**, *123*, 6768; *Angew. Chem. Int. Ed.* **2011**, *50*, 6657.

24 Transition metal complexes with cyclo-P_4^{2-} ligands: a) O. J. Scherer, J. Vondung and G. Wolmershäuser, *Angew. Chem. Int. Ed. Engl.* **1989**, *28*, 1355; b) M. Scheer, E. Herrmann, J. Sieler, M. Oehme, *Angew. Chem. Int.* **1991**, *103*, 1023; *Angew. Chem. Int. Ed. Engl.* **1991**, *30*, 969; c) M. Scheer, U. Becker, J. C. Huffman, M. H. Chisholm, *J. Organomet. Chem.* **1993**, *461*, C1; d) C. Schwarzmaier, A. Y. Timoshkin, G. Balázs, M. Scheer, *Angew. Chem.* **2014**, *126*, 9223; *Angew. Chem. Int. Ed.* **2014**, *53*, 9077.

25 F. Kraus, J. C. Aschenbrenner, N. Korber, *Angew. Chem.* **2003**, *115*, 4162; *Angew. Chem. Int. Ed.* **2003**, *42*, 4030.

26 a) A. Velian, C. C. Cummins, *Chem. Sci.* **2012**, *3*, 1003; b) C. Camp, L. Maron, R. G. Bergman, J. Arnold, *J. Am. Chem. Soc.* **2014**, *136*, 17652.

27 a) M. Scheer, U. Becker, M. H. Chisholm, J. C. Huffman, F. Lemoigno, O. Eisenstein, *Inorg. Chem.* **1995**, *34*, 3117; b) M. D. Walter, J. Grunenberg, P. S. White, *Chem. Sci.* **2011**, *2*, 2120.

28 Selected publications on the solvatochromism of square planar LLCT complexes: a) R. Benedix, H. Hennig, H. Kunkely, A. Vogler, *Chem. Phys. Lett.* **1990**, *175*, 483; b) S. D. Cummings, R. Eisenberg, *Inorg. Chem.* **1995**, *34*, 2007; c) S. D. Cummings, R. Eisenberg, *J. Am. Chem. Soc.* **1996**, *118*, 1949; d) C.-T. Chen, S.-Y. Liao, K.-J. Lin, C.-H. Chen, T.-Y. J. Lin, *Inorg. Chem.* **1999**, *38*, 2734; e) C. J. Adams, N. Fey, M. Parfitt, S. J. A. Pope, J. A. Weinstein, *Dalton Trans.* **2007**, 4446.

29 Selected publications on near-IR absorbing square planar LLCT complexes: a) A. E. Pullen, S. Zeltner, R.-M. Olk, E. Hoyer, K. A. Abboud, J. R. Reynolds, *Inorg. Chem.* **1997**, *36*, 4163; b) J.-F. Bai, J.-L. Zuo, Z. Shen, X.-Z. You, H.-K. Fun, K. Chinnakali, *Inorg. Chem.* **2000**, *39*, 1322; c) W. W. Kramer, L. A. Cameron, R. A. Zarkesh, J. W. Ziller, A. F. Heyduk, *Inorg. Chem.* **2014**, *53*, 8825; d) L. A. Cameron, J. W. Ziller, A. F. Heyduk, *Chem. Sci.* **2015**, *7*, 1807.

30 D. Herebian, E. Bothe, F. Neese, T. Weyhermüller, K. Wieghardt, *J. Am. Chem. Soc.* **2003**, *125*, 9116.

31 F. Spitzer, C. Graßl, G. Balázs, E. M. Zolnhofer, K. Meyer, M. Scheer, *Angew. Chem. Int. Ed.* **2016**, DOI:10.1002/anie.201510716.

32 T. Li, N. Arleth, M. T. Gamer, R. Köppe, T. Augenstein, F. Dielmann, M. Scheer, S. N. Konchenko, P. W. Roesky, *Inorg. Chem.* **2013**, *52*, 14231.

33 a) O. J. Scherer, M. Swarowsky, G. Wolmershäuser, *Organometallics* **1989**, *8*, 841; b) S. Dürr, D. Ertler, U. Radius, *Inorg. Chem.* **2012**, *51*, 3904; c) B. Zarzycki, F. M. Bickelhaupt, U. Radius, *Dalton Trans.* **2013**, *42*, 7468.

34 W. I. Dzik, J. I. van der Vlugt, J. N. H. Reek, B. de Bruin, *Angew. Chem.* **2011**, *123*, 3416; *Angew. Chem. Int. Ed.* **2011**, *50*, 3356.

35 a) C. Lichtenberg, L. Viciu, M. Vogt, R. E. Rodríguez-Lugo, M. Adelhardt, J. Sutter, M. M. Khusniyarov, K. Meyer, B. de Bruin, E. Bill, H. Grützmacher, *Chem. Commun.* **2015**, *51*, 13890; b) C. Lichtenberg, M. Adelhardt, T. L. Gianetti, K. Meyer, B. de Bruin, H. Grützmacher, *ACS Catal.* **2015**, *5*, 6230; c) C. Lichtenberg, L. Viciu, M. Adelhardt, J. Sutter, K. Meyer, B. de Bruin, H. Grützmacher, *Angew. Chem.* **2015**, *127*, 5858; *Angew. Chem. Int. Ed.* **2015**, *54*, 5766.

8.4 Supporting Information

8.4.1 General Procedures

All experiments were performed under an atmosphere of dry argon using standard Schlenk techniques or an MBraun UniLab glovebox. Solvents were dried and degassed with an MBraun SPS800 solvent purification system. Tetrahydrofuran and toluene were stored over molecular sieves (3 Å). Diethyl ether and *n*-hexane were stored over a potassium mirror. NMR spectra were recorded on Bruker Avance 300 and Avance 400 spectrometers at 300 K and internally referenced to residual solvent resonances. Melting points were measured on samples in sealed capillaries on a Stuart SMP10 melting point apparatus. UV/Vis spectra were recorded on a Varian Cary 50 spectrophotometer. NIR spectra were recorded on a Bruins Instruments Omega 20. Elemental analyses were determined by the analytical department of Regensburg University. The starting materials $[K(thf)_{0.2}][Co(1,5\text{-}cod)_2]$[1], BIAN[2] and *t*BuCP[3] were prepared according to literature procedures. CS_2 was purchased from Merck, degassed and dried over molecular sieves (3 Å) before use.

8.4.2 Synthesis of [K(OEt$_2$)][Co(BIAN)(cod)] (1)

A solution of BIAN (1.005 g, 2.01 mmol, 1.0 eq) in THF (70 mL) was added to a solution of $[K(thf)_{0.2}][Co(1,5\text{-}cod)_2]$ (660 mg, 2.01 mmol, 1.0 eq) in THF (10 mL). An immediate colour change to dark green was observed. After stirring the reaction mixture for two hours, the solvent was removed and the residue was extracted with diethyl ether (200 mL). The filtrate was concentrated to 75 mL and stored at room temperature. Dark green microcrystals of **1** formed upon storing for one day. Crystals suitable for X-Ray diffraction were obtained by diffusion of *n*-hexane into a concentrated THF solution of **1**. Yield 1.116 g (71%); m.p. >230 °C (decomp. to a black oil); UV/Vis (THF, λ_{max} /nm, (ε_{max} /L·mol^{-1}·cm^{-1})): 289 (26000), 441 (12000), 663 (8500), UV/Vis (Et_2O): 284 (24000), 436 (8500), 485 (9000); elemental analysis calcd. for $C_{52}H_{72}N_2CoKO_2$ (M = 855.19): C 73.03, H 8.49, N 3.28, found.: C 73.32, H 7.59, N 3.59; ^{1}H NMR (THF-d_8, 300 K, 400.13 MHz) δ /ppm = 0.96 (br m, 12H, CH(C*H*$_3$)$_2$), 1.12 (br m, 10H, Et_2O/cod-CH_2), 1.38 (br m, 12H, CH(C*H*$_3$)$_2$), 2.33 (br m, 4H, cod-CH_2), 2.91 (br m, 4H, cod-CH), 4.50 (br m, 4H, C*H*(CH$_3$)$_2$), 4.89 (br m, 2H, CH_{BIAN}), 6.20 (br m, 2H, CH_{BIAN}), 6.28 (br m, 2H, CH_{BIAN}), 7.00−7.09 (br m, 6H, *meta*-/*para*-CH_{Dipp}); ^{1}H NMR (THF-d_8, 333 K, 400.13 MHz) δ /ppm = 0.96−0.99 (br m, 16H, CH(C*H*$_3$)$_2$/cod-CH_2), 1.41 (d, $^3J_{HH}$ = 6.6 Hz, 12H, CH(C*H*$_3$)$_2$), 2.34 (br m, 4H, cod-CH_2), 2.90 (br m, 4H, cod-CH), 4.48 (sept., $^3J_{HH}$ = 6.6 Hz, 4H, C*H*(CH$_3$)$_2$), 5.01 (d, $^3J_{HH}$ = 6.3 Hz, 2H, CH_{BIAN}), 6.28 (t, $^3J_{HH}$ = 7.7 Hz, 2H, CH_{BIAN}), 6.34 (t, $^3J_{HH}$ = 7.7 Hz, CH_{BIAN}), 7.01−7.08 (br m, 6H, *meta*-/*para*-CH_{Dipp}); ^{13}C{^{1}H} NMR (THF-d_8, 300 K, 100.61 MHz) δ /ppm = 24.9 (CH(C*H*$_3$)$_2$), 25.4 (CH(C*H*$_3$)$_2$), 28.1 (*C*H(CH$_3$)$_2$), 32.6 (cod-CH_2), 64.1 (cod-CH), 114.3 (CH_{BIAN}), 118.6 (CH_{BIAN}), 122.7 (CH_{Dipp}), 122.9 (CH_{Dipp}), 127.3 (CH_{BIAN}), 127.5 (C_{BIAN}), 135.8 (C_{BIAN}) 137.8 (C_{BIAN}), 143.5 (C_{BIAN}), 145.2 (*ortho*-CH_{Dipp}), 154.8 (*ipso*-CH_{Dipp}).

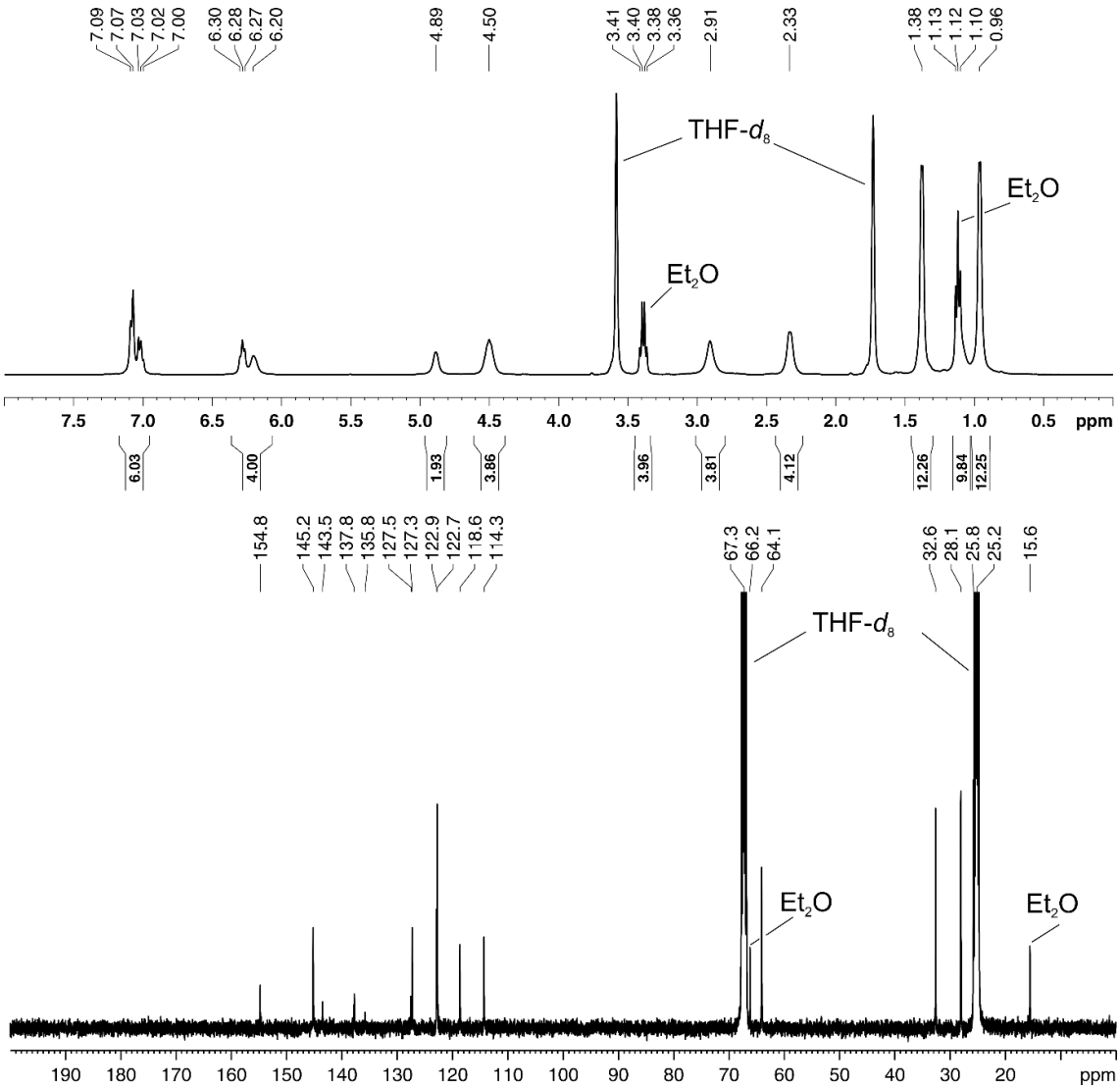

Figure S1. ^{1}H (top) and $^{13}C\{^{1}H\}$ NMR spectra (bottom) of **1** (400.16/100.61 MHz, THF-d_8, 300 K).

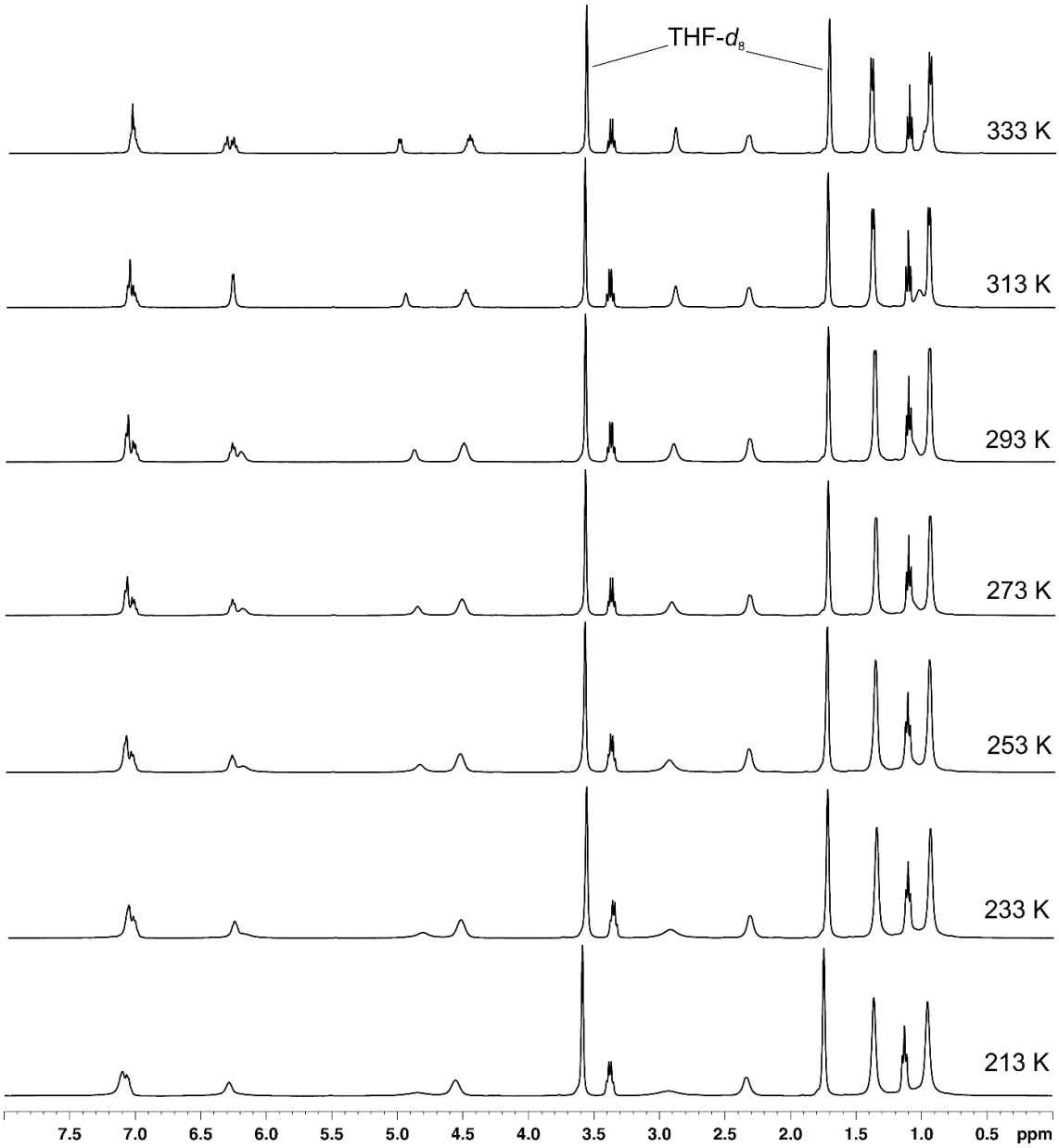

Figure S2. ^{1}H NMR spectrum of **1** (400.16 MHz, THF-d_8) at variable temperatures.

8.4.3 Synthesis of $[K(thf)_2]_2[\{(BIAN)Co\}_2(\mu\text{-}C_2S_4)]$ (2)

A solution of CS_2 (0.54 M, 0.30 mL, 0.16 mmol, 1.0 eq) in THF was added dropwise to a cooled (−70 °C) solution of **1** (125 mg, 0.160 mmol, 1.0 eq) in THF (12 mL). Afterwards the solution was warmed to room temperature and stirred for 40 hours. Subsequently, the reaction mixture was filtered and concentrated to 9 mL. Dark purple microcrystals formed upon layering this solution with diethyl ether (20 mL). Crystals suitable for X-Ray diffraction were obtained by storing a concentrated DME solution of **2** at room temperature. Yield 53 mg (40%); m.p. >295 °C (decomp. to a black and an orange oil); UV/Vis (THF, λ_{max} (nm, ε_{max} /L·mol^{-1}·cm^{-1})): 346 (27000), 463 (15000), 507 (23000), 687 (14000); NIR (THF, λ_{max} (nm, ε_{max} /L·mol^{-1}·cm^{-1})): sh940 (18700), 1056 (21600), sh1258 (9900); elemental analysis calcd. for $C_{80}H_{112}N_4Co_2K_2O_4S_4$ (M = 1638.21): C 65.99, H 6.89, N 3.42, found.: C 65.64, H 7.06, N 3.08; ^{1}H NMR (DMF-d_7,

300 K, 400.13 MHz) δ /ppm = 0.73 (br m, 24H, CH(C*H*$_3$)$_2$), 1.18 (br m, 24H, CH(C*H*$_3$)$_2$), 3.45−3.75 (br overlapping m, 24H, THF/C*H*(CH$_3$)$_2$), 6.30 (br m, 4H, CH$_{BIAN}$), 6.87 (br m, 4H, CH$_{BIAN}$), 7.21 (br m, 8H, *meta*-CH$_{Dipp}$), 7.48 (br m, 4H, *para*-CH$_{Dipp}$), 8.57 (br m, 4H, CH$_{BIAN}$); ^{13}C{^{1}H} NMR (DMF-d_7, 300 K, 100.61 MHz) δ /ppm = 24.7 (CH(*C*H$_3$)$_2$), 25.9 (CH(*C*H$_3$)$_2$), 28.8 (*C*H(CH$_3$)$_2$), 109.8 (CH$_{Dipp}$), 114.5 (CH$_{BIAN}$), 121.1 (CH$_{BIAN}$), 126.6 (CH$_{Dipp}$), 131.2, 133.8, 135.1 (CH$_{BIAN}$), 140.8, 153.2, 154.7, 155.9, 165.1.

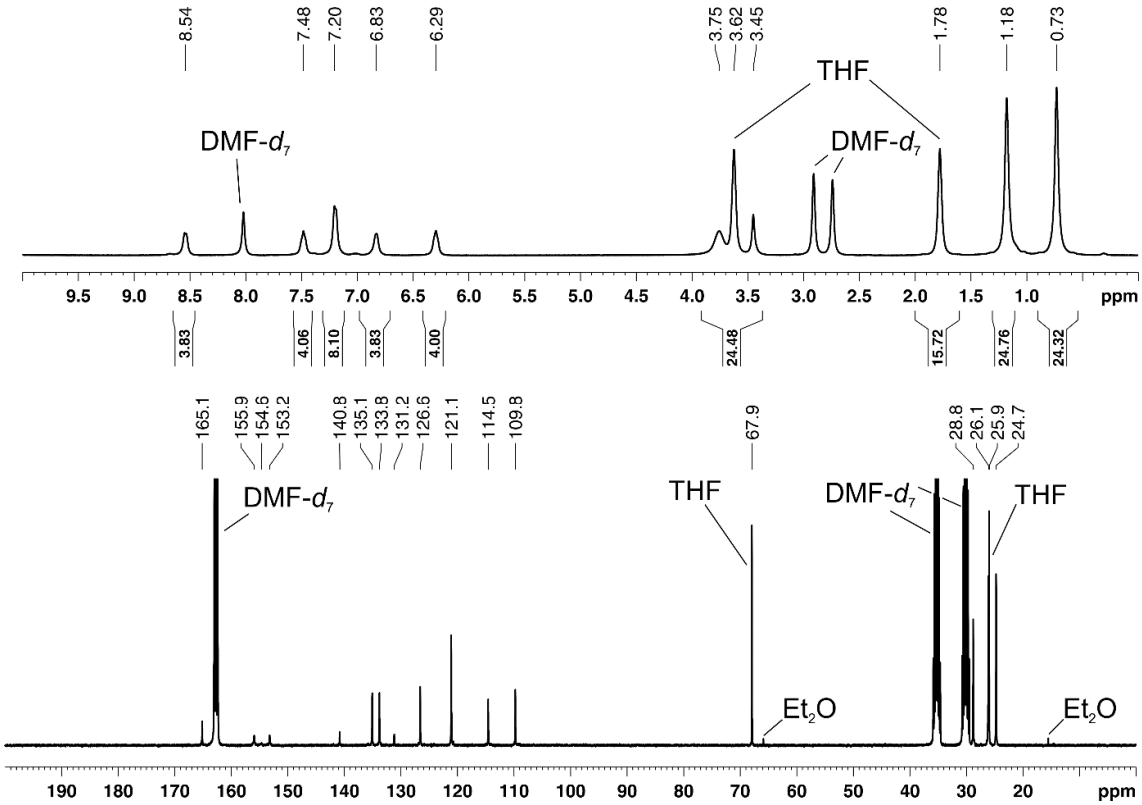

Figure S3. ^{1}H (top) and ^{13}C{^{1}H} NMR spectra (bottom) of **2** (400.16/100.61 MHz, DMF-d_7, 300 K bottom).

8.4.4 Synthesis of [K(thf)$_3$][Co(BIAN)(P$_2$C$_2$*t*Bu)] (3)

A solution of *t*BuCP (0.20 M, 0.70 mL, 0.14 mmol, 2.0 eq) in THF was added dropwise to a cooled (−70 °C) solution of **1** (56 mg, 0.071 mmol, 1.0 eq) in THF (5 mL). The solution was warmed to room temperature and stirred for 22 hours. After removal of the solvent, the residue was extracted with THF (1.0 mL). Dark turquoise X-ray quality crystals of **3** formed by diffusing *n*-hexane into this solution over the course of one day. Yield 51 mg (71%); m.p. 245 °C; UV/Vis (THF, λ_{max} (nm, ε_{max} /L·mol^{-1}·cm^{-1})): 294 (22800), 388 (6000), 605 (16700), 738 (7800); elemental analysis calcd. for $C_{58}H_{82}N_2CoKO_3P_2$ (M = 1014.48): C 68.62, H 8.14, N 2.76, found.: C 68.63, H 7.96, N 2.60; ^{1}H NMR (THF-d_8, 300 K, 400.13 MHz) δ /ppm = 0.80 (br m, 12H, CH(C*H*$_3$)$_2$), 0.93 (br s, 18H, C(CH$_3$)$_3$), 1.33 (br m, 12H, CH(C*H*$_3$)$_2$), 5.00 (br m, 6H, C*H*(CH$_3$)$_2$/CH$_{BIAN}$), 6.36 (br m, 2H, CH$_{BIAN}$), 6.61 (br m, 2H, CH$_{BIAN}$), 7.14 (br m, 6H, *meta*-/*para*-CH$_{Dipp}$); ^{13}C{^{1}H} NMR (THF-d_8, 300 K, 100.61 MHz) δ /ppm = 25.2 (CH(*C*H$_3$)$_2$), 26.4 (CH(*C*H$_3$)$_2$), 28.7 (*C*H(CH$_3$)$_2$), 32.5 (t, $^3J_{PC}$ = 4.9 Hz, C(*C*H$_3$)$_3$), 34.3 (t, $^2J_{PC}$ = 6.6 Hz, *C*(CH$_3$)$_3$),

89.4 (t, $^{1}J_{PC}$ = 49.5 Hz, P-C), 116.4 (CH_{BIAN}), 119.3 (CH_{BIAN}), 123.4 (CH_{Dipp}), 123.5 (CH_{Dipp}), 127.5 (CH_{BIAN}), 128.9 (C_{BIAN}), 136.1 (C_{BIAN}) 137.3 (C_{BIAN}), 143.5 (C_{BIAN}), 146.9 (*ortho*-C_{Dipp}), 160.5 (*ipso*-C_{Dipp}); $^{31}P\{^{1}H\}$ NMR (THF-d_8, 300 K, 161.98 MHz) δ /ppm = 1.8 (s).

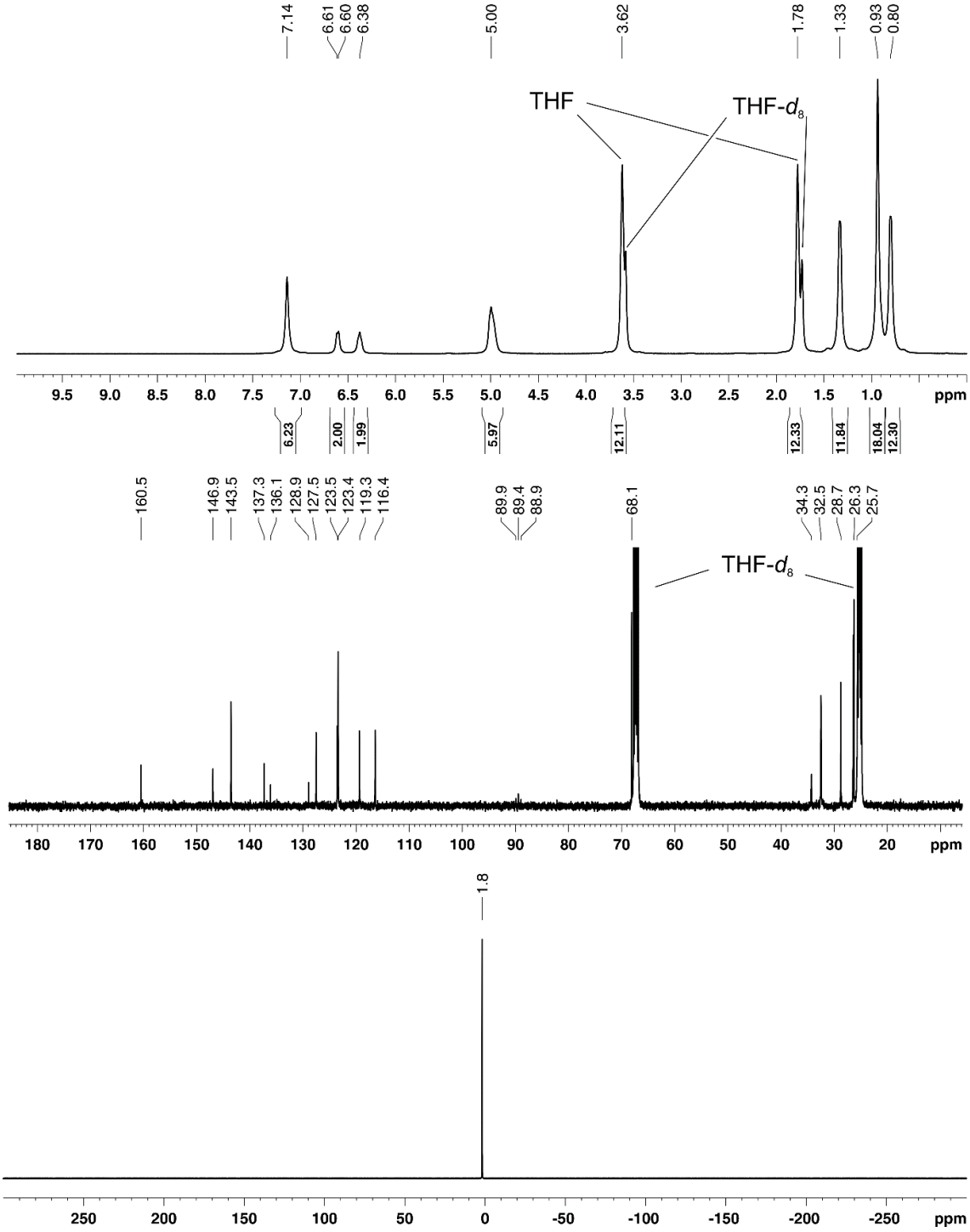

Figure S4. ^{1}H (top), $^{13}C\{^{1}H\}$ (middle) and $^{31}P\{^{1}H\}$ NMR spectra (bottom) of **3** (400.16/100.61/161.98 MHz, THF-d_8, 300 K).

8.4.5 Synthesis of $[K(thf)]_2[\{(BIAN)Co\}_2(\mu\text{-}\eta^4\text{:}\eta^4\text{-}P_4)]$ (4)

P_4 (26 mg, 0.21 mmol, 1.0 eq) was added at room temperature to a solution of **1** (328 mg, 0.420 mmol, 2.0 eq) in THF (10 mL). After the resulting violet reaction mixture was stirred for 23 hours the solution was filtered and the residue extracted with 2 mL of THF. The filtrate was concentrated to ~7 mL and layered with diethyl ether (~25 mL). Dark microcrystals of **4** formed upon storing the solution for one week at room temperature. X-ray quality crystals of **4** were obtained by storing a concentrated diethyl ether solution of **4** at room temperature. Yield 188 mg (61%). m.p. No melting point or decomposition was observed up to 300 °C; UV/Vis (THF, λ_{max} (nm, ε_{max} /L·mol^{-1}·cm^{-1})): 345 (24200), 585 (35200); elemental analysis calcd. for $C_{80}H_{96}N_4Co_2K_2O_2$ (M = 1465.63): C 65.56, H 6.60, N 3.82, found.: C 64.78, H 6.24, N 3.83; ^{1}H NMR (DMF-d_7, 300 K, 400.13 MHz) δ /ppm = 0.78 (br m, 24H, CH(CH_3)$_2$), 1.40 (br m, 24H, CH(CH_3)$_2$), 4.32 (br m, 8H, CH(CH$_3$)$_2$), 5.07 (br m, 4H, CH_{BIAN}), 6.31 (br m, 4H, CH_{BIAN}), 6.53 (br m, 4H, CH_{BIAN}), 7.05 (br m, 12H, *meta*-/*para*-CH_{Dipp}); ^{13}C{^{1}H} NMR (DMF-d_7, 300 K, 100.61 MHz) δ /ppm = 25.8 (CH(*C*H$_3$)$_2$), 26.0 (CH(*C*H$_3$)$_2$), 27.9 (*C*H(CH$_3$)$_2$), 114.2 (br s, CH_{BIAN}), 118.0 (br s, CH_{BIAN}), 122.2 (br s, *meta*-C_{Dipp}), 123.2 (br s, *para*-C_{Dipp}), 128.1 (br s, CH_{BIAN}), 128.7 (br s, C_{BIAN}), 137.2 (br s, C_{BIAN}), 141.5 (br s, C_{BIAN}), 144.0 (br s, *ortho*-C_{Dipp}), 157.6 (br s, *ipso*-C_{Dipp}) (One ^{13}C signal of a quarternary carbon atom of the BIAN ligand could not be detected probably due to broad and overlapping signals); ^{31}P{^{1}H} NMR (DMF-d_7, 300 K, 161.98 MHz) δ /ppm = −45.9 (s).

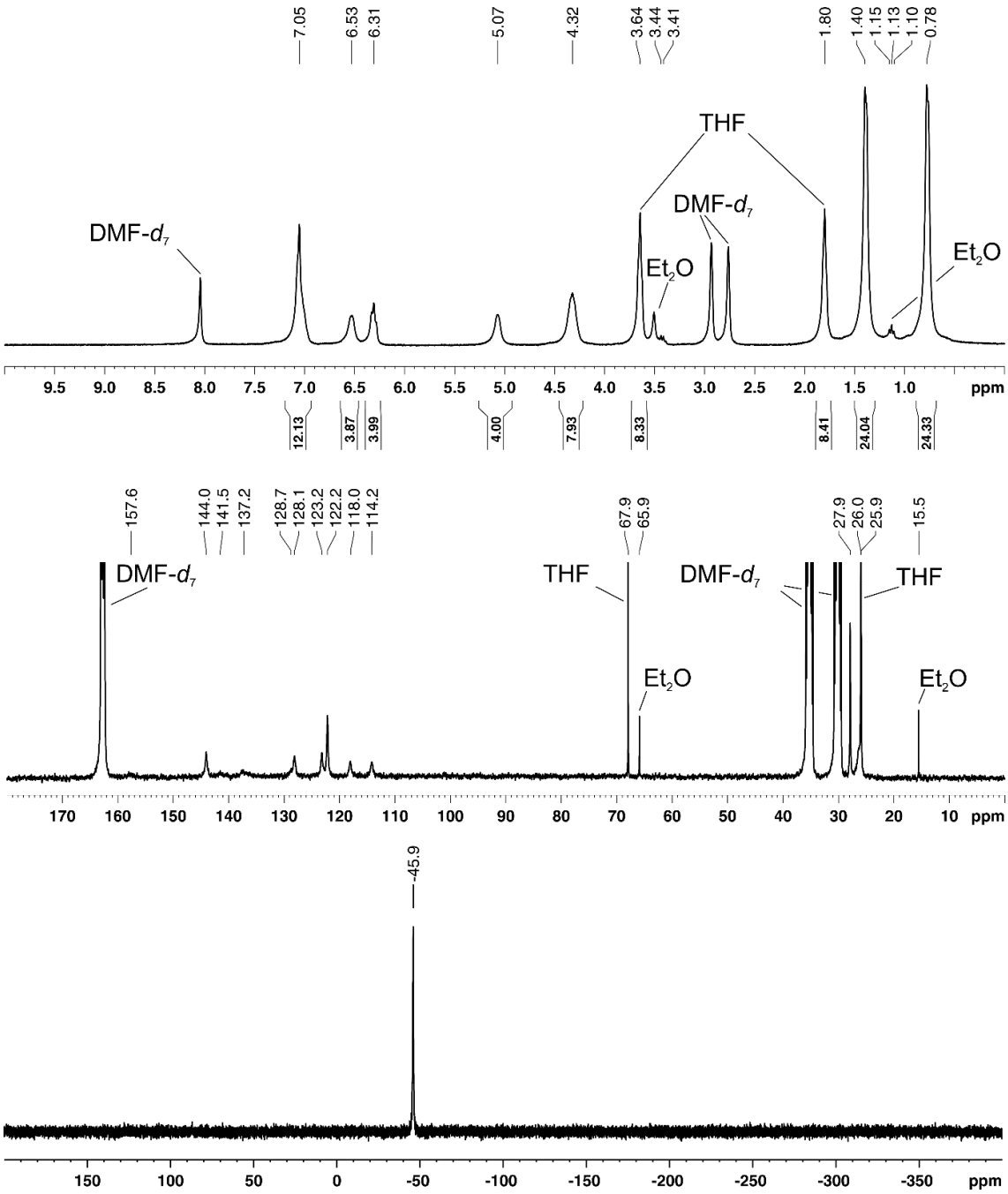

Figure S5. ^{1}H (top), $^{13}C\{^{1}H\}$ (middle) and $^{31}P\{^{1}H\}$ NMR spectra (bottom) of **4** (400.16/100.61/161.98 MHz, DMF-d_7, 300 K).

8.4.6 Synthesis of [K(OEt$_2$)][{(BIAN)Co}$_2$(μ-η^4:η^4-P$_4$)] (5)

A solution of [Cp$_2$Fe]BAr$^F_4$ (55 mg, 0.053 mmol, 1.0 eq) in THF (1 mL) was added dropwise to a suspension of **4** (77 mg, 0.053 mmol, 1.0 eq) in THF (3 mL). An immediate colour change to dark blue was observed. After stirring the reaction mixture for 24 hours, the solvent was removed and the residue was washed with *n*-hexane (7 mL) The residue was extracted with diethyl ether (8 mL), the filtrate was concentrated to 3 mL and stored at room temperature for five days. Dark blue X-ray quality crystals of **5** formed upon storing for one day. Yield 29 mg (41%); m.p. No

melting point or decomposition was observed up to 300 °C; UV/Vis (THF, λ_{max} (nm, ε_{max} /L·mol^{-1}·cm^{-1})): 337 (14500), 575 (19000); elemental analysis calcd. for $C_{76}H_{90}N_4Co_2KOP_4$ (M = 1356.44): C 67.30, H 6.69, N 4.13, found: C 68.29, H 6.73, N 4.11; Effective magnetic moment (THF-d_8): μ_{eff} = 2.0(1) μ_B.^{1}H NMR (THF-d_8, 300 K, 400.13 MHz) δ /ppm = −0.9 (br s), 0.8−1.2 (br m, overlap with Et_2O), 3.4 (br s, overlap with Et_2O), 7.29 (br s), 17.4 (br s), 19.3 (br s).

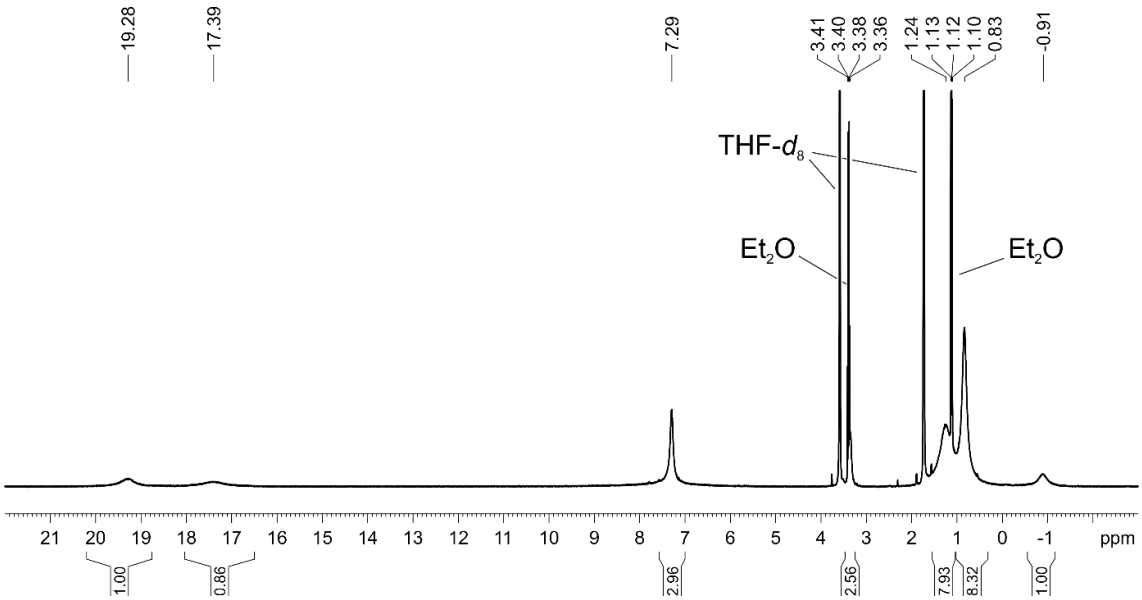

Figure S6. ^{1}H NMR spectrum of **3** (400.16 MHz,THF-d_8, 300 K).

8.5 X-ray Crystallography

The single crystal X-ray diffraction data were recorded on an Agilent Technologies Gemini Ultra R and in case of compound **3** on a GV1000 diffractometer with microfocus Cu K_α radiation (λ = 1.54184 Å). Emperical multi-scan[4] and analytical absorption corrections[5] and in case of **3** empirical[4] and numerical[6] ones were applied to the data. The structures were solved with SHELXT[5] and least-square refinements on F^2 were carried out with SHELXL.[8]

Table S1. Crystallographic data of **1**−**5**.

Compound	**1**	**2**	**3**
Empirical formula	$C_{52}H_{68}CoKN_2O_2$	$C_{60}H_{84}CoKN_2O_{3.5}P_2$	$C_{90}H_{120}Co_2K_2N_4O_8S_4$
Formula weight	851.11	1049.26	1710.19
Temperature [K]	123(1)	123(1)	123(1)
Crystal system	triclinic	monoclinic	triclinic
Space group	*P*-1	*Pn*	*P*-1
a [Å]	11.2499(4)	15.4510(2)	12.1308(3)
b [Å]	11.5370(4)	21.0207(2)	14.1427(4)
c [Å]	20.3034(6)	18.2194(1)	15.3246(4)
α [°]	91.310(3)	90	109.450(2)
β [°]	99.660(3)	102.473(1)	91.384(2)
γ [°]	119.140(4)	90	112.585(3)
Volume [Å^3]	2252.24(15)	5777.82(9)	2253.81(11)
Z	2	4	1
ρ_{calc} [g/cm^3]	1.255	1.206	1.260
μ [mm^{-1}]	4.127	3.837	5.004
F(000)	912.0	2248.0	908.0
Crystal size [mm^3]	0.277 × 0.143 × 0.048	0.255 × 0.153 × 0.044	0.178 × 0.137 × 0.0545
Radiation	CuK$_\alpha$ (λ = 1.54184)	CuK$_\alpha$ (λ = 1.54184)	CuK$_\alpha$ (λ = 1.54184)
2*Θ* range for data collection [°]	8.84 to 133.51	7.21 to 133.53	7.63 to 146.74
Index ranges	−13 ≤ h ≤ 13, −9 ≤ k ≤ 13, −23 ≤ l ≤ 24	−18 ≤ h ≤ 18, −24 ≤ k ≤ 25, −18 ≤ l ≤ 21	−13 ≤ h ≤ 14, −16 ≤ k ≤ 17, −18 ≤ l ≤ 19
Reflections collected	21844	70293	21099
Independent reflections	7903 [R_{int} = 0.0364, R_{sigma} = 0.0396]	17913 [R_{int} = 0.0384, R_{sigma} = 0.0348]	8724 [R_{int} = 0.0307, R_{sigma} = 0.0343]
Data / restraints / parameters	7903 / 0 / 542	17913 / 386 / 1369	8724 / 0 / 508
Goodness-of-fit on F^2	1.046	1.022	1.031
Final R indexes [I>=2σ (I)]	R_1 = 0.0403, wR_2 = 0.1036	R_1 = 0.0426, wR_2 = 0.1143	R_1 = 0.0318, wR_2 = 0.0787
Final R indexes [all data]	R_1 = 0.0450, wR_2 = 0.1072	R_1 = 0.0486, wR_2 = 0.1188	R_1 = 0.0352, wR_2 = 0.0815
Largest diff. peak/hole [e Å^{-3}]	0.40/−0.47	0.80/−0.47	0.88/−0.33
Flack parameter	-	−0.0324(14)	-

Compound	**4**	**5**
Empirical formula	$C_{44}H_{60}CoKN_2O_2P_2$	$C_{77}H_{92.5}Co_2KN_4O_{1.25}P_4$
Formula weight	808.91	1374.88
Temperature [K]	123(1)	123(1)
Crystal system	orthorhombic	triclinic
Space group	*Pbca*	*P*-1
a [Å]	18.1469(3)	11.6695(7)
b [Å]	20.2274(3)	13.5686(8)
c [Å]	24.0439(4)	14.0237(7)
α [°]	90	67.523(5)
β [°]	90	69.663(5)
γ [°]	90	83.206(5)
Volume [Å^3]	8825.6(2)	1923.6(2)
Z	8	1
ρ_{calc} [g/cm^3]	1.218	1.187
μ [mm^{-1}]	4.850	4.979
F(000)	3440.0	726.0
Crystal size [mm^3]	0.198 × 0.149 × 0.056	0.200 × 0.097 × 0.078
Radiation	CuK_α (λ = 1.54184)	CuK_α (λ = 1.54184)
2Θ range for data collection [°]	7.51 to 133.52	8.04 to 147.06
Index ranges	$-19 \le h \le 21$, $-23 \le k \le 24$, $-21 \le l \le 28$	$-14 \le h \le 11$, $-16 \le k \le 16$, $-17 \le l \le 17$
Reflections collected	36375	12427
Independent reflections	7766 [R_{int} = 0.0460, R_{sigma} = 0.0342]	7369 [R_{int} = 0.0360, R_{sigma} = 0.0560]
Data / restraints / parameters	7766 / 54 / 511	7369/160/448
Goodness-of-fit on F^2	1.025	1.136
Final R indexes [I>=2σ (I)]	R_1 = 0.0491, wR_2 = 0.1182	R_1 = 0.1340, wR_2 = 0.3342
Final R indexes [all data]	R_1 = 0.0625, wR_2 = 0.1261	R_1 = 0.1410, wR_2 = 0.3375
Largest diff. peak/hole [e Å^{-3}]	1.51/−0.40	1.50/−0.89

8.6 UV-Vis Spectrum of 1 and Vis-NIR Spectra of 1−4

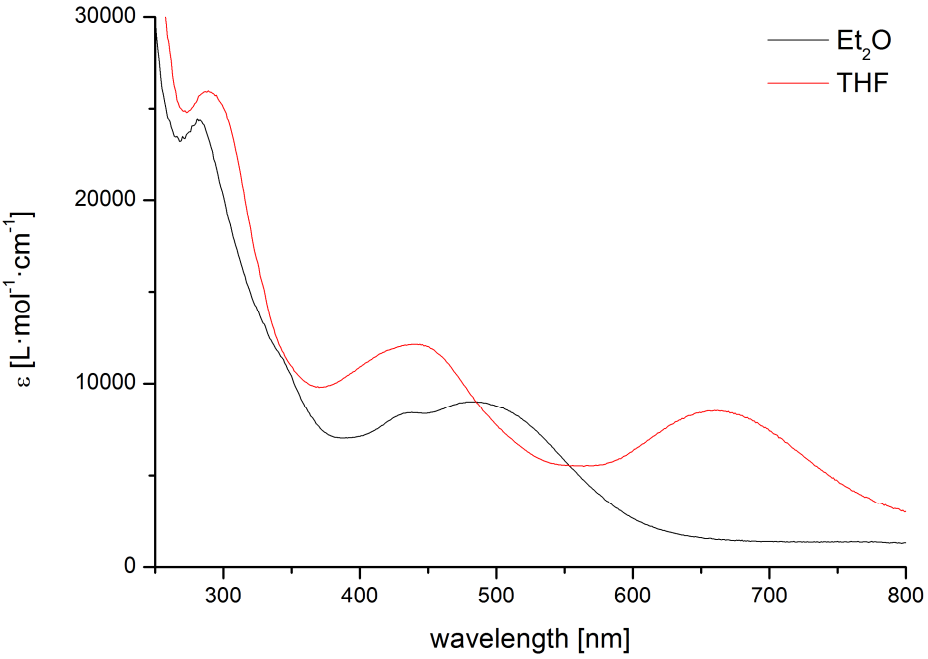

Figure S7. UV-Vis spectrum of **1** in diethyl ether (black) and THF (red).

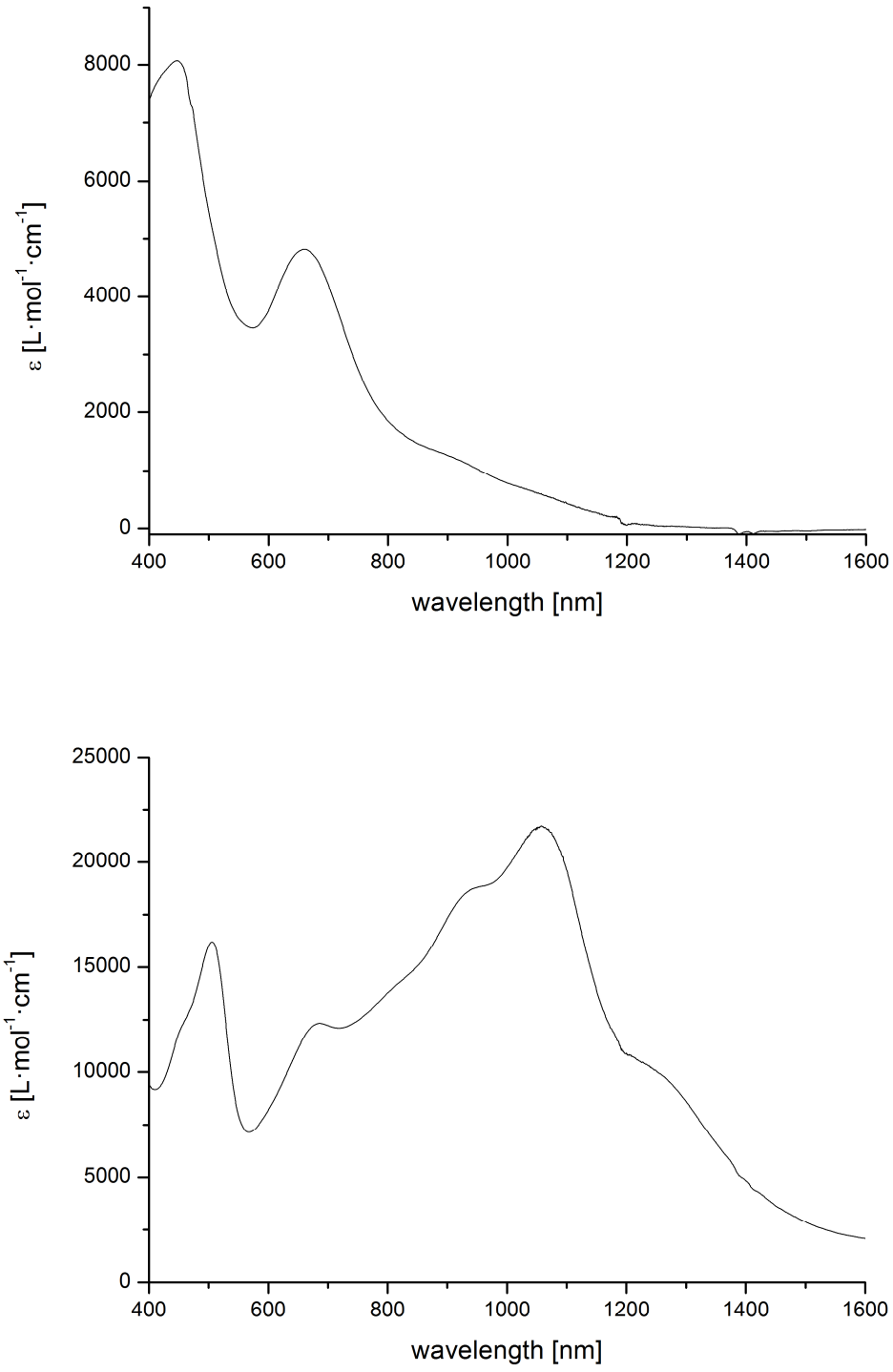

Figure S8. Vis/NIR spectra of **1** (top) and **2** (bottom) in THF.

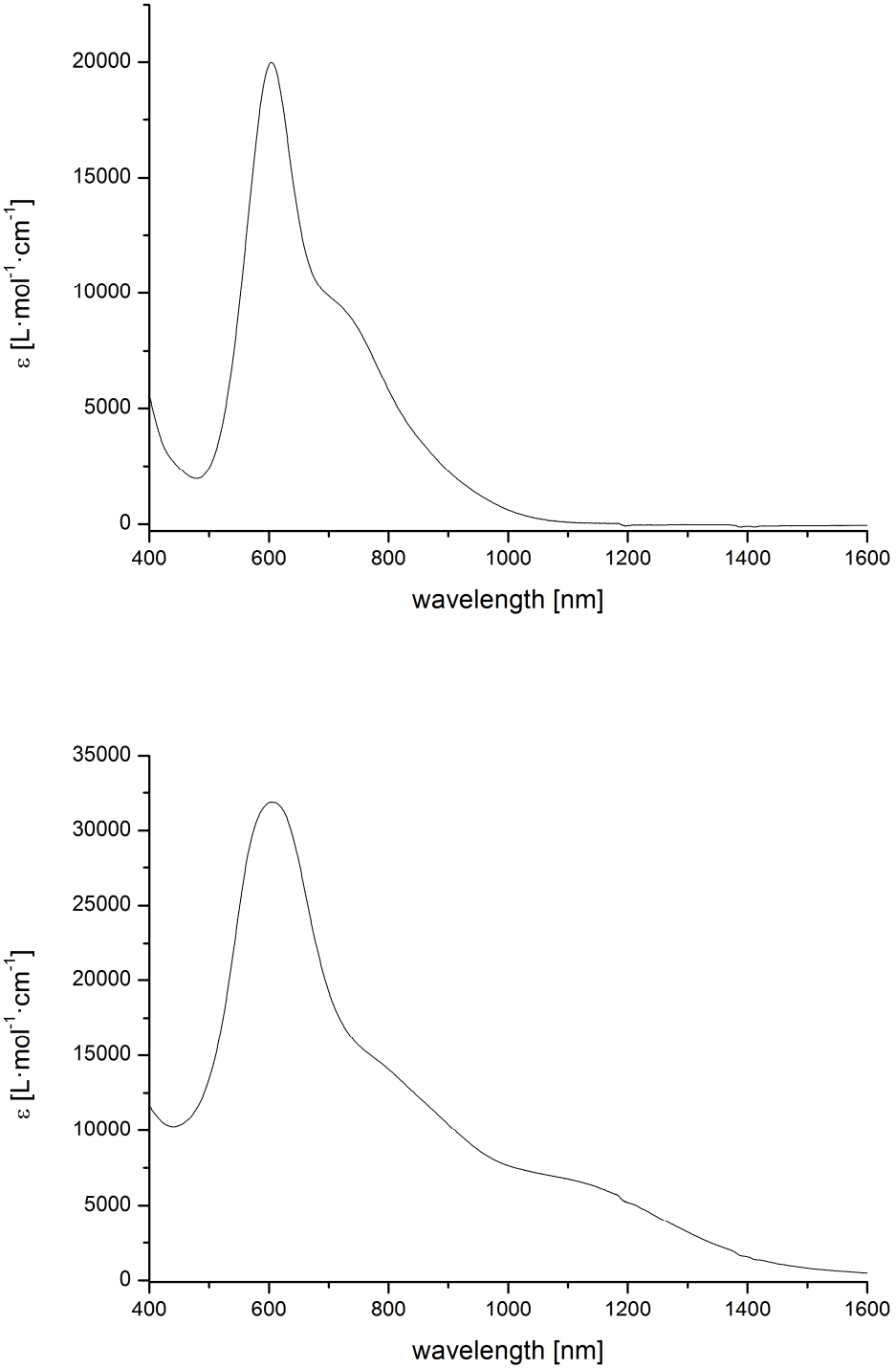

Figure S9. Vis/NIR spectra of **3** (top) and **4** (bottom) in THF.

8.7 Cyclic Voltammetry

Cyclic voltammetry experiments were performed in a single-compartment cell inside a nitrogen-filled glovebox using a CH Instruments CHI600E potentiostat. The cell was equipped with a platinum disc working electrode (1 mm diameter) polished with 0.05 µm alumina paste, a platinum wire counter electrode and a silver wire pseudoreference electrode. The supporting electrolyte, tetra-*n*-butylammonium hexafluorophosphate, was dried in vacuo at 110 °C overnight. All redox potentials are reported versus the ferrocenium/ferrocene (Fc^+/Fc) couple. The scan rate is v = 100 mV s^{-1} unless stated otherwise.

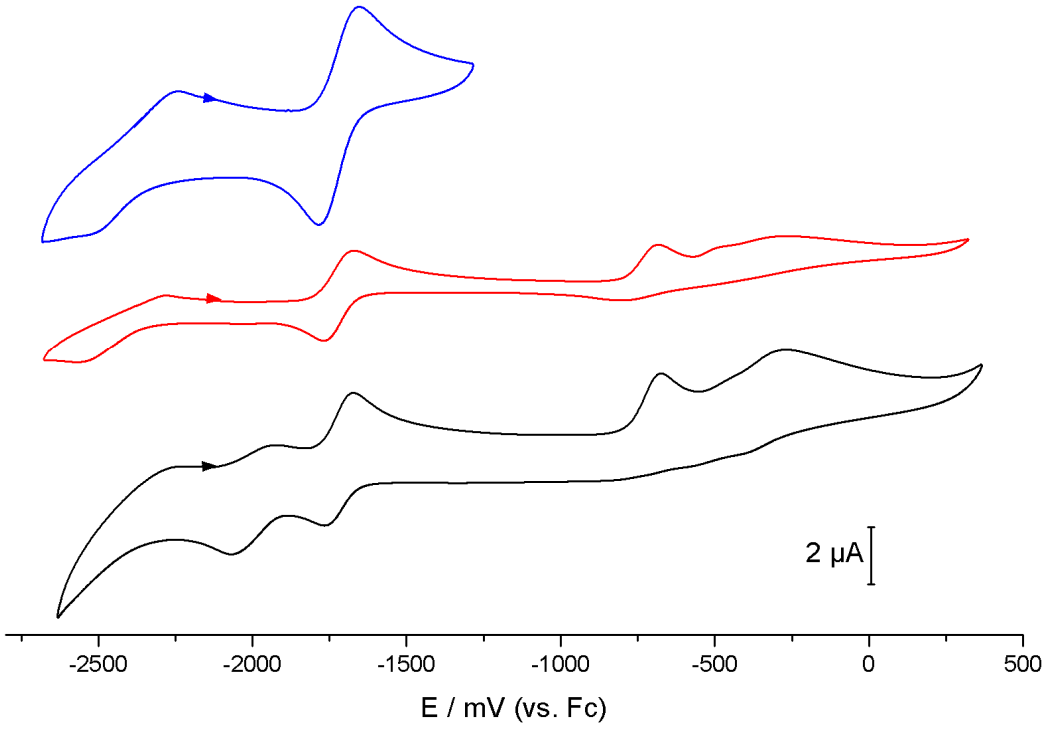

Figure S10. Cyclic voltammogram of **1** in THF at v = 100 mV s^{-1} (black), 20 mV s^{-1} (red) and 100 mV s^{-1} with limited scan range (blue).

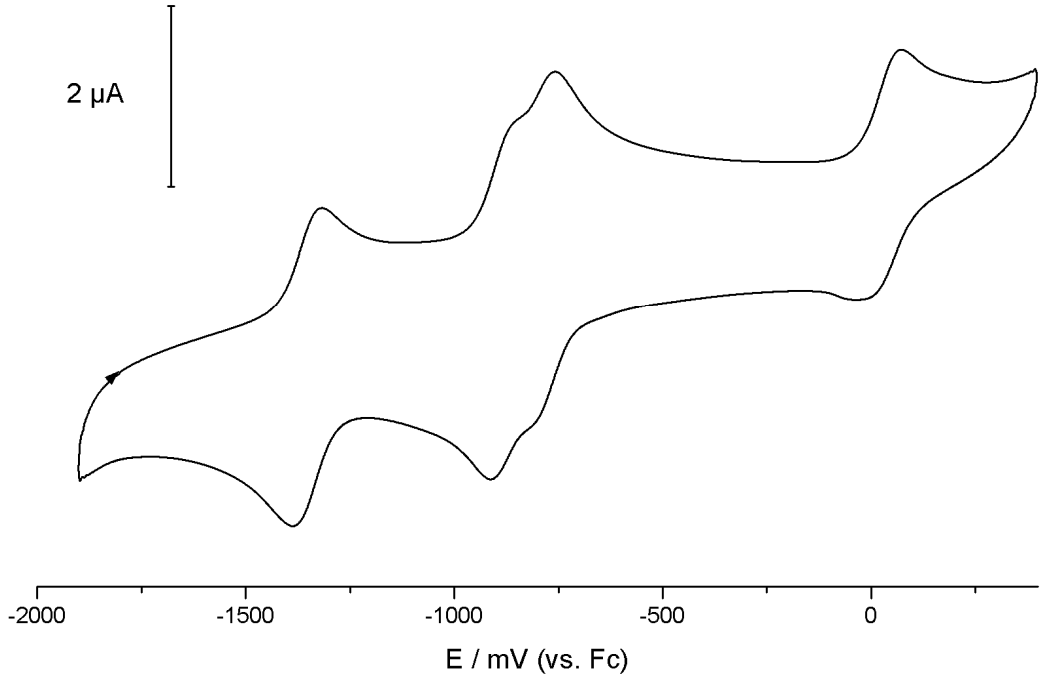

Figure S11. Cyclic voltammogram of **2** in acetonitrile.

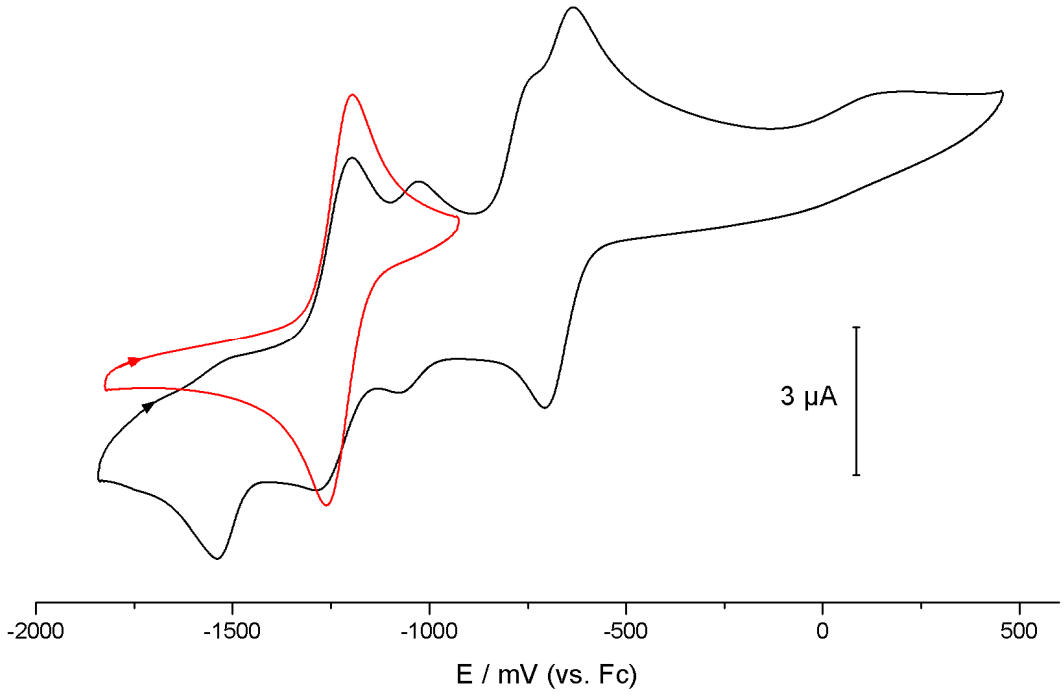

Figure S12. Cyclic voltammogram of **3** in THF (black); CV of **3** with limited scan range (red).

References

1 K. Jonas, *US patent 4169845*, **1979**.

2 A. Paulovicova, U. El-Ayaan, K. Shibayama, T. Morita, Y. Fukuda, *Eur. J. Inorg. Chem.* **2001**, 2641–2646.

3 G. Becker, G. Gresser, W. Uhl, *Z. Naturforsch. B* **1981**, *36*, 16.

4 a) SCALE3ABS, CrysAlisPro, Aglient Technologies Inc., Oxford, GB, **2015**; b) G. M. Sheldrick, SADABS, Bruker AXS, Madison, USA, **2007**.

5 R. C. Clark, J. S. Reid, *Acta Crystallogr. A* **1995**, *51*, 887.

6 CrysAlisPro, version 171.37.35, Agilent Technologies Inc., Oxford, GB, **2015**.

7 G. M. Sheldrick, *Acta Cryst.* **2015**, *A71*, 3.

8 G. M. Sheldrick, *Acta Cryst.* **2015**, *C71*, 3.

9 Summary

Chapter 1. *The Chemistry of Mononuclear Phosphane and N-Heterocyclic Carbene Nickel(I) Complexes: Synthesis, Structural Motifs, and Reactivity*

The introductory chapter reviews the chemistry of the dynamically emerging field of mononuclear NHC nickel(I) complexes and related phosphane compounds. The aim of this chapter is to highlight the analogies and differences between and within the two classes. Besides the synthesis and structural motifs of the monomers, this chapter covers the reactivity of the nickel(I) species. After a brief introduction about synthetic access strategies, this work is subdivided in phosphane nickel(I) halides and related cationic nickel(I) complexes with weakly coordinating counteranions, followed by phosphane complexes with ancillary N-donors, pincer complexes, phosphane complexes with additional S-donors, and a brief section on piano-stool hydrocarbyl complexes. Finally the chemistry of NHC nickel(I) complexes will be described.

Chapter 2. *Selective P_4 Activation by an Organometallic Nickel(I) Radical: Formation of a Dinuclear Nickel(II) Tetraphosphide and Related Di- and Trichalcogenides*[1]

The main goal of this thesis was to synthesize and characterize new monomeric cyclopentadienyl (Cp) nickel(I) complexes supported by NHCs and explore their reactivity. The results are summarized in Schemes 1−5.

Complexes **1**−**3** were synthesized according to Scheme 1 by reacting nickel(II) chlorides of type [(η^5-C_5R_5)Ni(NHC)] with potassium graphite in THF. Compounds **1**−**3** exhibit typical metalloradical character as indicated by EPR spectroscopy and cyclic voltammetry. Interestingly, these d^9 species show broad but characteristic ^{1}H NMR signals. Furthermore, the X-ray diffraction analysis revealed a bent structure in the solid-state as indicated by the $C_{carbene}$–Ni–$(C_5H_5)_{centroid}$ angle, which is probably caused by the asymmetric spin density distribution at the nickel center.

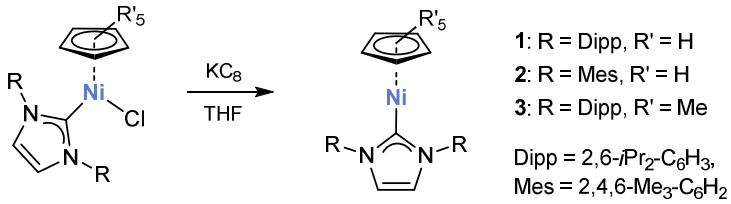

Scheme 1. Synthesis of new nickel(I) metalloradicals **1**−**3**.

In an initial study, we investigated the reactivity of the new nickel(I) radical **1** toward small molecules and typical radical traps (Scheme 2). The reaction of **1** with the mild oxidizing agent ferrocenium hexafluorophosphat gave the nickel(II) cation **4** with a two-legged piano stool

coordination environment for nickel. Upon converting **1** with the persistent radical TEMPO the square-planar nickel(II) complex **5** was formed in a very selective fashion.

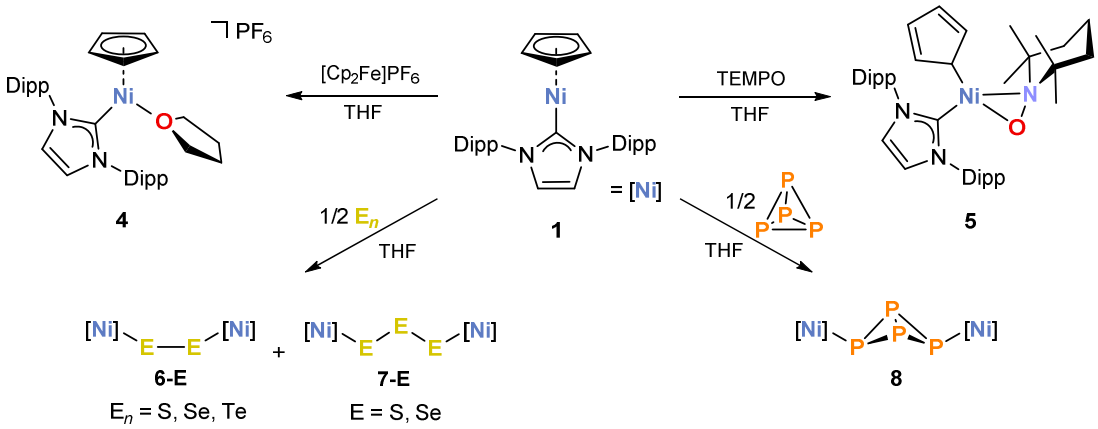

Scheme 2. Radical reactivity of complex **1**.

It is well known that radicals can be trapped by element-element bonds. Therefore, we tested the reactivity of **1** toward elemental chalcogenides sulfur, grey selenium, and grey tellurium, as well as white phosphorus (P_4). While the reactions with sulfur and selenium resulted in mixtures of di- and trichalcogenide-bridged complexes **6-E** and **7-E**, the only product observed was **6-Te** in case of tellurium. Remarkably, the reaction of **1** with P_4 resulted in the high-yield synthesis of new complex $[\{(C_5H_5)Ni(IDipp)\}_2(\mu\text{-}\eta^1\text{:}\eta^1P_4)]$ (**8**) with a bridging "butterfly" P_4^{2-} ligand, which represents the first example of a nickel complex bearing such ligand. All complexes were thoroughly characterized by X-ray crystallography, multinuclear NMR and UV-Vis spectroscopy.

Chapter 3. Half-Sandwich Nickel(I) Complexes of Ring-Expanded N-Heterocyclic Carbenes: A Structural and Quantum Chemical Study[2]

In a follow-up study, we were interested in designing new nickel(I) radicals by utilizing ring-expanded N-heterocyclic carbenes (RE-NHCs) and compare the influence of these unconventional carbenes on the structural and electronic properties of [CpNi(NHC)] complexes, as well as their reactivity toward P_4.

The three novel complexes **9**–**11** were prepared by reducing the nickel(II) bromides **9Br**–**11Br** with KC_8 in a similar manner as described for compounds **1**–**3** (Scheme 3). The nickel(II) precursors were obtained in the reaction of $[CpNiBr(PPh_3)]$ with the respective RE-NHC.

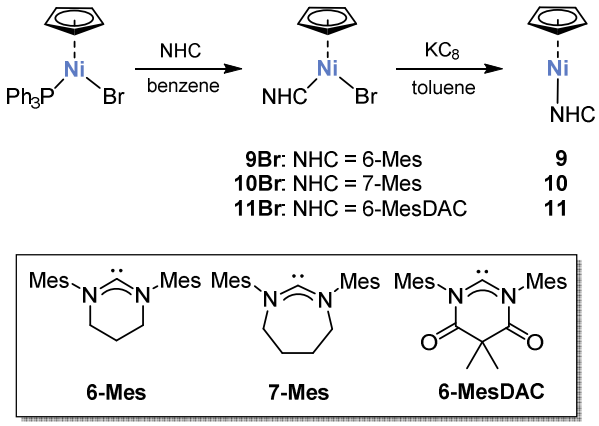

Scheme 3. Synthesis of cyclopentadienyl nickel(I) complexes with ring-expanded carbenes.

The X-ray diffraction analysis revealed that complexes **9**–**11** possess similar, though less bent structures as **1**–**3** (increased $C_{carbene}$–Ni–$Cp_{centroid}$ angles) in comparison with **1** and **2** and decreased $C_{carbene}$–Ni–$Cp_{centroid}$ angle as compared with **3**. According to DFT calculations complexes **9**–**11** also showed comparable electronic structures as **1**–**3**. Nevertheless, diamidocarbene complex **11** (Scheme 3) exhibits a distinct UV-Vis and ^{1}H NMR spectrum as compared with **1**–**3**, **9**, and **10**. Compound **9** and **10** readily react with white phosphorus at room temperature. The reaction of **9** affords tetraphosphide **12**. A mixture of the analogous complex **13** and unidentified products was obtained using **10** according to $^{31}P\{^{1}H\}$ NMR spectroscopy. In marked contrast, compound **11** did not react with P_4, further demonstrating its distinct electronic properties.

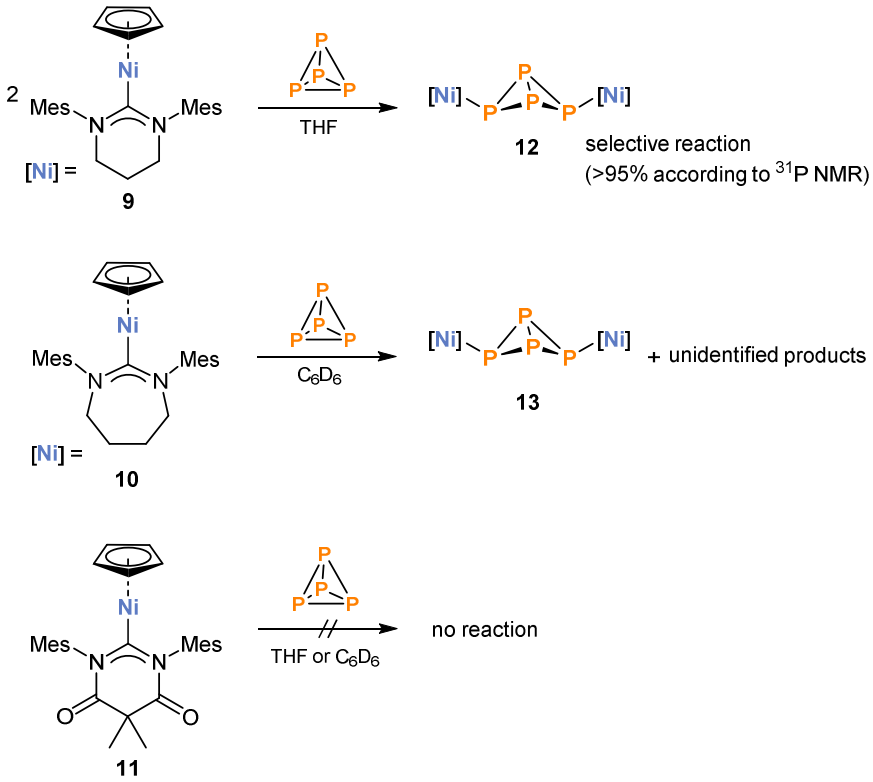

Scheme 3. Reactivity of complexes **9**–**11** toward white phosphorus.

Chapter 4. Formation of Heteronickelacycles through the Reductive Coupling of Phenyl Iso(thio)cyanate[3]

In extension to our reactivity studies toward element−element bonds in chapters 2 and 3, the reactivity of complex **1** toward heteroallenes was investigated.

The reaction of **1** with one equivalent phenyl isothiocyanate afforded compound **14**, which features the new $\{SC(NPh)N(Ph)CS\}^{2-}$ dianion as a result of the dimerization of the substrate in the coordination sphere of the metal atom (Scheme 4). The nickel(II) complex $[(\eta^5\text{-Cp})(\eta^1\text{-Cp})Ni(IDipp)]$ (**15**) is a stoichiometric by-product in this reaction. We presume that the reaction pathway probably involves the transfer of a Cp radical to a second equivalent of complex **1**, which then leads to a reactive intermediate that essentially acts as nickel(0) surrogate. In fact, complex **14** was cleanly produced in the reaction of the nickel(0) compound $[(IDipp)Ni(styrene)_2]$ (**A**) with two equivalents PhNCS. Interestingly, the reaction of **A** with phenyl isocyanate yields the new *γ*-lactam-nickellacycle $[(IDipp)Ni\{N(Ph)C(O)CH_2CHPh\}]$ (*rac*-**16**) as a result of the reductive coupling of PhNCO and a styrene ligand. The solid-state molecular structure of the unsaturated complex *rac*-**16** displays a rare T-shaped structure for nickel. In contrast, the reaction of PhNCO with the nickel(I) complex $[(\eta^5\text{-Cp})Ni(IDipp)]$ gave an inseparable mixture of diamagnetic products, showing that this complex has a distinct reactivity in this case with PhNCO and PhNCS.

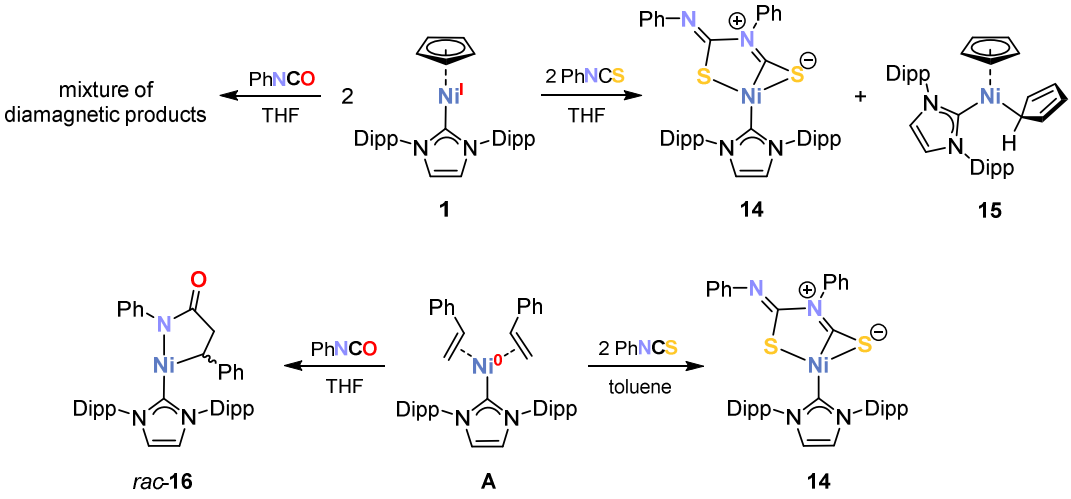

Scheme 4. Comparison of the reactivity of **1** and **A** toward heteroallenes.

Chapter 5. Insertion of Phenyl Isothiocyanate into a P−P Bond of a Nickel-substituted Bicyclo[1.1.0]tetraphosphabutane[4]

Encouraged by the good accessibility of phosphide complex **8**, we were interested in functionalizing the P_4 moiety in this complex. Therefore, we investigated the reactivity of **8** and derivative **17**, bearing the slightly less bulky IMes carbene instead of IDipp, toward phenyl

isothiocyanate. Complex **17** was obtained in an analogous fashion as described for **8** (chapter 2) and features a similar molecular structure and spectroscopic properties (Scheme 5).

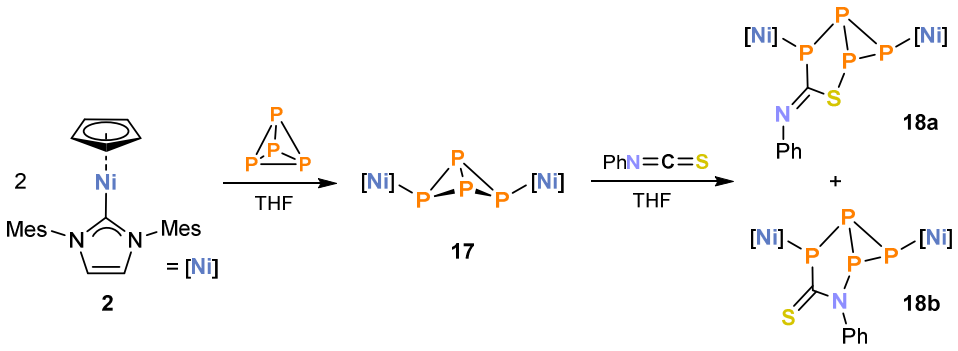

Scheme 5. Functionalization of the P_4 fragment in **17**.

Reactions of **8** and **17** with CS_2 gave products which feature ADMX spin systems in the $^{31}P\{^1H\}$ NMR spectra, but these products could not be isolated. Interestingly, the reaction of **17** with an excess of PhNCS yielded a mixture of two main products (ADMX spin systems) and one minor species (A_2MX spin system). Both main products, **18a** and **18b**, were obtained as pure compounds and fully characterized by X-ray diffraction as well as UV-Vis and multinuclear NMR spectroscopy. In addition, DFT calculations were performed in order to get further insight into the reaction mechanism. The novel complexes **18a** and **18b** feature unprecedented bicyclo[3.1.0]heterohexane fragments. Moreover, this reaction represent the first example of an insertion of a heteroallene into a bicyclo[1.1.0]tetraphosphabutane ligand.

The investigations of chapter 2-5 demonstrate that the presented NHC nickel(I) complexes exhibit typical metalloradical properties. Their high reactivity and radical nature enables mild reaction procedures for element-element bond activations, in particular P−P bonds of P_4. Moreover, the use of NHCs and cyclopentadienyl ligands enables the modification of the electronic and steric properties of these compounds. In case of complexes **9**−**11** our initial investigations indicate the presence of a distinct electronic structure of compound **11** in comparison with **1**−**3**, **9**, and **10**. Further investigations by EPR and ENDOR spectroscopy are ongoing to confirm this presumption and get deeper insight into the electronic structure.

In future work, it will also be of interest to investigate whether reactions of metal-substituted cyclopolyphosphanes with polar multiple bonds offer a general route toward “functionalized” polyphosphanes as exemplified by the reaction of complex **17** with PhNCS.

Chapter 6. Synthesis and Structural Characterization of Iron(II), Cobalt(II), and Nickel(II) Complexes of a Cyclic (Alkyl)(amino)carbene[5]

In the context of utilizing unconventional carbenes in 3d metal chemistry, we report on new cyclic (alkyl)(amino)carbene (CAAC) complexes of iron(II), cobalt(II) and nickel(II), which are potentially useful starting materials for further applications in catalysis and small molecule

activation. Complexes [FeCl(μ-Cl)(CAAC$_1$)]$_2$ (**19**), [CoBr(μ-Br)(CAAC$_1$)]$_2$ (**20**), and [NiBr(μ-Br)(CAAC$_1$)]$_2$ (**21**) were synthesized by reacting Bertrand's CAAC$_1$ with divalent iron, cobalt and nickel halides (Scheme 6). They represent the first CAAC complexes with these metals and are paramagnetic and highly air-sensitive, but appear to be thermally stable under an inert atmosphere. X-ray diffraction analyses revealed dimeric halide-bridged structures with distorted tetrahedral metal environments.

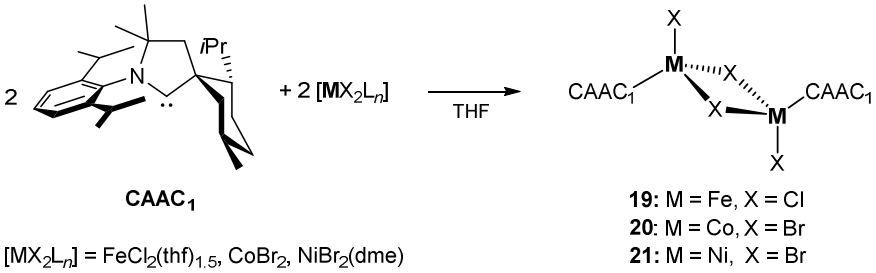

Scheme 6. Synthesis of CAAC complexes **19**–**21**.

Chapter 7. Preparation of a Trigonal Planar Manganese(II) Amido Complex Supported by an N-Heterocyclic Carbene[6]

In chapter 7 we describe a convenient synthesis of the NHC-stabilized manganese(II) chloride **22** from commercially available starting materials and investigated its ability as precursor for low-coordinate manganese(II) NHC complexes.

The X-ray diffraction analysis of **1-THF** indicate the dissociation of the dimer **22** in tetrahydrofuran solutions (Scheme 7).

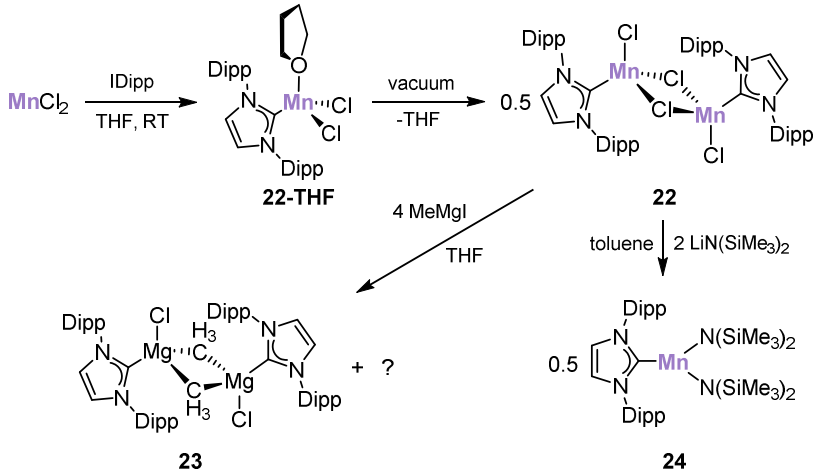

Scheme 7. Synthesis of the dimeric manganese(II) chloride **22** and reactivity toward MeMgI and LiN(SiMe$_3$)$_2$.

Furthermore, the lability of the manganese(II)-carbon bond in **22** was demonstrated in the reaction of **22** with four equivalents of MeMgI, which yielded the dinuclear compound [(IDipp)MgMeCl]$_2$ (**23**). As shown by single-crystal X-ray analysis of **23**, the IDipp and the chloride ligands were

transferred from manganese in **22** to the magnesium atom. The reaction of **22** with four equivalents lithium hexamethyldisilazide gave the monomeric amide **24** (Scheme 7), which features a trigonal planar coordination environment. Compound **24** represents a rare example of a three-coordinate NHC-stabilized manganese(II) complex. Solution magnetic moments showed the presence of d^5 high spin manganese(II) centers in **22** and **24**.

This initial study paves the way for further investigations regarding the use of complex **22** as precursor for further coordinatively and electronically unsaturated complexes. Future work should also focus on the exploration of the reactivity of **24** toward nucleophilic reagents.

Chapter 8. *Synthesis and Reactivity Studies of a Heteroleptic α-Diimine Cobalt Anion*[7]

Another aim of this thesis was to synthesize and characterize novel highly reduced cobalt complexes with redox-active α-diimine ligands, and investigate their reactivity toward small molecules.

The novel BIAN (BIAN = bis(2,6-diisopropylphenylimino)acenaphthene) cobalt complex **25** was synthesized from $[Co(cod)_2]^-$ via straightforward substitution of one cod ligand (Scheme 8).

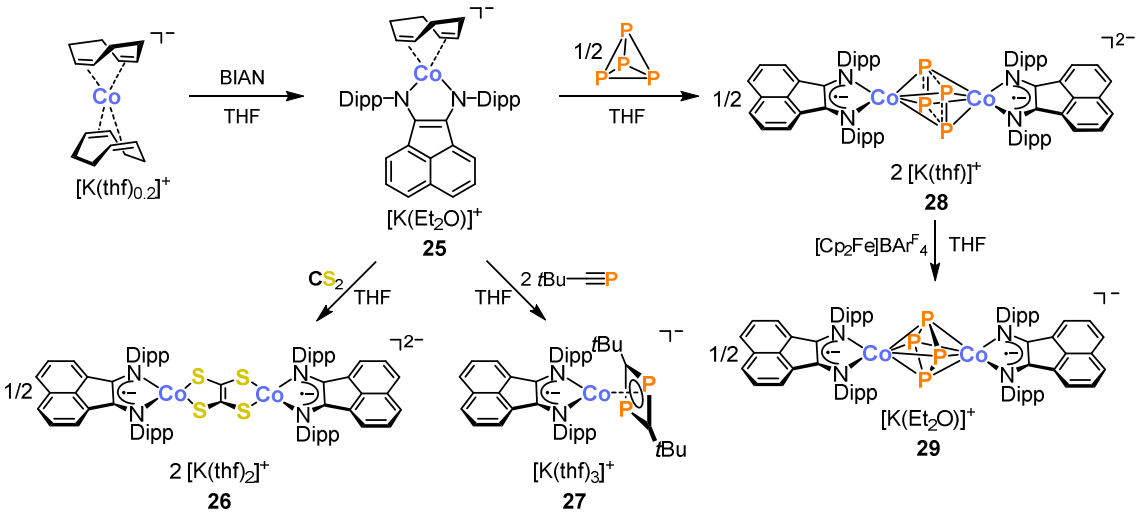

Scheme 8. Preparation of the heteroleptic BIAN complex **25** and its reactivity toward small molecules.

The reaction of **25** with carbon disulfide yielded the dinuclear complex **26** with a bridging ethylene tetrathiolate by the reductive dimerization of the substrate. Furthermore, complex **27** was obtained by converting **25** with two equivalents of *tert*-butylphosphaalkyne, containing an η^4-1,3-disphosphacyclobutadiene ligand. The dianionic complex **28**, which features an unusual rectangular P_4^{4-} framework, was formed by the selective activation of P_4. Its oxidation afforded monoanion **29** with a rare rhombic cyclo-P_4^{4-} ligand. Our investigations revealed that the use of the redox-active BIAN ligand appears crucial for achieving a high degree of P_4 reduction.

Phosphide anions **28** and **29** are potentially useful starting complexes for the functionalization of the P_4 moiety in the coordination sphere of the cobalt centers with electrophilic inorganic and organic molecules. In addition, the synthesis of complexes related to **25** with modified electronic and steric properties is promising in order to tune the highly reduced cobalt complexes for further reactivity studies toward other small molecules as well as potential catalytic applications.

References

1 S. Pelties, D. Herrmann, B. de Bruin, F. Hartl, R. Wolf, *Chem. Commun.* **2014**, 50, 7014–7016.

2 S. Pelties, E. Carter, M. F. Mahon, D. Murphy, M. K. Whittlesey, R. Wolf, manuscript in preparation.

3 S. Pelties, R. Wolf, manuscript in preparation.

4 S. Pelties, A. W. Ehlers, R. Wolf, *Chem. Commun.*, in revision.

5 S. Pelties, R. Wolf, *Z. Anorg. Allg. Chem.* **2013**, *639*, 2581–2585.

6 S. Pelties, D. Herrmann, T. Maier, R. Wolf, manuscript in preparation.

10 Acknowledgement

Zuletzt möchte ich mich bei folgenden Personen bedanken:

- Ganz besonders bei Prof. Dr. Robert Wolf für die hervorragende Betreuung, interessante Aufgabenstellung, anregenden Diskussionen, exzellenten Arbeitsbedingungen und große Freiheit bei meiner Forschung.
- Prof. Dr. Manfred Scheer (Zweitgutachter), Prof. Dr. Axel Jacobi von Wangelin (Drittprüfer) und Prof. Dr. Olga Garcia Mancheño (Vorsitz) für die Bereitschaft, die Plätze des Prüfungskomitees zu besetzen.
- Dr. Michael Bodensteiner, Dr. Stefanie Gärtner und Prof. Dr. Robert Wolf für die Hilfestellung bei der Röntgen-Einkristallstrukturanalyse.
- Den Mitarbeitern der zentralen Analytik und Werkstätten, insbesondere: Sabine Stempfhuber und Katharina Beier (Röntgenstrukturanalyse), Annette Schramm, Georgine Stühler und Fritz Kastner (NMR-Abteilung), Barbara Baumann, Wilhelmine Krutina und Helmut Schüller (Elementaranalyse), Markus Lindner (Glasbläserei), Peter Fuchs (Elektronikwerkstatt).
- Meinen Kooperationspartnern Prof. Dr. Bas de Bruin (University of Amsterdam), Prof. Dr. Frantisek Hartl (University of Reading), Prof. Dr. Jan J. Weigand und M.Sc. Felix Hennersdorf (TU Dresden), Dr. Andreas W. Ehlers (VU Amsterdam), Prof. Dr. Michael K. Whittlesey (University of Bath) Dr. Emma Carter und Prof. Dr. Damien Murphy (University of Cardiff) für ihren wertvollen Beitrag, ihr hohes Engagement und die interessanten Diskussionen.
- Meinen lieben Nachbarn von unten, oben und vom Gang, den Mitarbeitern der Arbeitskreise: Díaz-Díaz, Fleischer, Garcia Mancheño, Jacobi von Wangelin sowie Scheer, Thea Hering und Christian Götz (T. H. und C. G. auch für's Dirk-Sitten) für die wunderbaren Kaffeepausen, Grillabende, Weihnachtsfeiern, Konferenzen, oder einfach für's Zuhören und Quatschen.
- Dem AK Weigand: Maximilian Donath, Felix Hennersdorf, Rene Panzer, Chris Sala, Kathleen Schnaars, Robin Schoemaker, Stephen Schulz, Kai Schwedtmann, Fabian Watt, Jan J. Weigand und Sivathmeehan Yogendra für die besten und unterhaltsamsten Konferenztage, Unterstützung in vielerlei Hinsicht und die sehr freundschaftliche Atmosphäre.
- Andreas Ehlers and Jaap Borger for DFT support and a very nice and fun time in Amsterdam and at conferences.
- The "pretentions" Whittlesey group: Mateusz "my lost twin brother" Cybulski, Lee Collins, Ian "Kiwi" Riddlestone, and Mike Keith Whittlesey for a great atmosphere in the lab as well as in the pub, and an incredibly good time, which I'll never forget.
- Den aktuellen und früheren Arbeitskreismitgliedern: Philipp "😡😡😡" Büschelberger, Uttam „Der Uttinger" Chakraborty, Dirk „The Coach" Herrmann, Christian „Hoidini" Hoidn, Anna Kohl, Helge Lange, Julia "Solvent Girl" Leitl, Ulrich „Green Lennter" Lennert, Thomas „Nitrogen Boy" Maier, Nadine Maue, Jennifer „Dat Jennifa" Bißmeier (geb. Malberg), Der

bezauBERNDe Herr Mühlbauer, Markus “Monsieur Ploîs” Plois, Babak „Bobbse“ Rezaei Rad, Christian „Der Urlauber“ Rödl, Veronica Scheidler, Eva-Maria Schnöckelborg, Vanessa Tomanek, Franziska Urban, Katharina Weber, Anna Weigl, Anne-Kathrin Wiegel und Robert Wolf für die einmalige Stimmung im Arbeitskreis, sehr kollegiale Atmosphäre, lustigen Gin-Abende, musikalischen Mottotage, das fortwährende Planen einer Probe unserer Band *Organometallica,* für die Boarisch-Stunden… ihr seid einfach der Wahnsinn! So jung komma nimma z‘samm!

- All meinen Freunden aus Münster und der Heimat sowie meiner Familie: Helga und Heinz-Gerd, Anna und Christian, Cathrin und Christian für euer großes Verständnis und die Unterstützung in vielerlei Hinsicht.

Unendlich dankbar bin ich meiner Frau, Marta, für ihre Geduld und ihren Rückhalt während meiner gesamten Studien- und Promotionszeit, sowie für ihre grenzenlose Unterstützung, die sie mir tagtäglich entgegenbringt.

11 Curriculum Vitae

Education

Since Nov. 2012	**Ph.D.** at the *University of Regensburg, Germany* (Institute of Inorganic Chemistry) in the group of Prof. R. Wolf: "*Synthesis, Characterizsation, and Reactivity Studies of Low-valent 3d Metal Complexes with N-Heterocyclic Carbene and α-Diimine Ligands*"
2015, 2014	**Research Visits** during the Ph.D.: *University of Bath*, United Kingdom, Prof. Michael K. Whittlesey (June-July 2015, DAAD Kurzstipendium für Doktoranden) *Vrije Universiteit Amsterdam*, The Netherlands, Prof. Koop Lammertsma (May 2015) *Technical University of Dresden*, Germany, Prof. Jan J. Weigand (Dec. 2014)
Oct. 2010 – Sep. 2012	**MASTER OF SCIENCE** in **CHEMISTRY** at the *Westfälische Wilhelms-Universität* (WWU) in Münster, Germany **MASTER THESIS** in the group of Prof. W. Uhl (Institute of Inorganic and Analytical Chemistry): *"1,1-Carbogallation and generation of C_3Ge-heterocycles"*
Oct. 2007 – Sep. 2010	**BACHELOR OF SCIENCE** in **CHEMISTRY** at the *WWU* Münster **BACHELOR THESIS** in the group of Dr. R. Wolf: *"Heterometallic polyhydridorutheniumcomplexes with 3d metals"*
Aug. 2000 – Jun. 2006	**ABITUR** (A-level) Lise-Meitner-Gymnasium, Neuenhaus

Presentations

07. - 09.03.2016	Poster - 13th European Workshop on Phosphorus Chemistry 2016 in Berlin, Germany
23. - 28.08.2015	Talk - Wissenschaftliches Kolloquium von Arbeitsgruppen für Anorganische Chemie 2015 in Hirschegg, Austria
22. - 24.03.2015	Talk - Koordinationschemiker-Tagung 2015 in Paderborn, Germany
16. - 18.03.2015	Talk - 12th European Workshop on Phosphorus Chemistry 2015 in Kassel, Germany
24. - 26.09.2014	Poster - 17. Vortragstagung der Wöhler-Vereinigung für Anorganische Chemie in Saarbrücken, Germany
24. - 26.03.2014	Poster - 11th European Workshop on Phosphorus Chemistry 2014 in Sofia, Bulgaria
25. - 30.08.2013	Talk - Wissenschaftliches Kolloquium von Arbeitsgruppen für Anorganische Chemie 2013 in Hirschegg, Austria

12 List of Publications

5) S. Pelties, A. W. Ehlers, R. Wolf, *Chem. Commun.*, in revision, "*Insertion of Phenyl Isothiocyanate into a P−P Bond of a Nickel-substituted Bicyclo[1.1.0]tetraphosphabutane*"

4) W. Uhl, S. Pelties, J. Tannert, B. J. Ravoo, E.-U. Würthwein, *Chem. Eur. J.* **2015**, *21*, 2629, "*Germacyclobutenes: Generation by 1,1-Carbalumination or 1,1-Carbagallation and Their Photophysical Properties*"

3) S. Pelties, D. Herrmann, B. de Bruin, F. Hartl, R. Wolf, *Chem. Commun.* **2014**, *50*, 7014, "*Selective P_4 Activation by an Organometallic Nickel(I) Radical: Formation of a Dinuclear Nickel(II) Tetraphosphide and Related Di- and Trichalcogenides*"

2) W. Uhl, S. Pelties, M. Rohling, J. Tannert, *Eur. J. Inorg. Chem.* **2014**, 2809, "*Alkenyl-Alkynylgermanes Functionalised by Lewis Acids: Intramolecular Aluminium– and Gallium–Alkyne Interactions and Potential Ge–C Bond Activation*"

1) S. Pelties, R. Wolf, *Z. Anorg. Allg. Chem.* **2013**, *639*, 2581, "*Iron(II), Cobalt(II), and Nickel(II) Complexes of a Cyclic (Alkyl)(amino)carbene*"

Eidesstattliche Erklärung

Ich erkläre hier mit an Eides statt, dass ich die vorliegende Arbeit ohne unzulässige Hilfe Dritter und ohne Benutzung anderer als der angegebenen Hilfsmittel angefertigt habe; die aus anderen Quellen direkt oder indirekt übernommenen Daten und Konzepte sind unter Angabe des Literaturzitats gekennzeichnet.

Stefan Pelties